COUPLING OF THERMAL AND STRUCTURAL ANALYSIS TOWARDS AUTONOMOUS DESIGNING OF MASSIVE CONCRETE STRUCTURES AND RECOGNIZING SUSTAINABLE ALTERNATIVE MATERIALS INCLUDING METAKAOLIN

by

HIWA FAKHRADDIN HAMID

(Under the Direction of Mi Geum Chorzepa)

ABSTRACT

This dissertation includes both experimental and analytical investigations of concrete mixtures containing supplementary cementitious materials to identify sustainable alternatives to Class F fly ash for use in Georgia's mass concrete structures. The primary goal of this study is to optimize the long-term performance of massive concrete structures. This goal is achieved by identifying concrete mixtures that reduce the potential for thermal cracking caused by the heat of hydration of cementitious materials and by developing design charts that assist in design calculations of mass concrete structures. Through this study, ternary replacement mixtures are identified as potentially suitable for mass concrete placements. Additionally, temperature prediction models based on a coupled thermal-structural analysis are developed to aid in maximum temperature and temperature differential predictions. Among the 45% cement replacement mixtures considered in this study, the ternary mixture with 30% slag and 15% metakaolin replacements achieves superior performance in terms of mechanical properties, durability, and thermal cracking

potential from heat of hydration. The experimental and analysis results show that the maximum temperature differential limit of 35 °F (19.4 °C) specified in the current GDOT's Special Provision for mass concrete is adequate for limiting the crack width within 0.006 inch (0.1 mm). Placement conditions, including environmental conditions, significantly affect the maximum temperature and temperature differential. The sensitivity analysis of the bridge seal shows the maximum internal temperature limit of 158 °F (70 °C) will only be met in 70% cement replacement mixtures (SL55+MK15 and SL40+FA30). However, the 70% replacement mixtures will not meet the temperature differential requirement unless insulated formwork or cofferdam is used with R-value greater than 3 $ft^2 \cdot °F \cdot h/BTU$ (0.52 $m^2 \cdot °C/W$). For a given volume-to-surface area ratio (V/A) in a mass concrete structure, the charts and tables developed in this study should inform the temperature requirements conforming to a placement condition.

INDEX WORDS: Metakoalin, Slag Cement, Fly Ash, Heat of Hydration, Mass Concrete, Bridge Seal, Temperature, Temperature Differential, Binary, Ternary Mixture

COUPLING OF THERMAL AND STRUCTURAL ANALYSIS TOWARDS AUTONOMOUS DESIGNING OF MASSIVE CONCRETE STRUCTURES AND RECOGNIZING SUSTAINABLE ALTERNATIVE MATERIALS INCLUDING METAKAOLIN

by

HIWA FAKHRADDIN HAMID

B.S., University of Sulaimani, Iraq, 2009

M.S., Youngstown State University, 2013

A Dissertation Submitted to the Graduate Faculty of The University of Georgia in Partial Fulfillment of the Requirements for the Degree

DOCTOR OF PHILOSOPHY

ATHENS, GEORGIA

2019

COUPLING OF THERMAL AND STRUCTURAL ANALYSIS TOWARDS AUTONOMOUS DESIGNING OF MASSIVE CONCRETE STRUCTURES AND RECOGNIZING SUSTAINABLE ALTERNATIVE MATERIALS INCLUDING METAKAOLIN

by

HIWA FAKHRADDIN HAMID

Major Professor:	Mi Geum Chorzepa
Committee:	Stephan Durham
	S. Sonny Kim
	Xianqiao Wang

Electronic Version Approved:

Ron Walcott
Interim Dean of the Graduate School
The University of Georgia
December 2019

DEDICATION

To my parents and siblings: for your unconditional love, support, inspiration, and prayers throughout my life and education.

To my wife: for your endless sacrificial love and encouragement throughout our educational journey.

ACKNOWLEDGEMENTS

I would like to express my special appreciation and thanks to my advisor Professor Dr. Mi Chorzepa. You have been a tremendous mentor for me. Thank you for the opportunity to work under your supervision. I would also like to thank you for encouraging my research and for allowing me to grow as a scientist. Without your continuous support, this dissertation would not have been possible. Your care and advice on both research as well as on my career have been invaluable.

I would like to express my deepest appreciation to my PhD committee members, Drs. Stephan Durham, Sonny Kim, and Xianqiao Wang, for your valuable feedback, commitment, and time.

I am deeply indebted to my family. Thank you for your continued love, support, and unwavering belief in me. You have always encouraged and nurtured me. Without you, I would not be the person I am today. I am extremely grateful to my wife, Chnar. Thank you for your loving support, care, encouragement, and patience which made this dissertation possible. I am blessed to have you in my life.

I would like to extend my sincere thanks to my extended family and friends for their continuous support. I would like to thank my colleagues for contributing to the experimental work and for creating an amazingly friendly lab environment. Thank you for making my time at UGA such a wonderful experience. I would like to acknowledge the assistantship from Lewis Goode, Robert Chorzepa, Mathew Sullivan, Tofail Ahmed, Victor Lopez, Christopher Johnson, and Lewis Scruggs. I would like to thank Jeff Groh

from Calmetrix for generously providing his time. I am grateful to all the faithful friends for supporting me in a thousand ways over these past years.

I would like to acknowledge the contribution of Lewis Goode in the experimental work presented in Section 3.3.2. Section 1.1 of this dissertation is from Dr. Chorzepa's lecture notes. Sections 2.2, 2.3, and 2.4 are works performed by Mathew Sullivan (MS in Engineering, University of Georgia) during the Phase-I investigation of this study.

I would like to acknowledge the material donations by BASF, Lehigh Hanson, Argos Cement, Thiele Kaolin, Advanced Cement Technologies, Boral Resources, and Kingspan Insulation.

Finally, I would like to thank the funding agency GDOT for the financial support. Your contribution to this program has allowed me to obtain my PhD degree. A special thanks to Dr. Peter Wu (Office of Materials and Testing) who advised the research team in successfully performing the study and Mr. David Jared, P.E. (Office of Performance-based Management and Research) for his research support and provision of pertinent information.

TABLE OF CONTENTS

Page

LIST OF TABLES

Page

LIST OF FIGURES

Page

CHAPTER 1

INTRODUCTION

This chapter presents the background information, objectives, significance, and methodology employed in this study.

1.1 Background

The first subsection introduces the basic knowledge and design principles required to understand the thermal behavior of concrete structures. In addition, the benefits of supplementary cementitious materials (SCMs) (e.g., metakaolin (MK) and granulated blast furnace slag (hereafter referred to as 'slag' in the text and 'SL' in mixture notations)), particularly for improving durability and reducing the heat of cement hydration, are presented herein.

1.1.1 Concrete Behavior and Elevated Temperature

1.1.1.1 Simple facts about thermal loading and concrete behavior

Understanding the fundamental behavior of concrete structures subject to elevated temperatures is critical to a discussion of the thermal design procedures. Thermal loads are induced when natural changes in length or volume are fully or partially restrained due to temperature variations. In effect, thermal loading is strain loading due to temperature change in partially or fully restrained structural members. Increased temperature is represented by increased strain, ε_t, regardless of restraint conditions (free or fixed), as shown in Figure 1, where α denotes the coefficient of thermal expansion (e.g. 5.5×10^{-6}/°F

or $10x10^{-6}$/°C for concrete). In reinforced concrete structures, reinforcing steel generally expands as much as concrete when the temperature increases.

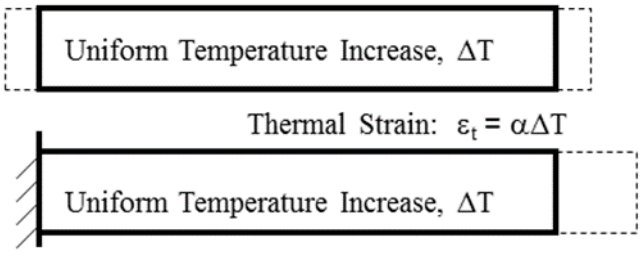

Figure 1 – 1D thermal expansion.

In designing concrete structures, concrete compressive strain and reinforcing steel tensile strain need to be evaluated for load combinations (i.e., combined structural and thermal loading). When a structure is restrained from a rotation but is subjected to a temperature gradient, the hotter side generally results in compression. In this situation, concrete crushing becomes the main concern, as in Figure 2, which shows a reinforced section of a foundation structure. On the other hand, the colder side (i.e., the other face) is in tension, ultimately causing the reinforcing steel to yield. As per the American Concrete Institute (ACI) 318 requirements for ultimate design, reinforcing steel can yield for temperature loading; however, the degree of concrete cracking may affect the serviceability of concrete members and thus may ultimately compromise the structure's primary function. Therefore, strains in reinforcing steel are often limited to $1.2\varepsilon_y$ (ACI 349, 2013) for controlling crack widths in leak-tight structures. Tolerable crack widths range between 0.004 inch (0.10 mm) and 0.016 inch (0.40 mm) according to the International Federation for Structural Concrete (fib) (fib, 2013) and ACI (ACI 224R-07, 2007) design guidelines, depending on a structure's environmental exposure.

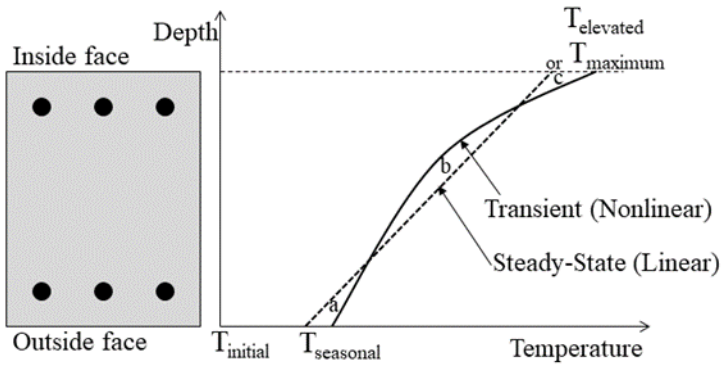

Figure 2 – Temperature profile through typical reinforced concrete section.

1.1.1.2 Temperature increase or decrease

Temperature changes in mass concrete structures are mainly attributed to temperature variations from the heat of cement hydration as well as seasonal temperature changes on surfaces exposed to air (or water). A temperature change is calculated with respect to an initial (or reference) temperature, $T_{initial}$. As the temperature increases to $T_{elevated}$ (or $T_{maximum}$) on one side of a reinforced concrete section, the temperature distribution throughout the section is nonlinear but ultimately converges to a linear steady-state condition as shown in Figure 2. This linear temperature profile is determined such that area 'b' is equivalent to areas 'a' and 'c' combined. Seasonal changes may reverse stress states, and thus both summer and winter conditions need to be evaluated unless inspection deems one condition more critical.

1.1.1.3 Uniform temperature increase and gradient temperature

Often, the linear temperature distribution is divided into a uniform temperature increase, T_u, and a temperature gradient, T_g, as shown in Figure 3. These values are described as increased and differential temperatures for analysis, respectively, and they do not exist as physical values in structures. A thermal model determines the time-dependent and

nonlinear temperature distributions for a structure. A structural model uses the temperature distribution (i.e., loading) at a selected time to generate elastic thermal strains. There is no need to linearize the temperature distribution as long as the same geometry is used in the structural analysis to read temperatures node-by-node from the corresponding thermal model; however, a temperature analysis is often simplified to provide a linear temperature profile for a structural analysis. This process sometimes results in multiple temperature profiles at different locations of a reinforced concrete structure, thereby creating discontinuous temperature assignments at junctions. For this reason, a nonlinear and coupled thermal-structural analysis is highly recommended. In general, a uniform temperature increase yields uniform strain, ε_u, and a gradient temperature yields both compressive and tensile strains, ε_g, in a section (see Figure 3).

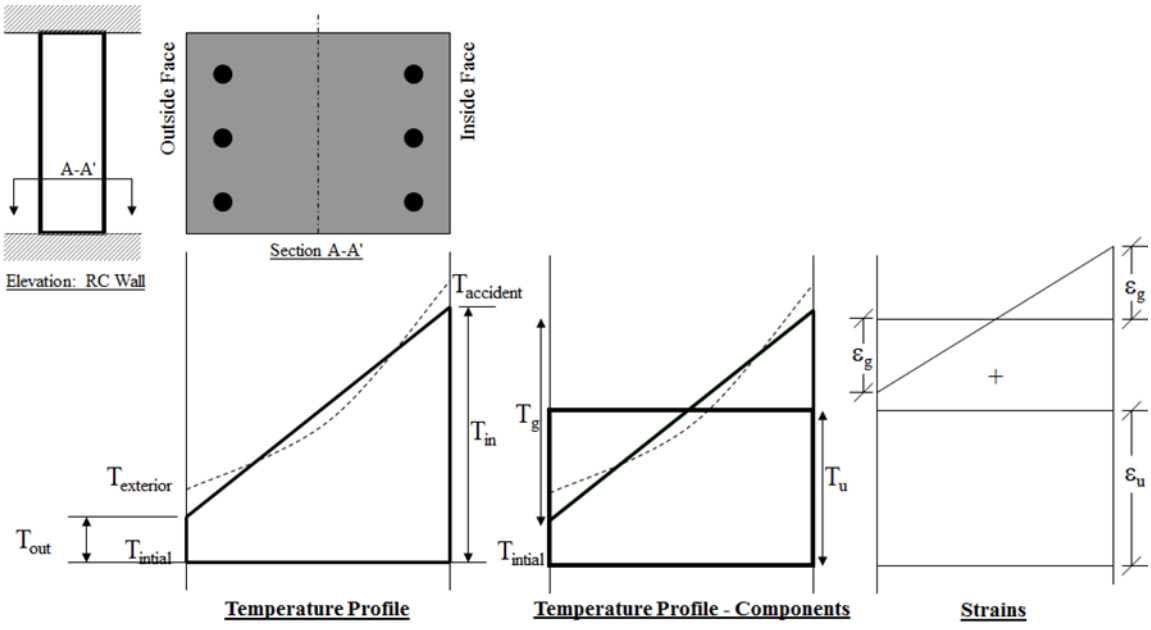

Figure 3 – Linear temperature profile.

1.1.1.4 Behavior of concrete members

Most concrete members are partially restrained from thermal expansion. Figure 4(a) presents the free expansion of a concrete beam as well as a fully-restrained beam member. When a concrete member is free to expand, there is no thermal stress. When the member is fully restrained, thermal stresses are generated. These in turn are used to determine internal thermal forces. Internal stress, σ, and force are simply determined by $\alpha.\Delta T.E$ and $\alpha.\Delta T.EA$, respectively, for a temperature change, ΔT. For other partially restrained structures, the axial force in the concrete member ranges from 0 to $\alpha.\Delta T.EA$. The same idea applies to calculations for member rotations, θ, and moment, M, as shown in Figure 4 (b). Young's modulus, cross-section area, gross section moment of inertia, and thickness of a reinforced concrete section are represented by E, A, I, and t, respectively, in Figure 4.

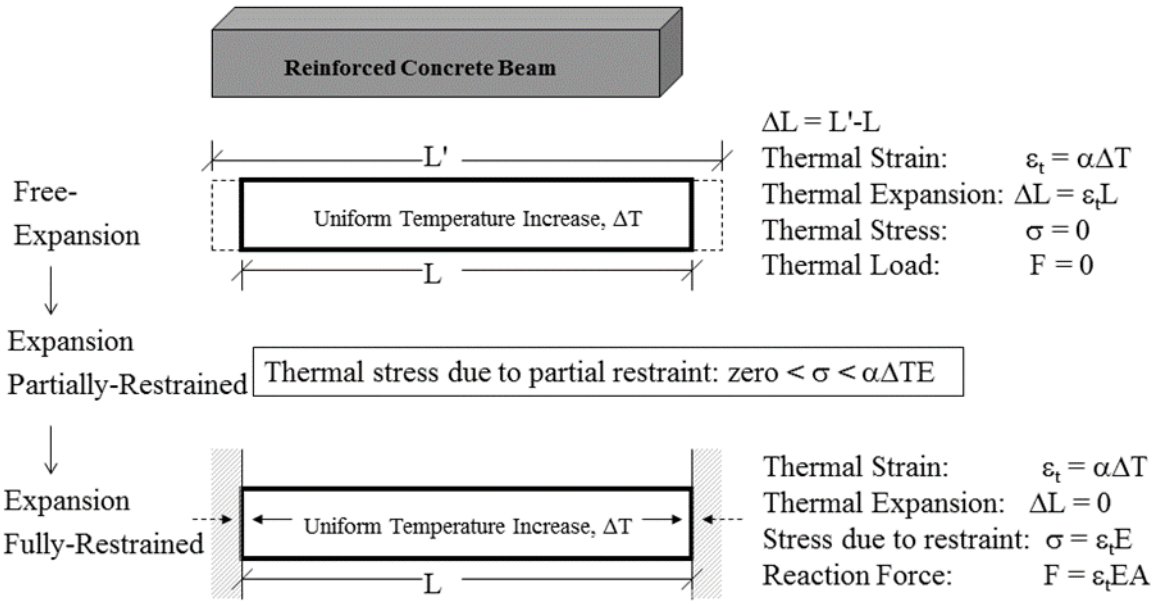

(a) expansion restrained

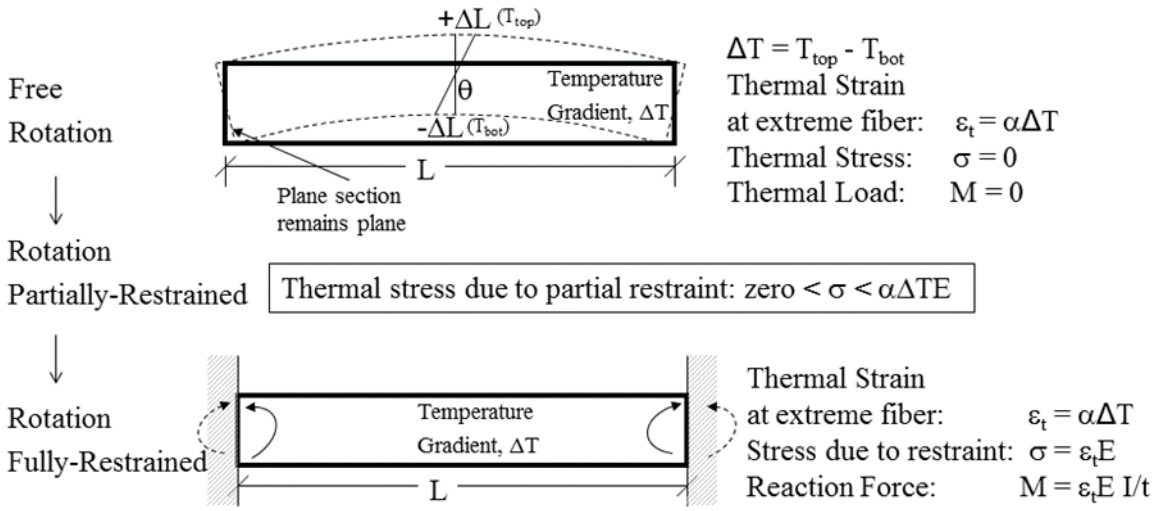

(b) rotation restrained

Figure 4 – Reinforced concrete members restrained from thermal expansion and rotation.

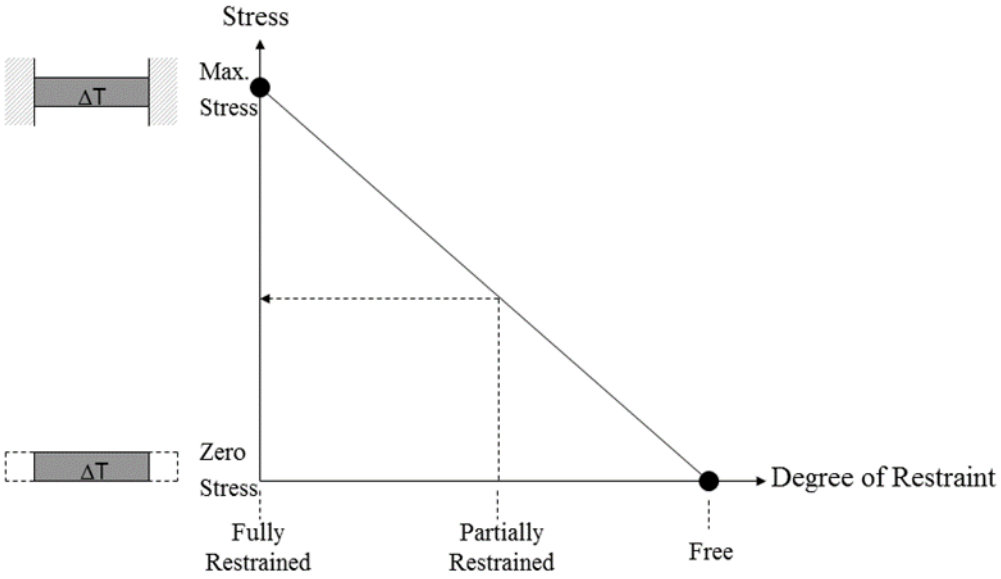

Figure 5 – Degree of restraints and thermal stresses.

1.1.1.5 Thermal stress and restraints

As shown above, the degree of restraints and the gradient temperature affect the amount of thermal stresses generated in a concrete member. Fully restrained concrete members yield

the worst design case, producing the largest thermal strains/stresses. In designing concrete structures for elevated temperatures, members should have as few restraints as possible. Figure 5 portrays an increase in thermal stress as a linear function of the degree of restraints in a concrete member to illustrate this important concept.

1.1.2 Supplementary Cementitious Materials

Natural pozzolans, such as metakaolin (MK), calcined shale, and calcined clay, are materials that contribute to the properties of hardened concrete through hydraulic or pozzolanic activity or both when used in conjunction with Portland or blended cement. Natural pozzolans are classified by ASTM C 618 (AASHTO M 295) as Class N pozzolans.

A pozzolan is a siliceous or alumino-siliceous material that chemically reacts in finely divided form and in the presence of moisture with the calcium hydroxide released by the hydration of Portland cement to form calcium silicate hydrate (CSH) and other cementitious compounds. Pozzolans and slags are generally categorized as supplementary cementitious materials (SCMs) or mineral admixtures (PCA, 2011). The most common natural pozzolans used today are processed materials, heat-treated in a kiln before they are ground to a fine powder; they include calcined clay, calcined shale, and MK. MK, a special calcined clay, is produced by the calcination of high purity kaolin clay at low temperatures. The product is ground to an average particle size of 1 to 2 mm (PCA, 2011).

Concrete mixtures including supplementary cementitious materials are generally defined as binary or ternary replacement mixtures. Binary replacement mixtures are defined as Portland cement and one supplementary cementitious material. Ternary mixtures are defined as Portland cement and two other supplementary cementitious materials, or blended cement and one other supplementary cementitious material.

When MK is used as a partial cement replacement, improved performance has been observed, as characterized by increased strength and reduced permeability, for instance (Marikunte & Phelps, 2012). Marikunte and Phelps (2012) statistically demonstrated that replacing cement with MK contributes more to concrete achieving high performance than reducing water content. San Nicolas et al. (2014) concluded that MK substitution (25% by weight) improves the durability of concrete. Ferreira et al. (2015) reported improved strength, durability properties, and chloride penetration resistance for concrete with MK. When MK is used as a cement replacement with Class F fly ash (hereafter referred to as 'fly ash' in the text and 'FA' in mixture notations), Khatib et al. (2009) found reduced concrete shrinkage. In addition, Lagier and Kurtis (2007) found that MK use accelerated the hydration process as a result of its higher surface area, though Brykov et al. (2015) reported that this acceleration depends on MK dosage. Due to the enhanced durability of highly reactive MK, the material is widely used for concrete overlay designs by Illinois, Iowa, and several other state departments of transportation (DOTs). Altogether, research has documented the following advantages of using MK as a partial cement replacement:

- Increased compressive and flexural strengths
- Increased resistance to chemical attack and durability
- Enhanced workability
- Improved color by lightening the color of concrete
- Reduced effects of alkali-silica reactivity (ASR)
- Reduced permeability and shrinkage
- Reduced potential for efflorescence

When the authors commenced this study in 2015, a brief review of how DOTs specify and/or use MK was conducted from publicly available DOT websites. Most DOTs refer to the chemical requirements of either the American Society for Testing and Materials (ASTM) C168 or American Association of State and Highway Transportation Officials (AASHTO) M321 for MK for use in hydraulic cement. The Illinois DOT shared a special provision for ASR mitigation requirements where the average alkali content ($Na_2O + 0.658\ K_2O$) of high reactivity MK must be less than 1.0%. In addition, the content of silicon dioxide (SiO_2), aluminum oxide (Al_2O_3), and iron oxide (Fe_2O_3) must exceed 80%. Meanwhile, the Texas DOT shared an 85% requirement for the same chemical composition (DMS-4635, 2014). For sulfate resistance, the Colorado DOT required high reactivity pozzolan mixtures to have less than 0.10% expansion at 18 months when tested according to ASTM C 1012; Class 2 concrete required less than 0.05% expansion within 6 months. The Minnesota DOT limited MK to 10% of Portland cement by weight, whereas the use of fly ash and slag was limited to 20% of Portland cement by weight. The Missouri DOT approved a maximum of 15% replacement of Portland cement on a pound for pound basis in all concrete. The California DOT recommended MK to be used in dosages ranging from 5%–10% by mass of the cementitious material. The Montana DOT allowed up to 20% replacement by weight of the total cementitious material. Ramezanianpour & Jovein (2012) recommended optimum replacement of MK between 12.5% and 10% at water-to-cement ratios of 0.4 and 0.35, respectively. In Nebraska, the maximum pozzolanic content should not exceed 15–25% of the total cementitious material. Wisconsin required MK suppliers to be included on the DOT's approved product list and have a quality management program in place with daily testing performed to determine uniformity. A previous investigation of

this study (see Chorzepa et al., 2017) and Chapter 3 of this dissertation provide a more detailed and recent literature review.

The Georgia Department of Transportation's (GDOT's) current specification for mass concrete (Special Provision to Section 500 (Concrete Structures) - Standard Specifications), hereafter referred to as "Special Provision" includes a maximum allowable internal temperature of 158 °F (70 °C) and a temperature differential of 35 °F (19.4 °C) between interior and exterior portions of the designated mass concrete element. The Special Provision also specifies that slag, fly ash, and a combination of different pozzolans may comprise no more than 75%, 40%, and 75% by mass of total cementitious and pozzolanic materials, respectively.

With a shortage of fly ash and imported slag in the state, SCMs such as MK are considered to control the heat of hydration (HoH) despite some disagreement in the literature on the effect of microsilica (or MK) on HoH. While in a previous study by (Meland, 1983), the replacement of cement by 10% and 20% microsilica slightly reduced early HoH, other studies (Alshamsi, 1997) showed an increase in HoH. This research highlights how the physical characteristics and chemical composition of MK influence its ability to affect HoH. Alshamsi (1997) limited cement replacement to 10%, and the chemical composition of MK at that time differed from what is available in today's market. Accordingly, it is necessary to evaluate currently available MK products to reduce HoH in mass concrete elements. In a recent study, increased MK replacement from 10% to 14% minimized the total heat evolved, although 10% was found optimal when also considering mechanical properties (Jiang et al., 2015).

An extensive survey of state DOTs' specifications and other available resources is necessary to fully understand current practices and challenges in relation to the usage of MK and other SCMs as partial replacements for cement. It is also important to determine whether and how MK should be specified.

1.2 Problem Statement

Fly ash is an important SCM used in mitigating deleterious cracking from large thermal gradients in mass concrete. However, the coal market may not be able to sustain the current volume of fly ash used in U.S. concrete structures. The Mid-Atlantic region has experienced a fly ash shortage, which in turn may impact cement concrete producers and thus construction material costs for GDOT projects. Thus, evaluating alternative SCMs is critical to maintain the market habits of the ready-mix industry. MK is a locally available option for Georgia, and several state DOTs have already adopted and specified commercial MKs for use in concrete. Even though Georgia is a world-leading kaolin producer, the use of MK has yet to be addressed in GDOT's standard specifications.

The United States Geological Survey (USGS) estimates that nearly 8.5 million metric tons of kaolin are mined from Georgia each year (USGS, 2013). Kaolin has many existing applications: ceramics, toothpaste, paint, cosmetics, and others. According to the Georgia Mining Association, the kaolin industry in Georgia employs over 4,400 Georgians, which amounts to over $232 million in pay and benefits (Georgia Mining Association, 2016). Unlike secondary materials such as fly ash, silica fume, and slag, MK is not the byproduct of another process.

Mass concrete placements demand considerable control of temperature rise due to the HoH of cementitious materials. Typical temperature rise in concrete mixtures ranges

between 80 °F (44.4 °C) and 100 °F (55.6 °C). The ACI recommends a placement temperature of 58 °F (14.4 °C) for 100 °F (55.6 °C) temperature rise concrete; however, this temperature requirement proves to be particularly challenging in Georgia. Generally, the temperature rise at concrete placements can be reduced to 70 °F (38.9 °C) with a large percentage of Portland cement replaced with fly ash or slag. However, there has been a shortage of fly ash and slag, so these materials have been replaced with alternative binder systems to allow reductions in temperature for mass concrete construction (e.g., large columns and foundations for bridges and other transportation structures).

Cement hydration produces an internal temperature rise; meanwhile, the outer concrete surface cools faster than the section core. Through thermal expansion/contraction, the temperature differential induces thermal stresses at the surface. Once the maximum interior temperature exceeds the accepted threshold value, delayed ettringite formation (DEF) can occur in mass concrete elements. Accordingly, DEF can be prevented by limiting the internal temperature of concrete from the outset. The maximum temperature suggested by prior research to prevent DEF in concrete elements is 160 °F (71.1 °C). This reduced temperature threshold can be achieved by specifying allowable initial temperatures, limiting cement content, or using low heat SCMs.

Currently, GDOT specifications do not explicitly specify the cement replacement limit on Class N pozzolan in concrete. With the availability of kaolin in middle Georgia, GDOT can take advantage of this material to decrease the demand for cement and fly ash as well as improve the overall properties of concrete mixtures. Furthermore, GDOT can control the maximum internal temperature and the temperature differential in mass concrete elements by incorporating SCMs such as MK and/or slag.

1.3 Research Objectives

This study aims to find natural, lightly processed, and economical alternatives to fly ash that perform similarly with regard to pozzolanic reactivity and provide comparable compressive strength, workability, drying shrinkage, thermal expansion properties, and resistance to ASR, sulfate attack, and chloride-ion penetration. Accordingly, this study investigates ternary replacement mixtures involving a combination of slag and MK products. As a pozzolan, MK would improve concrete performance through decreased permeability, improved strength and durability, and reduced shrinkage.

The study identifies the appropriate limits of MK to be used in mixtures and describes subsequent concrete performance. Appropriate usage of MK in both binary and ternary concrete mixtures will be discussed, along with preliminary specifications for its usage in GDOT mass concrete structures. Current GDOT specifications for mass concrete (Special Provision to Section 500) will be reviewed, and changes will be recommended based on the findings of this study.

1.4 Research Significance and Scope

The primary benefit of this study is to identify reasons for adopting Class N pozzolan MK as a viable option for inclusion in concrete specifications. This project will provide appropriate supporting information for its acceptance or rejection. Furthermore, the benefits of using commercially available slag products are investigated. If MK and/or slag are deemed acceptable, GDOT would have access to viable SCMs local to Georgia.

This study focuses on reducing the heat of hydration by means of cement replacement materials without relying on active cooling systems.

1.5 Research Methodology

To accomplish the aforementioned objectives, experimental and analytical methods are deployed in five specific tasks. These are outlined below.

1.5.1 Task 1. Perform Extensive Literature Review

A thorough review of specifications developed by other state DOTs is conducted to provide insight into current issues, practices, and challenges pertaining to MK (and/or slag) usage or in mass concrete mixtures.

1.5.2 Task 2. Design, Batch, and Test Concrete Mixtures with Three Metakaolin Products

This task includes designing, batching, and testing concrete mixtures with cement replacements of MK while evaluating the replacement threshold limit to satisfy the current performance requirements outlined in GDOT Section 430 – Concrete Pavement (Classes 1 and 2) and Section 500 Concrete Structures (Classes AAA, AA1, AA, A, B, and CS). Three locally sourced MK products, along with two slag products, are studied. Task 2 results are presented in Chapter 2.

1.5.3 Task 3. Design, Construct, and Quantify Temperature Rise in Mass Concrete

Results from this task are presented in Chapter 3. The following subsections provide a summary of Task 3.

1.5.3.1 Task 3.1 - Design test procedures for mass concrete mixtures

A test matrix consisting of different combinations of MK and other SCMs (e.g., slag) is developed to quantify temperature rise from the heat of cement hydration. Figure 6 illustrates the test layout and specimen size used for a similar study conducted by the CTL

Group (Gajda et al., 2014). Gajda et al. (2014) found the heat generated from cement hydration was rapidly dissipated even though 6-inch (15.24 mm)-thick insulation panels were employed. Accordingly, a more efficient insulation material is selected in this study, and the specimen size is reduced from a 3 foot x 3 foot x 3 foot (0.91 m x 0.91 m x 0.91 m) cube specimen to a 2 foot x 2 foot x 2 foot (0.61 m x 0.61 m x 0.61 m) cube specimen.

Figure 6 – Test layout for concrete cube placement (Gadja et al., 2014).

1.5.3.2 Task 3.2 – Construct cube molds and specimens

Cube molds are constructed with the 6-inch-thick (152.40 mm) Kingspan Kooltherm K20 Concrete Sandwich Board insulation panels shown in Figure 7. On all six sides of the cube specimen, these insulation panels are sandwiched between a 1-inch-thick (25.4 mm) plywood sheet and a stainless steel liner. A detailed procedure is presented in Chapter 3.

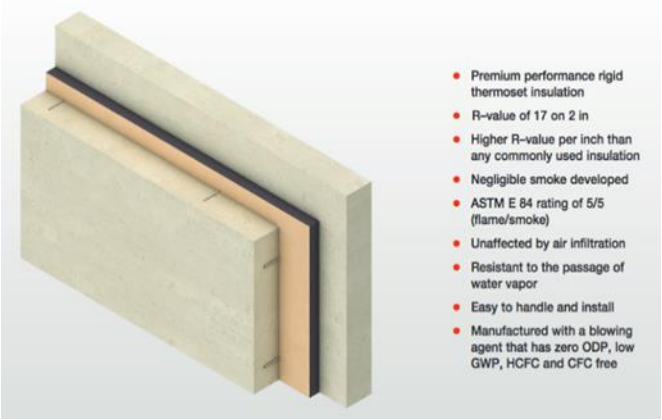

Figure 7 – Kingspan Kooltherm K20 Insulation (Kingspan USA, 2019)**.**

1.5.3.3 Task 3.3 – Internal temperature monitoring in test specimens

Concrete mixtures are placed in the mold constructed from Task 3.2. Temperature rise over time is monitored for each specimen using thermocouples for 14 days.

1.5.4 **Task 4. Evaluation of Maximum Temperature Limits**

Results from this task are presented in Chapter 4. The following subsections provide a summary of Task 4.

1.5.4.1 Task 4.1 – Thermal and structural modeling

A Finite Element Analysis (FEA) of a mass concrete structure is completed using the DIsplacement ANAlyser FEA software (DIANA FEA, Version 10.2). A transient thermal analysis and a nonlinear structural analysis (i.e., a coupled thermal-stress analysis) are performed by simulating the placement and boundary conditions of the mass concrete specimens from Task 3. The FEA model is validated using the experimental results from Task 3, as well as an experimental study conducted by others (Jung et al.'s (2017)).

1.5.4.2 Task 4.2 – Design and construct test specimens

Task 3 determines the maximum internal temperature of insulated cube specimens. In addition to the maximum allowable internal temperature, the maximum allowable temperature differential, ΔT, is needed to assess the extent of temperature-induced cracking in mass concrete. To identify a practical range of allowable temperature differentials and quantify tensile strains in mass concrete, concrete cylinders exposed to elevated temperatures are evaluated.

The following two temperature threshold scenarios are initially considered for implementation in GDOT's mass concrete specification (see Table 1):

1) Maximum allowable internal temperature of 158 °F (70 °C) & maximum temperature differential of 50 °F (27.8 °C), yielding the total temperature of 208 °F (97.8 °C).
2) Maximum allowable internal temperature of 170 °F (76.7 °C) & maximum temperature differential of 35 °F (19.4 °C) (if deemed feasible), reaching the total temperature of 205 °F (96.1 °C).

Table 1 – Maximum allowable internal and differential temperature limits.

Temperature Limits	
Maximum Allowable Temperature, °F (°C)	Maximum Temperature Differential, °F (°C)
158 (70)	50 (27.8)
170 (76.7)	35 (19.4)

1.5.4.3 Task 4.3 – Evaluation of temperature limits

This task includes a coupled thermal-structural analysis of mass concrete structures with varying placement configurations. The following placement configurations are evaluated:

1) 5-foot (1.5 m)-thick foundation,
2) 8-foot (2.4 m)-diameter column, and
3) 43.25 foot x 19.5 foot x 22.25 foot (13.2 m x 5.9 m x 6.9 m) seal (with rebar/steel cage in the middle).

The following two variables are considered to evaluate maximum temperatures and study the extent of cracking in mass concrete structures, and the results are presented in Chapter 5:

1) Varying surface temperature conditions (e.g., Georgia's winter/summer temperatures) and environmental conditions

2) Varying volume-to-surface area (V/A) ratios of mass concrete elements (e.g., concrete seals, foundation structures, and large columns)

1.5.5 Task 5. Data Analysis and Synthesis of Findings

The results, based on observations, previous studies, and data collected from laboratory testing, are analyzed to recommend whether and how to specify MK for GDOT. Further, allowable temperatures for maximum internal temperature and temperature differential are reviewed for implementation in the mass concrete provision.

1.6 Implementation

Appendices A and B present recommendations to the existing Special Provision to Section 500. Based on findings from this study, the following outcomes are provided:

1) Identification of appropriate limits of MK for implementation in GDOT specifications
2) Identification of the maximum allowable internal temperature and temperature differential for concrete mixtures incorporating SCMs such as fly ash, slag, and MK for implementation in GDOT specifications
3) Recommended changes to the Special Provision to Section 500 – Concrete Structures (GDOT, 2013)

1.7 Organization of the Dissertation

This dissertation is divided into seven chapters that describe test procedures for binary and ternary cement replacement mixtures and present results from these tests, which include

1) An experimental investigation of HoH and temperature rise in various mixtures,
2) An analytical investigation of mass concrete specimens and a bridge foundation seal, and

3) A sensitivity analysis of maximum temperatures and temperature differentials by varying V/A ratios and mixture designs.

Chapter 1 presents a general background on the thermal design of concrete structures and the use of SCMs, specifically MK and slag. Additionally, research objectives and significance are described.

Chapter 2 describes an experimental investigation of concrete mixtures containing various SCMs: MK, slag, and fly ash products. This chapter offers insight into the effect of different SCMs and replacement levels on HoH, mechanical properties, durability, and dimensional stability. This is a continuation of work performed by Chorzepa et al. (2017).

Chapter 3 presents an experimental investigation designed to measure HoH and temperature in mass concrete specimens. These specimens contain varying amounts of SCMs with various cement replacement levels. This chapter also provides a literature review on mass concrete specifications and other standard specifications across the state DOTs.

Chapter 4 outlines an analytical investigation of mass concrete structures using the Finite Element Analysis (FEA) method. Findings from existing research validate this simulation procedure. Finally, a case study involving a bridge seal structure is presented.

Chapter 5 presents a sensitivity analysis that considers the effects of different parameters (e.g., V/A ratios, mixtures designs, and placement conditions) on the maximum temperature and temperature differential of mass concrete structures.

Chapter 6 synthesizes the findings and presents the conclusions of this project. Chapter 7 provides recommendations.

Finally, Appendices A and B outline recommended changes to GDOT's current mass concrete special provision, Appendix C provides additional supplementary recommendations from the state DOTs, Appendix D presents the thermal analysis of a bridge seal with a rectangular column, Appendix E gives additional validation of strain from gradient temperature, and Appendix F presents detailed procedures for testing methodology and selecting suitable mixtures for mass concrete placements.

CHAPTER 2

COMPARISON OF BINARY AND TERNARY MIXTURES

A portion of this chapter was presented as part of the previous study (see Chorzepa et al., 2017). However, this study includes additional binary and ternary replacement mixtures. Results from both the previous study and this study are presented herein in order to synthesize results. Section 2.1 presents mixture designs based on the HoH of cementitious materials, and it is a portion of a study performed by Hamid et al. (2018). In Section 2.2, mechanical and durability properties of 19 selected mixtures are presented.

2.1 Preliminary Investigation into Heat of Cementitious Material Hydration

As a preliminary investigation, the HoH performance of selected binary and ternary replacement mixtures involving different SCMs is studied. Detailed HoH tests on all the mixtures are presented in Section 3.2.

2.1.1 Experimental Design

Eight mortar mixtures are prepared for the HoH test using the isothermal calorimeter shown in Figure 8. The mixtures consist of a Control mixture, a MK binary replacement mixture (15% MK), two slag binary replacement mixtures (30% and 45% slag), a fly ash binary replacement mixture (45% FA), and three ternary replacement mixtures including slag and MK for a total of 45% cement replacement. Replacement levels and mixture designations are shown in Table 2.

Table 2 – Mixtures used for HoH testing.

Percent Cement Replacement (%)	Mixtures
15	MK-15
30	SL-30
45	SL-45
	FA-45
	SL-40+MK-5
	SL-35+MK-10
	SL-30+MK-15

The external mixing method per ASTM C1702 (ASTM C1702, 2017) is used to prepare isothermal calorimetry specimens (120 mL or 4 oz.) for HoH testing. In this study, mortar specimens are prepared from large (4 cubic feet or 0.11 cubic meter) batch concrete mixtures by screening out the coarse/fine aggregate using a No. 5 sieve. This procedure is consistent with the ASTM procedure. In this method, the temperature of the calorimeter is maintained constant at 73.4 °F (23 °C), and data (e.g., power and energy output of the samples) is collected for seven days.

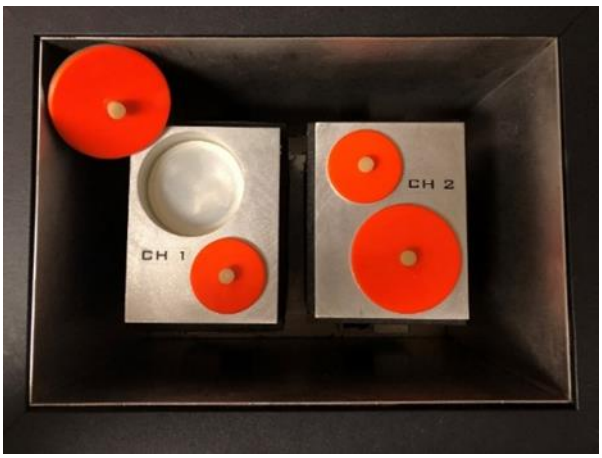

Figure 8 – Isothermal calorimeter used for HoH testing.

2.1.2 **Results**

HoH results are presented as well as the percentage reduction or increase in HoH in all binary and ternary mixtures, relative to the Control mixture, at 1, 3, and 7 day(s) of hydration. Table 3 presents a summary of the findings.

Table 3 – Percent reduction in HoH in binary and ternary mixtures.

Percent cement replacement (%)	Mixtures	% Reduction in HoH relative to the Control specimen		
		1 day (%)	3 day (%)	7 day (%)
15	MK-15	-9	-3	5
30	SL-30	-22	-13	-2
45	SL-45	-28	-18	-8
	FA-45	-42	-36	-32
	SL40+MK5	-30	-16	-7
	SL35+MK10	-26	-16	-8
	SL30+MK15	-36	-20	-13

2.1.2.1 Heat of hydration in binary mixtures including metakaolin

Figure 9 presents the thermal power per gram of cementitious materials for the MK binary replacement mixture. The rate of heat generation in the MK mixture is similar to the Control mixture while the amplitude of thermal power is reduced by about 4% in the MK mixture. Figure 10 presents HoH results for the MK mixture. Compared to the Control mixture, HoH at 1 and 3 days are reduced by 9% and 3%, respectively, in the MK15 mixture. The HoH for the MK-15 mixture is comparable to that of the Control mixture by 84 hours and exceeds it by 5% at 7 days. This corresponds with results found in the literature (Maia et al., 2011; Snelson et al., 2008).

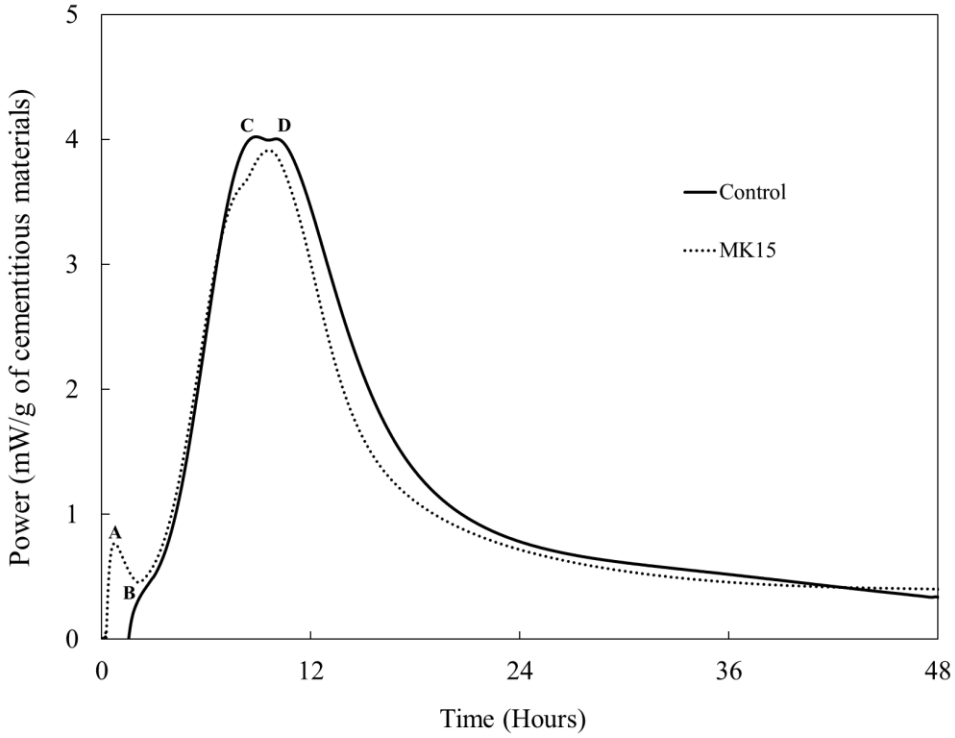

Figure 9 – Rate of heat flow in the Control and MK mixtures.

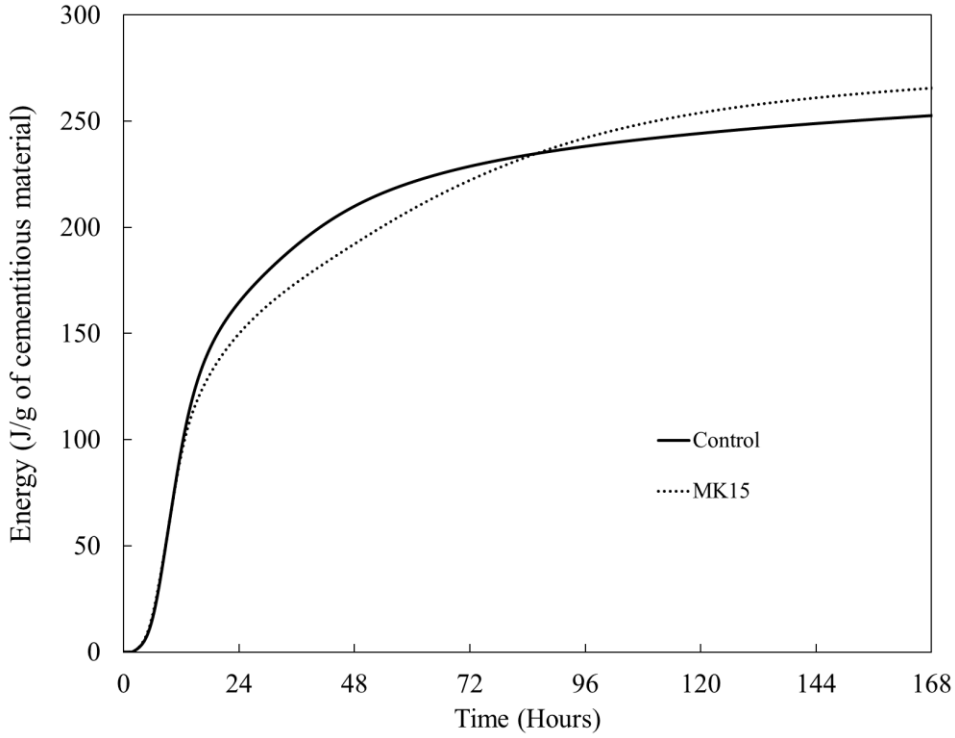

Figure 10 – HoH in the Control and MK mixtures.

The rate of heat flow from Figure 9 shows a negative value in the early age hydration of the Control mixture. This negative-valued endotherm results from early (<2 hrs.) temperature acclimation of the specimen and do not affect the main hydration peak. The hydration process of the mixtures is divided into stages as determined by letters A through D. Point A represents initial thermal power, which is caused by the rapid dissolution and initial hydration of the aluminate phase. Point B represents a dormant period associated with very low thermal power, indicating slow and well-controlled hydration (ASTM C1679-17, 2017). Point C represents the main hydration peak in the acceleration period, mainly attributed to the silicate reaction and initiation of the strength-generating alite or silicate hydration. Point D represents the accelerated calcium aluminate activity attributed to the second C_3A dissolution; this activity results from the high exothermic dissolution of aluminate and continued formation of ettringite (Berodier, 2015; Gallucci et al., 2010; ASTM C1679-17, 2017). In the Control mixture, the magnitude of point D is comparable to point C. However, in the MK binary mixture, point D is located much higher than point C on the y-axis. A similar trend is observed in the ternary and other binary mixtures, which are presented in the next section (Section 2.1.2.2). This is due to the pozzolanic reaction between calcium hydroxide (CH) and SCMs (Berodier, 2015; Wu et al., 1983).

2.1.2.2 Heat of hydration of ternary and other binary replacement mixtures

Figure 11 presents the thermal power for the ternary and alternate SCM binary mixtures. Figure 12, meanwhile, portrays the HoH for the ternary and alternate SCM binary mixtures over seven days. The 45% fly ash replacement mixture has a very slow rate of HoH and significantly reduces the heat energy by 42%, 36%, and 32% at 1, 3, and 7 days of

hydration, respectively. The HoH of the SL-30 mixture is lower than the Control mixture at all ages, but it is higher than the FA-45 mixture. The SL-30 mixture reduces the 1-, 3-, and 7-day HoH by 22%, 13%, and 2%, respectively. This result aligns with previous findings (Arora, Sant, & Neithalath, 2016; Boháč et al., 2014; Pane & Hansen, 2005), in which the 3- and 7-day HoH were reduced by approximately 15% and 3%, respectively, when 20–55% of cement was replaced by slag. The rate of heat generation is reduced in the binary slag mixtures, and this reduction is even more evident in the ternary SL-30+MK-15 mixture. A significant reduction in the rate of heat generation and total cumulative HoH is observed in this ternary mixture up to seven days. The 1-, 3-, and 7-day HoH are reduced by approximately 35%, 20%, and 13%, respectively, in the ternary mixture relative to the Control mixture.

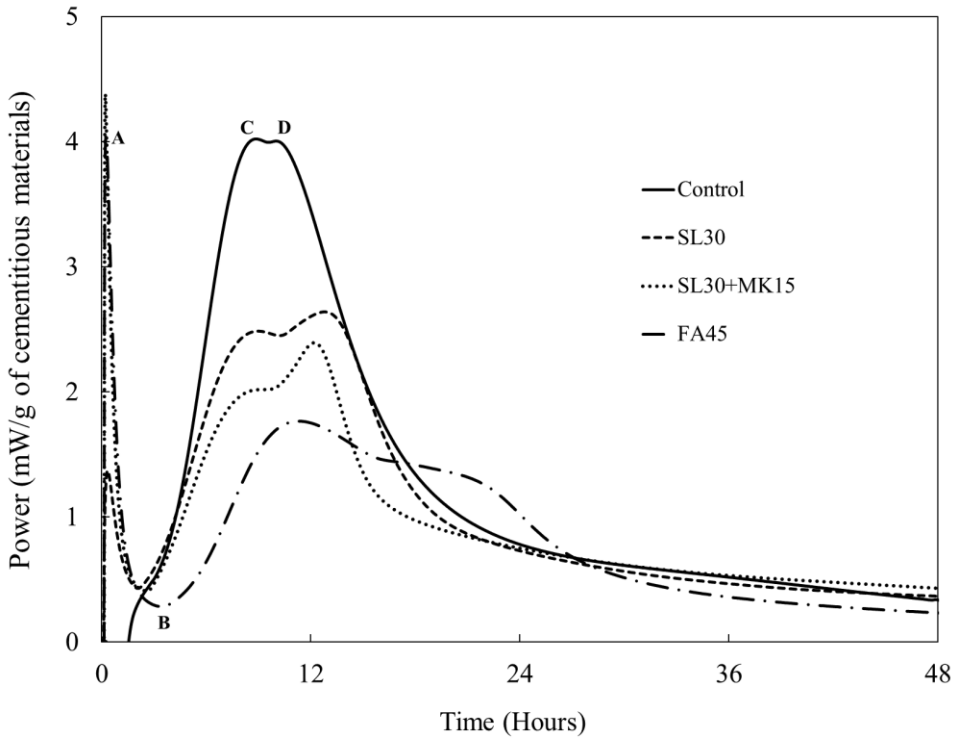

Figure 11 – Thermal power of the ternary and alternate binary mixtures.

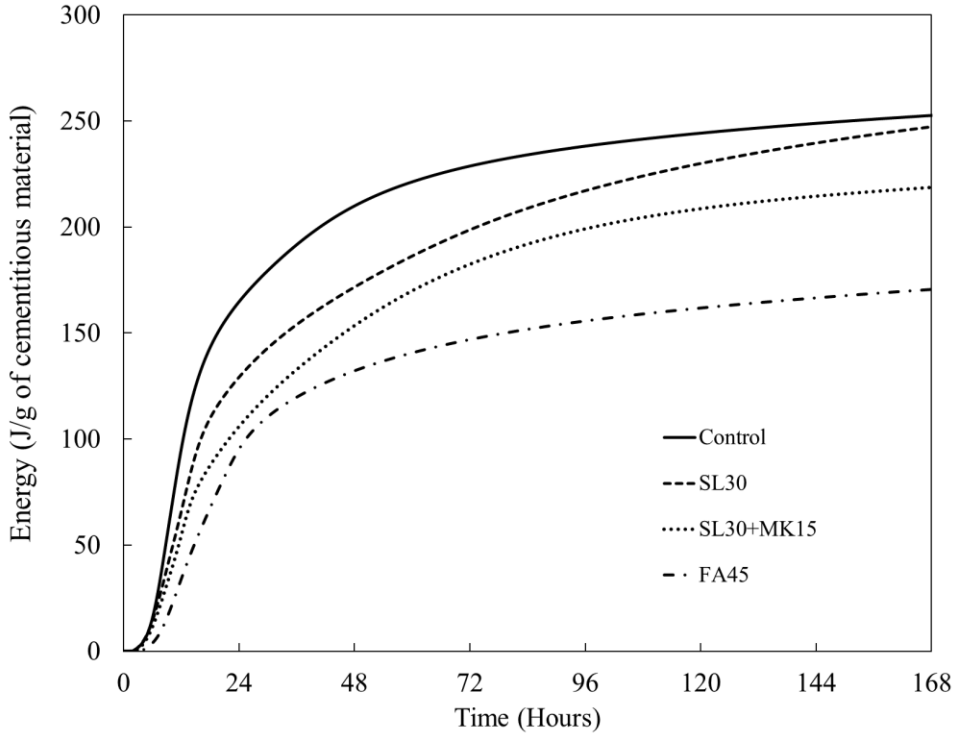

Figure 12 – HoH of the ternary and alternate binary mixtures.

2.1.2.3 Heat of hydration of ternary mixtures with various percentages of slag and metakaolin

Figure 13 and Figure 14 show the effect of ternary replacement mixtures containing various amounts of slag and MK on thermal power and HoH. Among the mixtures, SL-30+MK-15 offers the most reduction in heat energy, and this reduction is lower than that of the SL-45 mixture. Table 3 presents the percent reduction in HoH in all mixtures over the Control mixture.

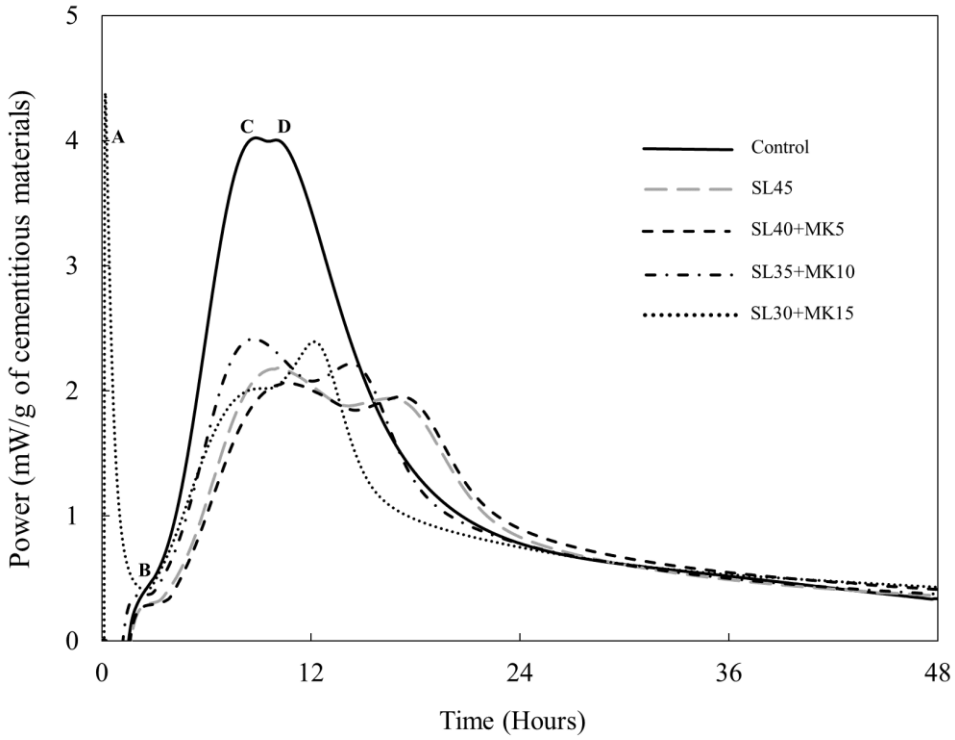

Figure 13 – Thermal power of ternary mixtures with various percentages of slag and MK.

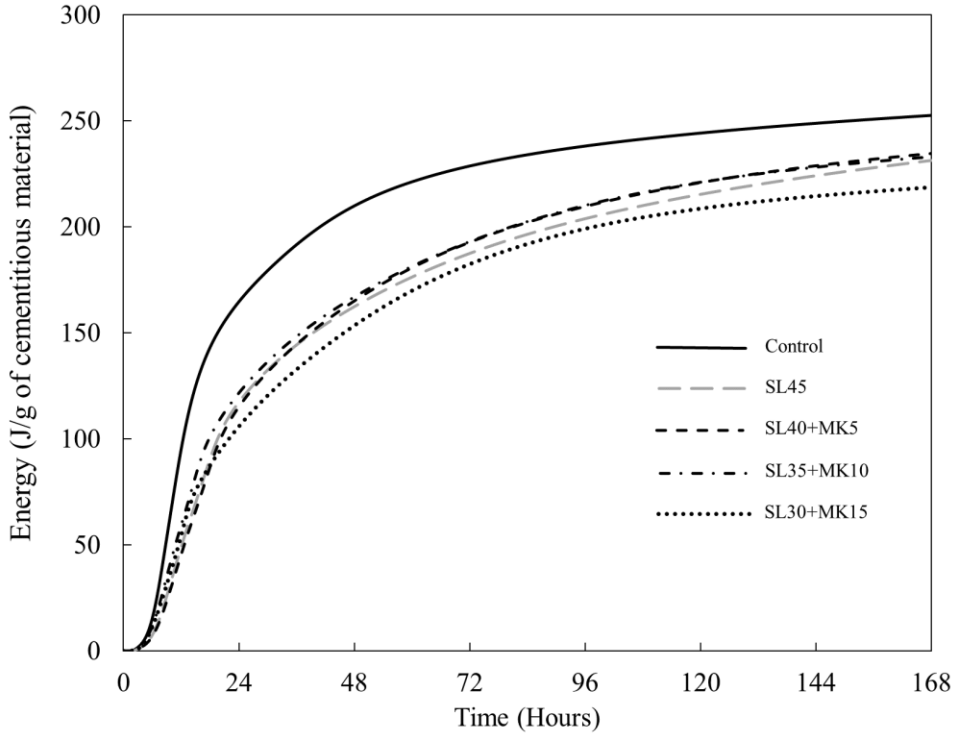

Figure 14 – HoH of ternary mixtures with various percentages of slag and MK.

Table 3 Repeated – Percent reduction in HoH in binary and ternary mixtures.

Percent cement replacement (%)	Mixtures	Percent reduction in HoH relative to the Control specimen		
		1 day (%)	3 day (%)	7 day (%)
15	MK-15	-9	-3	5
30	SL-30	-22	-13	-2
45	SL-45	-28	-18	-8
	FA-45	-42	-36	-32
	SL-40+MK-5	-30	-16	-7
	SL-35+MK-10	-26	-16	-8
	SL-30+MK-15	-36	-20	-13

This study employs 45% cement replacement mixtures. The optimal replacement composition of a ternary mixture is determined by studying HoH in the following mixtures: SL-45, SL-30+MK-15, SL-35+MK-10, and SL-40+MK-5. It was anticipated that SL-45 would result in the lowest HoH since other mixtures contain MK, which affords a greater capacity for pozzolanic activity than slag (Mindess et al., 2003). Contrary to this expectation, the SL-30+MK-15 mixture leads to the lowest HoH as shown in Figure 14. Table 3 shows that the ternary replacement mixture of SL-30+MK-15 comes in second to the FA-45 mixture in reducing HoH among all the mixtures. These results illustrate that the optimum ratio of pozzolans used in ternary replacement mixtures is 2SL:1MK when a 45% ternary replacement is considered.

2.1.3 **Analysis of Results**

2.1.3.1 Effect of metakaolin binary mixture on heat of hydration

The partial replacement of cement with 15% MK in the binary mixture results in no significant change in HoH. The heat of cement hydration is initially reduced by removing 15% of the Portland cement by weight; however, the pozzolanic reaction takes place after about two days and adds to the total heat generated.

2.1.3.2 Effect of binary mixtures containing fly ash and slag on heat of hydration

The slow rate of heat generation in the fly ash mixture is attributed to the relatively low specific surface area and the low solubility of the alumino-silicate glass in the alkaline environment of the Portland cement hydration (Snelson et al., 2008). The slag mixture has a higher calcium oxide (CaO) content compared to the fly ash mixture, which may in turn result in a corresponding increase in heat generation.

2.1.3.3 Effect of ternary mixtures on heat of hydration

In this study, SL-30+MK-15 reduces the 1-, 3-, and 7-day HoH by 36%, 20%, and 13%, respectively, compared to those of the Control mixture. These results align with a previous study by Boháč et al. (2014), where the 3-day HoH was reduced by about 60% in a SL-30+MK-5 mixture. In the same study by Boháč et al., however, a SL-40+MK-15 mixture unexpectedly increased the 3-day HoH by 27% from that of the SL-30+MK-5 mixture despite the increase in cement replacement from 35% to 55%. For Boháč et al. (2014), the percentage of SiO_2 and Al_2O_3 in MK was 57.3% and 38.6%, respectively, whereas in this study, MK contains 50.8% SiO_2 and 45.9% Al_2O_3. Thus, additional alumina content may confer different heat releases.

The ternary mixtures include aluminate, possibly a sufficient amount for the formation of calcium aluminate sulfate (AFt or ettringite). When pozzolans contain aluminate, AFt phases can form during the pozzolanic reaction. Moreover, the ternary mixtures also have a high level of silicate which results in the formation of additional C-S-H. Aluminate hydration reacts with CSH and releases calcium carbonate, which is known to convert AFt phases to monocarbonate. Boháč et al. (2014) indicate that little to no AFt is found in ternary mixtures including slag and MK, whereas it was found in binary mixtures with MK. The presence of water-rich AFt increases the total volume of hydration products, and thus the total amount of heat is relatively lower in ternary mixtures due to the absence of AFt. At the same time, combined alumina and silica content appears to affect the total amount of heat.

Based on the findings presented in this section, the presence of two pozzolanic materials with high contents of alumina and silica in ternary replacement mixtures results in reduced heat release, as well as adequate strength development as discussed in Section 2.2. Table 4 provides the ratios of calcium to alumina (Ca/Al), calcium to silica (Ca/Si), and calcium to alumina and silica (Ca/(Al+Si)) for the ternary and binary mixtures consisting of fly ash or slag at 45% replacement level. In the context of the findings discussed above, this table illustrates that the amount of heat is proportional to the Ca/(Al+Si) ratio.

Table 4 – Oxide ratios for select 45% replacements.

Mixtures	Ca/AL	Ca/Si	Ca/(AL+Si)
Control	13.5	3.2	2.6
SL-45	6.2	2.1	1.6
FA-45	3.1	1.1	0.8
SL-40+MK-5	5.0	1.9	1.4
SL-35+MK-10	4.1	1.8	1.3
SL-30+MK-15	3.49	1.7	1.1

2.1.4 Estimating the Heat Generated from Pozzolanic Materials

In order to isolate heat released from pozzolanic reactions, heat released solely from cement hydration in each binary and ternary mixture is estimated by linearly extrapolating the HoH obtained from the Control mixture as shown in Figure 15. Heat generated from the pozzolanic reaction in each mixture is then estimated by deducting heat released from cement hydration, as shown in Figure 15, from the total HoH of each mixture shown in Figure 10, Figure 12, and Figure 14. The same approach for separating the HoH of slag from that of Portland cement in blended mixtures is used by Gruyaert et al. (2010) and Meinhard & Lackner (2008). Figure 16 shows the estimated heat released solely from the presence of pozzolanic materials in each mixture. The shape and slope of the curves indicate the pozzolanic reaction's rate. Here, though, a comparison should only be made between mixtures of the same cement replacement levels. For instance, a fair comparison is made between the 45% replacement mixtures, SL-45 and SL-30+MK-15.

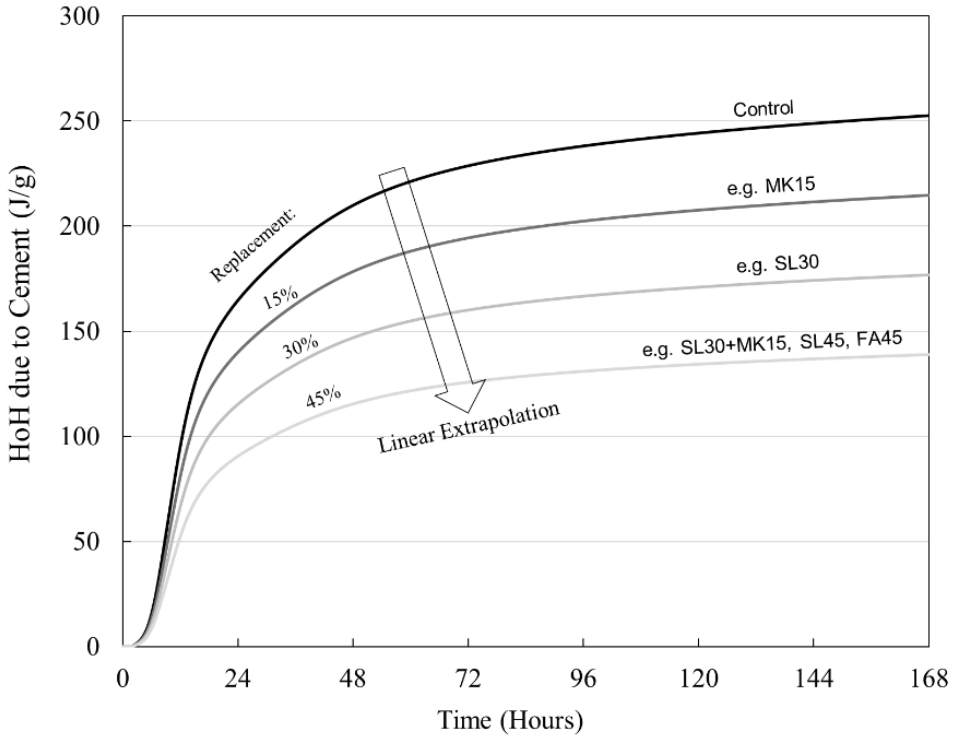

Figure 15 – Linear extrapolation of HoH for the Control mixture.

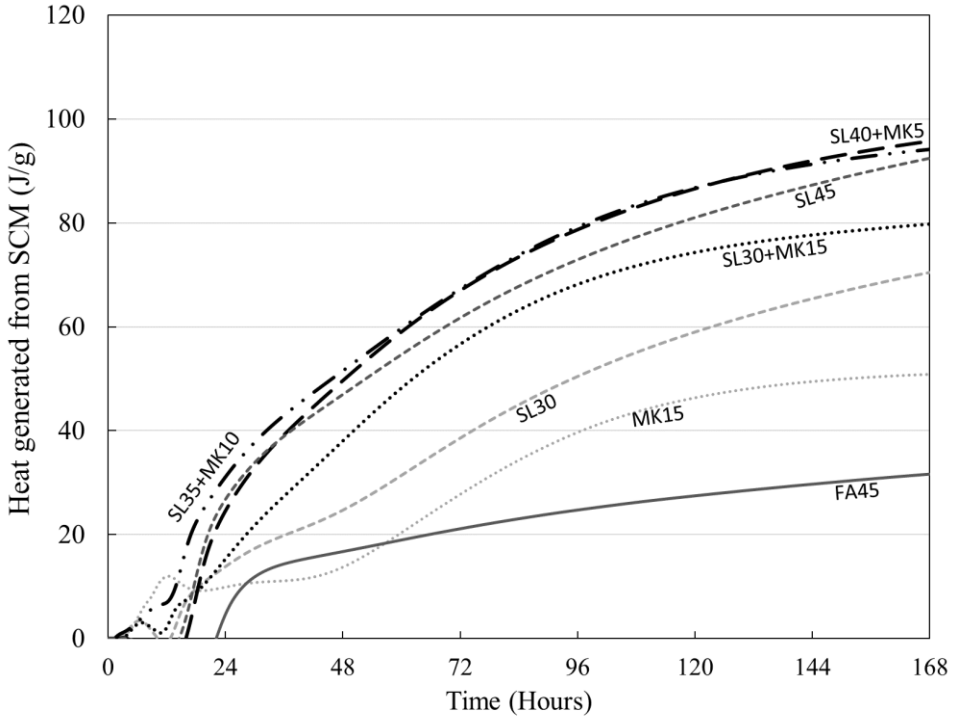

Figure 16 – HoH generated from the pozzolanic reaction.

2.1.4.1 Estimated heat of hydration in binary mixtures including metakaolin

Figure 16 shows that the pozzolanic reaction of the binary mixture MK-15 starts after two days and mainly occurs between two and five days. The heat release rate is initially high in the MK mixture. This may be attributed to the chemical composition of MK, which is high alumina content accelerates the pozzolanic reaction (Curcio et al., 1998). In the MK-15 mixture, the heat released reaches a plateau at seven days, indicating that the initial CH produced from cement hydration has been mostly depleted within a week (Mindess et al., 2003). This heat generation rate in the MK mixture is consistent with its compressive strength development, as shown in Section 2.2.2.1. In the MK-15 mixture, the rate of strength development is highest between one and seven days.

2.1.4.2 Estimated heat of hydration in ternary and alternate binary mixtures

Among the 45%-replacement-level mixtures, SL-35+MK-10 and SL-40+MK-5 have the highest rate of pozzolanic reaction followed by the SL-45 mixture. The ternary replacement SL-30+MK-15 mixture shows a lower pozzolanic reaction than the SL-45 mixture. On the other hand, the FA-45 mixture shows a very slow heat release rate (or pozzolanic reaction over time). This is consistent with the compressive strength development of this mixture, which occurs very slowly over time. The degree of crystallization of the SCM is directly related to the SCM/lime reactivity. MK exhibits a low degree of crystallization that leads to a high reactivity with lime; fly ash, meanwhile, has a higher degree of crystallization, so it requires a longer reaction time.

The amount of heat in SL-30+MK-15 is reduced by 13% over the amount in the Control mixture within a week. This reduction in HoH may be attributed to the limited amount of CH formed in the ternary mixtures. That is, two pozzolanic materials may

compete for CH. In turn, this deprivation may result in a relatively slow rate of HoH and a reduction in the total cumulative amount of heat released. The reduction in HoH is not fully explained by the CH content alone but appears to be correlated with the Ca/(Al+Si) ratio.

2.2 Mechanical Properties and Durability Results

Based on the results from Section 2.1 and the optimal MK replacement level determined from the previous study (Chorzepa et al., 2017), a total of 19 mixtures are studied. Proportions for these mixtures appear in Chorzepa et al. (2017).

Three MK (designated as '1', '2', and '3') and two slag (designated as 'a' and 'b') products are evaluated. MK1 is sourced from Sandersville, Georgia; MK2 is sourced from Aiken, South Carolina; and, MK3 is sourced from Sandersville, Georgia. All MK products used in this study are high-reactivity MKs that conform to ASTM C 618. The consensus within the literature is that a high-reactivity MK contains $SiO_2 + Al_2O_3 + Fe_2O_3 \geq 90\%$ by weight. A review of the physical and chemical characteristics of the MKs used in this study can be found in Chorzepa et al. (2017).

Two Grade 120, commercially available slag products were used in this study. The chemical composition and physical characteristics of these can also be found in Section 3.2.2. Table 5 presents a summary of findings from binary MK mixtures, while Table 6 provides a summary of findings from binary slag mixtures and the ternary mixtures.

Table 5 – Summary of binary MK performance.

		MK1			MK2			MK3		
		10%	15%	20%	10%	15%	20%	10%	15%	20%
Mechanical	Compression (28-day)	↑	↑	↑	↓	↑	↑	↑	↑	↑
		17%	29%	44%	-9%	19%	6%	21%	25%	15%
	Split-Cylinder Tension	↑	↑	↑	↓	↓	↑	↑	↔	↑
		18%	30%	14%	-8%	-1%	3%	7%	0%	13%
	MOR	↓	↑	↑	↓	↓	↑	↑	↑	↑
		-10%	38%	20%	-1%	-16%	1%	5%	5%	6%
	E_d	↓	↓	↓	↓	↓	↓	↔	↓	↓
		-2%	-4%	-4%	-12%	-1%	-9%	0%	-6%	-9%
Durability	RCPT Permeability	↓	↓	↓	↓	↓	↓	↓	↓	↓
		-67%	-79%	-65%	-38%	-75%	-75%	-74%	-81%	-81%
	Sulfate Resistance	-	-	-	-	-	-	-	-	-
		F	P	P	F	F	F	F	P	P
	ASR Resistance	-	-	-	-	-	-	-	-	-
		F	P	P	F	P	P	P	P	P
Dimensional Stability	CTE	↑	↑	↑	↑	↑	↑	↑	↑	↑
		4%	12%	6%	4%	6%	3%	12%	18%	18%
	Shrinkage	↑	↔	↓	↓	↓	↓	↓	↓	↓
		3%	0%	-10%	-7%	-11%	-19%	-9%	-15%	-35%

Note: F = Fail and P = Pass.

Table 6 – Summary of alternate binary and ternary SCM performance.

		Binary			Teranary					
		FA-45	SLa-30	SLb-30	MK1-15 _SLa-30	MK1-15 _SLb-30	MK2-15 _SLa-30	MK2-15 _SLb-30	MK3-15 _SLa-30	MK3-15 _SLb-30
Mechanical	Compression (28-day)	↓	↓	↑	↑	↓	↓	↓	↔	↓
		-51%	-2%	18%	10%	-9%	-8%	-10%	0%	-4%
	Split-Cylinder Tension	↓	↓	↑	↑	↓	↓	↑	↑	↓
		-24%	-15%	17%	1%	-4%	-8%	31%	11%	-4%
	MOR	↓	↑	↑	↔	↓	↓	↓	↓	↓
		-23%	4%	35%	0%	-8%	-21%	-25%	-15%	-5%
	E_d	↓	↑	↑	↓	↓	↓	↓	↓	↓
		-28%	3%	1%	-12%	-22%	-15%	-15%	-13%	-13%
Durability	RCPT Permeability	↑	↑	↓	↓	↓	↓	↓	↓	↓
		42%	4%	-48%	-74%	-83%	-69%	-85%	-84%	-85%
	Sulfate Resistance	-	-	-	-	-	-	-	-	-
		P	F	F	P	P	P	P	P	P
	ASR Resistance	-	-	-	-	-	-	-	-	-
		P	F	F	P	P	P	P	P	P
Dimensional Stability	CTE	↓	↑	↑	↑	↑	↑	↑	↑	↑
		-2%	3%	7%	1%	4%	4%	7%	4%	5%
	Shrinkage	↑	↔	↓	↓	↓	↓	↓	↓	↓
		10%	0%	-17%	-28%	-10%	-21%	-27%	-28%	-21%

Note: F = Fail and P = Pass.

2.2.1 **Fresh Properties**

Table 7 shows the fresh concrete properties for all concrete mixtures. Slumps ranged from 1 inch to 10 inches (25 mm–250 mm), and air contents typically ranged from 2.6%–5.5% with a single outlier of 8.5% for MK2-10. Temperatures are generally within acceptable limits, with two or three nearing the upper 80s °F (30 °C–32 °C).

Table 7 – Fresh concrete properties of mixtures.

Mixture Code	Slump		Air Content(%)	Unit Weight		Temperature	
	in	mm		pcf	kg/m^3	˚F	˚C
Control	2.5	64	4.1%	146.4	2345	73.0	22.8
MK1-10	8.5	216	5.5%	147.8	2367	75.7	24.3
MK1-15	1.3	32	3.8%	144.4	2313	73.4	23.0
MK1-20	2.0	51	3.6%	143.4	2297	66.6	19.2
MK2-10	3.0	76	8.5%	144.2	2310	82.7	28.2
MK2-15	1.5	38	3.9%	149.8	2399	59.7	15.4
MK2-20	2.0	51	3.6%	144.8	2319	75.2	24.0
MK3-10	6.5	165	3.5%	144.4	2313	78.1	25.6
MK3-15	3.8	95	3.1%	144.0	2307	78.8	26.0
MK3-20	1.5	38	2.6%	144.2	2310	84.6	29.2
SLa-30	1.0	25	4.3%	136.8	2191	68.2	20.1
SLb-30	1.0	25	3.0%	146.8	2351	82.4	28.0
FA-45	6.0	152	0.0%	146.0	2339	86.7	30.4
MK1-15_SLa-30	10.0	254	4.5%	140.6	2252	84.9	29.4
MK2-15_SLa-30	1.8	44	3.9%	141.4	2265	73.9	23.3
MK3-15_SLa-30	9.0	229	4.5%	136.4	2185	75.6	24.2
MK1-15_SLb-30	9.0	229	3.5%	144.6	2316	83.7	28.7
MK2-15_SLb-30	3.8	95	3.8%	143.6	2300	88.2	31.2
MK3-15_SLb-30	2.0	51	5.0%	144.8	2319	80.1	26.7

2.2.2 **Binary Metakaolin Hardened Properties**

Hardened properties of binary concretes and mortars that contain MK are presented. These include mechanical properties, durability properties, and the dimensional stability of these mixtures.

2.2.2.1 Mechanical properties

MK products varied widely in their effect on compressive strength in binary mixtures. MK1 showed a systematic increase in compressive strength with increasing levels of replacement; the highest compressive strength,11,170 psi (77 MPa), occurred at 28 days by MK1-20. Compressive strengths for all replacements were 17%–44% higher than that of the Control mixture at 28 days. Strength increase rates from 1–7 days were higher than those of the Control mixture for the 15% and 20% replacement levels, and the 1-day strengths for all replacement levels averaged 28% (580 psi or 4 MPa) higher than that of the Control mixture. Concretes incorporating MK2 saw an optimal 28-day compressive strength of 9,240 psi (64 MPa) at 15% replacement, which was 19% higher than that of the Control mixture. While MK2-20 also saw higher 28-day compressive strengths, MK2-10 saw a 7% reduction in compressive strengths and showed a lower rate of strength gain after one day of curing compared to the Control mixture. At the same time, the 15% and 20% replacement levels saw higher rates of strength gain compared to the Control mixture between 1 and 7 days. Overall, strength gains for MK2 ranged between 6%–19%. MK3 performed consistently across all replacement rates, with its highest 28-day strength of 9,700 psi (67 MPa, a 21% increase) attributed to the 15% replacement level. MK3-15 also showed a notable 43% higher compressive strength than that of the Control mixture at 1 day of age. Regardless of replacement rate, MK3 showed no lower than a 15% increase in compressive strength over the Control mixture at 28 days. Overall, only one mixture (MK2-10) did not exhibit a higher 28-day compressive strength than that of the Control mixture. For the rest of the mixtures, increases ranged between 6% and 44%. A graphical

representation of the compressive strength evolution of the binary MK mixtures appears in Figure 17 (a-d).

The split-cylinder tensile strength of the Control mixture was 420 psi (2.88 MPa), and the Modulus of Rupture (MOR) was 710 psi (4.90 MPa). MK1-15 recorded both the highest split-cylinder tensile strength and MOR, 30% and 38% higher than those of the Control mixture, respectively. Only one test of tension for MK1, MK1-10, produced a tensile value 10% less than that of the Control mixture. Otherwise, MK1 saw split-cylinder tensile strength increases between 14%–30% and increases of MOR between 20%–38%. MK2-20 recorded split-cylinder and MOR values similar to those of the Control mixture, while decreases in strength for the other two replacement levels, MK2-10 and MK2-15, were as high as 16% (MK2-15 MOR) when compared to the Control mixture. All measures of tension for MK3 were the same or higher than those of the Control mixture. The optimal replacement level for this MK product was 20%, with the split-cylinder tension 13% higher and the MOR 6% higher than the Control mixture. Overall, MK3 saw split-cylinder strength increases between 0%–13%, and MOR increases between 5%–6%. Finally, MK1 saw the most dramatic increases in tensile strength and indicated a clear optimal replacement level of 15%. MK3, meanwhile, saw moderate increases in strength that were consistent among replacement levels. MK2, on the other hand, caused a reduction in strength. A bar graph comparing the split-cylinder and MOR tensile strengths of the binary MK mixtures appears in Figure 18.

For the Control mixture, the dynamic measure of Young's modulus of elasticity was 5,440 ksi (37.5 GPa). Decreases in this measure across all replacement levels of MK1, MK2, and MK3 were observed, excluding MK3-10. Decreases ranged from 2%–4% for

MK1 concretes, 1%–12% for MK2 concretes, and 0%–9% for MK3 concretes. Figure 19 displays these values in a bar chart.

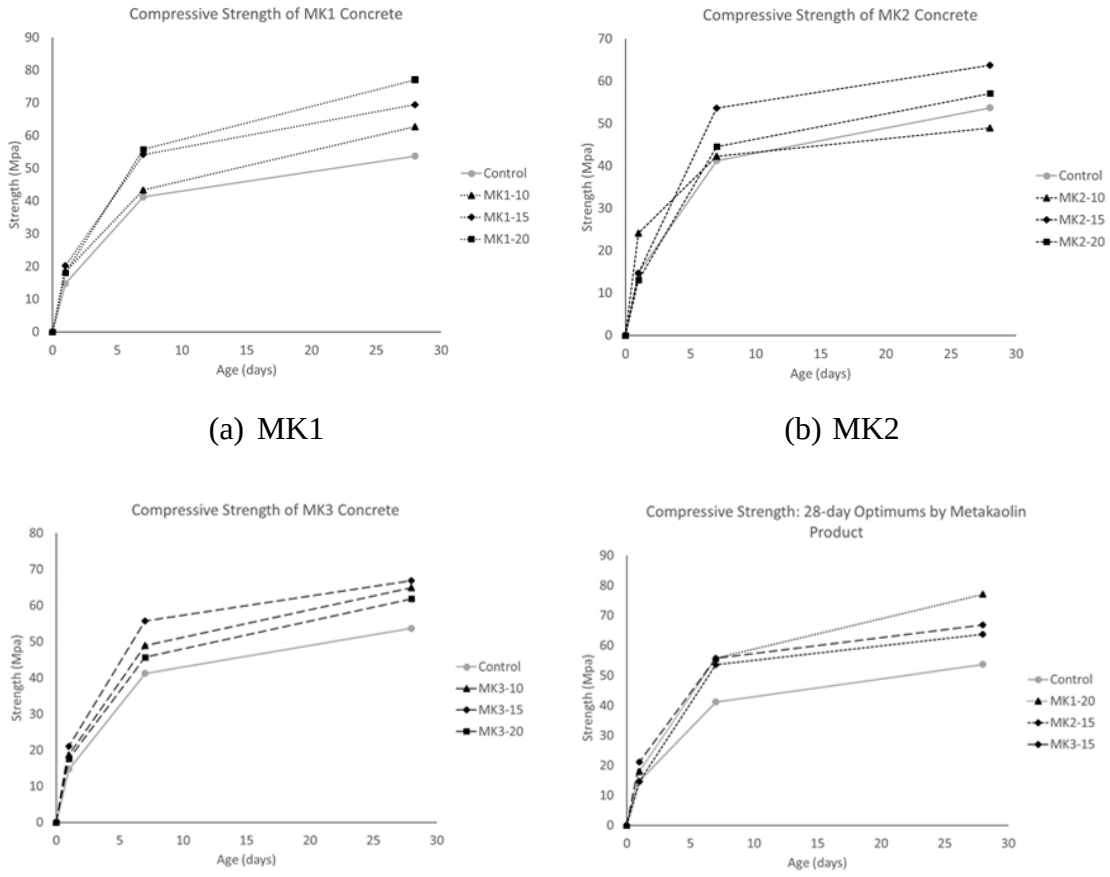

(a) MK1 (b) MK2

(c) MK3 (d) 28-day highest strength mixtures

Figure 17 – Compressive strength evolution for binary MK concrete mixtures.

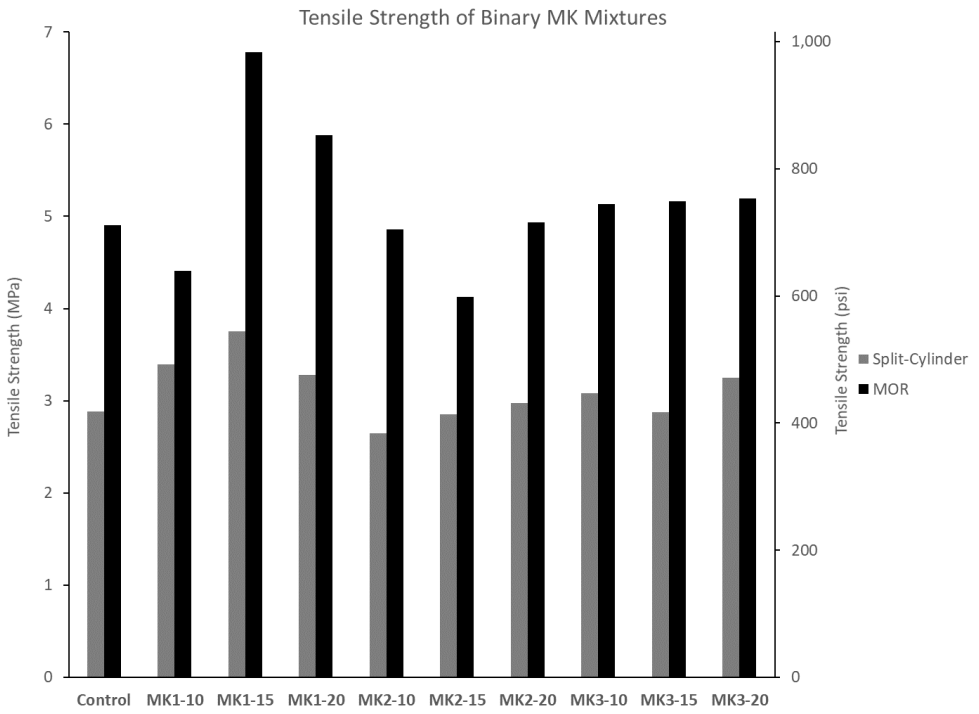

Figure 18 – Tension results for binary MK concrete.

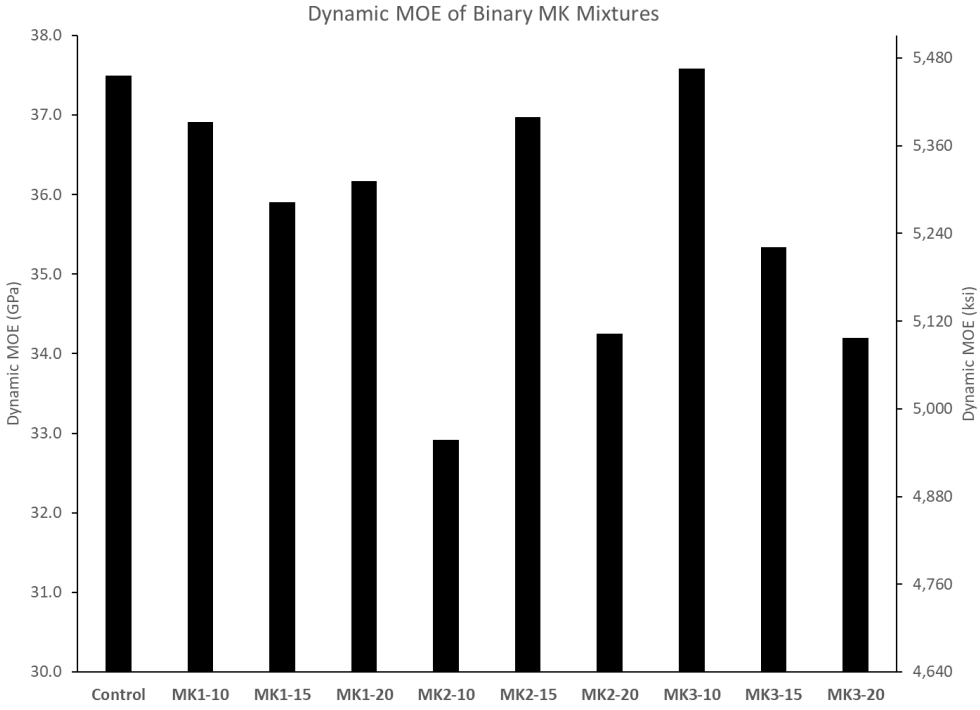

Figure 19 – Dynamic MOE for binary MK concrete.

2.2.2.2 Durability

The Rapid Chloride Permeability Test (RCPT) indicated that all binary MK mixtures achieved lower permeability to chloride ions compared to the Control mixture. All MK1 mixtures belong to the 'very low' permeability class (i.e., less than 1,000 C passed), with MK1-15 displaying the lowest permeability at 588 C. MK2 required a 15% or greater replacement level before reaching the same permeability class; MK2-10 passed 1,718 C while MK2-15 and MK2-20 passed 693 C and 697 C, respectively. MK3 achieved the lowest permeability, with its lowest at 496 C passed by MK3-20. However, other MK3 replacement levels performed similarly, with the highest recorded at 712 C. Overall, all MK concretes were classified as having a 'very low' permeability, excluding the MK2-10 mixture. Figure 20 provides a visual representation of these RCPT results along with indicators for permeability classes. Notably, while MK2-10 passed the most charge of any binary MK mixture, it was classified in a lower permeability class than the Control mixture.

The 6-month (168 day) expansion criterion set in ASTM C 1012 is 0.10% of the original length of the mortar bar. The Control mixture exceeded this expansion limit and ended the testing period with a total expansion of 0.47%. All mixtures with a 10% replacement failed to meet the expansion criterion. Most notably, mortar bars for mixtures MK2-10 and MK2-15 deteriorated before they could reach the end of the testing period (91 days and 112 days, respectively). MK2 and MK3 sufficiently limited expansion at replacement levels of 15% and 20%. The systematic increase in sulfate resistance for increasing replacement levels can be seen in Figure 21.

According to ASTM C1567, an SCM combination has sufficiently mitigated expansion due to Alkali-Silica Reactivity (ASR) if it expands less than 0.10% of its original

length at the end of a 14-day testing period. The ultimate expansion of the Control mixture was 0.17%. A consistent, systematic trend of increased ASR resistivity can be seen as binary MK replacement levels increase. For MK1 and MK2, a 15% replacement level was required to meet this expansion criterion. MK3 was the only MK that was able to meet this criterion at all replacement levels, though MK3-10 expansion was exactly 0.10% at the end of the 14-day testing period. MK1-15 and MK3-15 performed similarly, with an ultimate expansion of 0.04%. At the 20% replacement level, MK1-20 achieved the lowest ultimate expansion at below 0.02%, while MK3-20 was just over 0.02%. A time history of these expansions can be seen in Figure 22.

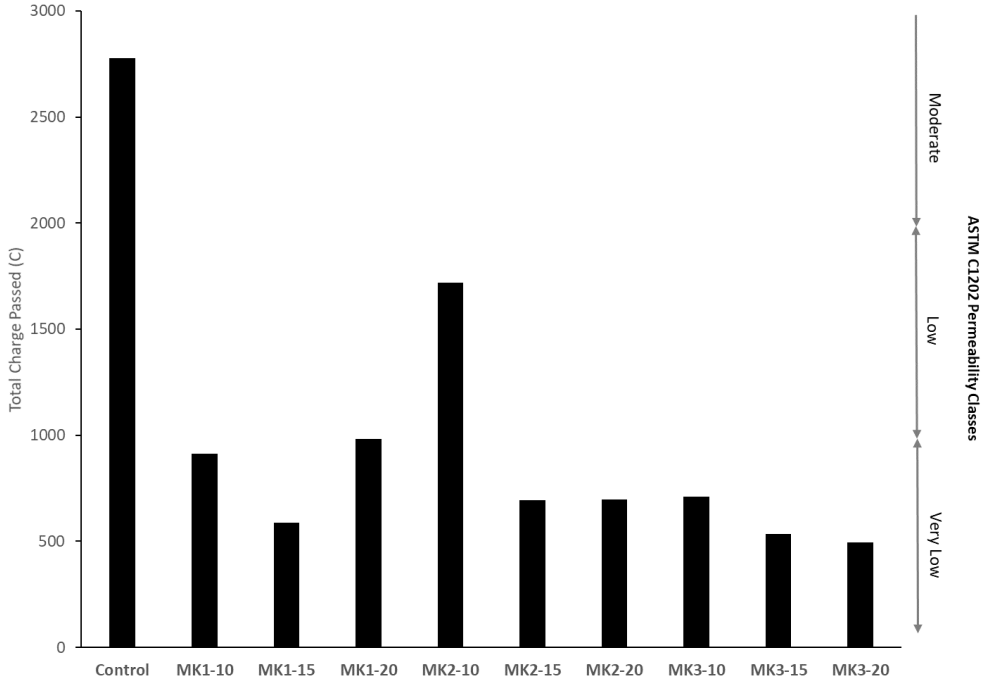

Figure 20 – RCPT results for binary MK concrete.

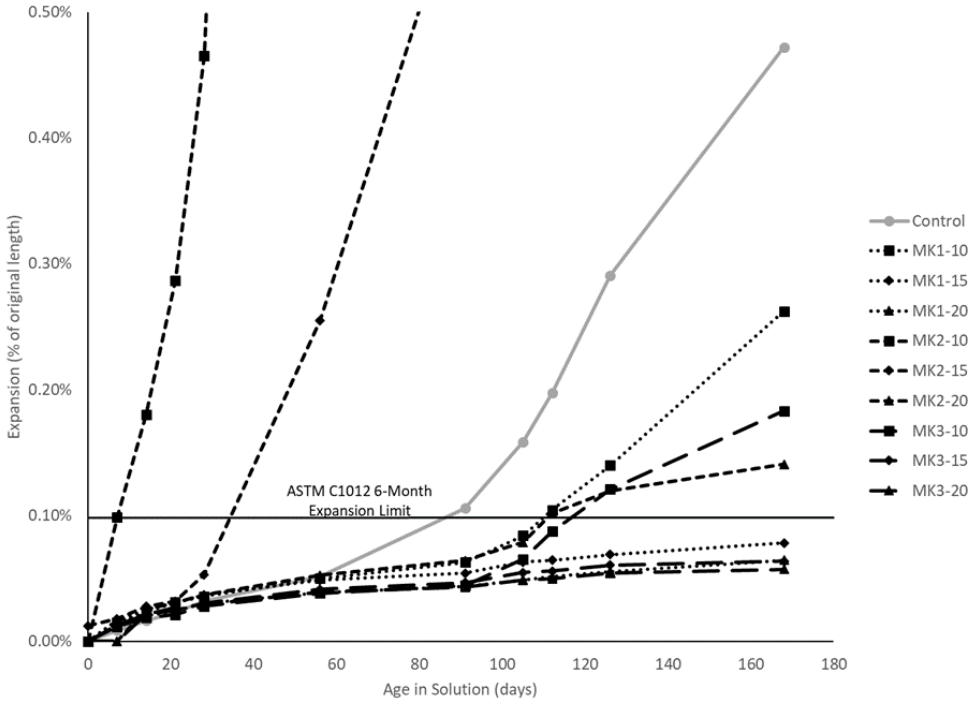

Figure 21 – Sulfate expansion of binary MK mortars.

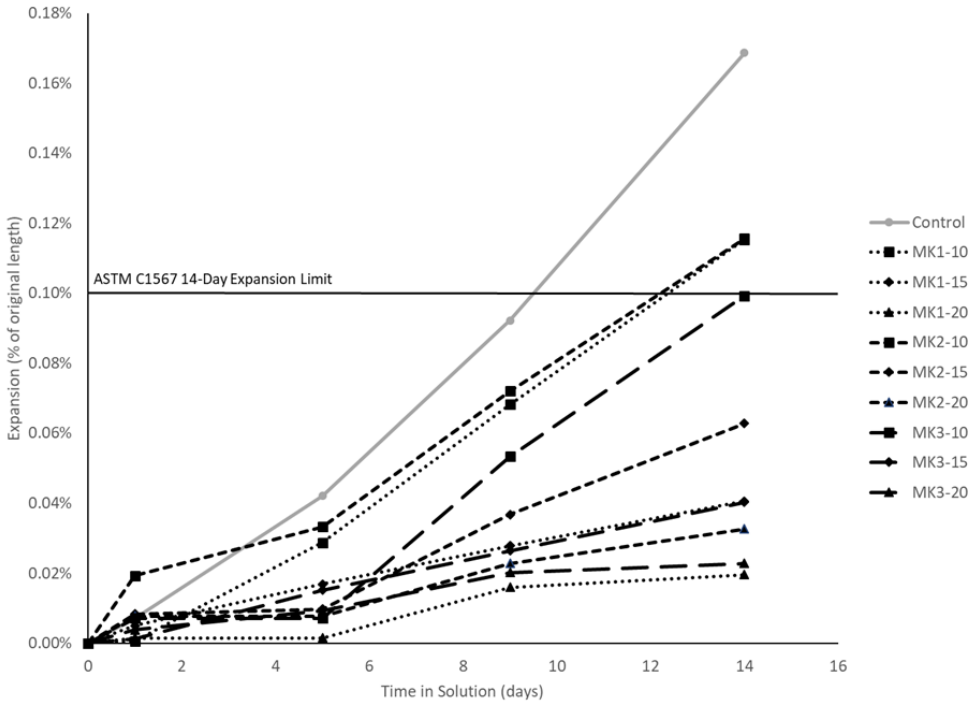

Figure 22 – ASR expansion of binary MK mortars.

2.2.2.3 Dimensional stability

Figure 23 indicates that the ultimate drying shrinkages of binary concretes containing MK were predominantly lower than that of the Control mixture. For the Control mixture, the 224-day drying shrinkage was 0.048%. One mixture, MK1-10, was slightly larger at 0.049%. For each product, the overall drying shrinkage decreased systematically with increasing replacement levels. For MK1, these values decreased from 0.049% to 0.039%. For MK2, shrinkage values decreased from 0.045% to 0.039%. Finally, MK3 concrete mixtures had shrinkage values that decreased from 0.044% to 0.031%, and MK3-20 showed the lowest drying shrinkage in this study.

The Coefficient of Thermal Expansion (CTE) of the Control mixture was 5.34×10^{-6} in/in/˚F (9.61×10^{-6} mm/mm/˚C). All binary concrete mixtures containing MK exhibited higher CTEs than the Control mixture. MK1 saw a high of 5.96×10^{-6} in/in/˚F (10.72×10^{-6} mm/mm/˚C) at the 15% replacement level and a low of 5.53×10^{-6} in/in/˚F (9.95×10^{-6} mm/mm/˚C) at the 10% replacement level. MK2 generally saw lower CTEs compared to MK1 and MK3, and had the lowest binary CTE at 5.5×10^{-6} in/in/˚F (9.88×10^{-6} mm/mm/˚C) for MK2-20. Finally, MK3 concretes consistently observed the highest CTEs, ranging from 6.0×10^{-6} in/in/˚F to 6.3×10^{-6} in/in/˚F (10.80×10^{-6} mm/mm/˚C to 11.38×10^{-6} mm/mm/˚C). MK1 and MK2 exhibited peak CTEs at the 15% replacement level. However, MK3 saw no reduction in CTE from the 15% replacement level to the 20% replacement level. A bar graph of these results can be seen in Figure 24.

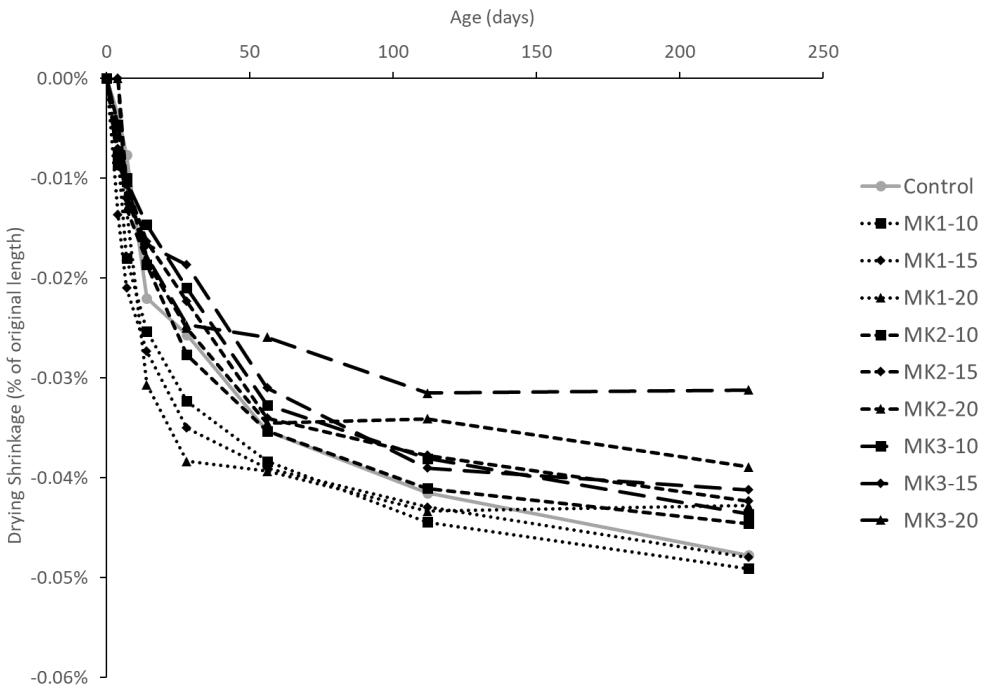

Figure 23 – Drying shrinkage of binary MK concrete.

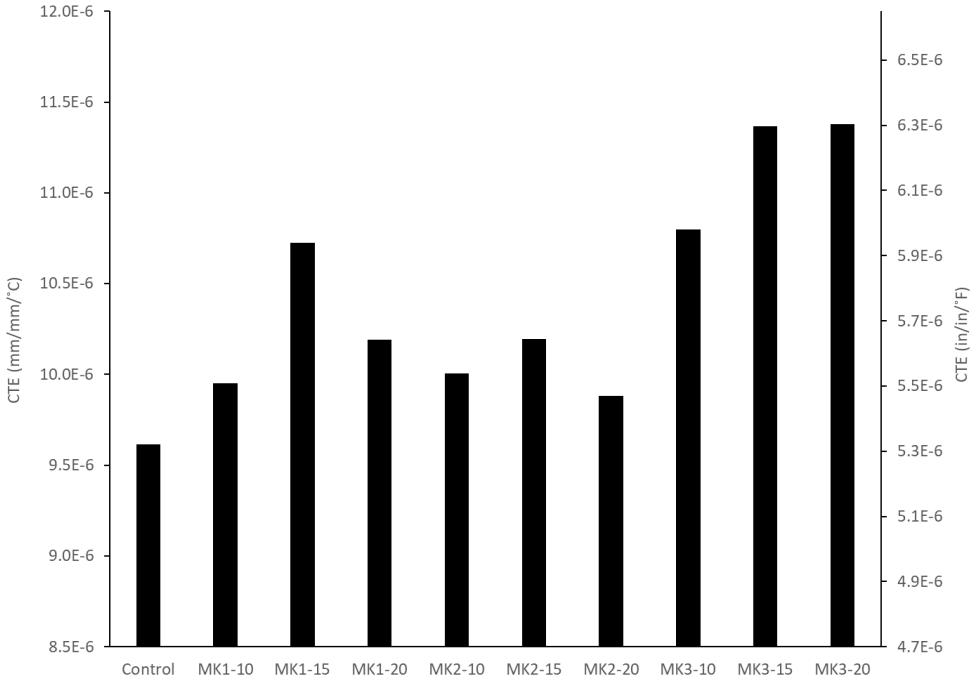

Figure 24 – CTEs of binary MK concrete.

2.2.3 **Ternary and Alternate Binary SCM Hardened Properties**

The hardened properties of alternate binary SCM and ternary SCM mixtures are discussed. These include mechanical properties, durability properties, and the dimensional stability of these mixtures.

2.2.3.1 Mechanical properties

Of the two binary mixtures including slag or fly ash, only one mixture achieved a 28-day strength higher than that of the Control mixture. SLb-30 exhibited a 28-day compressive strength of 9,222 psi (64 MPa), an increase of 18% over the Control mixture. Mixtures SLa-30 and FA-45 were 2% and 51% weaker in compression compared to the Control mixture, respectively. The rate of strength gain was relatively similar between the two binary slag mixtures, though SLb-30 was stronger than SLa-30 by slightly over 1,300 psi (9 MPa) at 1 day of age. This was nearly the same difference in strength at 28 days of age.

Of the ternary mixtures, only one mixture had a higher 28-day compressive strength than the Control mixture: SLa-30+MK1-15 finished with a compressive strength of 8,570 psi (59 MPa), 10% higher than that of the Control mixture. SLa-30+MK3-15 finished with a compressive strength similar to that of the Control mixture, at 7,770 psi (54 MPa). For all ternary concretes including SLa, 1-day strengths were similar or less than the 1-day strength of the Control mixture, ranging from 715 psi-1010 psi (5 MPa-7 MPa). Apart from SLa-30+MK1-15, 7-day strengths for concretes including SLa were lower than the 7-day strength for the Control mixture, as well. However, after seven days, all SLa ternary concretes gained compressive strength at a higher rate than the rates exhibited by SLb ternary concretes and the Control concrete. By contrast, ternary concretes with SLb did not suffer lower 1-day strengths (1,730 psi-2,110 psi, 12 MPa-14.5 MPa), though they were

still lower than that of the Control mixture. Moreover, ternary concretes consisting of SLb exhibited the highest strength gain rate from one to seven days but saw a less dramatic strength gain after seven days of age. Overall, excluding SLa-30+MK1-15, 28-day strengths for ternary concretes ranged from 6,970 psi-7,769 psi (48 MPa-54 MPa). Strength evolutions for all mixtures other than binary MK mixtures can be found in Figure 25.

Binary slag mixtures were, overall, stronger in tension compared to the Control mixture. SLa-30 produced a splitting tensile strength 15% lower than that of the Control mixture, while SLb-30's was 17% higher than the Control mixture. MOR values for these concretes were both higher than the Control mixture: 740 psi and 958 psi (5.1 MPa and 6.6 MPa), respectively. The fly ash mixtures saw a strength reduction in splitting-tension and MOR of 24% and 23%, respectively. Ternary SCM concretes typically displayed lower tensile strength compared to the Control mixture; however, SLa-30+MK1-15 performed similarly to the Control mixture for both split-tension and MOR. Further, apart from the SLb-30+MK2-15 split tension results, ternary concretes incorporating MK1 and MK3 appeared to have higher tensile strengths when compared to ternary concretes incorporating MK2. Meanwhile, the choice of slag product does not seem to affect the tensile strength of concrete in ternary mixtures. The tensile strength results of binary slag and fly ash concretes as well as ternary concretes are found in Figure 26.

Young's modulus for each of the binary slag concretes was higher than that of the Control mixture, while all other mixtures saw values lower than that of the Control mixture. Increases were on the order of 150 ksi and 60 ksi (1 GPa and 0.4 GPa) for SLa-30 and SLb-30, respectively. The greatest reduction in Young's modulus was exhibited by the fly ash mixture with a decrease of 28% from the modulus of the Control mixture. There were no

obvious trends among MK or slag products for the ternary concrete mixtures, and reductions in dynamic modulus, E_d, ranged from 12%–22% with an average reduction of 811 ksi (5.6 MPa). Young's modulus values for binary slag and fly ash mixtures and the ternary SCM mixtures are listed in Figure 27.

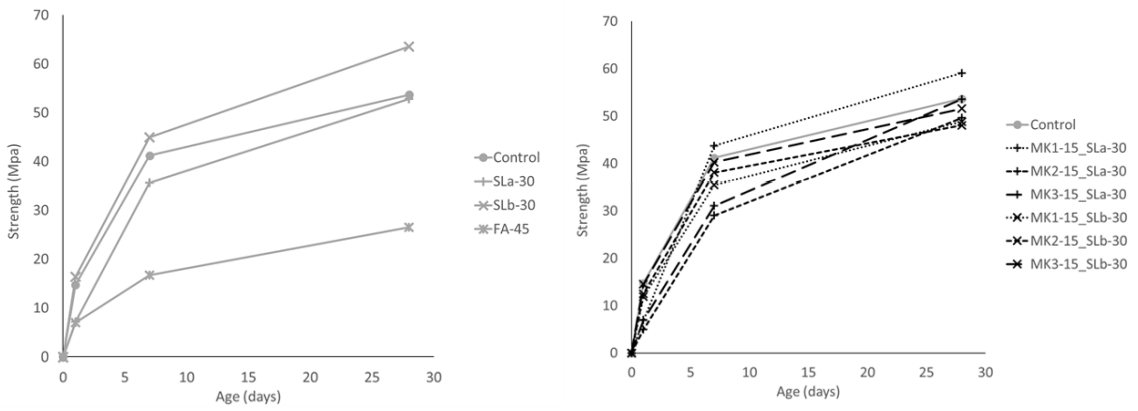

(a) alternate binary SCM concrete (b) ternary SCM concrete

Figure 25 – Compressive strength evolution for alternate binary SCM and ternary SCM concrete.

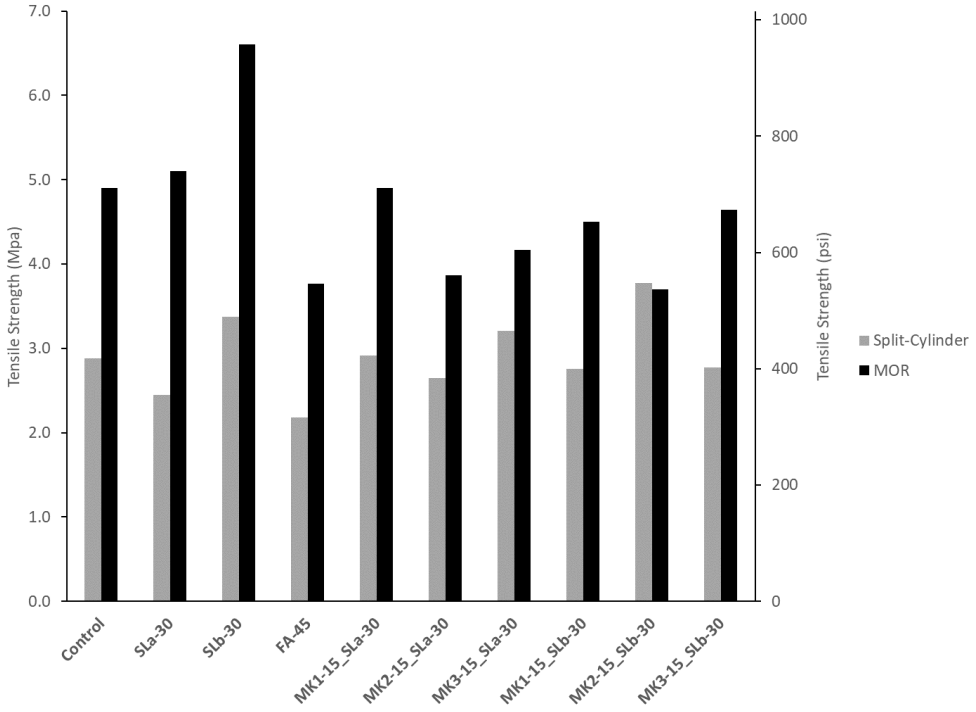

Figure 26 – Tensile strength of alternate binary SCM and ternary SCM concrete.

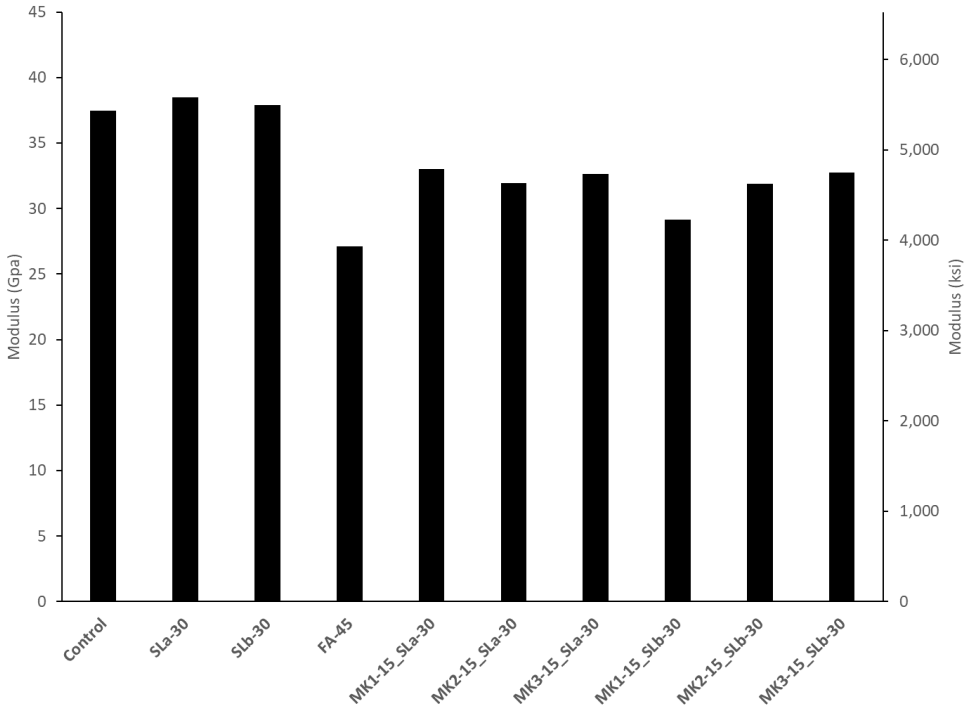

Figure 27 – Dynamic MOEs of alternate binary SCM and ternary SCM concrete.

2.2.3.2 Durability

Figure 28 shows that only one of three alternate binary SCM concrete mixtures were able to reduce chloride-ion permeability below the reduction afforded by the Control mixture. SLa-30 performed similarly to the Control mixture, while FA-45 almost reached the 'high' penetrability classification. SLb-30, however, was effective in reducing the total charge passed to 1,440 C, thereby earning a 'low' penetrability classification. All ternary SCM concretes fell below 1,000 C passed, and of those, four passed under 500 C. Penetrability classes and results for non-MK binary SCM concretes and ternary SCM concretes can be found in Figure 28.

Fly ash was the only SCM other than MK to sufficiently mitigate mortar expansion for the entire 6-month testing period. In fact, expansion of the binary slag mortars was more accelerated than the expansion of the Control mixture; this was especially so for the mortar incorporating SLa. All ternary mixtures were able to mitigate sulfate expansion during the 6-month window, and they typically resulted in less than 0.06% expansion. These results are presented in Figure 29.

As with the sulfate tests, binary slag mortars at a replacement level of 30% were not sufficient to limit expansion below acceptable limits (expansions of 0.11% and 0.12%). The binary fly ash mortar exhibited expansion similar to that of the ternary mixtures. All ternary mortars resulted in expansions less than 0.03%. Figure 30 presents these results.

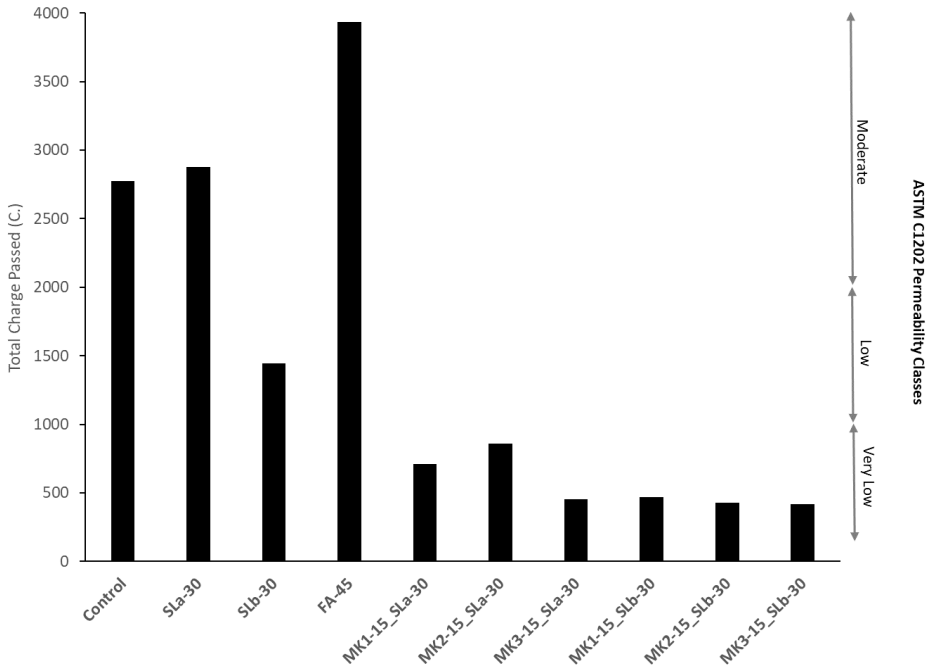

Figure 28 – RCPT results for alternate binary SCM and ternary SCM concrete.

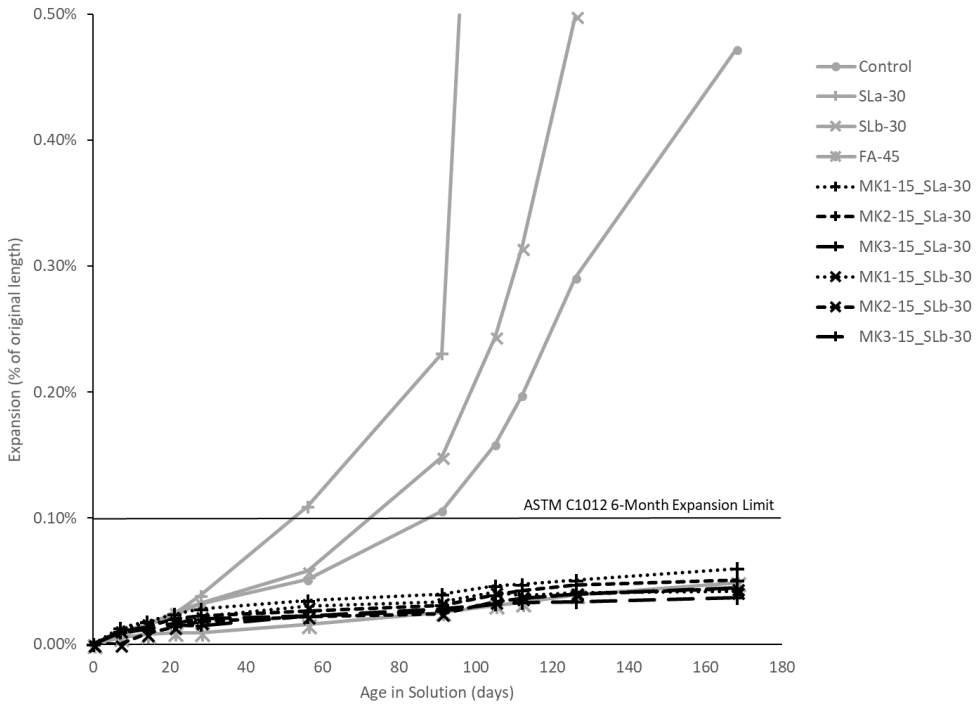

Figure 29 – Sulfate expansion of alternate binary SCM and ternary SCM mortars.

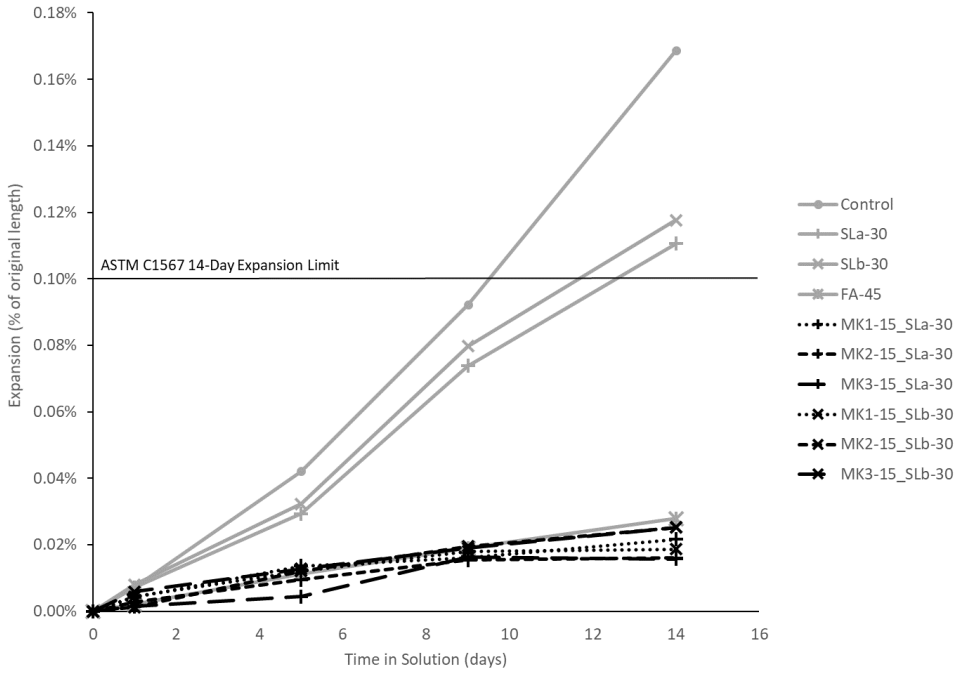

Figure 30 – ASR expansion of alternate binary SCM and ternary SCM mortars.

2.2.3.3 Dimensional stability

As evident from Figure 31, the fly ash binary mixture showed the highest drying shrinkage among all the mixtures, with the 224-day drying shrinkage of 0.058%. The 224-day drying shrinkage of the SLb-30 binary mixture was 0.04%, which was lower than the Control mixture by 17%. Meanwhile, Sla-30 mixture resulted in a similar shrinkage to that of the Control mixture. The ultimate drying shrinkage of ternary concretes containing slag and MK were predominantly lower than the shrinkage of the Control mixture. The SLa-30+MK1-15 and SLa-30+MK3-15 had the lowest 224-day drying shrinkage of 0.034%, which was about 28% lower than the Control mixture.

Figure 32 indicates that the binary fly ash concrete exhibited a 2% lower CTE than that of the Control mixture. SLa-30 and SLb-30 varied widely from one another at 3% and

7% higher CTE compared to the Control mixture, respectively. The latter was the highest CTE seen outside of the binary MK concretes. SLa-30+MK1-15 saw the lowest CTE in the ternary group with a value of 5.40 in/in/˚F ($9.73x10^{-6}$ mm/mm/˚C), an increase of 1% from that of the Control mixture. SLb-30+MK2-15 saw the highest CTE in the ternary group with a CTE of $5.70x10^{-6}$ in/in/˚F ($10.25x10^{-6}$ mm/mm/˚C), an increase of 7% over the CTE of the Control mixture. As a group, the ternary SCM concretes averaged a CTE of $5.53x10^{-6}$ in/in/˚F ($9.93x10^{-6}$ mm/mm/˚C), an increase of 3% compared to the CTE of the Control mixture. CTE results are presented in Figure 32.

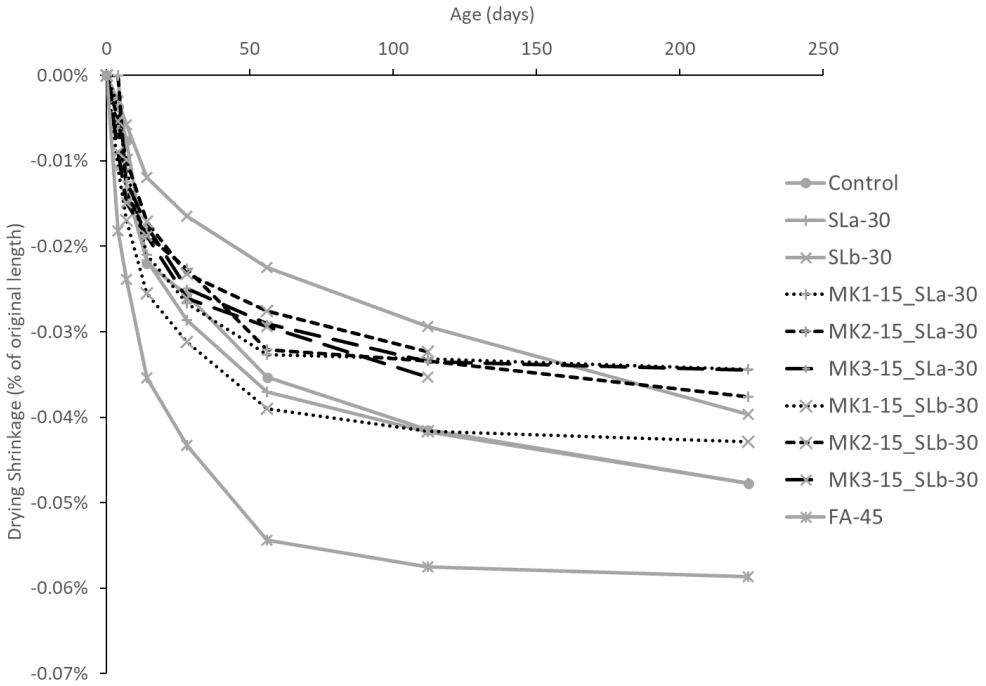

Figure 31 – Drying shrinkage of alternate binary SCM and ternary SCM concrete.

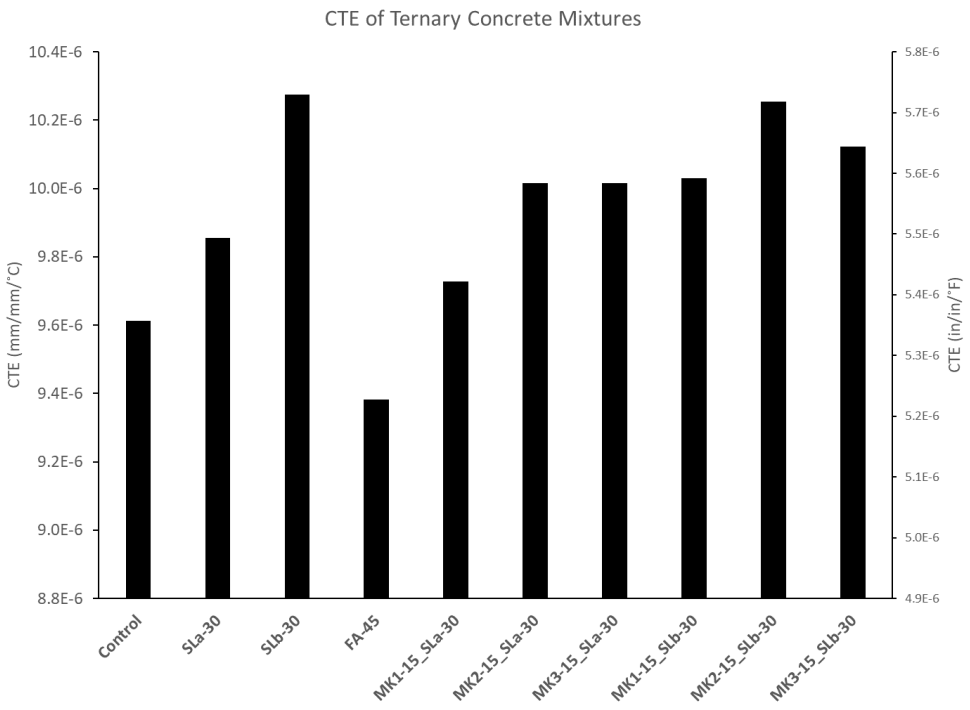

Figure 32 – CTEs of alternate binary SCM and ternary SCM concrete.

2.3 Discussion

This section discusses the results presented in Section 2.2 in the context of existing research. Binary mixtures including MK will be utilized to discuss important differences between the MK products. The performance of alternate binary SCM and ternary SCM mixtures will also be discussed.

2.3.1 Comparison of Binary Metakaolin Mixtures

Contrary to expectation, not every MK product benefitted concrete when part of a binary mixture. In particular, MK2 was inconsistent with respect to its effect on the mechanical strength of concrete. Moreover, a clear difference was observed in the durability test results of MK2 and the other MK products. The expansion of MK2-10 and MK2-15 mortars in the sulfate solution were the most aggressive in the entire testing program. The expansion

of MK2-20 in the sulfate solution most closely resembled the expansion of the other two products at a 10% replacement level. Figure 33 shows disintegration of the MK2-10 mortar bars as a result of deleterious expansion.

Figure 33 – Deleterious expansion by sulfate attack of MK2-10 mortar bars.

Table 5 Repeated – Summary of binary MK performance.

		MK1			MK2			MK3		
		10%	15%	20%	10%	15%	20%	10%	15%	20%
Mechanical	Compression (28-day)	↑	↑	↑	↓	↑	↑	↑	↑	↑
		17%	29%	44%	-9%	19%	6%	21%	25%	15%
	Split-Cylinder Tension	↑	↑	↑	↓	↓	↑	↑	↔	↑
		18%	30%	14%	-8%	-1%	3%	7%	0%	13%
	MOR	↓	↑	↑	↓	↓	↑	↑	↑	↑
		-10%	38%	20%	-1%	-16%	1%	5%	5%	6%
	E_d	↓	↓	↓	↓	↓	↓	↔	↓	↓
		-2%	-4%	-4%	-12%	-1%	-9%	0%	-6%	-9%
Durability	RCPT Permeability	↓	↓	↓	↓	↓	↓	↓	↓	↓
		-67%	-79%	-65%	-38%	-75%	-75%	-74%	-81%	-81%
	Sulfate Resistance	-	-	-	-	-	-	-	-	-
		F	P	P	F	F	F	F	P	P
	ASR Resistance	-	-	-	-	-	-	-	-	-
		F	P	P	F	P	P	P	P	P
Dimensional Stability	CTE	↑	↑	↑	↑	↑	↑	↑	↑	↑
		4%	12%	6%	4%	6%	3%	12%	18%	18%
	Shrinkage	↑	↔	↓	↓	↓	↓	↓	↓	↓
		3%	0%	-10%	-7%	-11%	-19%	-9%	-15%	-35%

With each product, the replacement levels that achieved the highest 28-day compressive strength also achieved the highest 7-day compressive strength. Overall, variation was low in these 7-day strengths. Figure 17 shows this tight clustering of 7-day strengths from all products at their optimal replacement levels (54 MPa-56 MPa). Notably, when these replacement levels were the same (i.e., for MK2-15 and MK3-15), strength

gain rates were very similar at all ages. Only when the optimal replacement is at 20% (MK1-20) does a higher compressive strength gain become evident after 7 days of age. The tight clustering of the 7-day compressive strength values is considered to be the result of similar oxide composition (see Section 3.2.1.1); this is not a poignant statement, as these MKs are being tested specifically because they are commercially-available high-reactivity metakaolins (HRMs) (Al_2O_3 + SiO_2 + Fe_2O_3 ≥ 90%). At the same time, because the majority of the pozzolanic reaction is completed between 7 and 14 days of age, comparable 7-day compressive strengths may indicate similar CH consumption and C-S-H formation rates across all MKs when their optimal replacement level is used (Wild et al., 1996). While this explanation would be consistent with MK1-20 showing additional strength gain between 7 and 28 days, (i.e., additional pozzolanic activity between 7–14 days), it is unknown why MK1 displays a higher optimal replacement level than that of the other two MKs.

Optimal replacement level trends in compressive strength tests did not translate to tensile strength results. MK1 saw optimal tensile strength at 15% replacement, while MK2 and MK3 reached their optimal strengths at 20% replacement. In addition, compared to the measures of tensile strength for MK3, larger variations were observed for MK1 and MK2 between replacement levels. This is consistent with the compressive strength findings, where MK3's compressive strength demonstrated less variation between replacement levels than the variation observed for the other two products. In fact, MK3 mixtures were more consistent across replacement levels than either of the other two MKs in all measures except the dynamic measure of Young's modulus. Here, MK3 saw the largest variation among any MK.

MK1 and MK3 were consistent in their ability to decrease permeability and increase resistance to chemical attacks. The inclusion of these MKs at all replacement levels resulted in very low RCPT permeability classifications, and beyond 15% replacement of both products sufficiently mitigated deleterious expansion in aggressive solutions. In addition, MK2 was able to achieve the same permeability classification as the other two MKs at or above a 15% replacement level, sufficiently mitigating ASR expansion only.

MK2 had the highest fineness of the three MKs, and a similar oxide composition. Increased fineness of MK has been shown to increase the rate of strength gain as well as the overall 28-day strength of concretes (Justice & Kurtis, 2007). Yet, the inclusion of MK2 does not result in higher performance across all hardened concrete tests in this study when compared to the other two MKs. Most dramatically, MK2-10 and MK2-15 deteriorated in sulfate solution more than the Control mixture. Similar performance has only been recorded once in the literature, using a MK with $Al_2O_3 + SiO_2 + Fe_2O_3 = 85\%$ and a loss on ignition (LOI) of 14% (Torres Agredo et al., 2008). In fact, Table 5 shows that MK2 exhibits a significantly reduced performance for all replacement levels.

Given this information, the following are possible explanations for MK2's poor performance:

- MK2's high fineness resulted in large agglomerations which were not properly deflocculated during the batching of the concrete.
    - This would explain tensile strengths lower than that of the Control mixture but not the inordinate deterioration of the sulfate mortar bars.

- MK2's alumina and silica contents were not amorphous, leading to an incomplete dehydroxylation of the MK (see (Brindley & Nakahira, 1957; Murray & Lyons, 1955)).
    - This would explain the mechanical performance as well as the rapid destruction of MK2 sulfate mortar bars, as the non-amorphous kaolin would act as inert material.
    - For compression and permeability, inert kaolin would still contribute to particle packing (Ramezanianpour, 2014), and the alumina content has been shown to increase chloride-binding capacity (Badogiannis et al., 2015; Wang et al., 2014). Moreover, the fine material would still provide additional nucleation sites for cement hydration (Wild et al., 1996).
    - This does not explain why the optimal replacement level for tensile strength was 20%.

All concretes containing MK exhibit increased expansion due to temperature change, as indicated by CTE values greater than that of the Control mixture. Concretes typically achieved a peak CTE value at 15% replacement. To date, no known research has been published on the CTE values of MK concretes. Existing research has concluded that the inclusion of fly ash, slag, and silica fume (SF) reduces the CTE of cement pastes (Shui et al., 2010). The mechanism by which the inclusion of SF reduces CTE is different from that of fly ash and slag inclusion: SF reduces CH contents, which have a higher CTE than that of plain cement pastes, while fly ash and slag reduce CTE by CH consumption and increased porosities, as an increase in porosity is expected to decrease CTE. This finding would support an increase in CTE by inclusion of MK only if the CTE reduction by CH

consumption is less than the increase in CTE due to the reduction of porosity. Temporarily ignoring MK2 and its poor performance, this explanation is supported by the finer MK (MK1) achieving lower CTE values than those of MK3, since finer MK likely exhibits a higher CH consumption with similar porosities (see the RCPT results). The deleterious results of jointed concrete pavements with CTE values higher than 5.5 in/in/˚F ($10x10^{-6}$ mm/mm/˚C) have been reported (Sabih & Tarefder, 2016).

Reduction in drying shrinkage with the inclusion of MK is supported by the literature (Brooks & Johari, 2001; Gleize et al., 2007; Wild et al., 1998). Some researchers have reported a systematic decrease in drying shrinkage with increasing replacement levels of MK (Gleize et al., 2007; Güneyisi, Gesoğlu, & Mermerdaş, 2008), while others have reported no observable benefit from higher replacements (Brooks & Johari, 2001).

2.3.2 Comparison of Ternary and Alternate Binary SCM Mixtures

Overall, ternary mixtures' mechanical strengths were equal to or just below those exhibited by the Control mixture. Only one mixture, SLa-30+MK1-15, managed to obtain a 28-day compressive strength higher (10%) than that of the Control mixture.

Table 6 Repeated – Summary of alternate binary and ternary SCM performance.

		Binary			Teranary					
		FA-45	SLa-30	SLb-30	MK1-15 _SLa-30	MK1-15 _SLb-30	MK2-15 _SLa-30	MK2-15 _SLb-30	MK3-15 _SLa-30	MK3-15 _SLb-30
Mechanical	Compression (28-day)	↓	↓	↑	↑	↓	↓	↓	↔	↓
		-51%	-2%	18%	10%	-9%	-8%	-10%	0%	-4%
	Split-Cylinder Tension	↓	↓	↑	↑	↓	↓	↑	↑	↓
		-24%	-15%	17%	1%	-4%	-8%	31%	11%	-4%
	MOR	↓	↑	↑	↔	↓	↓	↓	↓	↓
		-23%	4%	35%	0%	-8%	-21%	-25%	-15%	-5%
	E_d	↓	↑	↑	↓	↓	↓	↓	↓	↓
		-28%	3%	1%	-12%	-22%	-15%	-15%	-13%	-13%
Durability	RCPT Permeability	↑	↑	↓	↓	↓	↓	↓	↓	↓
		42%	4%	-48%	-74%	-83%	-69%	-85%	-84%	-85%
	Sulfate Resistance	-	-	-	-	-	-	-	-	-
		P	F	F	P	P	P	P	P	P
	ASR Resistance	-	-	-	-	-	-	-	-	-
		P	F	F	P	P	P	P	P	P
Dimensional Stability	CTE	↓	↑	↑	↑	↑	↑	↑	↑	↑
		-2%	3%	7%	1%	4%	4%	7%	4%	5%
	Shrinkage	↑	↔	↓	↓	↓	↓	↓	↓	↓
		10%	0%	-17%	-28%	-10%	-21%	-27%	-28%	-21%

For comparison, the average compressive strength increase over the Control mixture's compressive strength for all binary MK mixtures was 18% (ranging from -9% to 44%). SLa-30+MK1-15 also had the highest tensile strength of the ternary group, with a MOR equal to that of the Control mixture. Although the ternary mixtures outperformed binary concretes incorporating SLa, concretes incorporating SLb saw higher compressive (18% higher than that of the Control mixture) and tensile (MOR 35% higher than that of the Control mixture) strengths than the strengths exhibited by all ternary mixtures. Moreover, SLb-30 exhibited the highest tensile strength of all concretes tested.

The early-age strength properties of the ternary mixtures appear to be primarily dependent on the slag product used, with the SLb concrete mixtures recording higher 1-day and 7-day strengths. Ternary mixtures incorporating SLa and SLb exhibited nearly the same strengths as the SLa and SLb binary mixtures, respectively. The difference in compressive strengths between concretes incorporating SLa and SLb continued to be visible up to seven days, as Figure 25 shows. After this, the compressive strengths of all ternary mixtures approached that of the Control mixture.

Both MK and slag react pozzolanically with CH in ternary mixtures, which promotes optimal CH consumption and higher paste densities. This finding is evidenced by the durability results presented above, but it does not necessarily ensure higher mechanical strengths, as unreacted SCM is most likely present due to competing pozzolanic activity (Li et al., 2010). This explanation is supported by Khatib & Hibbert's (2005) study, which found that as the level of MK inclusion increased, optimal compressive strengths were found by reducing slag contents. Although slag is also a latent hydraulic material, its CaO content is less than that of ordinary Portland cement; thus, less CH is produced during hydration when slag replaces a portion of cement. In short, in ternary mixtures incorporating 30% slag and 15% MK, the slight reduction in compressive strength is a result of less CH for pozzolanic activity and more unreacted pozzolan. The increased density of the paste matrix and additional C-S-H via the pozzolanic reaction compensate for the unreacted material.

The most substantial benefits of the ternary mixtures were seen in the durability tests and most likely are the result of high CH consumption. All ternary mixtures indicated very low permeabilities. Five total mixtures passed less than 500 C, and ternary mixtures accounted for four of these five. The ternary mixtures including SLb recorded the lowest permeability, with a study low of 419 C recorded for a ternary mixture combining SLb with MK3. In addition, sulfate expansion of less than 0.60% was achieved by only one binary mortar mixture (MK1-20). By contrast, five of the six ternary mortars finished the 6-month testing period under this value. Similarly, all six ternary mortars met ASR expansion criteria. This indicates that, although durability performance varied widely

within binary slag and binary MK mortars (see Figures 21-23 and Figures 28-30), ternary mixture durability was consistently high regardless of product combinations.

All ternary concrete mixtures exhibited higher CTE values than that of the Control mixture; however, they were much lower than those of the binary MK mixtures. As mentioned, increased porosities in fly ash and slag concrete mixtures have been correlated with decreases in paste CTEs (Shui et al., 2010). This is a geometrical property. Only when high CH consumption exists (using SF) do low-porosity pastes exhibit CTEs lower than that of the Control mixture. This behavior is attributed to C-S-H, with a low CTE, replacing CH, with a higher CTE, and having a dominant effect. Figure 28 indicates that ternary concretes incorporating SLa have higher penetrability, and by inferred extension, higher porosities, than SLb concrete mixtures on average. Also, as Figure 32 illustrates, SLa concrete mixtures exhibit lower CTE values than SLb mixtures on average. It is hypothesized that a reduction in porosity leads to higher CTE values in SLb ternary blends. Further, the CTEs are higher for ternary blends than for the Control mixture but significantly lower than the CTEs of binary MK concrete mixtures, which would most likely have lower porosities than those of ternary concrete mixtures. Overall, CTEs of ternary concrete mixtures were well below the 5.5×10^{-6} in/in/˚F (10×10^{-6} mm/mm/˚C) limit for good performance in jointed concrete pavements (Sabih & Tarefder, 2016). Table 6 provides a summary of alternate binary SCM and ternary SCM mixture performance.

2.4 Conclusions and Recommendations from Chapter 2

This section further adds to the discussion presented in Section 2.3. Important results are summarized, and recommendations are made for the appropriate use of MK in binary and ternary concrete systems. Shortcomings of this study and future work are also presented.

2.4.1 **Summary of Findings**

Table 5 provides a summary of the performance of binary MK mixtures, while Table 6 provides a similar summary for the performance of alternate binary SCM and ternary SCM mixtures. The key findings in this study are as follows:

- All concretes incorporating MK as a cement replacement require a high dosage of superplasticizer (≥ 4 mL/kg of cementitious material or 6.1 oz./cwt), with higher dosage requirements at higher MK replacement levels.
- Binary usage of MK results in increased mechanical strengths, although the most significant increases are in compression. Increases up to 44% at 28 days of age were observed.
- Binary usage of MK results in increased chloride-ion penetrability and resistance to sulfate and ASR chemical attacks. A replacement level of 15% will ensure adequate resistance, although future work should include ASR tests with reactive aggregates.
- Binary usage of MK resulted in concretes with large CTE values and decreased drying shrinkage. Risk of crack development while using MK will likely depend on the type of concrete application (e.g., pavement, mass concrete, prestressing, etc.). A time history of CTEs should be studied so that expansion characteristics during hydration can be modeled.
- MK2 was an obvious outlier and did not perform well against sulfate attack. Caution should be exercised in choosing which MK products to put on Qualified Products List (QPL). Recommendations will be discussed in the next section, 2.4.2.

- Binary replacement mixtures containing a pozzolanic material such as MK (15%) offer no significant advantage in reducing HoH, although compressive strength increases up to 44% on the 28th day.
- The pozzolanic reaction of the binary mixture (MK15) starts after two days and mainly occurs between two and five days.
- Ternary concrete mixtures using slags and MKs (30% slag+15% MK) tend to perform similarly to one another and the Control mixture in both compression and tension at 28 days of age. Early-age strength characteristics of ternary mixtures resemble the early-age strength characteristics of the 30% mixture using the same slag.
- Ternary concrete mixtures using slags and MKs exhibit very high resistance to chemical attack and very low chloride-ion penetrability. All combinations of commercially available products performed similarly to one another.
- Ternary concrete mixtures using slags and MKs result in increased CTE values, although these values are much lower than the CTEs for binary MK mixtures. Values were near the threshold of $5.5x10^{-6}$ in/in/˚F ($10x10^{-6}$ mm/mm/˚C) reported to be deleterious in jointed concrete pavements. Drying shrinkage was lowered from the shrinkage of the Control mixture for these mixtures and was on average lower than the shrinkage of the binary MK mixtures. As with the binary MK mixtures, a time history of CTEs should be studied if ternary mixtures are to be used in mass concrete.
- The optimal weight ratio of pozzolans used in ternary replacement mixtures is 2 slag:1MK when a 45% ternary replacement is considered.

- The presence of two pozzolanic materials including high silica and alumina contents in ternary replacement mixtures results in approximately 13% reduction in the total amount of heat within 7 days and about 10% strength gain by 28 days, relative to the Control mixture. The amount of heat generated in ternary mixtures is proportional to the Ca/(Al+Si) ratio.
- The ternary replacement mixture of 30% slag and 15% MK results in a significant reduction in HoH, and its HoH is lower than that of the binary mixture with 45% slag replacement.
- Ternary replacements of cement with combined slag and MK significantly reduce HoH and enhance durability properties; thus, they could possibly alleviate the thermal cracking potential of concrete.

2.4.2 **Recommendations for Usage**

Binary replacements of cement by MK should be used if high mechanical strengths (at any age) are desired for the following reasons:

- MK provides similar compression benefits to SF (Duan et al., 2013; Güneyisi et al., 2012; Caldarone et al., 1994; Poon et al., 2006) but does not suffer from SF's dark coloration.
- MK is also less expensive than SF, and quality can be ensured because it is not a byproduct.

The authors recommend that concretes not incorporate MKs as a binary replacement for cement in massive concreting operations or in pavements. Figure 24 shows the dramatic effect of some MK products on CTE. According to the authors, the thermal

expansion evinced by these concretes under normal temperature fluctuations would quickly crack and degrade pavements and mass concrete.

Binary MK mixtures show dramatic benefits in resistance to chemical attack and durability as do ternary mixtures with slag. If mechanical strengths need only be similar to the Control mixture, it is recommended that a ternary mixture be used. Ternary mixtures see benefits beyond those of binary MK mixtures:

- Lower CTEs
- Lower HoHs
- Increased resistance to chemical attack
- Reduced permeability

2.4.3 **Future Work**

Further research should evaluate the following:

- The dispersion of high-fineness, plate-like MK in ready-mixed-sized concrete batching. Recommendations are provided by the Silica Fume Association (SFA, 2019).
- The pozzolanic reactivity (ASTM C311) of various commercially available MKs in the U.S., and its effect on concrete performance. The authors affirm that the commonly specified minimum of an 85% reactivity index (Florida, Texas) is insufficient to ensure quality. Particular attention should be paid to ensure that MKs appearing on QPLs have a high fraction of kaolinite converted to MK (amorphous, or glassy alumina and silica). Minimum contents should be set by future studies.

- Time-dependent CTEs of ternary mixtures. These mixtures have been shown to reduce HoH, and low CTEs during the hydration period would prove the reliability and durability of these mixtures for mass concreting.
- The relationship between MOE by forced resonance method and static MOE measurements for binary and ternary MK concrete.
- The relationship between HoH and pozzolanic activity (e.g., CH consumption).
- X-ray diffraction and scanning electron microscope tests for ternary mixtures.

CHAPTER 3

EXPERIMENTAL INVESTIGATION OF THE HEAT OF HYDRATION AND TEMPERATURE CHANGES

This chapter starts with a detailed literature review of available guides and state DOT specifications for mass concrete structures. This chapter also presents an experimental study to quantify maximum temperatures in 17 mass concrete specimens. These specimens include different SCMs and various combinations of binary and ternary replacement mixtures. Section 3.2 presents the methodology and procedures for testing the specimens. Sections 3.3 and 3.4 present the results and analysis of the results, respectively. A summary of the literature review from the mass concrete standard specifications is presented in Appendix C.

3.1 Literature Review

GDOT Special Provision to Section 500 (GDOT, 2013) has been approved by the Federal Highway Administration (FHWA) and is currently acceptable for any mass concrete project in Georgia. In light of the current provision, this section provides a literature review of ACI standards and other state DOT mass concrete specifications.

3.1.1 U.S. Mass Concrete Specifications and Guides

3.1.1.1 American Concrete Institute specifications for structural concrete (ACI 301-16)

The ACI does not use specific size limits to define mass concrete. The characteristic that distinguishes mass concrete from other concrete elements is its thermal behavior, which

may “cause a loss of structural integrity and monolithic action” (ACI 301-16, 2016). ACI 301-16 “Specifications for Structural Concrete” defines mass concrete as “any volume of structural concrete in which a combination of dimensions of the member being cast, the boundary conditions, the characteristics of the concrete mixture, and the ambient conditions can lead to undesirable thermal stresses, cracking, deleterious chemical reactions, or reduction in the long-term strength as a result of elevated concrete temperature due to heat of hydration.” The following temperature limits apply for mass concrete placements:

- The maximum temperature in concrete after placement shall not exceed 160 °F (71.1 °C).
- The maximum temperature difference between the center and the surface of the placement (i.e., gradient temperature) shall not exceed 35 °F (19.4 °C).

For mass concrete placements, the ACI specification requires the use of hydraulic cement with moderate to low HoH (ASTM C150 Type I or Type II cement), or the use of Portland cement with fly ash or slag cement, or the use of both. No specific limits are stated for the percentage of cementitious materials used; however, the maximum percentage replacement by mass (i.e., 25% for fly ash conforming to ASTM C618 and 50% for slag conforming to ASTM C989/C989M) is specified for concrete assigned to Exposure Class F3. This class includes concrete exposed to severe freezing and thawing cycles in continuous contact with moisture and to deicing chemicals. For any mass concrete placement, the specifications typically require a thermal control plan by the contractor. The thermal control plan includes the following items:

- Concrete mixture proportions

- Calculated or measured adiabatic temperature rise of concrete
- Upper limit for concrete placement temperature
- Calculated maximum temperature and temperature difference in placement
- Description of specific measures and equipment that will be used to ensure that the maximum temperature and temperature difference will not exceed specified limits
- Drawing that shows locations for temperature sensors and a description of the equipment and procedures that will be used to monitor and log temperatures and temperature differences
- Format and frequency of providing temperature data
- Description of curing methods and formwork removal procedures

The temperature and temperature difference within the concrete "shall be controlled from time of placement until time when the internal temperature has cooled from its maximum so that the difference between average daily ambient and internal temperatures is less than a specified temperature difference limit." To monitor concrete temperature, ACI recommends placing one temperature sensor at the mass placement center and another sensor at a depth of two inches from the center of the nearest exterior surface. Additional backup sensors need to be placed at each location. Finally, a temperature sensor must be placed in a shaded location for monitoring ambient on-site temperature.

ACI specifications also require mass concrete to be cured and protected for a minimum of seven days. The use of water curing is not recommended, though the following methods are: "ponding, continuous fogging or sprinkling, application of mats or fabric kept continuously wet, continuous application of steam kept under 150 °F (65.6 °C), application of sheet materials conforming to ASTM C171, and application of curing compound

conforming to ASTM C309 or C1315." For surfaces not in contact with forms, one of the aforementioned curing methods is recommended.

3.1.1.2 ACI guide to mass concrete (ACI 207.1R)

This document (ACI 207.1R-05, 2012) covers the history of the development of mass concrete practice and a discussion of materials and concrete mixture proportioning, properties, construction methods, and equipment. Detailed guidance in proportioning mass concrete is presented in ACI 211.1 (Standard Practice for Selecting Proportions for Normal, Heavyweight, and Mass Concrete), mainly in Appendix 5 (ACI 211.1-91, 2009). Type II moderate heat cements are recommended for use in mass concrete placements as they generate moderate heat during hydration. Type II cement must be specified with the moderate heat option and contain no more than 8% tricalcium aluminate (C3A), a compound that contributes to early heat development. Type IV and low-heat cements are also recommended, although they are difficult to obtain and infrequently used in cement production today.

The ACI 207.1R recommends controlling the temperature of concrete by implementing the following measures to reduce thermal stresses and control cracks:

- Control the cementitious material content and use suitable type of materials to lower the heat-generating potential of the concrete.
- Pre-cool ingredients and post-cool the concrete to lower temperature.
- Protect the structure from excessive temperature differentials through construction management.

The guide further recommends that temperature control measures for mass concrete placements can include a prudent selection of low-heat-generating cement systems, such as

- using pozzolans,
- controling aggregate grading and the use of large-size aggregate in mixtures with low cement contents,
- lowering the placement temperature by pre-cooling the aggregate and mixing water or using ice instead of mixing water,
- using chemical admixtures to improve both fresh and hardened properties of concrete,
- using appropriate block dimensions for placement and coordinating construction schedules with seasonal changes to establish lift heights and placing frequencies,
- using special mixing and placing equipment to quickly place cooled concrete with minimum absorption of ambient heat,
- post-cooling by circulating cold water through embedded piping,
- properly curing the surface, and
- insulating surfaces to minimize thermal differentials between the interior and exterior of the concrete.

Lastly, the guide states that mass concrete should be water-cured for at least 14 days, or up to twice this amount of time if a pozzolan is used as one of the cementitious materials.

3.1.1.3 ACI technical report on mass concrete (ACI 207.2R)

The ACI 207.2R report on "Thermal and Volume Change Effects on Cracking of Mass Concrete" (ACI 207.2R-07, 2007) presents a discussion of the effects of heat generation, restraint, and volume change on the design and behavior of mass concrete elements and structures. Discussion of various factors that influence mass concrete cracking and volume change is presented. What differs ACI 207.1R from ACI 207.2R is that the former is a general guide on mass concrete, whereas the latter provides additional information and detailed discussion on cement types and effects on heat generation, thermal issues, thermal properties, thermal property values for some mass concrete, factors influencing cracking, and example computations.

3.1.1.4 AASHTO and FHWA construction specifications

Two specifications are noteworthy although they are not specific to mass concrete structures. The American Association of State Highway and Transportation Officials (AASHTO) (AASHTO LRFD, 2017) specify that the maximum temperature within concrete should not exceed 158 °F (70 °C) if a known potential for ASR or DEF exists. Otherwise, the maximum concrete temperature is 180 °F (82 °C). A maximum temperature of 160 °F (71.1 °C) is specified for precast concrete. The Standard Specifications (FP-14) for Construction of Roads and Bridges on Federal Highway Projects (FHWA FP-14, 2014) specifies temperature limits for high performance concrete in bridge decks, approach slabs, and other structural elements as follow:

- The placement temperature should be maintained between 50 °F and 80 °F (10 °C and 26.7 °C).
- The maximum internal temperature should not exceed 140 °F (60 °C).

- The minimum surface temperature is 45 °F (7.2 °C).
- The maximum temperature differential should not exceed 35 °F (19.4 °C).
- Maturity meter probes need to be installed to monitor concrete temperatures according to AASHTO T 325.
- Internal cooling, external heating, or insulation needs to be provided to insure the temperature differential does not exceed 35 °F (19.4 °C) during placing, curing, cooling, form stripping, and after curing ends.
- Flatwork needs to be cured for at least 14 days and structural elements for at least 10 days.
- The maximum temperature in prestressed concrete should not exceed 160 °F (71.1 °C).

For structural concrete, the maximum percent of total cementitious material by mass should be limited to 25% for fly ash or other pozzolans (AASHTO M 295), 50% for slag (AASHTO M 302), and 50% for fly ash and slag together. The maximum water-to-cementitious material ratio of 0.54 is used for concrete Class S (Seal).

3.1.2 **U.S. State DOTs Mass Concrete Specifications**

The authors have reviewed available state DOT specifications to gain a comprehensive understanding of mass concrete temperature and other requirements. A reasonable effort was made to locate and identify specifications on each state DOT website. Only 23 states appeared to have mass concrete specifications or mass concrete special provisions publicly available. Table 8 lists these states, Table 9 presents available document types, and Figure 34 shows a map of US states which have mass concrete specifications or provisions

publicly available. Mississippi and New Hampshire provide maximum temperature limits only for normal concrete placements in their specifications. A summary of the mass concrete requirements is organized by eleven subtitles:

1. Mass concrete definition
2. Maximum temperature and temperature differential limits
3. Maximum placement temperature
4. Maximum and minimum total SCM content
5. Percentage of SCM replacement allowed
6. Compressive strength and/or HoH requirements
7. Water to cementitious material ratio and slump requirements
8. Curing requirements
9. Formwork removal time
10. Methods to cool down concrete temperature
11. Temperature monitoring requirements

Table 10 through Table 21 summarize these requirements. Figure 34 through Figure 40 provide visual representations of selected items on maps. For these figures, a US map template was obtained from yourfreetemplates.com and modified to present the differences in state DOT mass concrete requirements.

Table 8 – State DOTs that publish mass concrete specifications.

Publish	Do Not Publish (or are not found)
	Alabama
	Alaska
	Arizona
Arkansas, 2014	Colorado
California, 2015	Connecticut
Delaware, 2017	Connecticut
Florida, 2017	District of Colombia
Georgia, 2013	Hawaii
Idaho, 2017	Indiana
Illinois, 2016	Kansas
Iowa, 2015	Maine
Kentucky, 2012	Maryland
Louisiana, 2018	Michigan
Massachusetts, 2015	Missouri
Minnesota, 2018	Montana
Mississippi*	Nebraska
New Hampshire*	Nevada
New Jersey, 2016	New Mexico
New York, 2019	North Dakota
North Carolina, 2018	Oklahoma
Ohio, 2016	Oregon
Rhode Island, 2016	Pennsylvania
South Carolina, 2007	South Dakota
Texas, 2014	Tennessee
Virginia, 2016	Utah
West Virginia, 2010	Vermont
	Washington
	Wisconsin
	Wyoming

Note: * indicates state published concrete specifications in which mass concrete requirements are provided.

Table 9 – Mass concrete document type by state DOT.

DOTs	Type of Mass Concrete Specification
Arkansas	Standard Specifications for Highway Construction (ArDOT, 2014)
California	Standard Specifications (Caltrans, 2015)
Delaware	Standard Specifications for Road and Bridge Construction (DelDOT, 2016)
Florida	Standard Specifications for Road and Bridge Construction (FDOT, 2017)
Georgia	Special Provision (GDOT, 2013)
Idaho	Standard Specifications for Highway construction (IDT, 2017)
Illinois	Standard Specifications for Road and Bridge Construction (IDOT, 2016)
Iowa	Standard Specifications (Iowa DOT, 2015)
Kentucky	Standard Specifications for Road and Bridge Construction (KYTC, 2012)
Louisiana	Standard Specifications for Roads and Bridges (DOTD, 2016)
Massachusetts	Supplemental Specifications (MassDOT, 2015)
Minnesota	Standard Specifications for Construction (MnDOT, 2018)
Mississippi	Standard Specifications for Road and Bridge Construction (MDOT, 2017)
New Hampshire	General Provisions (NHDOT, 2016)
New Jersey	Standard Specifications for Road and Bridge Construction (NJDOT, 2007)
New York	Standard Specifications (NYSDOT, 2019)
North Carolina	Standard Specifications for Roads and Structures (NCDOT, 2018)
Ohio	Construction and Material Specifications (ODOT, 2016)
Rhode Island	Special Provisions (RIDOT, 2016)
South Carolina	Standard Specifications for Highway Construction (SCDOT, 2007)
Texas	Standard Specifications for construction and Maintenance of Highways, Streets, and Bridges (TxDOT, 2014)
Virginia	Road and Bridge Specifications (VDOT, 2016)
West Virginia	Standard Specifications for Roads and Bridges (WVDOT, 2010)

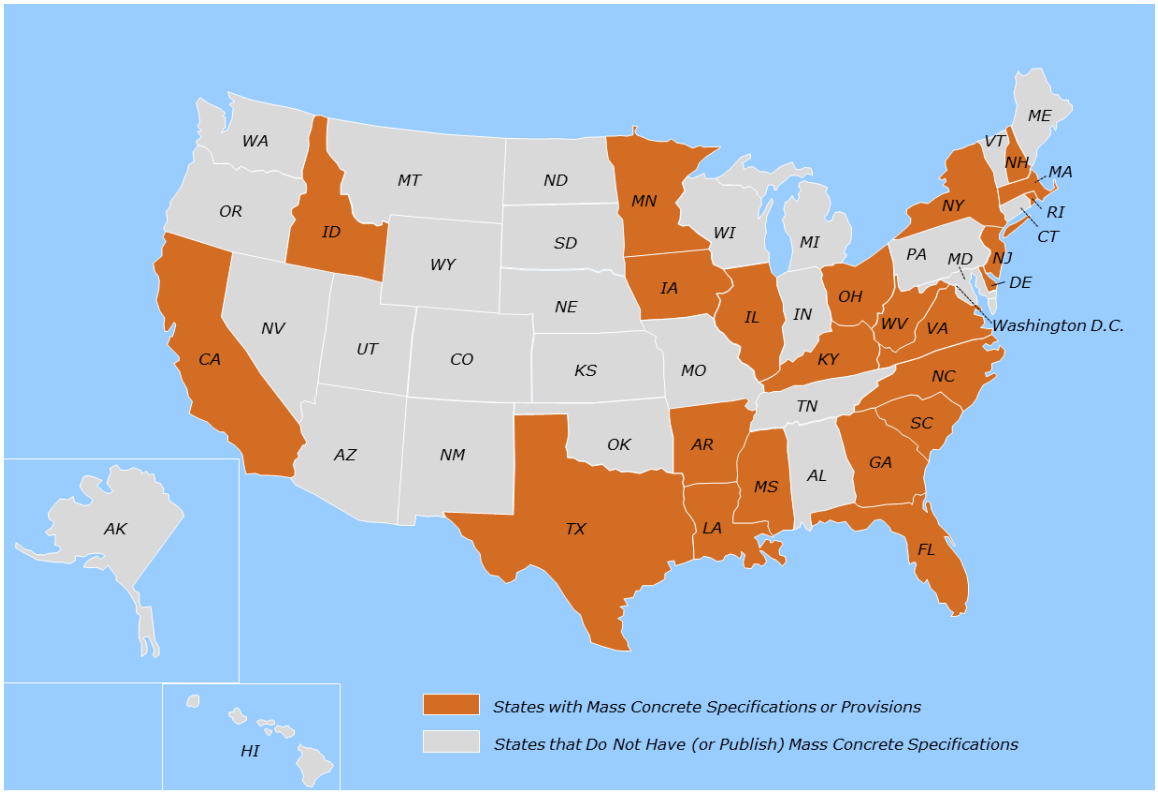

Figure 34 – US states with mass concrete specifications publicly available.

Table 10 – Mass concrete definition by state DOT.

DOTs	Mass Concrete Definition
California	Minimum dimension exceeding 7 feet shall be constructed as mass concrete. Any large volume of cast-in-place concrete with dimensions large enough to require that measures be taken to cope with generation of heat and attendant volume change to minimize cracking.
Delaware	Designers are responsible to identify.
Florida	• Concrete with a minimum dimension exceeding 3 feet and the ratio of volume of concrete to the surface area greater than 1 foot. • All drilled shafts with design diameters greater than 6 feet.
Georgia	• Any large volume of cast-in-place concrete with dimensions large enough to require measures be taken to cope with the generation of heat and attendant volume change to minimize cracking. • Any substructure concrete element whose least dimension is greater than 5 feet (excluding drilled shafts).
Idaho	Placements thicker than 4 feet.
Illinois	Concrete structures when the least dimension for a drilled shaft, foundation, footing, substructure, or superstructure concrete pour exceeds 5 feet (1.5 m).
Iowa	• Any concrete footing with a least dimension greater than 5 feet. • Other concrete placements with a least dimension greater than 4 feet.
Kentucky	Any concrete placement, excluding drilled shafts, with a least plan dimension of 6 feet or greater.
Louisiana	Structural concrete placement with a least dimension of 4 feet or greater, or if designated on the plans or in the project specifications as mass concrete.
Massachusetts	• Cement concrete placements where all volumetric dimensions of the placement are 4 feet (1.2 m) or greater. • Cement concrete placements of other dimensions where measures must be taken to mitigate potential cracking caused by heat of hydration when such placements are specifically designated as mass cement concrete on the plans.
Minnesota	Least dimension of 4 feet.
North Carolina	Substructure components (footings, columns, or caps) when the smallest dimension of that component is between 6 feet and 8 feet.
Ohio	• Components with a minimum dimension of 5 feet (1.5 m) or greater. • Drilled shafts with a dimension of 7 feet (2.1 m) diameter or greater.
Rhode Island	Any element with the ratio of the total volume to the surface area equal to or exceeding 0.6 and a minimum dimension of 3 feet in any of the 3 planes.
South Carolina	Pour that has dimensions of 5 feet or greater in 3 different directions. For circular cross-sections, a pour with a diameter of 6 feet or greater and a length of 5 feet or greater. Mass concrete requirements do not apply to Drilled Shafts (Class 4000DS) and Foundation Seals (Class 4000S).
Virginia	All reinforced concrete elements (pier, abutment, footing, or drilled shaft cap) with minimum dimension exceeding 5 feet.
West Virginia	Concrete placements with least dimension exceeding 4 feet, excluding Drilled Caissons, tremie seals, and Class D Concrete.

Note: 1foot = 0.3 meter.

Table 11 – Temperature limit requirements by state DOT.

State DOT	Maximum Temperature (°F)	Maximum Temperature Differential (°F)
Arkansas	NS	36
California	160	must not exceed the limit in control plan
Delaware	160	Varies (30-60) °F • First 24 hours: 30 °F • 24 to 48 hours: 40 °F • 2 to 7 days: 50 °F • 7 to 14 days: 60 °F
Florida	180	35
Georgia	158	35
Idaho	NS	35
Illinois	150	35 (option to propose up to 50 °F justified through strength and mathematical method)
Iowa	160	Varies (20-50) °F • First 24 hours: 20 °F • 24 to 48 hours: 30 °F • 48 to 72 hours: 40 °F • After 72 hours: 50 °F
Kentucky	160	35
Louisiana	160	35
Massachusetts	154	38
Minnesota	160	Varies (45-60) °F • First 48 hours: 45 °F • 2 to 7 days: 50 °F • After 8 days: 60 °F
Mississippi	160	35
New Hampshire	160	NS
New Jersey	160	35
New York	160	35
North Carolina	158	35
Ohio	160	36
Rhode Island	155	35
South Carolina	NS	35
Texas	160	35
Virginia	• 160 for fly ash mixtures • 170 for slag mixtures	35
West Virginia	160	40

Note: (°C x 9/5) + 32 = °F.

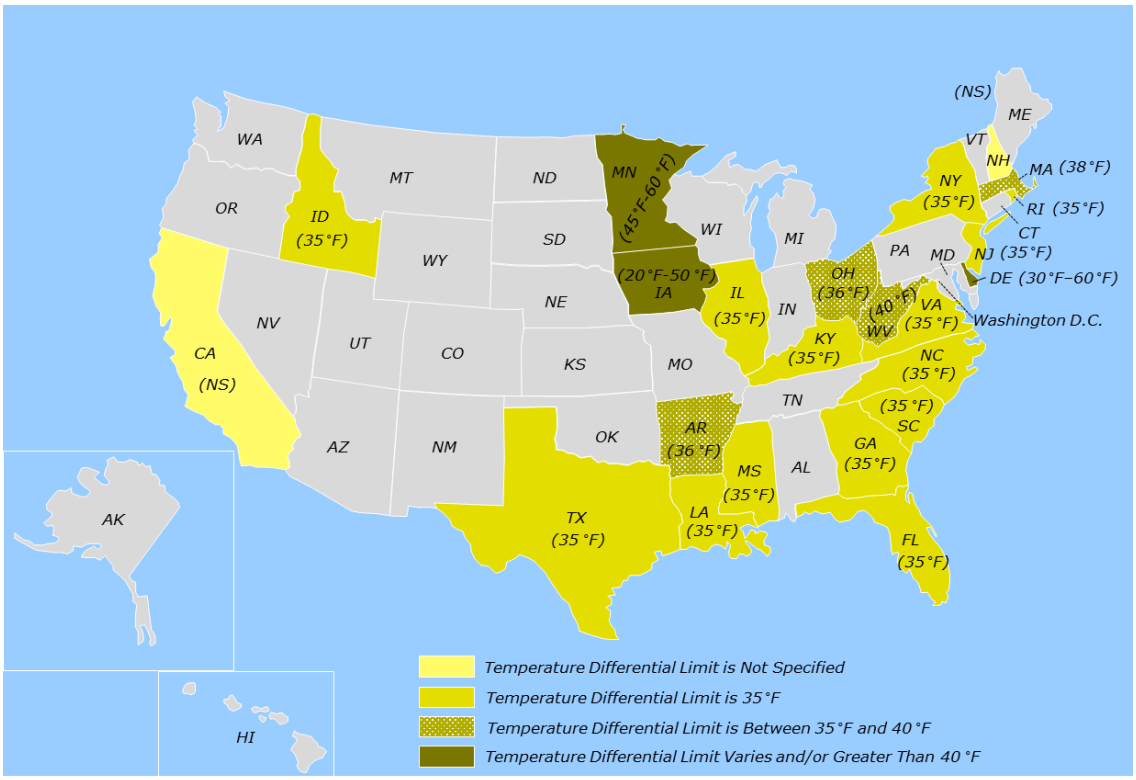

* NS = Not Specified

Figure 35 – Temperature differential limits by state DOT.

Table 12 – Maximum concrete placement temperature requirements by state DOT.

State DOT	Maximum Placement Temperature, °F
Arkansas	75
Delaware	70
Georgia	85
Illinois	Maximum: article 1020.14 Minimum 40
Iowa	Maximum 70 Minimum 40
Kentucky	70 (60 for Seal)
Massachusetts	90
Mississippi	95
New Hampshire	85
New Jersey	Maximum 90 Minimum 60
North Carolina	Maximum 75 Minimum 40
Ohio	95
Rhode Island	85 for hot weather 65 for cold weather
South Carolina	80
Texas	Maximum 75 Minimum 50
Virginia	95

Note: (°C x 9/5) + 32 = °F.

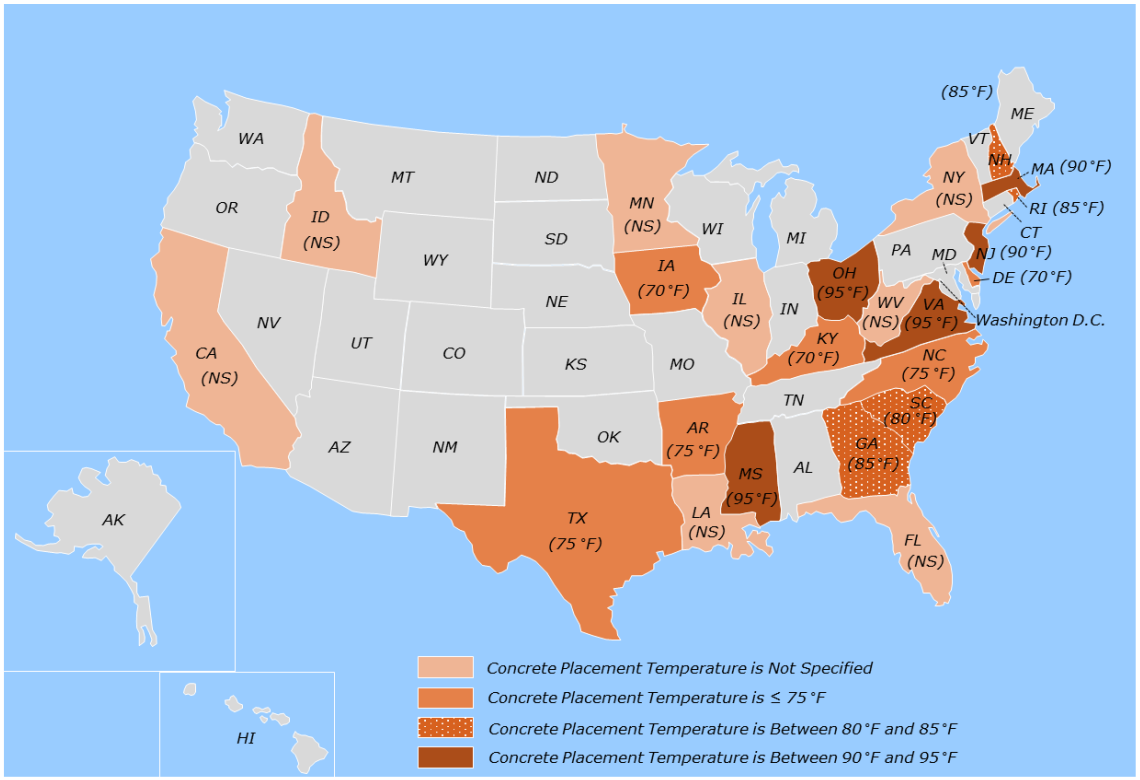

* NS = Not Specified

Figure 36 – Concrete placement temperature limits by state DOT.

Table 13 – Minimum and maximum SCM content requirements by state DOT.

State DOT	Minimum SCM Content, lb/cy	Maximum SCM Content, lb/cy
Arkansas	Class B	Class B
California	N/A	For CIP Pile: 750 for diameter between 8’ to 10’ 720 for diameter between 10’ to 14’
Florida	470 for type ll Concrete 658 for type lV Concrete 611 for Seal (not considered as MC) 658 for Drilled Shaft	N/A
Idaho	660 for Seal Concrete	N/A
Illinois	520 for central mixed 550 for truck or shrink mixed Underwater: 550 for central mixed Underwater: 580 for truck mixed 605 for Drilled Shaft 635 for underwater or self-consolidating	N/A
Iowa	560	N/A
Kentucky	564	N/A
New Hampshire	Concrete Class T for Foundation Seal	N/A
New Jersey	611 for Drilled Shaft 658 for Seal	N/A
New York	N/A	700
North Carolina	N/A	600
Ohio	470 for Mass Concrete 470 or 520 for Drilled Shaft	N/A
Rhode Island	500 for Mass Concrete Class X for Drilled Shaft 400 for Tremie Seal	600 for Mass Concrete 700 for Tremie Seal
South Carolina	625 for Drilled Shaft 682 for Foundation Seal	N/A
Texas	N/A	700
Virginia	494 for massive or lightly reinforced 423 for massive unreinforced 635 Tremie Seal	N/A
West Virginia	494	N/A

Table 14 – Fly ash and slag replacement content requirements by state DOT.

State DOT	Fly ash	Slag
Arkansas	Maximum 120 lb/cy	Maximum 25%
California	At least 25% for CIP Pile	
Delaware	Maximum 75%	Maximum 75%
Florida	Must 18 to 50% if core temperature is < 165 °F Must 35 to 50% if core temperature is > 165 °F Must 33 to 37% for drilled shaft	Must 50 to 70% Must 58 to 62% for Drilled Shaft
Georgia	Class F fly ash may comprise no more than 40% by mass of total cementitious and pozzolanous materials	Slag may comprise no more than 75% by mass of total cementitious and pozzolanous materials
Illinois	Maximum 40%	Maximum 65%
Iowa	Maximum 20%	Maximum 35%
Kentucky	25 to 30% with substitution rate of 1 to 1.25 lb of fly ash for 1 lb of cement	Maximum 50% With substitution rate of 1 lb of slag for 1 lb of cement
Louisiana	20 to 50%	50 to 70%
Minnesota	Maximum 30%	Maximum 70%
Mississippi	20 to 25%	45 to 50%
New Jersey	Maximum 25%	Maximum 50%
New York	20 to 50%	30 to 70%
North Carolina	25%	25%
South Carolina	2:1 ratio by weight for fly ash not more than 20%	50%
Ohio	Maximum 25% or 50%	Maximum 30% or 50%.
Rhode Island	Maximum 30%	Up to 75%
Texas	Maximum 45%	35 to 50%
Virginia	25 to 40%	50 to 75%
West Virginia	Maximum 25%	Maximum 50%

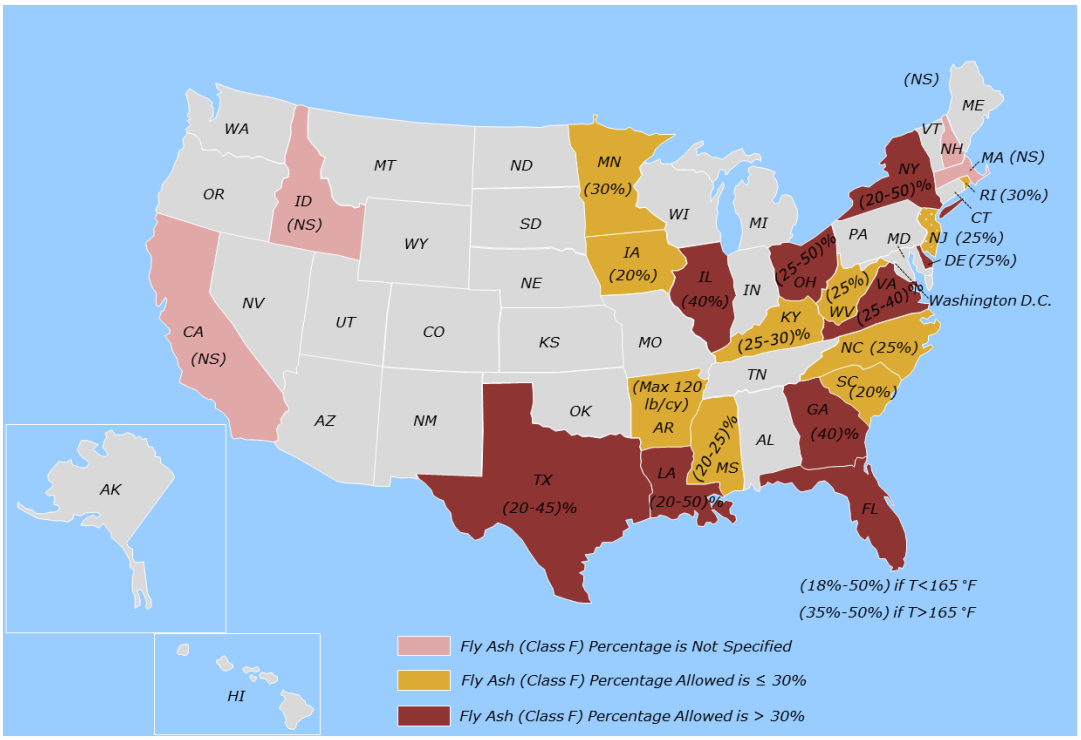

* NS = Not Specified

Figure 37 – Fly ash (Class F) content limits by state DOT.

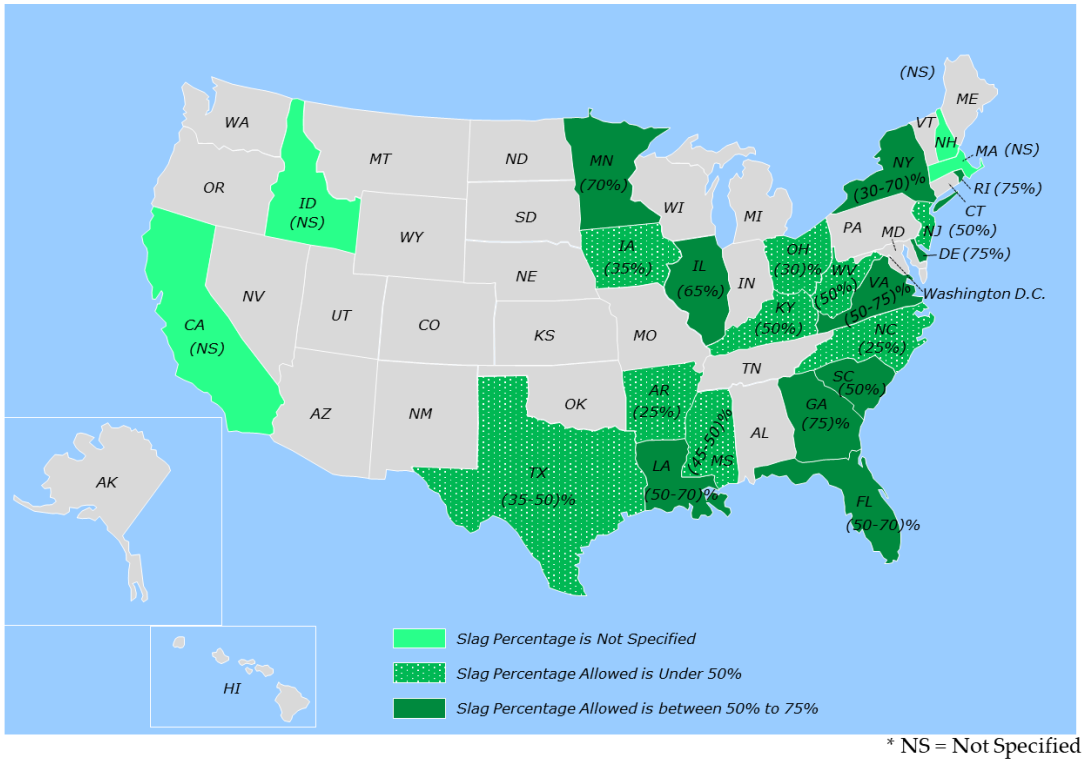

* NS = Not Specified

Figure 38 – Slag content limits by state DOT.

Table 15 – Ternary replacement and other SCM limits by state DOT.

State DOT	Ternary and Other SCM Mixture Content Limits
Florida	Use 50% to 55% slag of total SCM when used in combination with SF, ultra-fine fly ash, and MK.
Georgia	When a combination of multiple different pozzolans is used, the total amount may be no more than 75% by mass of total cementitious and pozzolanous materials.
Illinois	• Microsilica or high reactivity MK portion used together or separately shall not exceed 5.0 percent. • Mixture may contain a maximum of two finely divided minerals.
Iowa	• Maximum total substitution of Portland cement shall not exceed 50%, including the amount in the blended cement. • Use any combination of GGBF slag or Class F fly ash. • Maximum substitution of 20% with Class C fly ash.
Kentucky	For mixtures with both GGBF slag and Class F fly ash, permit up to but no more than 20% of the 50% GGBF slag maximum as Class F fly ash.
Louisiana	Ternary mixture meeting specification requirement.
Minnesota	• Maximum replacement of 70% by weight in ternary mixtures. • SF maximum 5%.
New Jersey	Maximum of 5 % SF by weight.
Ohio	Microsilica 10% maximum.
Rhode Island	Mass concrete mixture may have a total SCM of 75% of total SCM material when using either slag or combination of slag and other SCMs.
Texas	Replace 35% to 50% of the cement with a combination of Class F fly ash, slag cement, modified F fly ash (MFFA), ultra-fine fly ash (UFFA), MK, or SF; however, no more than 35% may be fly ash, and no more than 10% may be SF. 4.2.6.4.
West Virginia	Combination of total fly ash and slag of 50%.

Table 16 – Strength and heat generation criteria by state DOT.

State DOT	Other Criteria	
	Compressive Strength	**Heat of Hydration/ Temperature Rise**
Arkansas	3000 psi at 28 days 3500 psi at 90 days	N/A
Florida	4000 psi at 28 days for Drilled Shaft	N/A
Georgia	Meet 28 or 56-day strength requirement	N/A
Kentucky	2600 psi at 7 days 3500 psi at 28 days	N/A
Louisiana	N/A	HoH of less than 70 calories/gm at 7 days
Minnesota	4000 psi for abutments and piers at 28 days 4500 psi for footing at 28 days Same criteria for mixtures including SCM but at 56 days of strength	N/A
Mississippi	3000 psi at 28 days	N/A
New Jersey	4600 psi at 28 days for Drilled Shaft 2000 psi at 28 days for Tremie Seal	N/A
New York	6000 psi at 56 days	N/A
Ohio	4000 psi at 28 or 56 days 4500 psi at 28 or 56 days	N/A
Rhode Island	3500 psi at 28 days 5000 psi at 56 days	Maximum Adiabatic Temperature Rise of 75 °F
South Carolina	4000 psi at 28 days for Drilled Shaft 4000 psi at 28 days for Foundation Seal	Mass concrete requirements do not apply to Drilled Shafts (Class 4000DS) and Foundation Seals (Class 4000S).
Texas	3600 psi at 28 days for Drilled Shaft	N/A
Virginia	2200 psi at 28 days for B2 1500 psi at 28 days for C1 3000 psi at 28 days for T3	N/A
West Virginia	2500 psi at 28 days	N/A

Table 17 – Water-to-cementitious material ratio and slump by state DOT.

State DOT	Water to Cementitious Ratio	Slump (inch)
Arkansas	Maximum 0.49	1 - 4
Florida	Maximum 0.53 for Type ll Concrete Maximum 0.41 for Type lV Concrete Maximum 0.41 for Drilled Shaft	5 - 8.5
Iowa	Maximum 0.45	Maximum 6
Kentucky	Maximum 0.47	4 - 8
Louisiana	Maximum 0.53 for Mass A1 Maximum 0.46 for Mass A2 Maximum 0.36 for Mass A3 Maximum 0.53 for Class S	2 - 4 Maximum 8 if water reducers used
Minnesota	0.3 - 0.45	2 - 5
Mississippi	Maximum 0.55	4 - 8
New Hampshire	Maximum 0.559	1 - 3
New Jersey	Maximum 0.443 for Class A	6 - 8
New York	Maximum 0.4	7 - 9
Ohio	Maximum 0.44	1 - 4 for MC 5 - 7 for DS
Rhode Island	Maximum 0.4	2 - 4
South Carolina	N/A	7 - 9
Texas	Maximum 0.45 for Drilled Shaft	N/A
Virginia	Maximum 0.4	N/A
West Virginia	Maximum 0.58	N/A

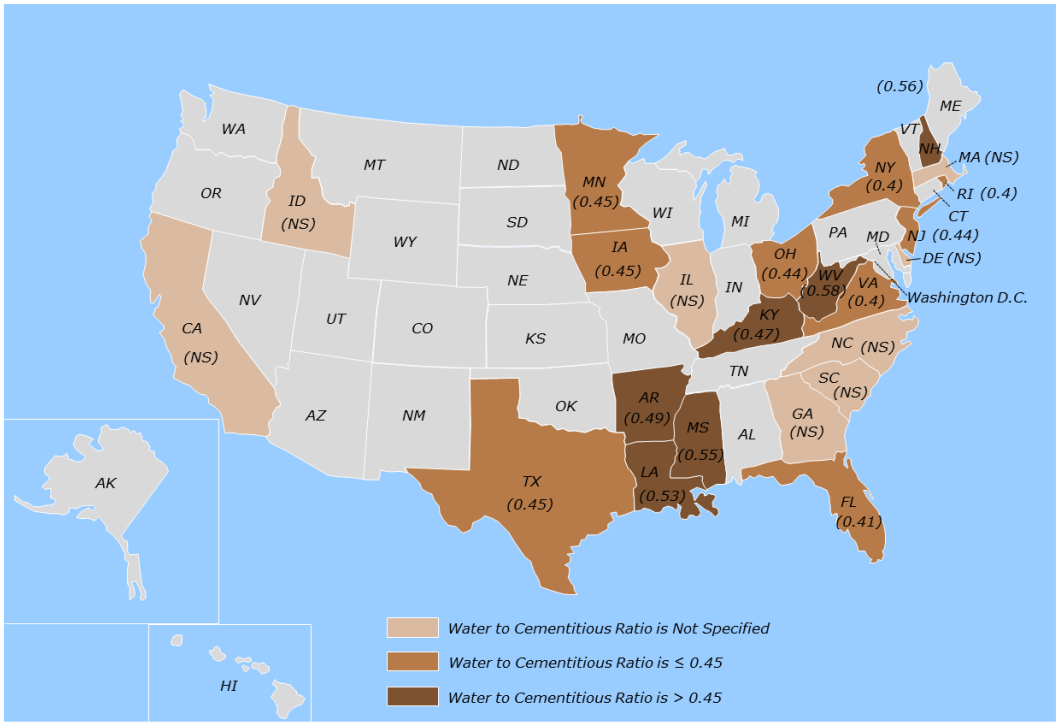

* NS = Not Specified

Figure 39 – Water-to-cementitious material ratio recommended for mass concrete by state DOT.

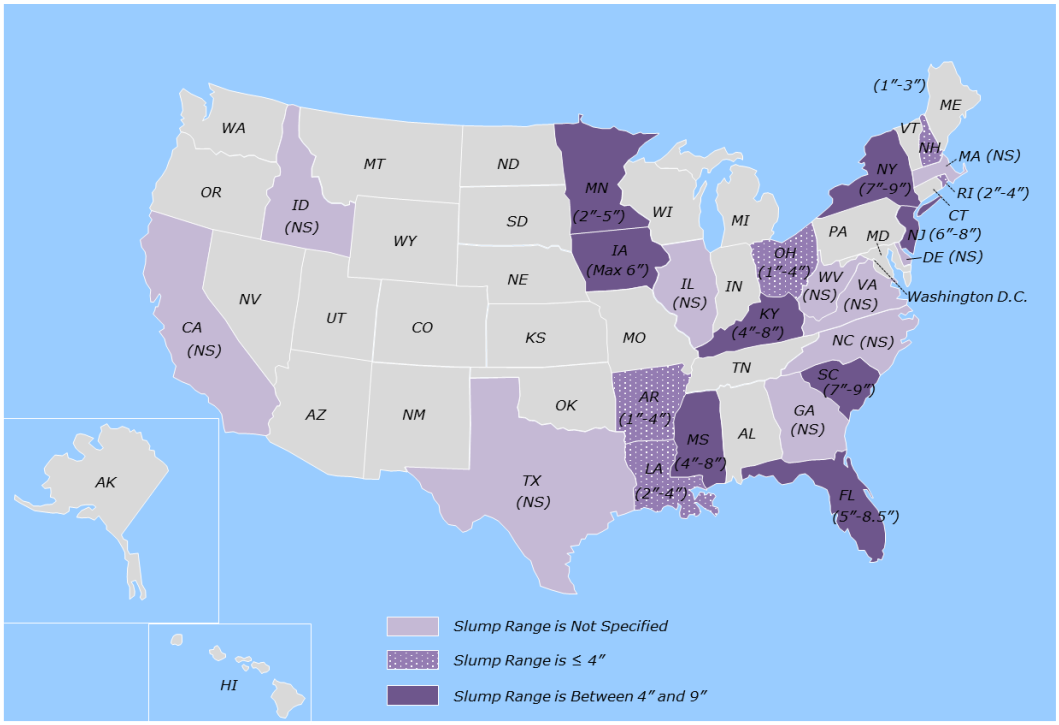

* NS = Not Specified

Figure 40 – Slump recommended by state DOT.

Table 18 – Curing period requirements by state DOT.

State DOT	Curing Requirement
Arkansas	• Class B concrete shall be cured by free moisture. • Water curing shall be provided for all exposed surfaces for 14 days.
Delaware	Maintain curing methods in place until the full 5 days have elapsed or the compressive strength of the concrete has reached 2,000 psi.
Florida	Continuously cure the freshly placed concrete for a period of 72 hours, exclusive of any periods when the temperature of the surface of the concrete falls below 50 ºF.
Illinois	The time to obtain the specified strength may be increased to a maximum 56 days, provided the curing period is increased to a minimum of 14 days
Louisiana	Allow foundation concrete for roadway barriers and pier protection systems a minimum of three days curing time.
Massachusetts	• The area of concrete to be cured shall be covered by wet burlap blankets placed as soon after concrete finishing as the Engineer determines will not cause damage to the concrete surface. However, in no case will the foregoing time period exceed 1 hour after placing of concrete. • Fog spray or covers shall be used continuously during this period. • The burlap shall be completely saturated over its entire area by being submerged in water for at least 8 hours before the start of the placement.
Mississippi	After the 4-hour curing period, the material shall show no tackiness or no tendency to stick to your finger when pressed.
New York	Temperature/time relation (interior of concrete with autogenous curing boxes) for 7 days measuring at hourly intervals.
Rhode Island	• Mass concrete placements shall be continuously moist cured for at least 14 days and until the 28-day compressive strength as indicated by the approved Maturity Curve is achieved. • Maintaining moisture on the top surface with forms in place shall be considered adequate moist curing. • If strength and thermal control are achieved prior to 14 days, forms may be removed but moist curing must be continued.
South Carolina	• If curing blankets used, they shall conform to the requirements found in Subsection 702.3.4, and remain in place for a minimum of 4 days. • Re-wetting of the curing blankets may not be required if they remain wet and the edges remain sealed throughout the 7-day curing period.
Virginia	The minimum curing period shall be 1 week.
West Virginia	• All mass concrete elements shall be kept completely and continuously moist by means of moisture retention. • White polyethylene sheeting per standard requirements shall be used. • Water curing shall not be permitted. • Curing shall be continued for a period of at least 7 calendar days.

Table 19 – Formwork removal time requirements by state DOT.

State DOT	Formwork Removal Time Requirement
Arkansas	• Forms shall remain in place 4 days after placing any time the temperature is below 40 °F or forecast to drop below 40 °F. • Exposed top surfaces of the concrete shall be protected with an insulated blanket. • Surface of the concrete shall not be saturated when it is exposed to freezing air temperatures.
Idaho	Protect concrete with forms for at least 7 calendar days.
Minnesota	• Maximum peak temperature is reached and drops by more than 3 °F. • Maximum temperature differential is reached and drops by more than 3 °F. • Temperature difference between the ambient and the point 2 inches from the surface has reached its maximum, drops by more than 3 °F, and doesn't exceed 35 °F. • Minimum of 72 hours for bridge substructures and 96 hours for bridge superstructures. • Gradually discontinue heating or cooling protection in a manner such that the rate of temperature reduction adjacent to the concrete surface does not exceed 20 °F during any 12-hour period until the surface temperature reaches that of the ambient temperature outside any cold weather protection.
Rhode Island	• Forms shall remain in place until the estimated strength of the concrete surface exceeds 2500 psi based on the lowest indicated maturity from the data loggers and until the differential between the mean center temperature and ambient temperature is less than 30 °F and decreasing. • Ambient temperatures must be rising at the time of form removal. • Forms shall not be removed prior to meeting all other requirements listed elsewhere in the Contract Documents.
Texas	Keep forms for mass placements in place for 4 days following concrete placement unless otherwise approved based on the outcome of the heat control plan.
Virginia	• The forms may be stripped when the concrete strength is high enough to withstand the anticipated thermal gradient between the core temperature and the 48-hour average air temperature, or as directed by the Engineer. • In no event will form stripping be allowed before the surface concrete reaches at least 80% of its design strength. After form striping, concrete shall be protected from freezing temperatures for 48 hours by the use of insulating blankets or other methods approved by the Engineer.
West Virginia	Under good weather conditions, side forms may be removed 24 hours after placing concrete, but the entire pile shall remain supported for at least seven days and shall not be subjected to any handling stress until the concrete has set for at least 14 days or for a longer period in cold weather, according to the judgment of the engineer.

Table 20 – Methods to cool down concrete temperature by state DOT.

State DOT	Methods to Cool Down Concrete Temperature
Arkansas	• Using ice in the mixing water. • Storing cement and aggregates in cool or shaded locations. • Watering down coarse aggregates. • Installing cooling pipes in the concrete. • Insulating via tenting, quilts, or sand on polyethylene sheeting. • Cooling by watering of fine aggregates not allowed.
California	• Coolant circulation shall be in progress at the time that concrete placement begins. The mechanical cooling system shall be embedded within mass concrete elements, and surface connections to cooling pipes shall be removable to a depth of 4 inches from the surface.
Delaware	• Addition of controlled quantities of ice in lieu of equal quantities of mixing water or cooling tubes; however, the mix shall contain no frozen pieces of ice after blending and mixing components. • Use of liquid nitrogen is permitted if included in the Design-Builder's Plan.
Georgia	Mechanical cooling system may be used to control the internal temperature of mass concrete during curing but shall be designed in conformance with the Thermal Control Plan. If a mechanical cooling system is used, the plans for the cooling system operation and final grouting after cooling shall be submitted to the Engineer for approval.
Illinois	• Pre-cooling. • Post-cooling. • Surface insulation methods. • For reinforcement that extends beyond the limits of the pour, the Contractor shall indicate if the reinforcement is required to be covered with insulation.
Iowa	• Cooling component materials prior to adding to the mix. • Adding crushed or shaved ice to the mix water. • Sprinkling coarse aggregate with water or wetting the stockpile. • Controlling rate of concrete placement (low lifts). • Insulating the forms and the surface of the concrete. • Placing concrete at times of day when the ambient temperature is lowest (in summer) or highest (in winter).

State DOT	Methods to Cool Down Concrete Temperature
Kentucky	• Sprinkle the mixer trucks' drums for cooling. • Arrange with supplier to avoid delivery of hot cement. • Cool aggregate stockpiles. • Use a nitrogen gas cooling system to cool the concrete mass before placement. • Use shaved, flaked, or chipped ice as part of the mixing water. • Embed cooling system in structural mass concrete. • Place concrete during the coolest part of the day or during cooler weather.
North Carolina	Methods for reducing thermal differential may involve but are not limited to a combination of the following: • Selecting materials that minimize the heat generated by hydration of the cement. • Cooling materials to reduce the temperature of the concrete in its plastic state. • Controlling the rate of concrete placement. • Insulating the concrete surface to prevent heat loss. • Providing supplemental heat at the concrete surface to prevent heat loss.
Rhode Island	• Use low-heat concrete mixtures. • Pre-cool the concrete. • Insulate curing blankets. • Insulate forms. • Cool pipes and other measures.
Texas	The heat control plan may include a combination of the following elements: • Selection of concrete ingredients including aggregates, gradation, and cement types to minimize heat of hydration. • Use of ice or other concrete cooling ingredients. • Use of liquid nitrogen dosing systems. • Controlling rate or time of concrete placement. • Use of insulation or supplemental external heat to control heat loss. • Use of supplementary cementing materials. • Use of a cooling system to control the core temperature. • Variation in the duration formwork remains in place.

Table 21 – Temperature monitoring requirements by state DOT.

State DOT	Temperature Monitoring Requirement
Arkansas	Monitor temperature for 7 days.
Georgia	Monitor and maintain records of the concrete temperature, beginning with casting and continuing until the maximum temperature is reached and begins decreasing to a differential of no more than 35 °F from the mean annual ambient temperature of the surrounding environment, for three consecutive days.
Illinois	Temperature monitoring may be discontinued after the maximum concrete temperature has been reached, post-cooling is no longer required, and the maximum temperature differential between the internal concrete core and the ambient air temperature does not exceed 35 °F. The Contractor has the option to select a higher maximum temperature differential, but the proposed value shall not exceed 50 °F.
Iowa	Thermal control of each placement shall be maintained until the temperature of the interior is within 50 ºF of the average outside air temperature.
Kentucky	• Maintain thermal control of each placement until the temperature at the center is within 35 °F of the average outside air temperature. • Begin measuring temperature differential 12 hours after the last concrete placement.
New Jersey	Monitor the temperature until the interior temperature is within 35 °F of the lowest ambient temperature or a maximum of 15 days.
New York	Temperature readings will continue until the maximum temperature differential (not maximum temperature) is reached and a decreasing temperature differential is confirmed as defined in the Thermal Control Plan.
North Carolina	Mass concrete should remain covered and monitored until the difference between the core temperature and the average daily ambient temperature is below 35 °F. All mass concrete pours shall remain covered and protected a minimum of 7 days unless otherwise directed by the Engineer.
Rhode Island	Mass concrete temperature control procedures shall remain in effect until the temperature differential between the average peak temperature and the 3-day mean ambient low temperature is less than 35 °F.
South Carolina	Continue monitoring temperature until the interior temperature is within 35 ºF of the lowest ambient temperature or a maximum of 2 weeks.

3.1.3 **Thermally Induced Cracking**

As introduced in Section 1.1.1, one of the most important characteristics of mass concrete is its thermal behavior. Thermal behavior is related to temperature changes within a mass concrete element which, if not controlled, will result in significant cracking. Thermal cracking caused by elevated temperatures in mass concrete structures is an important phenomenon, mainly originated and induced by a hydration reaction of cementitious binders present in concrete mixtures. The key factor contributing to temperature rise in cement is heat development as a result of an exothermic chemical reaction. In most structural concrete elements, this heat is rapidly dissipated from exposed surfaces, minimizing temperature differentials within the elements. In contrast, in mass concrete structures such as foundations, the heat dissipation is uneven and problematic if not actively controlled. Furthermore, if such structures are allowed to cure while exposed to cold environments, significant differential temperatures will arise between the center of the foundation and its exposed surface. The volume change associated with an increase or decrease in temperature and thermal restraints results in tensile strains and stresses that may cause cracking detrimental to the design, serviceability, or appearance of the structure (ACI 207.2R-07, 2007).

3.1.3.1 Thermal gradient

As concrete volume increases with a constant exposure surface, the heat from cement hydration is trapped within the concrete element. Thus, the heat takes much longer to dissipate. In addition, the outer surfaces of the element cool down at a faster rate since they are in contact with surrounding ambient and environmental temperatures. This creates a structure with a very hot interior temperature and a cooler surface temperature; hence, a

large temperature differential occurs, which can potentially impair structural integrity. This temperature change through a structural section is referred to as a thermal gradient (ACI 207.2R-07, 2007). Significant differences in temperature between the inner and outer parts of a mass concrete element cause thermal gradients. In turn, damage occurs when the cooler outside concrete resists thermal expansion of the inner concrete. This resistance results in the development of thermal strains and stresses. When these thermal strains exceed the tensile strain of concrete, cracks form.

Thermal gradients are categorized as either mass gradient or surface gradient (ACI 207.2R-07, 2007). A mass gradient is the differential temperature between that of a mass concrete structure and a restraining foundation, which acts as an external restraint to the movement of the structure (ACI 207.2R-07, 2007). It is measured as the long-term maximum internal temperature of the mass concrete structure as it cools down from its internal peak temperature to a stable temperature equal to approximately the annual average temperature. Accordingly, this type of gradient relates to time, as the temperature at a given point in the concrete varies over time. The geometry of the structure, properties of the mass concrete and foundation bedrock, and the nature of the contact between the structure and the foundation determine how a mass gradient and its consequent volume change develop into strains and stresses that can cause thermal cracking.

Surface gradients are the result of the concrete surface cooling to the ambient temperature relative to the more stable and high internal temperature (ACI 207.2R-07, 2007). The concrete surface contracts with cooling, and this contraction is restrained by the hot interior of the concrete, which acts as an internal restraint. This type of gradient is the result of temperature differences at any given time between two points in the concrete,

which leads to the development of tensile strains on the surface of the concrete that in turn may result in cracking. The temperature differential, relative to the core of the element, is the highest at the surface of the concrete and rapidly deteriorates with distance from the surface. Thus, the effect of an internal restraint and its consequent stress and cracking is strongest at the surface of the concrete and is dissipated rapidly with distance from the surface. As a result, surface cracking due to ambient temperature changes is usually confined and limited to shallow regions/depths at or near the surface. At times, however, conditions develop where this surface cracking penetrates deeply into the structure and, when combined with mass gradient volume changes or other load conditions, may compound cracking conditions.

3.1.3.2 Degree of thermal restraints

The degree of restraints is defined as the ratio of the actual stress resulting from the volume change to the stress that would result if the elements were completely unrestrained (ACI 207.2R-07, 2007). Restrained volume change can induce tensile, compressive, or flexural stresses in the element. Concrete is weak in tension, and therefore the primary concern is with the tensile stress. Restraints to movements occur externally and internally, and both restraint types exist in mass concrete placements. External and internal restraints are interrelated and usually exist to some degree in all concrete elements.

External restraints exist along the contact surface of concrete and the material it is cast against. They are developed by the supporting element or foundation against the volume change or movement of the mass concrete structure. The degree of this restraint is a function of the structural shape and dimensions of the mass concrete, as well as the stiffness or rigidity of the foundation material. If completely unrestrained and fully

insulated, concrete expands and contracts without creating any stress; however, partial restraints often exist leading to the development of stresses.

Internal restraints develop when one part of the freshly placed concrete expands or contracts differently compared to another part of the same section (Bamforth, 2007). In mass concrete, it is the restraint of the core against the cooling and contracting of the surface. Internal restraints are the result of a temperature differential and its consequent nonuniform volume change on the mass concrete cross-section. The stress caused by this situation is referred to as a self-stress (Bofang, 2014). Internal restraints "may lead to both surface cracking and internal cracking that may not be observed from the surface" (Bamforth, 2007). Internal restraints are dominant in mass concrete placements, while external restraints are dominant in thinner sections. The effects of both restraints add algebraically together, except that their summation never exceeds the effects of 100% external restraint (ACI 207.2R-07, 2007). The development of internal cracking due to internal restraints is graphically illustrated in Figure 41.

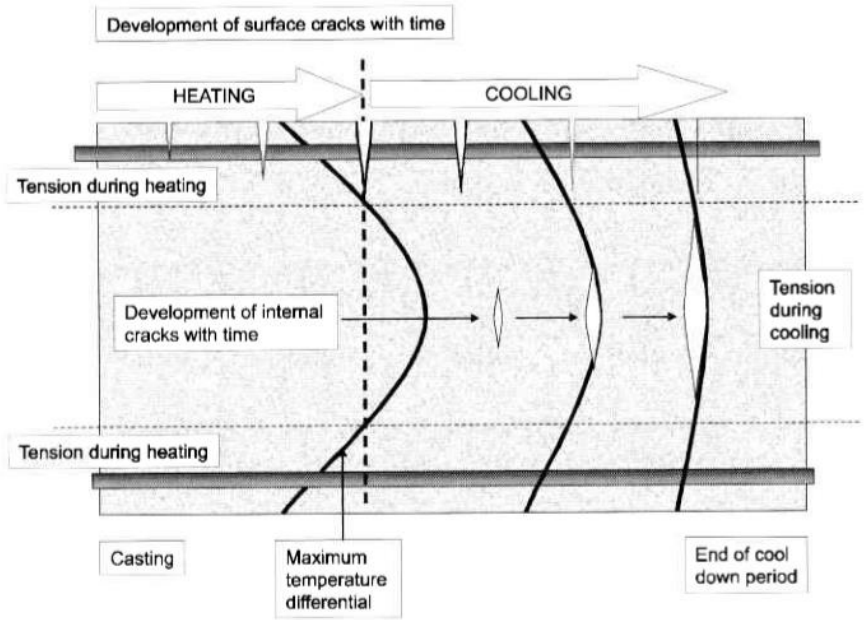

Figure 41 – Schematic of crack development in mass concrete (Bamforth, 2007)**.**

3.2 Procedures for Quantifying Temperatures

An experimental study is designed to quantify temperature rise in mass concrete mixtures. Cement is partially replaced according to weight by three different MK products, two slag products, and one fly ash product. Polymer-modified and phase-changing materials are also studied. The mixtures contain 711 lb/yd^3 (422 kg/m^3) of cementitious materials and have a water-to-cementitious material ratio of 0.43. Paste and mortar samples are prepared for HoH measurements using an isothermal calorimeter. In addition, seventeen 2 foot x 2 foot x 2 foot (0.61 m x 0.61 m x 0.61 m) cube specimens are prepared for temperature measurements.

3.2.1 Introduction

3.2.1.1 General background and motivation

Mass concrete is defined as "any volume of structural concrete in which a combination of dimensions of the member being cast, the boundary conditions, the characteristics of the concrete mixture, and the ambient conditions lead to undesirable thermal stresses, cracking, deleterious chemical reactions, or reduction in the long-term strength as a result of elevated concrete temperature due to heat of hydration" (ACI 301-16, 2016). Material selection is among the most effective methods for reducing thermal stresses and controlling cracking.

In mass concrete elements, an early-age concrete temperature above 155 °F–165 °F (68 °C–74 °C) results in the development of unstable hydration products which in turn causes internal expansion and impairs durability and structural integrity. DEF is a long-term adverse effect that may not be evident for months or years after the time of construction (Gadja & Alsamsam, 2006). Accordingly, most of the mass concrete standard specifications limit the maximum concrete temperature threshold below 160 °F (71.1 °C)

to prevent DEF. A higher maximum concrete temperature of 180 °F (88 °C) is also specified (Bamforth, 2007; FDOT, 2017), particularly when SCMs are used in mass concrete. This higher allowable maximum temperature is attributed to the role of SCMs in reducing the risk of DEF (Bamforth, 2007). A detailed review of the DEF phenomenon is well documented in the literature (Diamond, 1996; Taylor et al., 2001).

SCMs rich in Al_2O_3 content, such as MK, when used at low replacement levels; slag and fly ash, when used at high replacement levels, have been shown to be very effective in controlling and suppressing expansion. Cement with a sulfate-to-alumina ratio ($(SO_3)^2/Al_2O_3$) smaller than 2.0 may not be susceptible to DEF-related damage (Heinz et al., 1989). Therefore, incorporating SCMs rich in Al_2O_3 content in cement mixtures reduces the sulfate-to-alumina ratio.

SCMs can be used as a partial cement replacement to control the HoH and temperature rise in mass concrete mixtures. Among SCMs, fly ash and slag are well known to have a low and slow rate of HoH and early-age strength development. Fly ash is typically used to replace 20% to 40% of cement, and cement weight replacement up to 50% is specified by some agencies. On the contrary, higher cement replacement levels are often used with slag, ranging between 50% and 75% (see Section 3.1.2, (Gadja & Alsamsam, 2006)). Meanwhile, pozzolans such as MK and SF are known to yield HoH at a similar level when compared to Portland cement. The strength of the concrete, however, is significantly increased when cement is partially replaced with these minerals. Thus, when carefully selected, SCMs have the potential to lower internal heat generation, reduce the risk of DEF, and increase strength and durability.

Fly ash is mainly used as a partial replacement for cement in mass concrete structures. However, due to a limited supply of fly ash, alternative SCMs are considered in mass concrete placements. This experimental study examines the feasibility of using cementitious materials including different types of locally available MK and slag products in controlling the temperature rise in binary and ternary replacement mixtures. Furthermore, a literature review has suggested the use of polymer-modified and phase-changing materials (Choi et al., 2014; Ismail et al., 2016) in concrete mixtures. Therefore, additional polymer-modified polyvinyl acetate (PVA) and phase-changing Barium Oxide (BaO) materials are considered in this study.

Heat generation and temperature rise from concrete mixtures are generally measured by means of calorimetry. Paste, mortar, and concrete specimens are tested for HoH and temperature rise measurements. Several approximation methods available in the literature are studied in order to predict temperature rise in mass concrete structures. The Portland Cement Association (PCA) (PCA, 2011) provides a method for predicting the maximum temperature rise for structures with a dimension of at least 6 feet (1.8 m) and cement content between 500 lb/yd^3 and 1000 lb/yd^3 (300 kg/m^3 and 600 kg/m^3). ACI 207.1R (ACI 207.1R-05, 2012) slightly adjusts the PCA method for temperature rise prediction by incorporating the effect of pozzolans (specifically fly ash). Additionally, several charts and equations are provided by ACI 207.2R (ACI 207.2R-07, 2007) for calculating temperature rise that account for the effect of member size, V/A ratio, cement type and fineness, surface exposure condition, use of fly ash or slag, and placement temperature. Gajda et al. (2014) provide a method to estimate temperature rise for concrete placements with a minimum dimension greater than 6 feet (1.83 m) containing Type I or

I/II cement. This method incorporates the effect of different SCMs on maximum temperature rise.

3.2.1.2 Study objectives

This study aims to answer the following five research questions:

1. What are the differences in HoH measurements between paste and mortar samples containing different SCMs using isothermal calorimetry?
2. Do polyvinyl acetate (PVA) and Barium Oxide (BaO) affect HoH?
3. How do different SCMs and replacement levels in binary and ternary mixtures affect temperature rise in mass concrete elements?
4. Do HoH measurements from isothermal calorimetry give a good representation of the temperature rise observed in mass concrete elements?
5. Binary and ternary replacement mixtures are expected to affect temperature rise. Can existing equations predict changes in temperature?

3.2.1.3 Scope of experimental study

An experimental study consisting of binary and ternary replacement paste, mortar, and concrete mixtures is designed. The research is divided into three parts, as shown in Figure 42, and each part provides answers for specific research questions as follows:

- In Part 1, paste and mortar samples are prepared for HoH measurements using an isothermal calorimeter. This part provides answers to research questions No. 1 and 2
- In Part 2, mass concrete specimens (hereafter referred to as ‘cube specimens’) are prepared for temperature measurements. This part provides answers to research questions No. 3 and 4.

- In Part 3, the maximum temperature rise measurements from Part 2 are compared with the maximum temperature rise predictions calculated from the commonly available methods. This part answers the research question No. 5.

(a) Part 1: HoH from paste and mortar specimens.

(b) Part2: Temperature measurements from cube specimens.

(c) Part 3: Temperature comparisons with available prediction equations.

Figure 42 – Specimen photos and a schematic showing three parts of the study.

3.2.2 **Experimental Investigation**

3.2.2.1 Materials

Type I/II ordinary Portland cement was used for all mixtures. In binary and ternary replacement mixtures, cement was partially replaced according to weight by three different locally available MK products, two locally available slag products, and fly ash. The coarse aggregate per ASTM C33 was no. 57 graded granite stone sourced from Athens, Georgia, with a specific gravity of 2.65, and an absorption capacity of 0.49%. The fine aggregate per ASTM C33 was river sand sourced from Watkinsville, Georgia, with a specific gravity of 2.65 and an absorption capacity of 1.53%. Polycarboxylate ether (PCE)-based high-range water-reducing admixture (HRWRA) with 33% solids, which conforms to ASTM C494 Type A and F requirements, was used in the mixtures to maintain adequate workability. The chemical composition and physical properties of all cementitious

materials in this study are presented in Table 22. Properties were obtained from their manufacturers.

In addition to the aforementioned SCMs, two other materials, namely PVA, a polymer modifier generated from manufacturing paint, and BaO, a phase-changing material, were utilized to study the effect of polymer-modified and phase-changing materials on the HoH of paste mixtures. The PVA, sourced from Oregon, was a milky white paste with a total solid content of 50–60% by weight. The BaO, sourced from Virginia, was an off-white powder consisting of 97% BaO.

Table 22 – Chemical composition and physical properties of cementitious materials.

Chemical Composition and Physical Properties	**Cement**	**MK-1**	**MK-2**	**MK-3**	**Slag-a**	**Slag-b**	**Fly Ash**
SiO_2 (%)	19.7	50.75	54 - 56	51.66	33.33	34.07	49.27
Al_2O_3 (%)	4.7	45.91	40 - 42	43.99	13.5	12.73	20.9
Fe_2O_3 (%)	3	0.45	< 1.4	0.47	0.68	0.47	16.76
CaO (%)	63.3	0.06	< 0.1	0.01	41.28	40.41	3.88
MgO (%)	3.1	0	< 0.1	0.03	5.53	6.56	0.83
Na_2O (%)	0 - <0.1	0.23	< 0.05	1.89	0.21	0.17	1.04
TiO_2 (%)	0 - <0.1	1.87	< 3	1.89	0.56	0.52	-
S (%)	-	-	-	-	0.9	-	-
SO_3 (%)	3.2	0.08	< 0.05	-	2.3	-	1.87
Loss on Ignition (%)	2.7	0.42	< 1.0	0.5	-	1.05	1.65
Moisture Content	-	0.43	-		-	-	0.13
Fineness, Amount retained on #325 Sieve, %	-	0	-	0.1	3	-	14.53
Specific Gravity	3.16	2.6	2.6	2.5	2.8	2.87	2.44
Blaine m^2/kg	387	14,200	20,000	11,000	472	531	-
C_3S	54%						
C_2S	15%						
C_3A	7%						
C_4AF	9%						

3.2.2.2 Design and testing for parts 1 and 2 mixtures

The mixtures used in Parts 1 and 2 were designed based on a mixture proportion used for mass concrete placements by GDOT. Total cementitious content in all mixtures was 711 lb/yd^3 (422 kg/m^3). The coarse aggregate content was maintained at a constant 1660 lb/yd^3 (984 kg/m^3) in all mixtures, and the sand contents slightly varied by mixture based on the absolute volume method to attain an equal volume between mixtures per ACI 211 (ACI 211.1-91, 2009). A constant water-to-binder (w/b) ratio of 0.43 was used for all mixtures. Table 23 presents the saturated surface dry mixture proportions for all concrete mixtures. The proportions for the paste and mortar mixtures correspond to the proportions of the concrete mixtures.

In this study, a total of 56 paste, mortar, and concrete mixtures were prepared, which consisted of the Control mixture, binary replacement mixtures, and ternary replacement mixtures. In the binary mixtures, cement was partially replaced according to weight by 15% of 3 different types of MK, 30% of two types of slag and a fly ash, and 45% of two types of slag and a fly ash. In the ternary mixtures, cement was partially replaced according to weight by a combination of 30% of each type of slag with 15% of each type of MK.

Table 23 – Concrete mixture proportions, lb/yd^3 (1 lb/yd3 = 0.5933 kg/m^3).

Replacement (%)	Mixture Code	Cement	Metakaolin	Slag	Fly Ash	Water	Fine Aggregate	Coarse Aggregate
0	Control	711	0	0	0	306	1220	1660
15 (binary)	MK1-15	604	107	0	0	306	1198	1660
	MK2-15	604	107	0	0	306	1198	1660
	MK3-15	604	107	0	0	306	1198	1660
30 (binary)	SLa-30	498	0	213	0	306	1202	1660
	SLb-30	498	0	213	0	306	1202	1660
	FA-30	498	0	0	213	306	1150	1660
45 (binary)	SLa-45	391	0	320	0	306	1193	1660
	SLb-45	391	0	320	0	306	1193	1660
	FA-45	391	0	0	320	306	1119	1660
45 (ternary)	SLa-30+MK1-15	391	107	213	0	306	1183	1660
	SLa-30+MK2-15	391	107	213	0	306	1183	1660
	SLa-30+MK3-15	391	107	213	0	306	1183	1660
	SLb-30+MK1-15	391	107	213	0	306	1183	1660
	SLb-30+MK2-15	391	107	213	0	306	1183	1660
	SLb-30+MK3-15	391	107	213	0	306	1183	1660

The designation of each mixture is indicated by the cement replacement material followed by the product number and percent weight replacement of cement, respectively. For example, MK1-15 indicates a binary mixture with a 15% replacement of cement by the first MK product (MK-1). SLa-30+MK2-15 indicates a ternary mixture with a 30% and 15% replacement of cement by the first slag product (SLa) and the second MK product (MK-2), respectively.

Part 1 Mixtures:

For this part, a total of 39 paste and mortar mixtures were prepared for calorimeter testing. Figure 43 presents the steps used in Part 1 to prepare and test the paste and mortar samples for measuring HoH using an isothermal calorimeter.

Of the total 39 mixtures, 16 binary and ternary paste mixtures containing different SCMs were prepared in a controlled environment for HoH testing. A total of 50 gm cementitious material with a fixed w/b ratio of 0.43 was used in each mixture. Table 24 presents the mixture proportions used in preparing the paste mixtures for HoH testing. Additionally, seven paste mixtures containing PVA and BaO were prepared for HoH testing. The effect of adding 5% and 10% PVA and 3.5% BaO on the HoH of the Control, MK1 binary, and SLa-30+MK1-15 ternary mixtures were investigated. The total water content in the PVA was 45% by weight and was accounted for in the mixture proportions to maintain a fixed w/cm ratio of 0.43. Table 25 presents the proportions of PVA and BaO in the paste mixtures for HoH testing.

All the paste samples were prepared using an external mixing method according to ASTM C1702 (ASTM C1702, 2017) HoH testing. All the materials were kept at a room temperature of 73.4 °F (23 °C) before mixing. The materials were thoroughly hand mixed for two minutes by using a spatula inside a plastic vial, and the sample was then placed in the calorimeter. Consistency in preparing all mixtures was maintained.

(a) raw materials

(b) mixing of a paste specimen

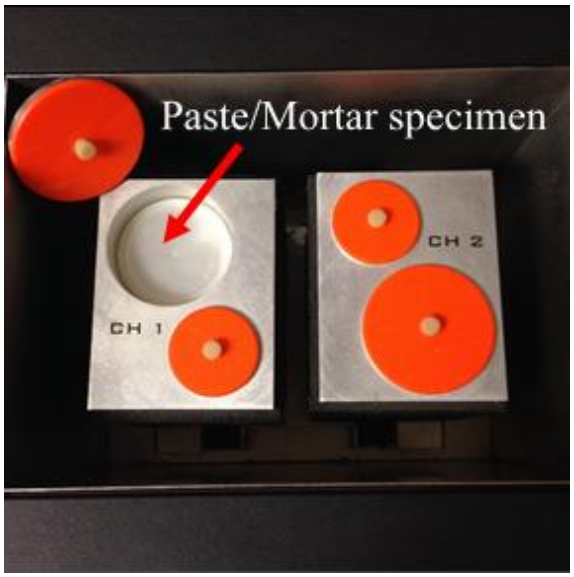

(c) placing the specimen in calorimeter

(d) samples of specimens

Figure 43 – Part 1 experimental work: HoH measurements from paste and mortar specimens.

Meanwhile, 16 mortar samples were prepared for HoH testing from the concrete mixtures presented in Table 23 after screening out the coarse aggregate through sieve No. 5. These samples were cast inside 120 mL plastic cups, and they were placed in the

calorimeter. The initial time when water was added to the mixture was recorded and included in the calorimeter. Consistency in preparing all mortar samples was maintained.

HoH testing was conducted on all paste and mortar mixtures using an isothermal calorimeter following HoH testing per ASTM C1702 (ASTM C1702, 2017). The temperature of the calorimeter was maintained at a constant 75 °F (23.9 °C), and HoH data were collected every minute for 7 days.

Table 24 – Paste mixture proportions for HoH testing (gram).

Replacement (%)	Mixture Code	Cement	Metakaolin	Slag	Fly Ash	Water
0	Control	50	0	0	0	21.5
15 (binary)	MK1-15	42.5	7.5	0	0	21.5
	MK2-15	42.5	7.5	0	0	21.5
	MK3-15	42.5	7.5	0	0	21.5
30 (binary)	SLa-30	35	0	15	0	21.5
	SLb-30	35	0	15	0	21.5
	FA-30	35	0	0	15	21.5
45 (binary)	SLa-45	27.5	0	22.5	0	21.5
	SLb-45	27.5	0	22.5	0	21.5
	FA-45	27.5	0	0	22.5	21.5
45 (ternary)	SLa-30+MK1-15	27.5	7.5	15	0	21.5
	SLa-30+MK2-15	27.5	7.5	15	0	21.5
	SLa-30+MK3-15	27.5	7.5	15	0	21.5
	SLb-30+MK1-15	27.5	7.5	15	0	21.5
	SLb-30+MK2-15	27.5	7.5	15	0	21.5
	SLb-30+MK3-15	27.5	7.5	15	0	21.5

*Note: (1 gram = 0.0022 lb.)

Table 25 – Proportions of PVA and BaO in paste mixtures for HoH testing (gram).

Replacement (%)	Mixture Code	Cement	MK	Slag	PVA	BAO	Water
0	Control	50	0	0	0	0	21.5
	Control+PVA 5%	50	0	0	2.5	0	20.38
	Control+PVA 10%	50	0	0	5.0	0	19.25
	Control+BaO 3.5%	50	0	0	0	1.75	21.5
15 (binary)	MK1-15	42.5	7.5	0	0	0	21.5
	MK1-15+PVA 10%	42.5	7.5	0	5	0	19.25
	MK1-15+BaO 3.5%	42.5	7.5	0	0	1.75	21.5
45 (ternary)	SLa-30+MK1-15	27.5	7.5	15	0	0	21.5
	SLa-30+MK1-15+PVA 10%	27.5	7.5	15	5.0	0	19.25
	SLa-30+MK1-15+BaO 3.5%	27.5	7.5	15	0	1.75	21.5

*Note: (1 gram = 0.0022 lb.)

Part 2 Mixtures:

In this part, seventeen 2 foot x 2 foot x 2 foot (0.61 m x 0.61 m x 0.61 m) concrete cube specimens were prepared for temperature measurements: two Control mixtures in summer and winter conditions, nine binary mixtures, and six ternary mixtures. These cube specimens were prepared to verify the peak temperature decrease/increase observed in binary and ternary mixtures from Part I. Table 23 presents the saturated surface dry mixture proportions for all the concrete mixtures. The mixtures were prepared per ASTM C192 (ASTM C192/C192M, 2018) using a 12.5 ft^3 (0.35 m^3) portable revolving drum mixture. The superplasticizer was then added to the mixing water and thoroughly agitated before the water was added to the mixer.

3.2.2.3 Design of mass concrete specimens

Figure 44 presents the steps used in Part 2 to prepare and test the cube specimens for temperature measurements using thermocouples.

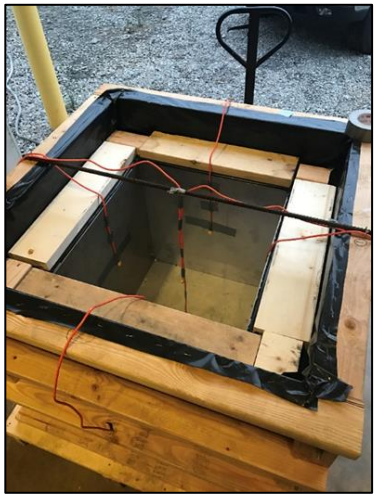

(a) assembling the formwork

(b) thermocouples in the specimen

(c) concrete placement

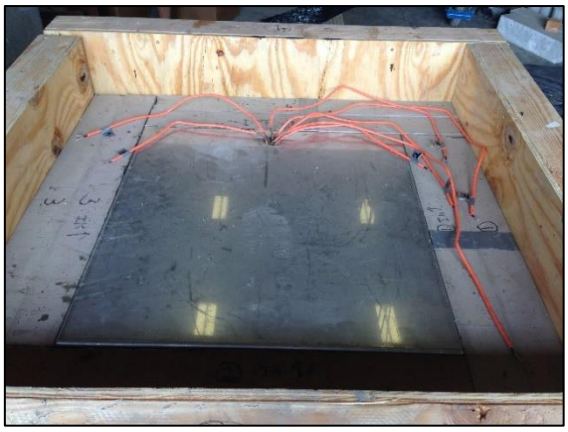

(d) putting top lid on

(e) adding top insulation and formwork and tightening the specimens

Figure 44 – Part 2 experimental work: Temperature rise measurement from mass concrete cube specimens.

To replicate the peak temperature at the core of a mass concrete element, 17 2 foot x 2 foot x 2 foot (0.61 m x 0.61 m x 0.61 m) cube concrete specimens were cast in stainless

steel molds insulated on all 6 sides by 6 inch (150 mm) rigid insulation panels with a total R-value of 50 °F·ft^2·h/BTU (8.8 °C·m^2/W), which is considered very high, and 1 inch (25.40 mm) plywood formwork. The formwork and insulation panels were designed to provide a near-adiabatic temperature boundary condition. Embedded thermocouples were placed at critical locations inside each of the concrete specimens for temperature measurements (Figure 44 a and b). After casting the specimens (Figure 44 c and d), the top insulation layers and then the formwork were placed on top of the cubes, and the formwork was tightened to minimize heat loss and provide a nearly adiabatic condition (Figure 44 e). The specimens were kept in a controlled lab environment for the internal temperature measurements. The temperature in the mass concrete cube specimens was monitored and recorded every 30 minutes for 2 weeks using the thermocouples.

The Control-summer specimen was cast first and instrumented with seven thermocouples (Figure 44 a and b): one placed at the center of the specimen and the other six placed at the middle of all six surfaces of the specimen. An additional thermocouple was placed on the formwork to monitor the ambient air temperature. The temperature profile results for all seven thermocouples inside the specimen showed a similar temperature rise over the two weeks, which confirmed the efficiency of the insulation material used in this study in terms of holding the temperature. Thus, for the rest of the 16 mass concrete specimens, and in addition to the ambient thermocouple, only three thermocouples were used inside the specimens to monitor temperature rise: one at the center, one at the middle of the bottom face, and one at the middle of the side surface of the specimen.

3.2.2.4 Insulation material for mass concrete specimens

Several insulation materials are available in the market with different R-values. The higher the R-value, the better the insulation is at keeping the temperature and providing a nearly adiabatic temperature rise environment. Insulations such as expanded polystyrene foam (with an R-value of about 4 $ft^2 \cdot °F \cdot h/BTU$ per inch), extruded polystyrene foam (with an R-value of about 5 $ft^2 \cdot °F \cdot h/BTU$ per inch), and fiberglass (with an R-value of about 3 $ft^2 \cdot °F \cdot h/BTU$ per inch) are commonly used in research to insulate specimens with the goal of creating a nearly adiabatic temperature environment for temperature rise measurements.

Gajda et al. (2014) cast 3 foot x 3 foot x 3 foot (0.91 m x 0.91 m x 0.91 m) cube concrete specimens and used 3 layers of 2-inch (50 mm) extruded polystyrene board insulation (total R-value of about 30 $ft^2 \cdot °F \cdot h/BTU$) on all sides of the specimen. Tia et al. (2010) cast 3.5 foot x 3.5 foot x 3.5 foot (1.1 m x 1.1 m x 1.1 m) cube concrete blocks and used 1 layer of a 3-inch (75 mm) polystyrene plate (total R-value of about 15 $ft^2 \cdot °F \cdot h/BTU$) as insulation material on all 6 sides of the blocks for temperature rise measurements. Bouzoubaâ et al. (1997) cast a circular concrete block with a diameter of 3 ft (0.92 m) and a length of 3.3 ft (1 m) to simulate a part (9.2 m in diameter and 10 m in thickness) of a concrete gravity dam. The lateral surface of the concrete block was covered with a 6-inch (150 mm) fiberglass mat for insulating material (total R-value of about 18 $ft^2 \cdot °F \cdot h/BTU$) to prevent heat loss in the radial direction. Siang (2017) cast 5 foot x 5 foot x 5 foot (1.5 m x 1.5 m x 1.5 m) concrete blocks and used 4-inch (100 mm) molded, reinforced expanded polystyrene foam board as insulation material (total R-value of about 16 $ft^2 \cdot °F \cdot h/BTU$) on all sides of the blocks.

In this study, two layers of 3-inch (76.2 mm) thick Kingspan Kooltherm K20 Concrete Sandwich Board insulation were used (Figure 7 and Figure 44), for a total R-value of 50 $ft^2 \cdot °F \cdot h/BTU$ per 6 inches (R-value of about 8.3 $ft^2 \cdot °F \cdot h/BTU$ per inch). This insulation has a premium performance, and it is used for concrete insulated sandwich wall systems. It has a glass tissue-based facing, adhesively bonded to the insulation core, which is a premium performance rigid thermoset fiber-free phenolic insulant. Table 26 presents the properties of this insulation. This high R-value insulation is used in this study to quantify the temperature in mass concrete cube specimens and provide a condition more adiabatic in the smaller concrete cube specimens than in those used in previous studies.

Table 26 – Properties of the Kooltherm K20 Concrete Sandwich Board Insulation (Kingspan USA, 2019)**.**

Compressive Strength Psi (MPa)	Density lb/ft^3 (Kg/m^3)	Water Absorption (% by volume)	Air Permeance cfm/ft^2 ($L/S/m^2$)	Water Vapor Permeance Perm
21 (0.14)	2 (32)	1.21	0.000 (0.001)	0.79

3.3 **Results**

The experimental results from Part 1 and Part 2 mixtures are presented in this section. Part 1 results consist of HoH measurements from the paste and mortar mixtures. Part 2 results consist of the temperature rise measurements from the mass concrete specimens.

3.3.1 **Part 1 Results: Calorimetry of Paste and Mortar Specimens**

3.3.1.1 Effect of SCMs and replacement levels on heat of hydration of paste specimens

Figure 45 shows the effect of all SCMs and different replacement levels in binary and ternary replacement mixtures on the HoH of paste mixtures.

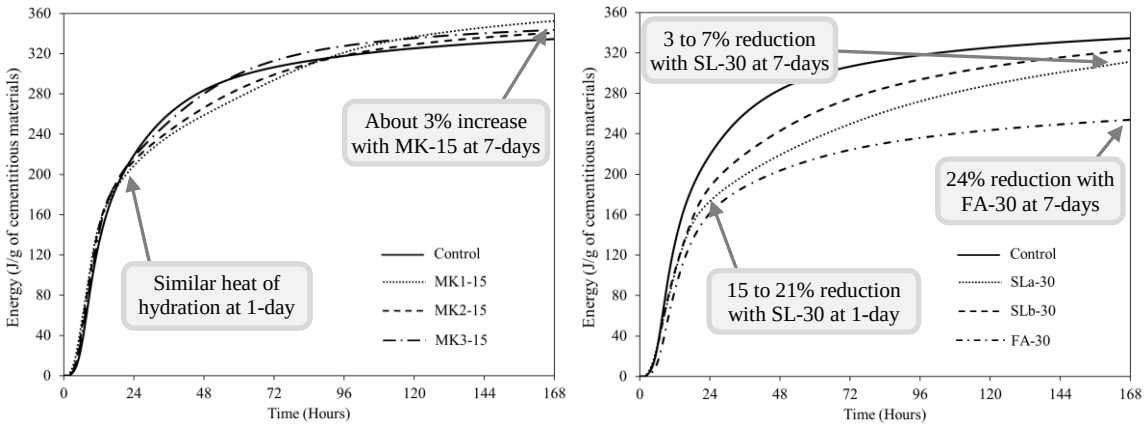

(a) 15% MK binary mixture (b) 30% slag or fly ash binary mixture

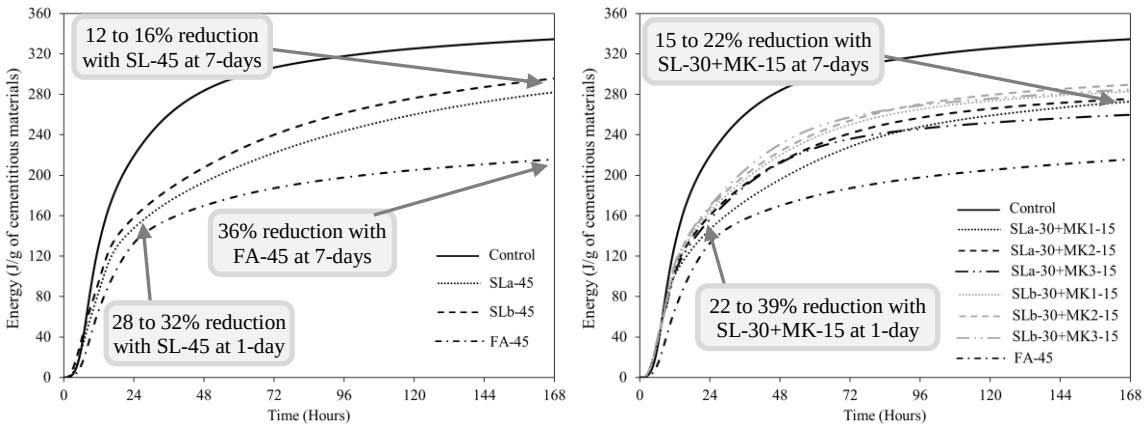

(c) 45% slag or fly ash binary mixture (d) 45% slag and MK ternary mixture

Figure 45 – Effect of SCMs and replacement levels on HoH of paste mixtures.

3.3.1.2 Effect of PVA and BaO addition on heat of hydration

The effects of PVA and BAO additions on the HoH of the Control, binary replacement mixtures, and ternary replacement mixtures are shown in Figure 46 and Figure 47, respectively.

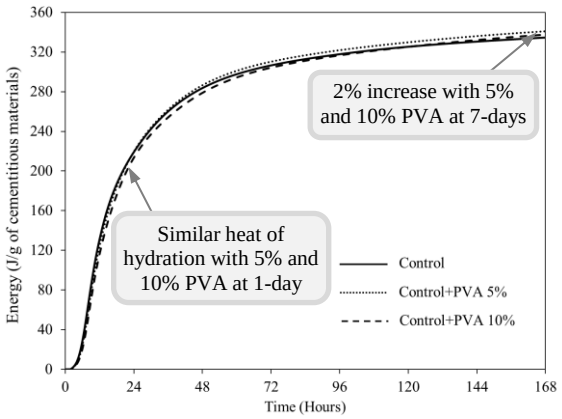

(a) Control mixture

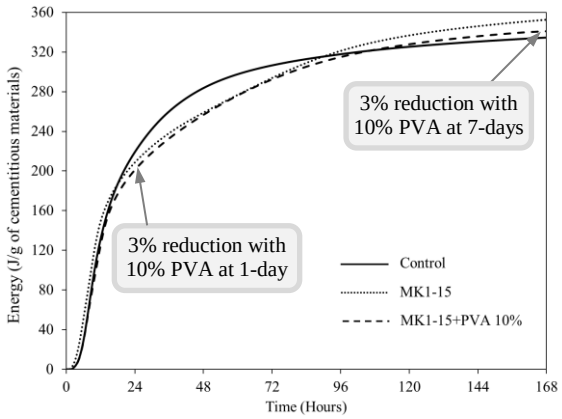

(b) 15% MK binary mixture

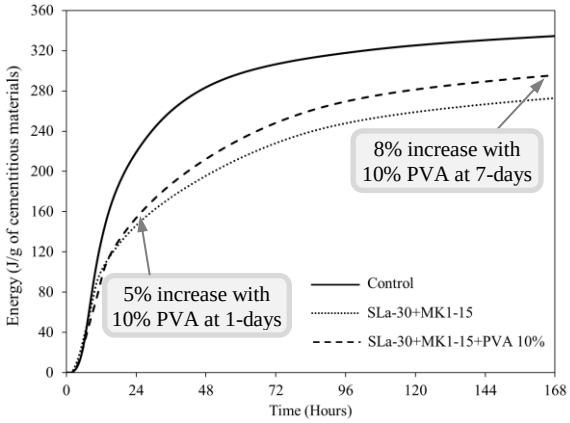

(c) 45% slag and MK ternary mixture

Figure 46 – Effect of PVA addition on HoH.

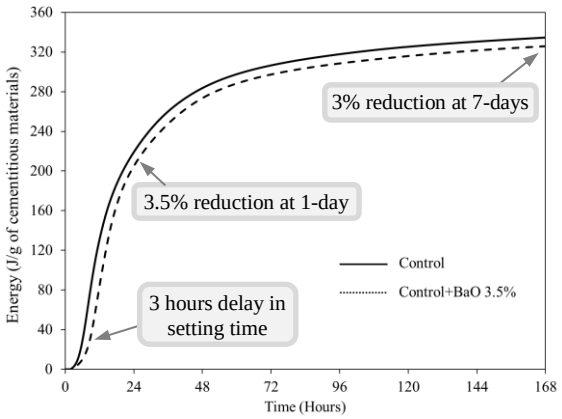

(a) Control mixture

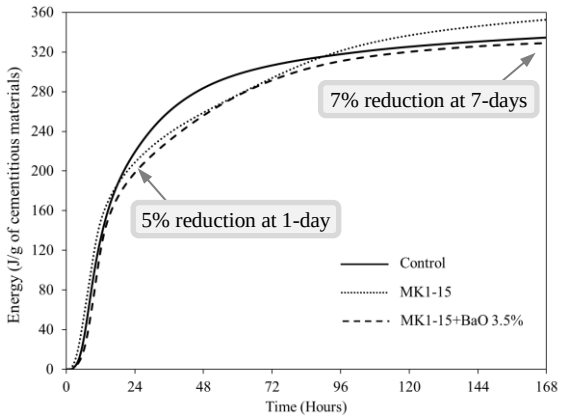

(b) 15% MK binary mixture

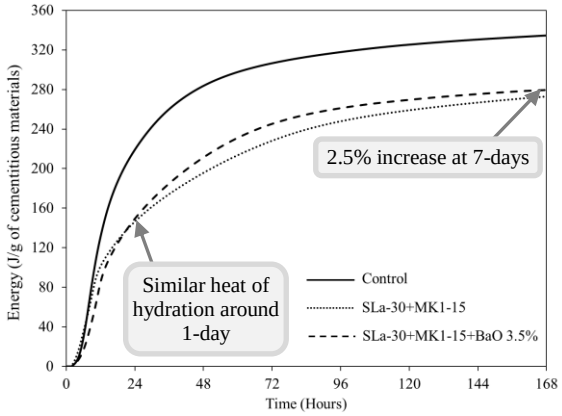

(c) 45% slag and MK ternary mixture

Figure 47 – Effect of BaO addition on HoH.

3.3.1.3 Effect of SCMs and replacement levels on heat of hydration of mortar specimens

Figure 48 presents the effect of different SCM products and different replacement levels in binary and ternary replacement mixtures on the HoH of mortar mixtures sampled from the concrete mixtures.

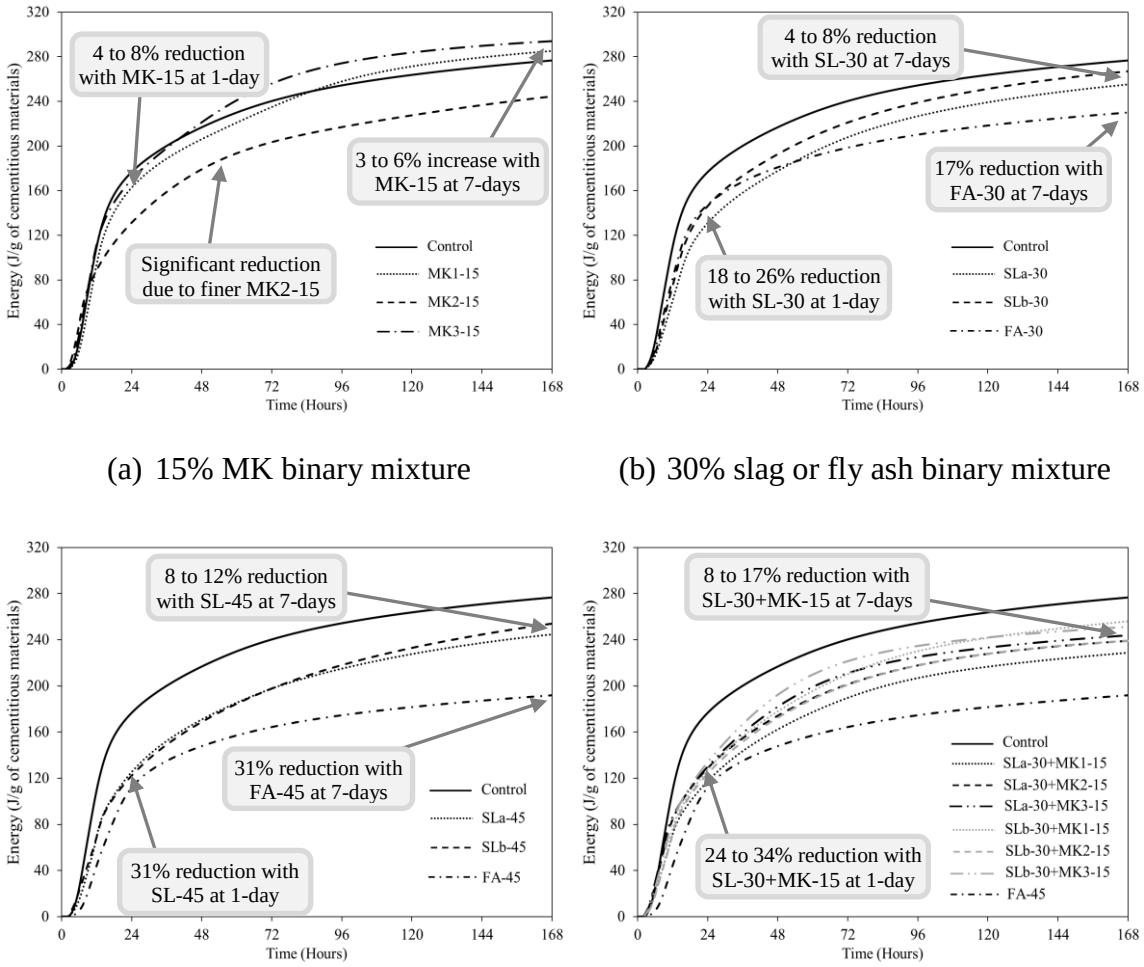

(a) 15% MK binary mixture (b) 30% slag or fly ash binary mixture

(c) 45% slag or fly ash binary mixture (d) 45% slag and MK ternary mixture

Figure 48 – Effect of SCMs and replacement levels on HoH of mortar mixtures.

3.3.2 **Part 2 Results: Temperature Rise Measurements from Concrete Cube Specimens**

The internal temperature of the concrete mixtures was continuously measured for two weeks using thermocouples. The internal temperature is the sum of the placement temperature and the temperature rise of the concrete mixture specimen. Therefore, the temperature rise for each mixture is calculated by deducting the placement temperature from the internal temperature.

3.3.2.1 Effect of summer and winter placements on temperature rise

Figure 49 illustrates the effect of summer and winter placement conditions on the temperature rise of the Control specimen.

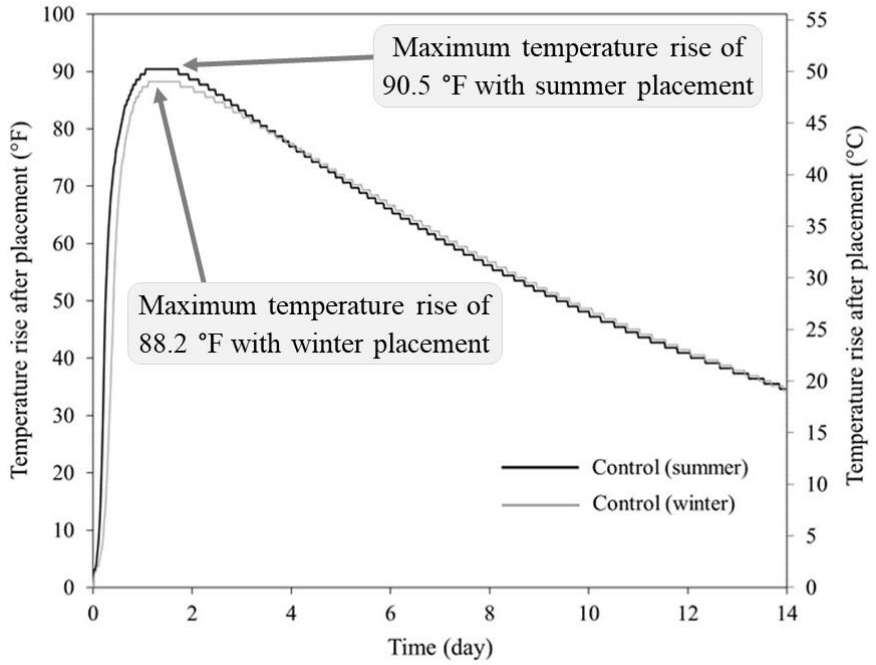

Figure 49 – Effect of placement temperature on temperature rise in the mass concrete Control specimen.

Note: (°C x 9/5) + 32 = °F.

3.3.2.2 Temperature rise of binary and ternary replacement mixtures

Figure 50 presents the temperature rise of all cube specimens containing different SCMs and different replacement levels in binary and ternary mixtures. The temperature rise of the Control-summer mixture is shown in comparison to temperature rise results from the binary and ternary replacement mixtures.

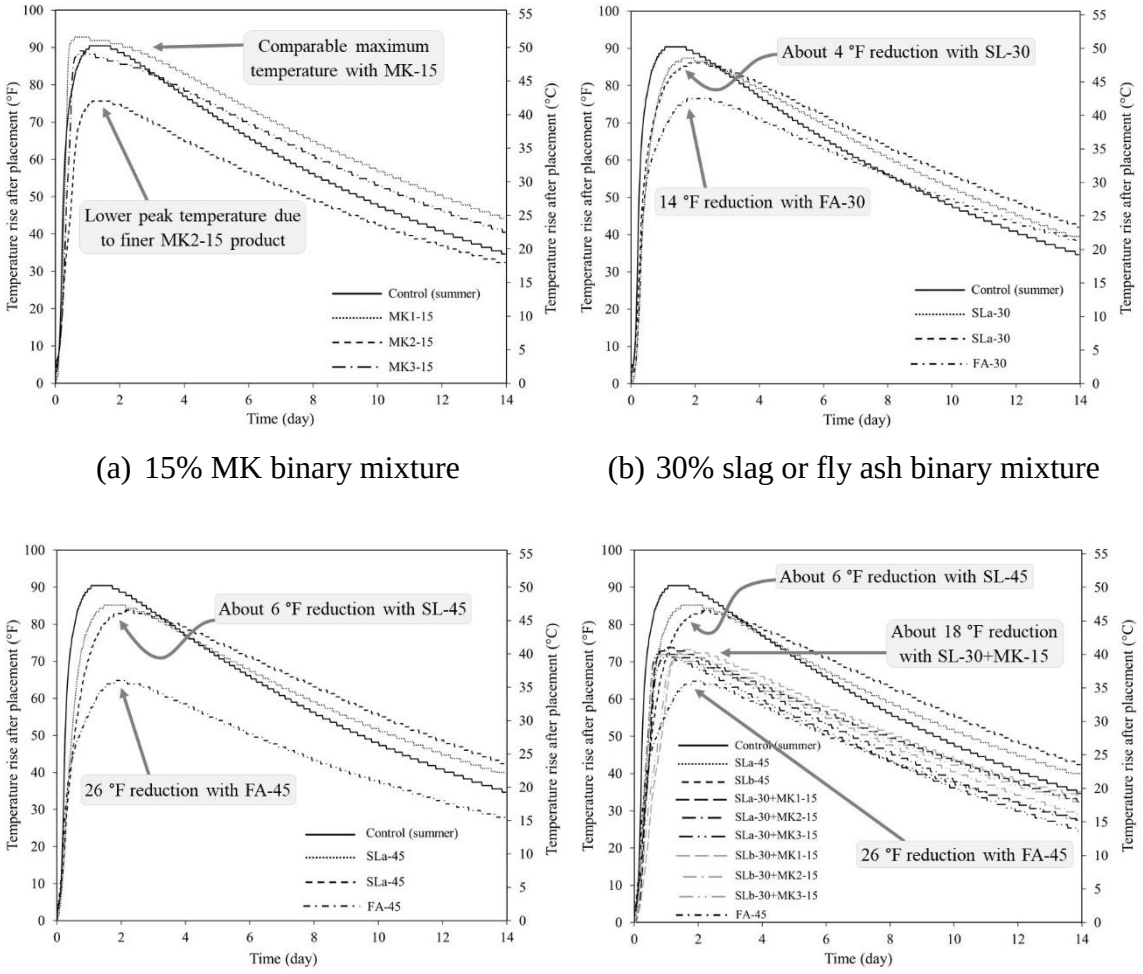

(a) 15% MK binary mixture (b) 30% slag or fly ash binary mixture

(c) 45% slag or fly ash binary mixture (d) 45% slag and MK ternary mixture

Figure 50 – Temperature rise in cube specimens.

3.4 **Analysis of the Results**

3.4.1 **Analysis of Results from Part 1 Mixtures**

3.4.1.1 Effect of SCMs on heat of hydration from paste and sampled mortar mixtures

The results from both paste and mortar samples are shown in Figure 45 and Figure 48, respectively. The partial replacement of cement with 15% MK1 and MK3 products in binary mixtures results in an HoH comparable to that of the Control mixture. The MK mixtures result in a slightly lower 3-day HoH and an increase of 3%–6% in the 7-day HoH.

The MK2 mortar mixture is notable here as it has a low HoH compared to those of the Control and the other MK mixtures. The low HoH of this mixture is due to its high fineness, as shown in Table 22, which results in an unworkable mortar mixture. The HoH of the MK2 paste mixture (Figure 45 a) shows that this mixture also has a HoH comparable to that of the Control mixture as well as those of the MK1 and MK3 mixtures.

The increase in partial replacement of cement with slag from 30% to 45% in binary mixtures results in a systematic reduction in HoH, even though the reduction at 7 days is only about 14% and 10% in the SL-45 paste and mortar specimens, respectively. At the same replacement level, SLa mixtures show a slightly lower HoH than that of the SLb mixtures.

The HoH of the ternary mixtures is significantly lower than that of the Control mixture. Ternary mixtures result in 17% and 12% reductions over the 7-day HoH in the paste and mortar mixtures, respectively. Similar to the binary mixtures, the ternary mixtures containing SLa have a lower HoH compared to that of the ternary mixtures containing SLb. Moreover, the HoH of the ternary mixtures is lower than the HoH of the SL-45 binary mixtures, and it is comparable to the HoH recorded for the FA-30 mixture.

3.4.1.2 Heat of hydration from paste and sampled mortar mixtures

The paste samples were prepared in a controlled way such that all ingredients had the same mixing temperature. Meanwhile, the mortar mixtures were sampled from the mass concrete placements after screening out the coarse aggregate; thus, they represent more realistic mixtures. The results from both methods are consistent and agree well with each other in terms of reduction or increase in HoH compared to the Control mixture. They only differ by about 3% for 15% replacement with MK, 1% for 30% replacement with slag, 7% for

30% replacement with fly ash, 4% for 45% replacement with slag, 5% for 45% replacement with fly ash, and 5% for 45% replacement with slag and MK in ternary replacement mixtures.

The accumulative HoH measurements per gram of cementitious materials of the mortar mixtures are lower than those of their corresponding paste mixtures, in which they are expected to be similar or comparable to each other. The reason for this difference is that the mixing energy and its associated friction between the particles are higher in preparing the paste mixtures compared to preparing the mortar samples; this results in a lower temperature and HoH in the mortar mixtures. Additionally, when the coarse aggregate is screened out in the mortar samples, some of the paste is possibly retained on the surface of the coarse aggregate and is left out. This results in mixtures with less paste for given mixture proportions specified in the calorimeter and hence lower HoH values compared to those of the paste mixtures.

The results illustrate that the HoH values from paste samples represent accurate values per gram of cementitious materials. Accordingly, they are used in Chapter 4 to calculate the adiabatic temperature rise of concrete mixtures. Since the HoH values from the mortar mixtures are affected by the sampling procedure, they are only useful for qualitative comparison between different mixtures.

3.4.1.3 The heat of hydration of PVA and BaO mixtures

The HoH results from PVA paste mixtures presented in Figure 46a show that the addition of 5% PVA to the Control mixture results in about a 5% reduction within the first 12 hours of hydration, a similar HoH at 24 hours of hydration, and about a 2% increase in HoH by 7 days of hydration. The increase in PVA content from 5% to 10% in the Control mixture

results in about an 11% reduction within the first 12 hours of hydration, only about a 2.2% reduction at 24 hours of hydration, and a slight increase, about 1%, in HoH within a week. A study on vinyl acetate effluents by Ismail et al. (2016) observed about a 4.9% reduction in the maximum temperature rise when up to 5% PVA by weight was used as an addition to a Control mixture. In their study, the maximum temperature occurred at 21 hours after casting. These results align with the HoH results of 5% and 10% PVA from this study, which showed about a 2.2% reduction in HoH within 24 hours of hydration.

The effect of PVA on HoH seems to be more pronounced in the binary mixture containing 15% MK as shown in Figure 46b. The addition of 10% PVA to the MK1-15 mixture results in approximately a 15% reduction within the first 12 hours of hydration, about a 3.9% reduction within 24 hours, and about a 3% reduction in HoH within a week.

Meanwhile, the effect of PVA on the HoH of ternary replacement mixtures, as shown in Figure 46c, is less pronounced. The addition of 10% PVA to the ternary mixture containing 30% slag and 15% MK (SLa-30+MK1-15) results in 8% reduction in the HoH within the first 12 hours of hydration, but an increase of approximately 5% and 8% by 24 hours and 7 days of hydration, respectively. The mechanism by which the initial HoH is reduced may be attributed to the formation of a protective skin by the PVA around the cement grains, which delays contact between the cement particles and water in the mixture. Also, during the hydration of cement–polymer composites, the vinyl acetate is hydrolyzed and acetate ions are produced, which react with Ca^{2+} ions from cement hydration to generate calcium acetate. As the Ca^{2+} ions are consumed by this process, the unreacted sulfate ions left behind delay hydration. Increasing the polymer content (from 5% to 10%)

reduces the yield of Ca^{2+} ions generated from cement hydration owing to an increase in viscosity, and this delays early hydration in the mixture (Kang et al., 2015).

The HoH results of the BaO paste mixtures presented in Figure 47a indicate that the addition of 3.5% BaO to the Control mixture results in a reduction of about 35% within the first 12 hours of hydration, about 6% within 24 hours, and about 2.5% within a week. A previous study by Choi et al. (2014) on latent heat materials showed that the partial replacement of cement with 3.5% barium hydroxide 8-hydrate ($Ba(OH)_2 \cdot 8H_2O$) resulted in the lowest hydration heat value among latent heat materials and reduced temperature rise by about 36 °F (20 °C) compared to a Control mortar specimen. The BaO in this study decreased HoH, especially within the first 24 hours of hydration; however, the reduction over seven days was not as significant as the observed temperature rise measurements from Choi et al. (2014) on mortar specimens. Reduction in HoH is due to the ability of the BaO to absorb a large amount of heat when transitioning from a solid phase to a liquid phase using latent heat (Kim et al., 2015).

Figure 47b shows that the addition of 3.5% BaO to the binary mixture containing 15% MK results in reductions of approximately 19% within the first 12 hours of hydration, about 4.7% by 24 hours of hydration, and about 6.5% within a week. The addition of 3.5% BaO to the ternary replacement mixture containing 30% slag and 15% MK, as shown in Figure 47c, results in a reduction of approximately 8% in HoH within the first 12 hours of hydration, but an increase of approximately 2% and 2.4% in HoH at 24 hours and 7 days of hydration, respectively.

Figure 51 below illustrates the effects of PVA and BaO on HoH for the Control, the binary replacement mixtures, and the ternary replacement mixtures by day 7.

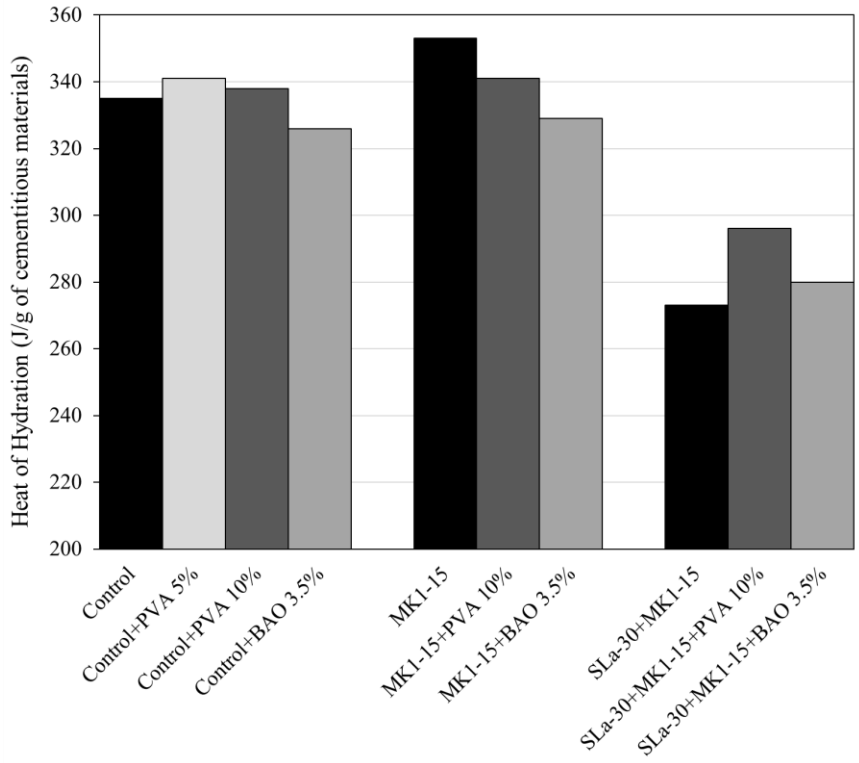

Figure 51 – Comparison of the effects of PVA and BaO on the HoH of Control, binary mixtures, and ternary mixtures at seven days of hydration.

As shown above, the addition of PVA increases the HoH of the Control and ternary replacement mixtures and reduces the HoH of the binary (MK1-15) mixture over seven days. Meanwhile, the addition of 3.5% BaO results in an HoH reduction in the Control and binary (MK1-15) mixtures and an increase in the HoH of the ternary replacement (SLa-30+MK1-15) mixture. Interestingly, the effects of PVA and BaO on reducing HoH are more pronounced in the binary mixture containing 15% MK (MK-15). The addition of BaO performs better than the addition of PVA in all mixtures; however, the cost of BaO is approximately $1.4 per gram ($40 per ounce), whereas the cost of PVA is approximately $0.2 per gram ($0.62 per ounce). Especially in light of the price of BaO, about 65 times higher than the cost of PVA, the relative reduction in HoH due to BaO compared to the reduction due to PVA is small. Thus, due to the insignificant reduction in HoH for PVA

and the high cost of BaO, the effects of these materials on temperature rise in the cube specimens were not studied.

3.4.2 Analysis of Results from Part 2 Mixtures

3.4.2.1 Effect of placement temperature on temperature rise

Figure 49 presents the effect of placement temperature on the temperature rise of the Control cube specimens. As expected, the summer mixture has a steeper rise and yields a higher maximum temperature rise over the winter mixture. Temperature rise is also shifted to the right for the winter placement by about five hours. Placement temperature, however, does not appear to influence the time when the maximum temperature occurs, as it is the same for both summer and winter mixtures; it occurs about 26 hours after placement.

The maximum temperature rise is about 90.5 °F (32.5 °C) in the Control-summer mixture and 88.2 °F (31.2 °C) in the Control-winter mixture. The higher placement temperature in the summer accelerates temperature rise (ACI 207.2R-07, 2007). These results show that the placement temperature between summer and winter conditions yields a difference of about 2.3 °F (1.3 °C) (less than 3%) for the maximum temperature rise. Therefore, the temperature rise of the Control-summer mixture is considered in the following section.

3.4.2.2 Effect of SCMs on temperature rise from cube specimens

Temperature rise measurements from all cube specimens are presented in Figure 50. The partial replacement of cement with 15% MK1 and MK3 products in binary mixtures (Figure 50a) results in a rate of temperature rise and peak temperature comparable to those of the Control mixture. The peak temperature is increased by about 2 °F (1.1 °C) in the MK1 mixture, and it is reduced by about 2 °F (1.1 °C) in the MK3 mixture. Thus, the partial

replacement of cement with 15% MK could slightly increase or decrease the temperature rise based on the composition and type of MK. The MK2 mixture resulted in a significant reduction in temperature rise compared to the Control and other MK mixtures; however, the lower temperature rise of the MK2 mixture is due to its high level of fineness, which caused the sizable specimens to become unworkable (0.1 inch or 2.54 mm slump). Otherwise, results comparable to MK1 and MK3 mixtures are expected from the MK2 mixture, as well.

The partial replacement of cement with 30% SLa and SLb products (Figure 50b) results only in a slight reduction (about 4 °F or 2.2 °C) in the peak temperature compared to that of the Control mixture. The increase in partial replacement of cement with slag from 30% to 45% in binary mixtures (Figure 50c) results only in a 2 °F (1.1 °C) additional reduction in peak temperature. At the same replacement level, the SLa shows a slightly lower temperature rise than SLb in binary mixtures.

The partial replacement of cement with a combination of 30% of different slag products and 15% of different MK products in ternary mixtures (SL-30+MK-15) results in a significant reduction of about 18 °F (10 °C) in peak temperature compared to that of the Control mixture (see Figure 50d). Moreover, at the same replacement level of 45%, the peak temperature in the ternary mixtures is lower than the SL-45 binary mixtures by about 12 °F (6.7 °C), which is approximately 14% more reduction in the maximum temperature rise compared to the binary mixtures containing 45% slag. Similar to the binary mixtures, the ternary mixtures containing SLa have a lower temperature rise compared to the ternary mixtures containing SLb.

The partial replacement of cement with 45% fly ash results in the greatest reduction (about 27 °F or 15 °C) in peak temperature compared to that of the Control mixture (Figure 50d). The temperature reduction achieved in the ternary mixtures comes close to the reduction level obtained in the 30% cement replacement mixture with fly ash. The temperature rise from the ternary mixtures are comparable, yet slightly lower by about 4 °F (2.2 °C) than the temperature rise from the FA-30 mixture; they are higher than the FA-45 mixture by about 8 °F (4.4 °C). These results show the effectiveness of a combination of slag and MK in ternary mixtures in reducing temperature rise in cube specimens.

3.4.2.3 Effect of SCMs on time and duration of the maximum temperature

Table 27 presents the maximum temperature rise, the time of its occurrence, and the duration for which the maximum temperature was maintained in the cube specimens. The time of maximum temperature is when the maximum temperature first occurs. The duration that maximum temperature maintains is the period that the concrete is exposed to the maximum temperature.

Table 27 shows that the maximum temperature occurs in the Control mixture at about 26 hours after placement. The maximum temperature is reached earlier in the MK binary mixtures, and it is delayed in the slag and fly ash binary mixtures. Meanwhile, the ternary mixtures with a combination of slag and MK products show both slight acceleration and slight delay in the time of maximum temperature compared to that of the Control mixture.

For the Control mixture, the duration maintained at the maximum temperature is 16.8 hours. This time is reduced in all binary mixtures except MK2-15, FA-30, and SLb-45, which had the same maximum temperature duration as the Control mixture. On the

other hand, this time is significantly reduced, by about 8 hours, in the ternary mixtures. The maximum temperature, the time to maximum temperature, and the time spent at elevated temperatures are critical parameters in predicting the possibility of DEF occurrence and thermal shock susceptibility (Day, 1992).

Table 27 – Time of maximum temperature occurrence and its maintained duration.

Replacement Level (%)	Mixture Code	Maximum Temperature Rise °F (°C)	Time of Maximum Temperature Occurrence (Hours)	Duration that Maximum Temperature Maintained (Hours)
0	Control-Summer	90.5 (50.3)	26.4	16.8
	Control-Winter	88.2 (49.0)	26.4	16.8
15 (binary)	MK1-15	92.8 (51.6)	14.4	12.0
	MK2-15	75.6 (42.0)	26.4	16.8
	MK3-15	89.1 (49.5)	19.2	2.4
30 (binary)	SLa-30	87.4 (48.6)	38.4	9.6
	SLb-30	86.1 (47.8)	43.2	14.4
	FA-30	76.5 (42.5)	43.2	16.8
45 (binary)	SLa-45	85.2 (47.3)	38.4	16.8
	SLb-45	83.8 (46.6)	52.8	4.8
	FA-45	64.8 (36.0)	45.6	7.2
45 (ternary)	SLa-30+MK1-15	73.8 (41.0)	24.0	7.2
	SLa-30+MK2-15	72.9 (40.5)	19.2	7.2
	SLa-30+MK3-15	71.3 (39.6)	21.6	9.6
	SLb-30+MK1-15	73.3 (40.7)	36.0	9.6
	SLb-30+MK2-15	72.0 (40)	19.2	7.2
	SLb-30+MK3-15	72.0 (40)	38.4	9.6

3.4.2.4 Efficiency of temperature measurements from mock-up specimens

Temperature rise measurements from this study are compared to those from a study performed by Gadja et al. (2014) in which 3 foot x 3 foot x 3 foot (0.91 m x 0.91 m x 0.91 m) mock-up cube specimens insulated on all sides by three layers of 2-inch (50.8 mm) polystyrene (XPS) board insulation (with a total R-value of about 30) were cast. This concrete mixture design is comparable to the mixture design used in the current study, including the use of a mixture with cement replacement of 30% fly ash; at the same time, total SCM content in the previous study was 658 lb/yd^3 (390 kg/m^3), which is close to the 711 lb/yd^3 (422 kg/m^3) total SCM used in the current study. Figure 52 presents a comparison of the temperature rise results between the mixture used in Gadja et al. (2014) and the FA-30 mixture used in this study.

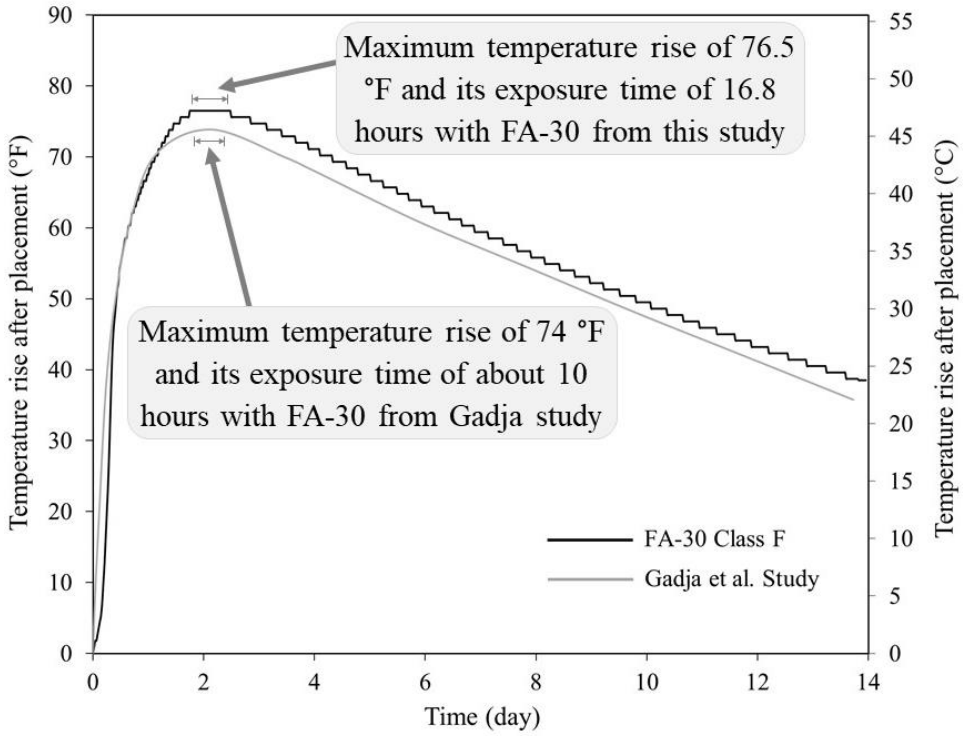

Figure 52 – Comparison of temperature rise between FA-30 mixture and Gadja et al. (2014) mixture.

Interestingly, the temperature rise results over two weeks seem very comparable; the FA-30 mixture from the current study has a slightly higher (by 2.5 °F or 1.4 °C) temperature rise due to its slightly higher total SCM content (about 53 lb/yd^3 or 31.44 kg/m^3). Further, maximum temperature durations for the Gadja et al. (2014) mixture and the FA-30 mixture from this study are 10 hours and 16.8 hours, respectively.

These results confirm the effectiveness of the system and the insulation material used in this study in creating nearly adiabatic temperature boundary conditions. In addition, they show the efficiency of the mock-up specimens in quantifying the maximum temperature even though they were smaller mock-up specimens (2 foot x 2 foot x 2 foot or 0.61 m x 0.61 m x 0.61 m) than those used in previous studies (3 foot x 3 foot x 3 foot or 0.91m x 0.91m x 0.91m). The current system thus saves time and money by creating small yet effective mock-up specimens for temperature rise measurements.

3.4.2.5 Comparison between heat of hydration and temperature rise results

From HoH results, Figure 45 and Figure 48, and temperature rise measurements, Figure 50, comparison bar charts are developed in Figure 53 to enable the comparison of the relative reduction in HoH and temperature rise measurements together. Figure 53 presents the normalized 7-day HoH results from paste and mortar mixtures along with the maximum temperature rise measurements with respect to their corresponding Control mixtures. The X-axis presents the mixtures, and the Y-axis presents the relative reduction or increase in HoH or temperature rise with respect to the Control mixture. The straight dotted red line with a value of 1.0 represents the normalized Control mixture. Any mixture with values higher than 1.0 exemplifies a relative increase in HoH or temperature rise compared to the

Control mixture, whereas values lower than 1.0 exemplify a relative reduction in HoH or temperature rise compared to the Control mixture.

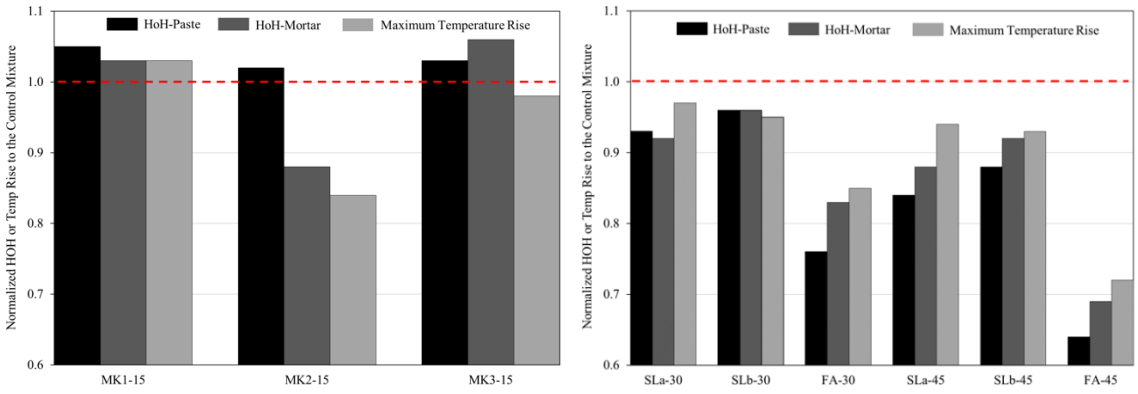

(a) 15% MK binary mixture (b) 30% slag or fly ash binary mixture

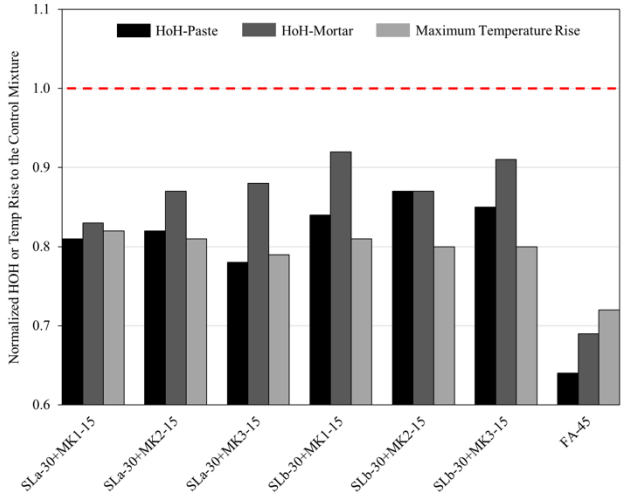

(c) 45% slag and MK ternary mixture

Figure 53 – Normalized HoH and maximum temperature rise with respect to the Control mixture.

In general, the normalized HoH results from mortar mixtures give slightly closer results to the maximum temperature rise measurements in binary mixtures. Meanwhile, the HoH results from paste mixtures yield results closer to the maximum temperature rise measurements in ternary mixtures. However, the difference between the HoH of the two

mixtures is small, less than 4% on average. Both paste and mortar mixtures represent well a relative increase or decrease in maximum temperature rise measurements. Therefore, the normalized HoH results from paste mixtures are selected for relative comparison to the normalized maximum temperature rise measurements in cube specimens.

Figure 53a presents a bar chart with results for binary mixtures containing 15% of different MK products. HoH results and maximum temperature rise measurements in all three MK products are consistent. HoH results show that the 15% cement replacement with different MK products in binary mixtures effects an increase of about 2% to 5% compared to that of the Control mixture. Similarly, temperature rise results show that MK1 and MK3 products have a temperature rise comparable to that of the Control mixture. Meanwhile, the maximum temperature increases by 3% in MK1 and decreases by 2% in MK3 compared to the maximum temperature of the Control mixture. As discussed in Sections 3.4.1.1 and 3.4.2.2, the high fineness of the MK2 product made its sizable concrete specimen and its corresponding mortar sample unworkable. The lower maximum temperature rise in the MK2 concrete mixtures is well reflected in the HoH of the MK2 mortar mixture. Otherwise, comparable results to MK1 and MK3 mixtures are expected from the MK2 mixture. It is concluded here that the HoH results for mixtures containing 15% MK can very well predict the relative change in temperature rise in cube specimens.

Figure 53b presents the bar chart results for binary replacement mixtures containing 30% and 45% slag or fly ash. HoH results seem to slightly overestimate the relative reduction in maximum temperature rise measurements; however, observed differences are small. The HoH of SL-30 mixtures shows a reduction of about 4%–8% compared to that of the Control mixture, whereas the reduction in maximum temperature rise is up to 5%.

The HoH of SL-45 mixtures show a reduction of about 12–16% compared to that of the Control mixture, whereas the reduction in maximum temperature rise is about 7%. The HoH of FA-30 and FA-45 mixtures show about 24% and 36% reduction, respectively, compared to that of the Control mixture, whereas the reduction in maximum temperature rise is about 15% and 28%, respectively. Therefore, the HoH results align with the temperature rise measurements; at the same time, sample size made a difference, specifically in the binary slag mixtures, as the reduction in maximum temperature rise is only about half of what is observed in the HoH results.

Figure 53c presents a bar chart with results for ternary mixtures containing 30% slag and 15% MK. The HoH results show great consistency across the maximum temperature rise measurements in all six ternary replacement mixtures. In the three mixtures containing the SLa product, the same reduction percentage is observed in both HoH and the maximum temperature rise. In the other three ternary mixtures containing the SLb product, HoH results show a 15% reduction compared to the 20% reduction observed in the maximum temperature rise.

Altogether, these results indicate a strong relative consistency between the HoH from small mixtures and the maximum temperature rise measurements from the cube specimens. HoH from an isothermal calorimeter can provide a practical evaluation of a mixture's suitability for mass concrete placements. If casting mock-up cube specimens is not possible, HoH results can afford a reasonable prediction of the relative reduction or increase in the maximum temperature rise for different binary and ternary replacement mixtures.

Maximum temperature rise, however, still needs to be validated in a mass concrete element since it is challenging to predict from HoH results as the specific heat value of each mixture is required to convert HoH to temperature rise. The time of maximum temperature rise in mass concrete elements also changes when different SCMs are used. It is, therefore, challenging to select an HoH value that corresponds to the time of maximum temperature rise. Thus, HoH alone is not sufficient to accurately predict temperature rise measurements in mass concrete elements; actual measurements from cube specimens may be necessary to quantify temperature rise in mass concrete elements more realistically and accurately.

Ultimately, the reduction in HoH observed in different mixtures using an isothermal calorimeter provides significant information about the suitability of specific mixtures to be used for mass concrete placements. This information further helps in predicting the relative reduction or increase in maximum temperature rise in different mixtures and minimizing the number of mass concrete mock-up specimens needed to be built for further temperature rise measurements.

3.4.3 **Part 3 – Comparison with Available Equations to Predict Maximum Temperature Rise**

In this section, the maximum temperature rise measurements from Part 2 are compared with the maximum temperature rise calculated from the existing prediction methods described in Section 3.2.1.1 and in more detail in the following section. In each of these methods, adding the estimated temperature rise to the initial concrete temperature provides a prediction for the maximum concrete temperature.

The Portland Cement Association (PCA, 2011) provides a method for predicting the maximum temperature rise as shown in Eq. 1, where T_{max} is the predicted maximum concrete temperature, °F (°C), T_i is the concrete placement temperature, °F (°C), and W_c is the weight of cement per unit volume of the mixture, lb/yd^3 (kg/m^3). This method assumes that temperature increases by 12.8 °F for every 100 lb/yd^3 (12 °C for every 100 kg/m^3) of cement used. It does not, however, provide any guidance regarding mixtures containing SCMs.

$$T_{max} = T_i + \left(12.8 * \frac{W_c}{100}\right) \quad \text{Equation 1}$$

The ACI (ACI 207.1R-05, 2012) slightly adjusts the PCA method by incorporating the effect of pozzolans (specifically Class F fly ash). Temperature rise per this method is given in Eq. 2, where W_{SCM} is the weight of SCMs per unit volume of the mixture, lb/yd^3 (kg/m^3). This method (called PCA-ACI Method here) assumes that temperature decreases by 6.4 °F for every 100 lb/yd^3 (6 °C for every 100 kg/m^3) of cement replaced by SCMs (i.e., fly ash).

$$T_{max} = T_i + \left(12.8 * \frac{W_c}{100}\right) + \left(6.4 * \frac{W_{SCM}}{100}\right) \quad \text{Equation 2}$$

The equation proposed by Gajda et al. (2014) to estimate temperature rise is given in Eq. 3 in a format consistent with the previous two equations (Eqns. 1 and 2). It linearly adds the temperature increases from the cement (W_c), fly ash (W_{FAsh}/W_{CAsh}), SF (W_{SF}), MK (W_{MK}), and slag (W_{Slag}). The W in Eq. 3 is the weight of each SCM per unit volume of the mixture, lb/yd^3 (kg/m^3). This method assumes that for every 100 lb/yd^3 (100 kg/m^3) of cement replaced, Class F fly ash decreases the temperature by 8 °F (7.5 °C), Class C fly ash decreases the temperature by 3.2 °F (3 °C), SF and MK each increase the temperature

by 3.2 °F (3 °C), and slag changes the temperature by a $Factor$, which varies based on the percent replacement level.

$$T_{max} = T_i + \left(16 * \frac{W_c}{100}\right) + \left(8 * \frac{W_{FAsh}}{100}\right) + \left(12.8 * \frac{W_{CAsh}}{100}\right) + \left(19.2 * \frac{W_{SF/MK}}{100}\right) + \left(16 * Factor * \frac{W_{Slag}}{100}\right) \quad \text{Equation 3}$$

In Eq. 3, $Factor$ is a variable, which depends on the percentage of cement replaced (1.0 to 1.1 for 0–20% replacement, 1.0 for 20–45% replacement, 0.9 for 45–65% replacement, and 0.8 for 65–80% replacement). Based on Eq. 3, a partial replacement of cement with 30% slag and 15% MK in a total of 711 lb/yd^3 (422 kg/m^3) ternary replacement mixture results in a temperature increase of about 3.4 °F (1.9 °C) compared to that of a mixture without supplementary material.

Table 28 presents the maximum temperature comparisons between the experimental results from the cube specimens and the results calculated from Eqns. 1, 2, and 3. The PCA method only gives a prediction for mixtures containing cement. Therefore, no predictions are provided for mixtures containing SCMs under the PCA method column. The PCA-ACI method yields predictions for mixtures containing cement and fly ash; accordingly, the values for other mixtures are left blank in this column. The maximum temperature rise measurements of all mixtures are also graphically compared to the temperature rise values predicted by Eq. 3 (Gajda et al., 2014) and presented in Figure 54.

Table 28 – Maximum temperature rise comparisons, °F (°C).

Replacement (%)	Mixture Code	Experimental Results	PCA	PCA-ACI	Gadja
0	Control	90.5 (50.3)	91.0 (50.6)	91.0 (50.6)	113.8 (63.2)
15 (binary)	MK1-15	92.8 (51.6)	-	-	117.2 (65.1)
	MK2-15	75.6 (42.0)	-	-	117.2 (65.1)
	MK3-15	89.1 (49.5)	-	-	117.2 (65.1)
30 (binary)	SLa-30	87.4 (48.6)	-	-	113.8 (63.2)
	SLb-30	86.1 (47.8)	-	-	113.8 (63.2)
	FA-30	76.5 (42.5)	-	77.4 (43)	96.7 (53.7)
45 (binary)	SLa-45	85.2 (47.3)	-	-	108.7 (60.4)
	SLb-45	83.8 (46.6)	-	-	108.7 (60.4)
	FA-45	64.8 (36.0)	-	70.5 (39.2)	88.2 (49.2)
45 (ternary)	SLa-30+MK1-15	73.8 (41.0)	-	-	117.2 (76.1)
	SLa-30+MK2-15	72.9 (40.5)	-	-	117.2 (76.1)
	SLa-30+MK3-15	71.3 (39.6)	-	-	117.2 (76.1)
	SLb-30+MK1-15	73.3 (40.7)	-	-	117.2 (76.1)
	SLb-30+MK2-15	72.0 (40)	-	-	117.2 (76.1)
	SLb-30+MK3-15	72.0 (40)	-	-	117.2 (76.1)

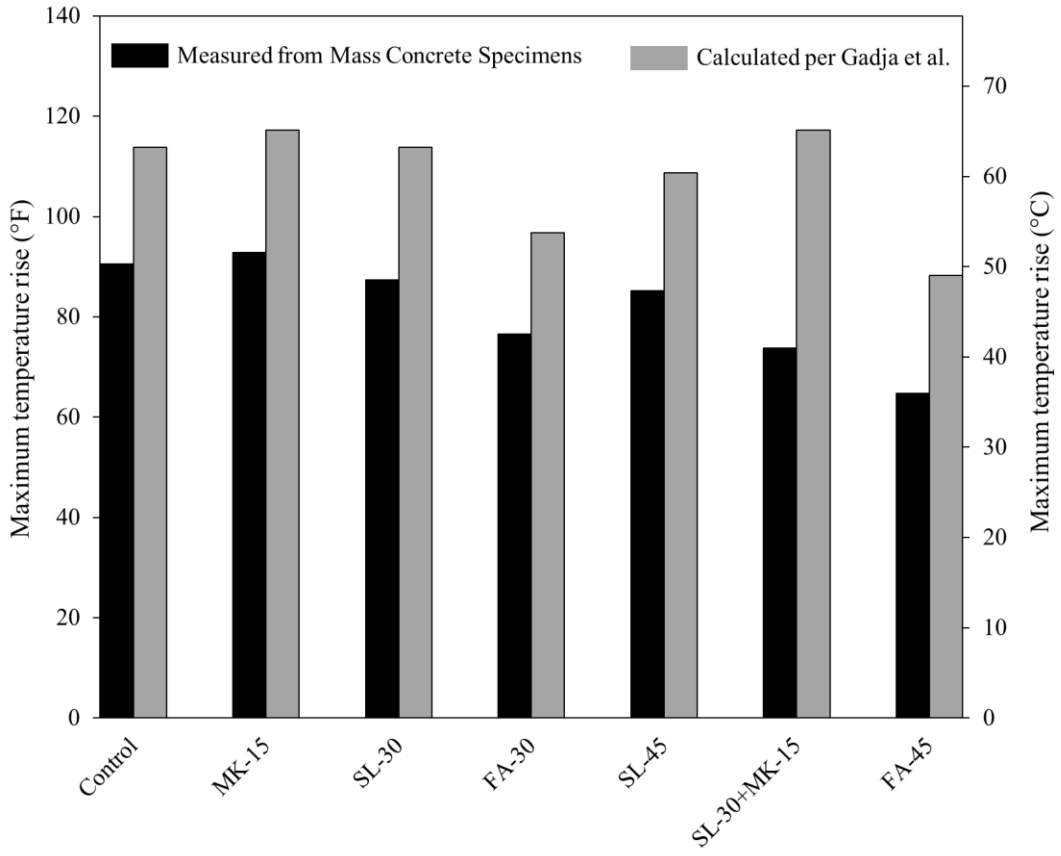

Figure 54 – Experimental and calculated maximum temperature rise comparison.

The results presented in Table 28 show that the maximum temperature rise of the Control mixture is well predicted by both the PCA and PCA-ACI methods, and it is overestimated by the Gadja et al. (2014) method. The PCA-ACI method also gives a close prediction on the maximum temperature rise for binary mixtures containing 30% and 45% fly ash. The Gadja et al. (2014) method predicts the relative increase or decrease in the maximum temperature rise in the binary mixtures as shown in Table 28 and Figure 54, though it overestimates the temperature by about 25 °F (13.9 °C). At the same time, this method significantly overpredicts temperature rise in the ternary mixtures containing slag and MK (SL-30+MK-15). Based on this method, the SL-30+MK-15 mixtures result in an increase of about 3.4 °F (1.9 °C) in the maximum temperature rise compared to that of the

Control mixture, whereas, a significant reduction of about 18 °F (10 °C) is observed from the experimental results of this study. The reason for this overprediction is that the Gadja et al. (2014) method is not designed to consider the combined effect of slag and MK, and it linearly adds the temperature rise effect first from slag and then from MK. In contrast, the temperature measurements and the HoH results from this study indicate that the combination of slag and MK in ternary replacement mixtures results in a significant reduction in temperature compared to the Control mixture.

These results show that existing equations well predict the maximum temperature rise in binary mixtures, yet they fail to predict the maximum temperature from ternary replacement mixtures containing slag and MK. Therefore, the results of this study provide a baseline for additional research necessary to fully develop a prediction method for ternary replacement mixtures.

3.5 Conclusions

An experimental program consisting of binary and ternary replacement paste, mortar, and concrete mixtures is implemented to study the effect of different SCMs and phase-changing and polymer-modified materials on HoH and temperature rise measurements from cube specimens. The research is divided into three parts, and each part provides answers for specific research questions as follow:

3.5.1 Findings from Part 1

- The HoH results from paste and mortar samples including different SCMs are consistent with each other. The mortar mixtures, however, may only be used for qualitative comparison as they result in lower HoH per gram of SCMs than their corresponding paste mixtures. The lower HoH is due to a lower mixing energy and

its associated friction between the particles in the mortar samples, as well as cement paste lost when preparing the mortar mixtures from concrete mixtures after screening out the coarse aggregate.

- The 10% cement weight addition of PVA paste to cementitious mixtures results in a negligible reduction in HoH.
- The addition of a 3.5% BaO powder, consisting of 97% BaO, to cementitious mixtures results in a significant (3 hours) delay in the HoH peak and setting time in the early period after concrete placement, while only a slight reduction in the HoH (by 3%) is achieved over the course of a week.

3.5.2 **Findings from Part 2**

- Partial replacements (15%) of cement with three different MK products in binary replacement mixtures do not negatively affect the maximum temperature.
- Partial replacements (with up to 45%) of cement with two different slag products in binary replacement mixtures result in a slight reduction (≤ 6.7 °F or 3.7 °C) in the maximum temperature rise.
- 45% cement replacement with (30%) slag and (15%) MK in ternary replacement mixtures results in a significant reduction (approximately 18 °F (10 °C)) in the maximum temperature rise.
- The temperature reduction achieved in the ternary replacement mixtures results in a reduction level similar to that obtained in the 30% cement replacement mixture with fly ash.
- HoH results from small mixtures provide an effective tool to predict the relative reduction or increase in maximum temperature rise measurements from cube

specimens. HoH from an isothermal calorimeter can provide a practical evaluation for quantifying the maximum temperature rise, although HoH results are relatively higher than temperature measurements in binary MK and ternary mixtures and relatively lower than temperature measurements in slag and fly ash binary mixtures.

- The duration of time the maximum temperature is maintained is about 17 hours in the Control mixture and is shortened in the ternary replacement mixtures by about 7 to 10 hours. This shorter exposure time in the ternary mixtures is beneficial in reducing the possibility of DEF occurrence.

3.5.3 Findings from Part 3

- Existing prediction methods estimate the maximum temperature rise in binary mixtures effectively; however, they fail to predict the maximum temperature in ternary replacement mixtures containing slag and MK. The combined effect of both slag and MK results in a significant reduction in the maximum temperature rise, but the existing equations are not designed to consider a reduction from this combined effect.

3.6 Discussion

The results from this study suggest that existing equations for predicting the maximum temperature increase do not consider reductions achieved from ternary replacement mixtures. Future work is needed to study the effect of ternary replacement mixtures on the maximum temperature rise at different replacement levels.

CHAPTER 4

ANALYTICAL INVESTIGATION OF MASS CONCRETE STRUCTURES

This chapter presents an analytical investigation of mass concrete elements in transportation structures. DIANA is a finite element analysis (FEA) software program and is used to numerically simulate mass concrete structures with different configurations. The main objective of this investigation is to develop an FEA model capable of predicting temperature distribution and determining its consequent strains, stresses, and cracking in mass concrete structures. In addition, validation of the model is achieved by a case study, an investigation of cracks observed in a bridge seal structure.

4.1 Motivation, Background, and Procedure

4.1.1 Motivation

Experimental investigations are often time-consuming and costly, and their scope is limited by the large size and complex geometry of the structures. Conducting an analytical investigation of mass concrete structures provides great insight into structural performance when funding and time are limited. In turn, developing a verified, validated, and thus reliable computer simulation model is vital to predict structural performance, such as a thermal distress in mass concrete structures. Such a model can also inform investment decisions and aid in performance-based design (FHWA, 2017). For instance, computer simulation capacities and associated technologies enable predictions of distress, such as cracking in bridge foundation structures. Proper resolutions, design changes, and necessary precautions can then be taken by state DOTs and their contractors.

In summary, having a reliable analytical model capable of accurately analyzing and developing alternative designs is vital when developing mass concrete structures. More specifically, such a model is able to evaluate thermal stresses from the heat of cement hydration in complex mass concrete structures without investing a large amount of time and effort.

4.1.2 **Background**

Thermal forces in concrete structures in an elastic analysis are fictitious. If fictitious thermal forces are used for design, an increase in tensile strain will in reality crack a concrete section. Concrete cracking in fact relieves thermal stresses and is a desired behavior to a certain extent. To simulate this nonlinear behavior and illustrate the extent of cracking, a coupled thermal-structural model with a nonlinear concrete material model is developed in the FEA program DIANA.

When analyzing mass concrete structures, temperature input from the HoH of cementitious materials is necessary. The process by which this heat (or temperature history) is applied and dissipated in an analytical model is complex and depends on many factors: the size and geometry of a structure, constituents and proportions of concrete mixtures, and boundary conditions. This study investigates the effects of different mixture designs, structural configurations, and boundary conditions on the thermal and structural behavior of mass concrete structures using the FEA method. The goal of this analytical investigation is to develop a reliable FEA model capable of predicting temperature distribution and defining the degree of cracking in mass concrete structures for varying V/A ratios and mixture designs.

4.1.3 **Research Procedure**

First, 14 of the 17 mass concrete specimens tested in Chapter 3 are simulated. This step is achieved by using HoH data from Chapter 3 as input data in a thermal analysis model. The resulting temperature distribution and maximum temperature are compared with the experimentally measured temperatures in Chapter 3. Subsequently, a validation study is conducted using a time-dependent mass concrete placement study available in the literature (Jung et al., 2017).

A transient thermal analysis coupled with a nonlinear structural analysis is then conducted. A comparison of results from the coupled thermal-structural analysis and the validation study is presented. Finally, a case study of a concrete bridge seal structure exhibiting distress is studied using the DIANA software. Sections 4.9.4 through 4.9.6 present the outcomes.

The following list presents and describes mass concrete specimens and structures investigated through a coupled thermal-structural analysis:

- A validation study including 14 mass concrete cube specimens from Chapter 3. The mixtures consist of 2 Control mixtures in summer and winter placements, 6 binary mixtures containing 30% or 45% slag or fly ash, and 6 ternary mixtures containing 30% slag and 15% MK. Predicted maximum temperature results are compared to the experimental results.
- A validation study involving a 13 foot x 13 foot x 13 foot (4 m x 4 m x 4 m) mass concrete member cast on a rigid concrete slab. This was an experimental study conducted by Jung et al. (2017), from which they present detailed results regarding

temperature and crack size. Predicted temperature, strain, and crack width are compared against these experimental results.

- A case study involving a bridge seal member in Georgia is conducted. Predicted crack size is compared with crack sketches produced by divers during an underwater inspection.
- In Appendix E, an experimental program is designed to quantify the total strain in concrete. It consists of small concrete cylinder specimens exposed to elevated temperature (i.e., the total temperature described in Section 1.5.4.2) reflecting the total effect of both temperature increase and temperature differential.

4.2 Material Properties and Models

4.2.1 Thermal Properties

Concrete is a complex material made up of cement, water, fine aggregate, coarse aggregate, and often chemical admixtures. Its mechanical and thermal properties vary with age as well as temperature and humidity conditions. The thermal properties of concrete and boundary elements affect the rate of heat generation and dissipation in the concrete. Two properties are particularly important: thermal conductivity and specific heat. These properties are either constant or depend on variables such as temperature, time, or degree of reaction in concrete mixtures.

4.2.1.1 Thermal conductivity

Thermal conductivity, commonly represented by the symbol, k, is a measure of concrete's ability to conduct heat. It is defined as the rate of heat flow per unit temperature gradient causing the heat movement (ACI 207.2R-07, 2007). It can further be explained as the thermal energy (heat), Q, transmitted through a length or thickness L in the direction normal

to a surface area A, under a steady-state temperature difference T_h and T_c (Zhao et al., 2016). Figure 55 presents the thermal conductivity of solid bulk material using Fourier's law of heat conduction in a one-dimensional heat flow system. The techniques used to measure thermal conductivity are broadly classified under steady-state and transient methods. Concrete has a low thermal conductivity and therefore has a low rate of heat transfer. This low thermal conductivity results in an increase in the temperature at the core of mass concrete elements, as it takes a long time for the heat to dissipate.

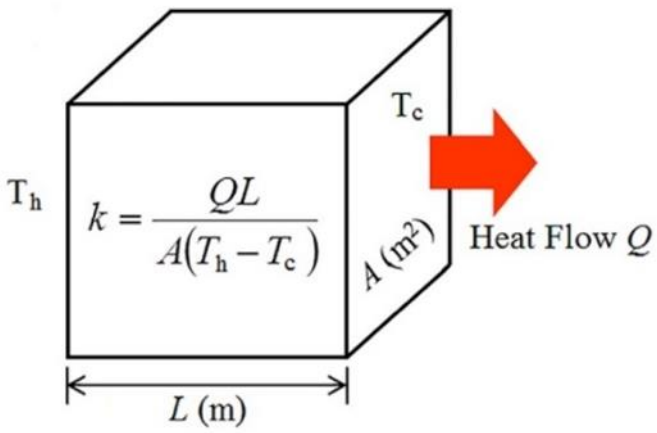

Figure 55 – One-dimensional heat flow system (Zhao et al., 2016)**.**

For a three-dimensional case, as shown in Figure 56, the Fourier equation for heat transfer becomes (Lawrence, 2009):

$$q^n = -k\Delta T = -k(i\frac{\partial T}{\partial x} + j\frac{\partial T}{\partial y} + k\frac{\partial T}{\partial z}) \qquad \text{Equation 4}$$

where:

x, y, z = the axes of the coordinate system.

i, j, k = the vector directions in the coordinate system.

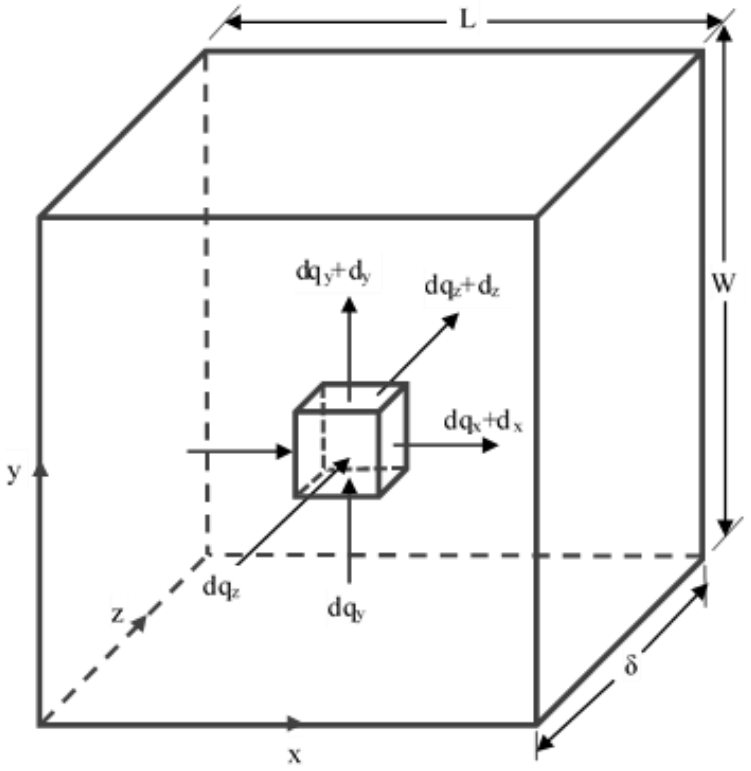

Figure 56 – Three-dimensional heat flow system (regenerated from Lawrence, 2009)**.**

Thermal conductivity of a solid-phase material can span several orders of magnitude at room temperature, with a value of 0.015 W/m·°C for aerogels at the low end to 2000 W/m·°C for diamond and 3000 W/m·°C for single-layer graphene at the high-end (Zhao et al., 2016). The thermal conductivity of conventional normal strength concrete at room temperature ranges between 1.4 and 3.6 W/m·°C (ACI 207.2R-07, 2007; Bažant et al., 1996). Table 29 shows the thermal properties of concrete mixtures used in a variety of mass concrete structures (ACI 207.2R-07, 2007). Here, temperatures ranging from 50 °F–150 °F (10 °C–65 °C) in mass concrete structures do not significantly affect thermal conductivity. The average change in thermal conductivity is less than 3% when the temperature rises from 50 °F (10 °C) to 150 °F (66 °C), which is a reasonable temperature range in mass concrete structures.

Table 29 – Thermal properties of mass concrete mixtures (ACI 207.2R-07, 2007)**.**

Structure	Coarse aggregate type	Temperature, °F (°C)	Coefficient of expansion,† millionths/°F (millionths/°C) 1-1/4 in. (37.5 mm) max.	Coefficient of expansion,† millionths/°F (millionths/°C) 4-1/2 in. (114 mm) max.	Thermal conductivity,‡ Btu/ft·h·°F (kJ/m·h·°C)	Specific heat, Btu/lb·°F (kJ/kg·°C)	Density, lb/ft^3 (kg/m^3)	Diffusivity,§ ft^2/h ([m^2/h] × 10^{-3})
Hoover	Limestone and granite	50 (10)	5.3 (9.5)	4.8 (8.6)	1.70 (10.6)	0.212 (0.887)	156.0 (2500)	0.051 (4.7)
		100 (38)			1.67 (10.4)	0.225 (0.941)		0.047 (4.4)
		150 (66)			1.65 (10.3)	0.251 (1.050)		0.042 (3.9)
Grand Coulee	Basalt	50 (10)	4.4 (7.9)	4.6 (8.3)	1.08 (6.74)	0.219 (0.916)	158.1 (2534)	0.031 (2.9)
		100 (38)			1.08 (6.74)	0.231 (0.967)		0.029 (2.7)
		150 (66)			1.09 (6.78)	0.257 (1.075)		0.027 (2.5)
Friant	Quartzite granite and rhyolite	50 (10)	—	—	1.23 (7.66)	0.216 (0.904)	153.8 (2465)	0.037 (3.4)
		100 (38)			1.23 (7.66)	0.230 (0.962)		0.035 (3.2)
		150 (66)			1.24 (7.70)	0.243 (1.017)		0.033 (3.1)
Shasta	Andesite and slate	50 (10)	—	4.8 (8.6)	1.32 (8.20)	0.219 (0.916)	156.6 (2510)	0.039 (3.6)
		100 (38)			1.31 (8.16)	0.233 (0.975)		0.036 (3.3)
		150 (66)			1.31 (8.16)	0.247 (1.033)		0.034 (3.2)
Angostura	Limestone	50 (10)	4.0 (7.2)	—	1.49 (9.29)	0.221 (0.925)	151.2 (2423)	0.045 (4.2)
		100 (38)			1.48 (9.20)	0.237 (0.992)		0.041 (3.8)
		150 (66)			1.46 (9.08)	0.252 (1.054)		0.038 (3.5)
Kortes	Granite gabbros and quartz	50 (10)	5.2 (9.4)	4.5 (8.1)	1.61 (10.0)	0.208 (0.870)	151.8 (2433)	0.050 (4.6)
		100 (38)			1.60 (9.96)	0.221 (0.925)		0.047 (4.4)
		150 (66)			1.59 (9.87)	0.234 (0.979)		0.044 (4.1)
Hungry Horse	Sandstone	50 (10)	6.2 (9.7)	5.7 (9.4)	1.72 (10.1)	0.217 (0.895)	150.1 (2425)	0.053 (4.6)
		100 (38)			1.71 (10.0)	0.232 (0.937)		0.049 (4.4)
		150 (66)			1.69 (9.87)	0.247 (0.983)		0.046 (4.2)
Monticello	Sandstone, metasiltsone, quartzite, and rhyolite	50 (10)	5.2 (9.4)	—	1.57 (9.79)	0.225 (0.941)	151.3 (2454)	0.046 (4.3)
		100 (38)			1.55 (9.67)	0.237 (0.992)		0.043 (4.0)
		150 (66)			1.53 (9.54)	0.250 (1.046)		0.040 (3.7)
Anchor	Andesite, latite, and limestone	50 (10)	5.6 (10.1)	4.5 (8.1)	1.14 (7.11)	0.227 (0.950)	149.0 (2388)	0.034 (3.2)
		100 (38)			1.14 (7.11)	0.242 (1.013)		0.032 (3.0)
		150 (66)			1.15 (7.15)	0.258 (1.079)		0.030 (2.8)
Glen Canyon	Limestone, chert, and sandstone	50 (10)	—	—	2.13 (13.3)	0.217 (0.908)	150.2 (2407)	0.065 (6.0)
		100 (38)			2.05 (12.8)	0.232 (0.971)		0.059 (5.5)
		150 (66)			1.97 (12.3)	0.247 (1.033)		0.053 (4.9)
Flaming Gorge	Limestone and sandstone	50 (10)	—	—	1.78 (11.1)	0.221 (0.925)	150.4 (2411)	0.054 (5.0)
		100 (38)			1.75 (10.9)	0.234 (0.979)		0.050 (4.6)
		150 (66)			1.73 (10.8)	0.248 (1.038)		0.046 (4.3)
Yellowtail	Limestone and andesite	50 (10)	—	4.3 (7.7)	1.55 (9.67)	0.226 (0.946)	152.5 (2444)	0.045 (4.2)
		100 (38)			1.52 (9.46)	0.239 (1.000)		0.042 (3.9)
		150 (66)			1.48 (9.20)	0.252 (1.054)		0.039 (3.6)
Dworshak	Granite gneiss	100 (38)	—	5.5 (9.9)	1.35 (8.41)	0.220 (0.920)	154 (2467)	0.040 (3.9)
Ilha Solteira	Quartzite and basalt	100 (38)	—	6.9 (12.5)	1.73 (10.8)	0.220 (0.920)	159 (2552)	0.049 (4.6)
Itaipu	Basalt	100 (38)	—	4.3 (7.8)	1.06 (6.61)	0.233 (0.975)	158 (2537)	0.029 (2.7)
Theodore Roosevelt Modification	Granite	50 (10)	4.3 (7.7)	—	1.71 (10.7)	0.234 (0.979)	148.7 (2380)	0.049 (4.6)
		100 (38)			1.73 (10.9)	0.248 (1.037)		0.047 (4.4)
		150 (66)			1.70 (10.6)	0.260 (1.088)		0.044 (4.1)
Olivenhain	Granodiorite	100 (38)	5.4 (9.7)	—	0.94 (5.86)	0.210 (0.880)	147.4 (2360)	0.030 (2.8)

*(U.S. Army Corps of Engineers 1966; U. S. Bureau of Reclamation 1961; Pacellidede et al. 1982).
†1-1/2 in. (37.5 mm) and 4-1/2 in. (114 mm) max. refer to maximum size of aggregate in concrete.
‡Procedure for calculating thermal conductivity is described in CRD-44 (U.S. Army Corps of Engineers 1949).
§Diffusivity is often expressed in ft^2/day (m^2/day) for convenience in calculations.

The ACI report (2007) also states that for normal concrete temperatures in mass concrete construction, and for the high moisture content existing in concrete at early ages, thermal conductivity values should resemble the values shown in Table 30.

Table 30 – Typical thermal conductivity values for concrete selected by type of aggregate (U.S. Bureau of Reclamation 1940) (ACI 207.2R-07, 2007)**.**

Aggregate type	Thermal conductivity, Btu·in./h·ft^2·°F (KJ/kg·°C)
Quartzite	24 (4.5)
Dolomite	22 (4.2)
Limestone	18 to 23 (2.6 to 3.3)
Granite	18 to 19 (2.6 to 2.7)
Rhyolite	15 (2.2)
Basalt	13 to 15 (1.9 to 2.2)

According to Table 30, for a concrete made with limestone, the thermal conductivity coefficient should fall between 2.6 and 3.3 W/m·°C. Mass concrete structures studied in the current investigation contain limestone; thus, a thermal conductivity coefficient of 3.0 W/m·°C is selected for the analysis. Finally, the thermal conductivity of commonly used formwork and insulation materials are shown in Table 31.

Table 31 – Thermal conductivity of common formwork and insulation materials.

Materials	**Thermal Conductivity**
Plywood sheathing	0.12
Steel	50
Insulating blanket	0.058
Fiberglass	0.037
Extruded polystyrene (XPS) foam	0.029
Expanded polystyrene (EPS) foam	0.036
Kingspan Kooltherm K20	0.017
Dry clay	0.25
Saturated clay	1.589
Dry sand	0.30
Saturated sand	2.3

4.2.1.2 Specific heat

Specific heat is defined as the amount of energy needed to raise the temperature of 1 gm of a material by 1 °C, or the quantity of heat energy in BTU required to raise the temperature of 1 pound of a material by 1 °F. In the context of this study, specific heat is a function of the specific heat capacities of the concrete mixture ingredients, moisture content, porosity, and mixture temperature. For normal weight concrete, ACI states that specific heat capacities of 0.20–0.25 Btu/lb·°F (0.84 to 1.05 KJ/kg·°C) should be used across a wide range of conditions and materials (ACI 207.2R-07, 2007), whereas the Japan Society of Civil Engineers (JSCE) recommends that specific heat capacities range from 0.251 Btu/lb·°F (1.05 KJ/kg·°C) to 0.300 Btu/lb·°F (1.26 KJ/kg·°C) (JSCE, 2007). Table 29 shows typical thermal properties used in a variety of mass concrete structures (ACI 207.2R-07, 2007), as well as specific heat capacities ranging from 0.208 to 0.260 Btu/lb·°F (0.87 to 1.09 J/g·°C) in various mass concrete placements. The increase in mass concrete temperature from 50 °F to 150 °F (10 °C to 66 °C) results in about a 10% to 20% increase in specific heat. Specific heat is theoretically calculated using the law of mixtures as a mass-weighted average of the specific heat capacity of each ingredient in the concrete. For a material made with two or more constituent materials, Eq. 5 is used to determine the specific heat (ASTM C1702, 2017). Table 32 shows specific heat capacities for constituent materials.

$$C = \sum M_i * C_i \qquad \text{Equation 5}$$

Where:

C = specific heat of concrete, J/g-c; M_i = mass percentage of the ith constituent; and C_i = specific heat of the ith constituent, J/g-C.

Table 32 – Specific heat value of concrete ingredients (ASTM C1702, 2017)**.**

Materials	Specific Heat Capacity J/g-C
Cement	0.75
Fly ash	0.8
Slag	0.8
Metakaolin	0.93
Sand	0.8
Limestone	0.84
Water	4.18

A reduction of about 10% to 20% in the specific heat of concrete during hardening is reported by many researchers (Brown & Javaid, 1970; Hansen et al. 1982; Reinhardt et al., 1982; De Schutter & Taerwe, 1995). This reduction is a function of the degree of hydration or time. In the current study, specific heat values are calculated for each concrete mixture as the mass-weighted average of the specific heat capacity of each constituent, as shown in Table 32. A 15% reduction in specific heat as a function of the degree of hydration is considered for the FEA simulation. Furthermore, slight adjustments are made for the specific heat values of each concrete mixture in the FEA models based on the experimental results. Further discussion of the specific heat values used for analysis is provided in Section 4.7.4.

4.2.2 **Mechanical Properties**

The structural behavior of mass concrete depends on its mechanical properties. Temperature differences within a section create a differential volume change, which in turn develops strains across the section: compressive strain at the center and tensile strain at the surface zone of the section. Concrete is strong in compression but is weak in tension, and it cracks when the induced tensile strain exceeds its tensile strain capacity, which varies

with time. Additionally, the MOE changes considerably in the early ages of concrete and affects tensile strain capacity. Therefore, the time evolution of the modulus of elasticity affects tensile strain capacity and the extent of cracking.

A temperature change in concrete results in volume expansion or contraction. The coefficient of thermal expansion (CTE) determines the degree of expansion (or contraction). Concrete structures are more likely to experience deformation when their CTEs are higher.

The mechanical properties of concrete include compressive strength, tensile strain/strength, modulus of elasticity, coefficient of thermal expansion, density, slump, and air content. Experimental work is performed to determine these mechanical properties as discussed in Chapter 2. A constant Poisson's ratio ν of 0.2 is considered.

4.2.3 Material Models

The DIANA FEA software offers nonlinear material (i.e., concrete) models that are highly efficient for the convergence of displacement/strain solutions. Two concrete model codes, fib Model Code and ACI Model Code, are selected for defining the nonlinear properties of concrete. Both model codes are based on total-strain-crack models, which follow a smeared approach for measuring fracture energy. The cracking behavior of the fib Model Code is described by the total-strain-rotating-crack model, whereas the cracking behavior of the ACI Model Code is described by the total-strain-fixed-crack model. These rotating and fixed crack features play an important role in representing cracks and crack orientations. A detailed description of both models is provided in the DIANA Theory Manual (2017).

4.3 Element Types

The CHX60 solid element is selected for modeling concrete behavior in a structural analysis. This element, shown in Figure 57, is a twenty-node isoparametric solid brick element and is based on the 3x3x3 Gauss-Legendre quadrature formulae. Results are calculated at the Gauss integration points in each element. The basic variables are translations (or displacements), and the derived variables are the Green-Lagrange strains and Cauchy stresses (DIANA FEA, Version 10.2).

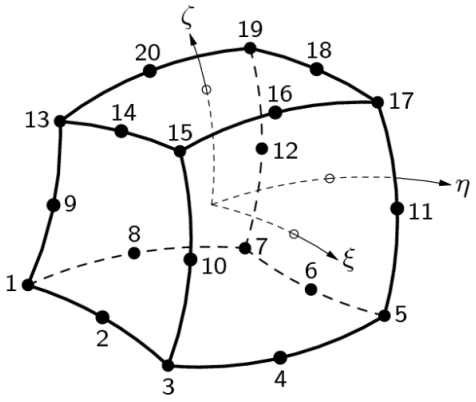

Figure 57 – CHX60 solid element in DIANA (DIANA, 2017)**.**

Reinforcing steel is modelled by line elements and are constrained in the concrete continuum by the Constrained Lagrange feature in DIANA. Figure 58 presents a bar reinforcement embedded in a solid element.

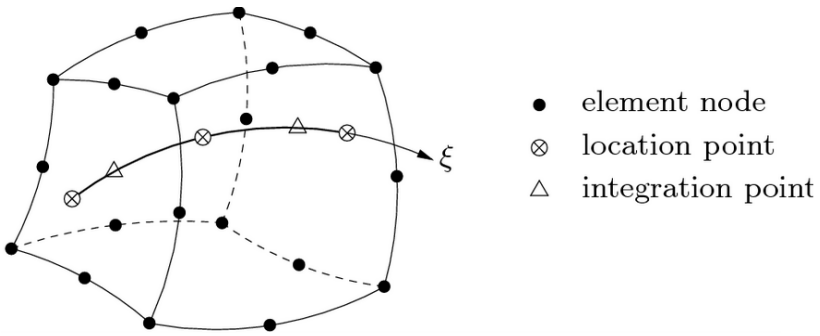

Figure 58 – Modeling reinforcing steel in a solid element (DIANA, 2017)**.**

The BQ4HT element is used for describing thermal boundaries. This element, shown in Figure 59, is a four-node isoparametric quadrilateral boundary surface element. It is based on linear interpolation and Gauss integration and used to describe boundaries such as a convective surface in a three-dimensional potential (or heat) flow analysis (DIANA FEA, Version 10.2).

The CQ481 element is used for modeling a structural interface. This element formulation is based on a quadratic interpolation. It is used to define properties between two planes in a three-dimensional configuration and has three nodes at each edge, with a total of eight nodes on each face of the element as shown in Figure 60 (DIANA FEA, Version 10.2).

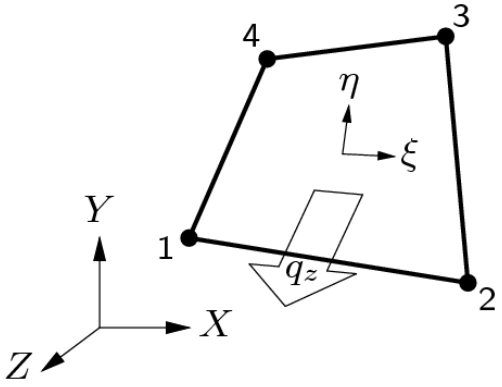

Figure 59 – BQ4HT boundary element (DIANA, 2017)**.**

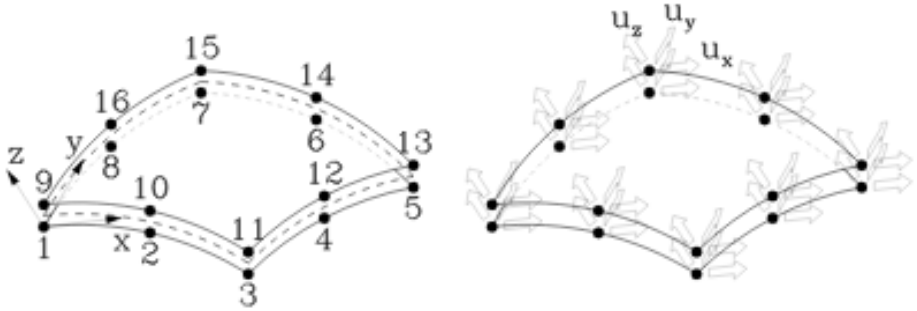

Figure 60 – CQ481 interface element (DIANA, 2017)**.**

4.4 Boundary Conditions

The use of accurate and reasonable boundaries reflecting the conditions surrounding the structure is vital in an analysis of finite element models. Boundary conditions include thermal and structural conditions. Thermal boundary conditions consist of external environment temperatures and surface convections. Structural boundary conditions include the restriction to displacement of the structure and the defining property of contact or interface layers.

4.5 Development of Temperature Input Data

When there is no heat transfer to or from the environment, an increase in temperature of a concrete mixture as a result of an exothermic chemical reaction is referred to as adiabatic temperature rise. To simulate the heat generation from cementitious materials, an adiabatic temperature-time history of a concrete mixture is required as input for a thermal analysis in DIANA. The adiabatic temperature rise of a concrete mixture is obtained from its HoH using the first rule of thermodynamics:

$$\Delta T = \frac{\Delta Q}{C_p * m} * SCM\% \qquad \text{Equation 6}$$

where,

ΔT= incremental change in temperature, C;

ΔQ= incremental change in energy, J/g;

C_p= specific heat of the concrete mixture, W/g.C;

m= unit weight of the concrete, kg/m^3; and

$SCM\%$= weight percent of total cementitious materials in the concrete mixture.

Therefore, HoH, specific heat, and unit weight are required for each concrete mixture to calculate adiabatic temperature development. Accordingly, the HoH test is

performed using an isothermal calorimetry on all the mixtures used in the 14 cube specimens, a 13 foot x 13 foot x 13 foot (4.0 m x 4.0 m x 4.0 m) mass concrete element, and the bridge seal structure. Meanwhile, the specific heat for each concrete mixture is calculated per Eq. 5 as the mass-weighted average of the specific heat capacity of each constituent in the concrete mixture. The unit weight of each concrete mixture is experimentally measured. Finally, Eq. 6 is used to calculate adiabatic temperature development, values which are then used as the input temperature load for the thermal analysis. Calculation details are presented with the description of each FEA model in the following sections (Sections 4.7, 4.8, and 4.9).

4.6 Coupled Thermal-Structural Analysis

A heat flow analysis and a subsequent structural analysis are known as a staggered flow-stress analysis. DIANA automatically reads the results from a thermal analysis for a structural analysis. A staggered flow-stress (or coupled thermal-structural) analysis comprises sequential execution of the following steps:

- Prepare a finite element model.
- Perform a heat flow analysis.
- Perform a structural analysis.

According to the DIANA Users' Manual (DIANA, 2019), the model for staggered flow-stress analysis consists of two domains: one for heat flow analysis and the other for structural analysis. A transient thermal analysis is first carried out to compute the temperature field in the concrete. The time-dependent flow results from a nonlinear transient heat analysis are converted to temperatures at each node in the model. These temperatures determine strains for a stress-field (transient nonlinear structural) analysis.

4.7 Validation – Experimental Results from Cube Specimens

4.7.1 FEA Model Description

For the fourteen 2 foot x 2 foot x 2 foot (0.61 m x 0.61 m x 0.61 m) cube specimens, a transient thermal analysis is performed for a duration of 2 weeks. The model reflects the HoH from the binary and ternary concrete mixtures studied in Chapter 3. The analysis results (e.g., maximum temperature) are compared with the experimental results. Figure 61 presents the geometry of the cube specimens used in the experimental work. A three-dimensional model is simulated in DIANA, and this simulation appears in Figure 62. Figure 63 presents the finite element mesh of the formwork and insulation panels inside the cube specimens.

(a) formwork and insulation materials (b) cube specimen after formwork removal

Figure 61 – Geometry of the cube specimens.

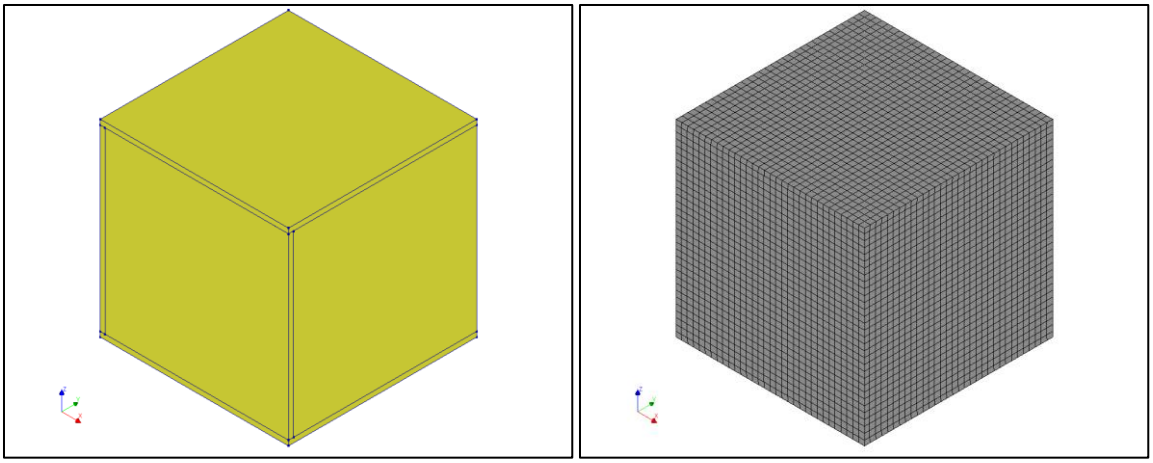

(a) three-dimensional geometry (b) element mesh

Figure 62 – Cube specimen in DIANA.

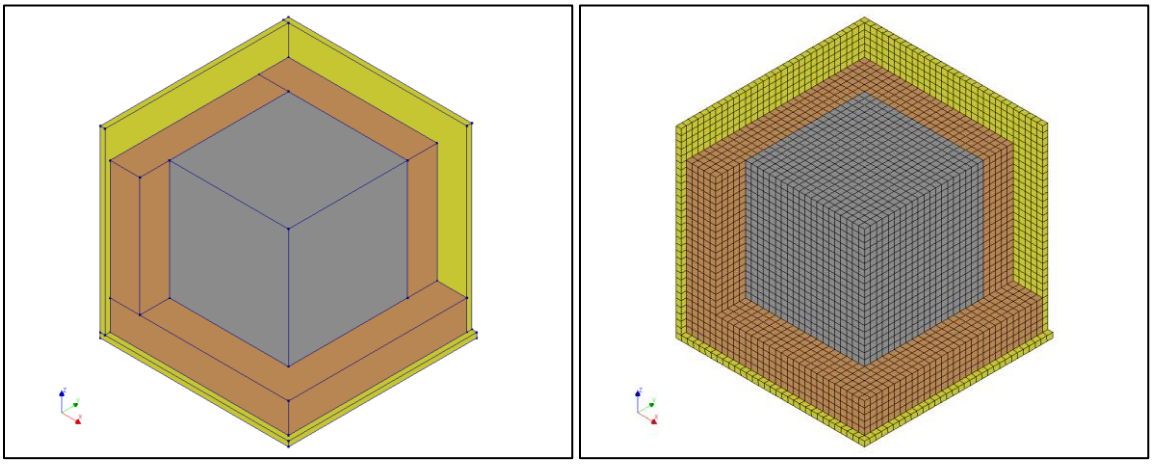

(a) three-dimensional geometry (b) element mesh

Figure 63 – Cube specimen interior in DIANA.

Figure 64 presents the HoH of the mixtures used in the 14 cube specimens. The unit weight and specific heat for each concrete mixture used for analysis are listed in Table 33. The time-temperature rise history for each concrete mixture serves as input for analysis; these are shown in Figure 65.

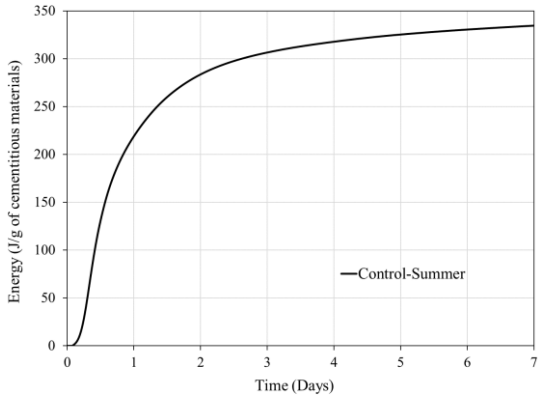

(a) Control mixture in summer placement

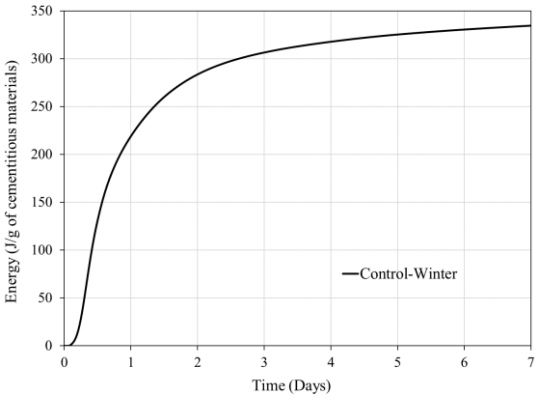

(b) Control mixture in winter placement

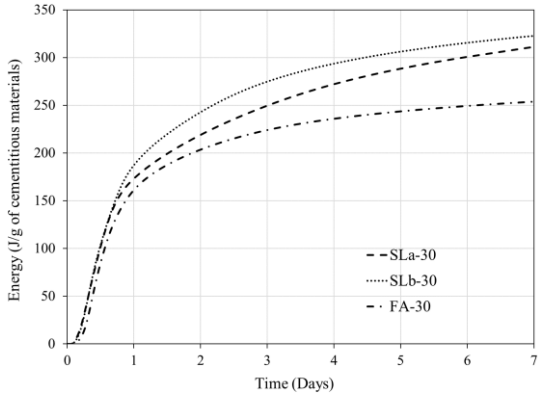

(c) 30% replacement binary mixtures

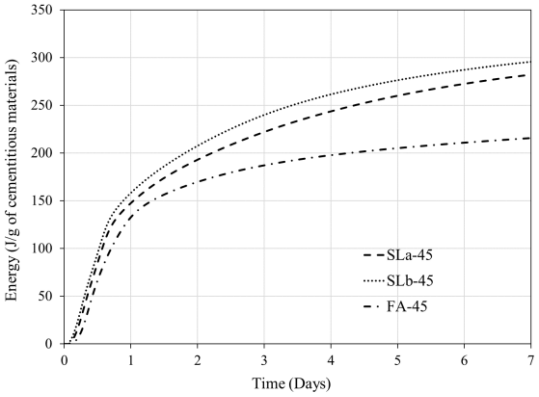

(d) 45% replacement binary mixtures

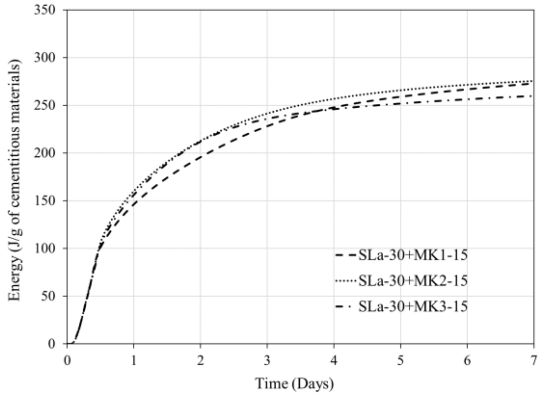

(e) 45% ternary mixtures of slag-a and MK

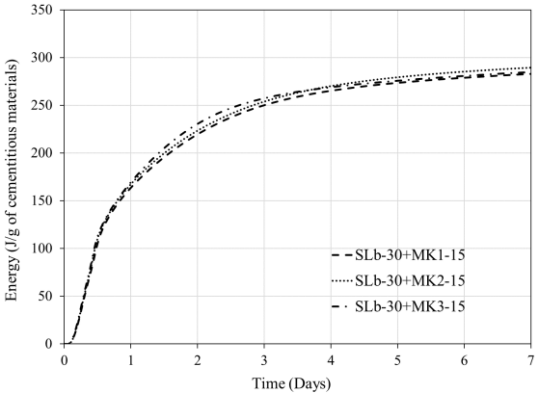

(f) 45% ternary mixtures of slag-b and MK

Figure 64 – HoH of mixtures used in the 14 cube specimens.

Table 33 – Unit weight and calculated specific heat values for concrete mixtures containing different SCMs.

Mixtures	Unit Weight (Kg/m^3)	Specific Heat (W/g.C)
Control	2345	1.09
SLa-30	2278	1.12
SLb-30	2351	1.09
FA-30	2297	1.11
SLa-45	2393	1.07
SLb-45	2329	1.10
FA-45	2339	1.09
SLa-30+MK1-15	2252	1.14
SLa-30+MK2-15	2265	1.13
SLa-30+MK3-15	2185	1.17
SLb-30+MK1-15	2316	1.11
SLb-30+MK2-15	2300	1.11
SLb-30+MK3-15	2319	1.11

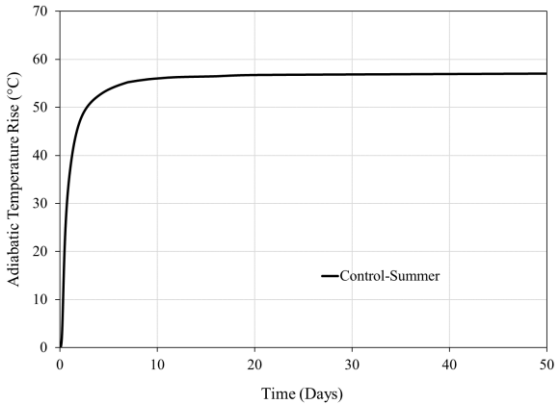

(a) Control mixture in summer placement

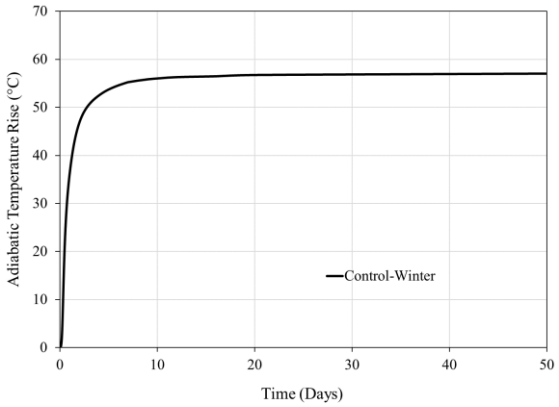

(b) Control mixture in winter placement

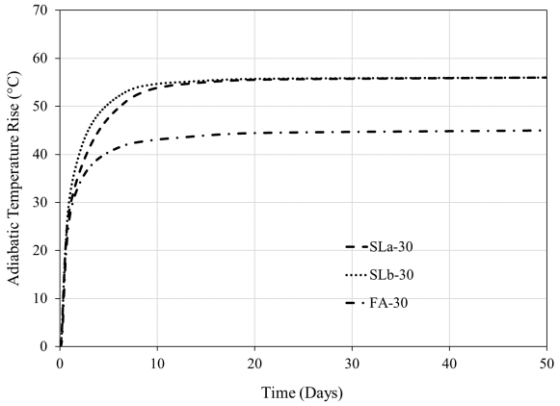

(c) 30% replacement binary mixtures

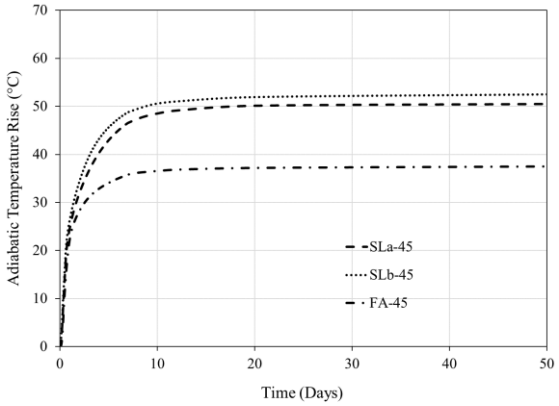

(d) 45% replacement binary mixtures

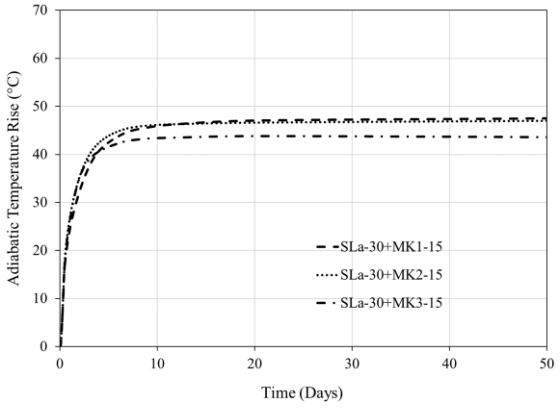

(e) 45% ternary mixtures of slag-a and MK

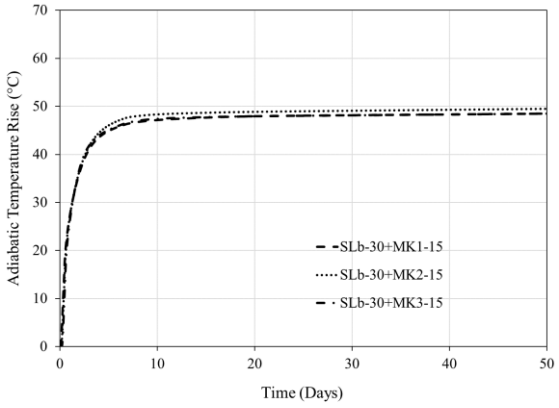

(f) 45% ternary mixtures of slag-a and MK

Figure 65 – Adiabatic temperature rise of mixtures used in the 14 cube specimens.

4.7.2 **Boundary Condition**

Thermal boundary conditions consist of external (or ambient) temperature and surface convection. During the experimental work, the specimens were kept inside a temperature-controlled lab with a constant temperature of 77 °F (25 °C). Therefore, an external temperature of 77 °F (25 °C) is applied to the model. A heat transfer coefficient of 2.11 Btu/h·ft^2·°F (12 W/m^2·C) is also used for air convection. The experimental placement temperature of each concrete mixture is used as the initial condition for the thermal analysis.

4.7.3 **Temperature Results**

The temperature results from the transient thermal analysis are presented in this section. Figure 66 illustrates a predicted temperature distribution inside a cube model. The temperature-time histories of all cube specimens are presented in Figure 67 through Figure 70. Figure 67 presents the temperature rise predictions for the Control mixtures for both summer and winter placement conditions. Figure 68 presents the temperature rise estimates for specimens containing binary replacement mixtures, 30% slag or fly ash. Figure 69 presents the temperature rise predictions for specimens with binary replacement mixtures containing 45% slag or fly ash. Figure 70 presents the temperature rise histories of the cube models with ternary replacement mixtures, 30% slag and 15% MK. The predicted temperature increases are then compared to the empirically determined temperatures in Chapter 3.

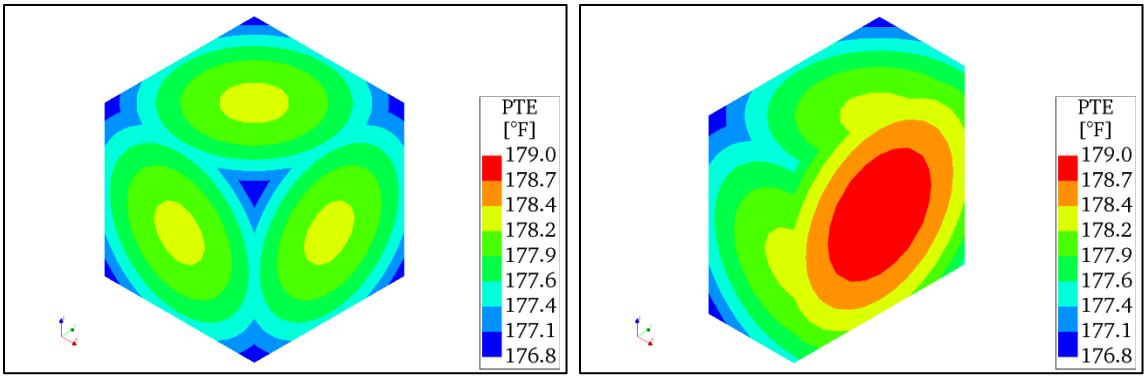

(a) full three-dimensional model (b) half of the model

Figure 66 – Temperature distribution in a cube specimen.

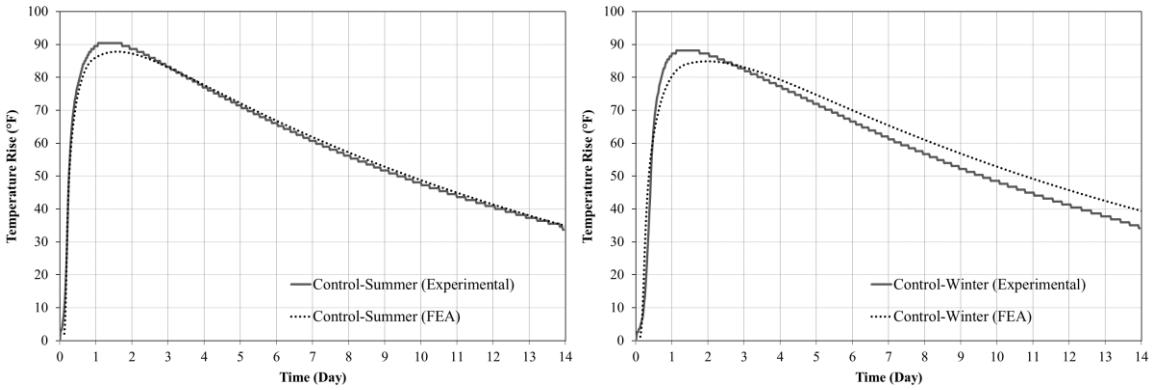

(a) summer placement (b) winter placement

Figure 67 – Temperature rise development in cube specimens from experimental and FEA studies using Control mixtures and calculated specific heat values.

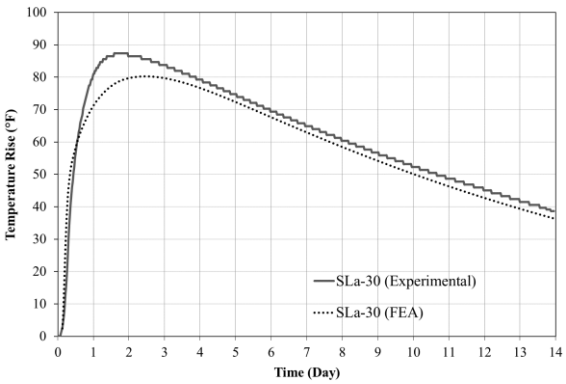

(a) slag-a mixture

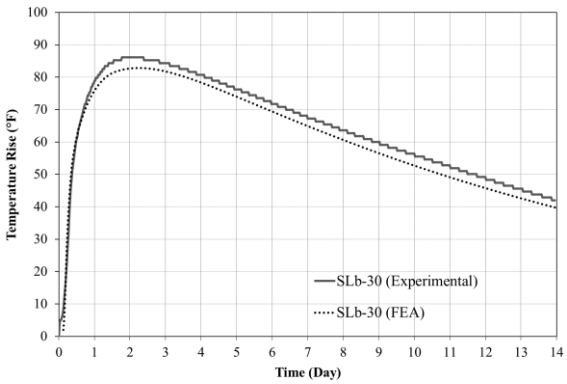

(b) slag-b mixture

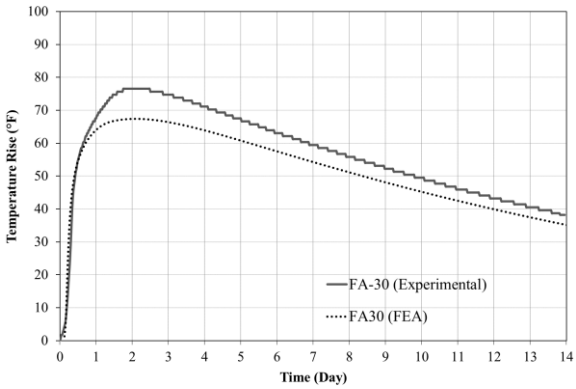

(c) fly ash mixture

Figure 68 – Temperature rise development in cube specimens from experimental and FEA studies using 30% binary mixtures and calculated specific heat values.

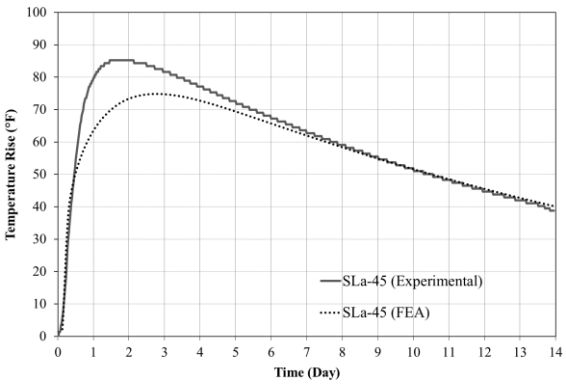

(a) slag-a mixture

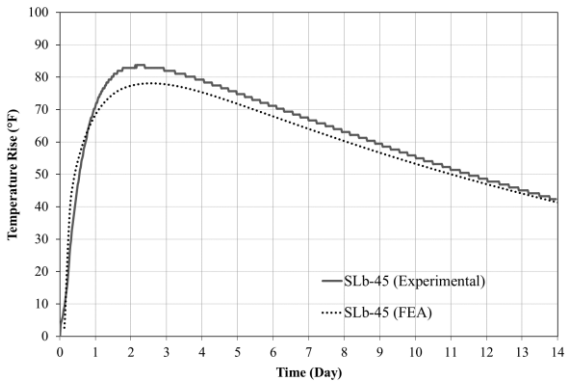

(b) slag-b mixture

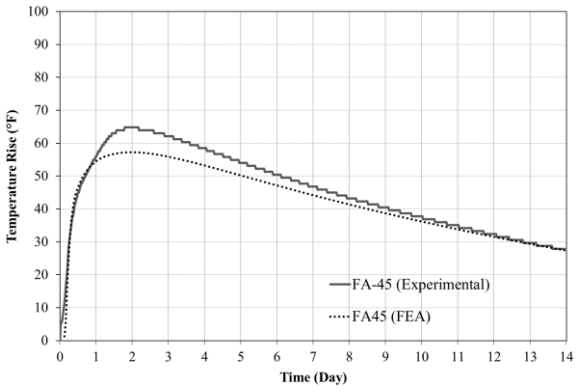

(c) fly ash mixture

Figure 69 – Temperature rise development in cube specimens from experimental and FEA studies using 45% binary mixtures and calculated specific heat values.

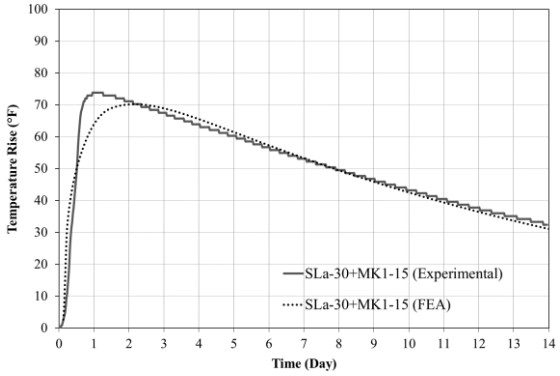

(a) slag-a and MK1 mixture

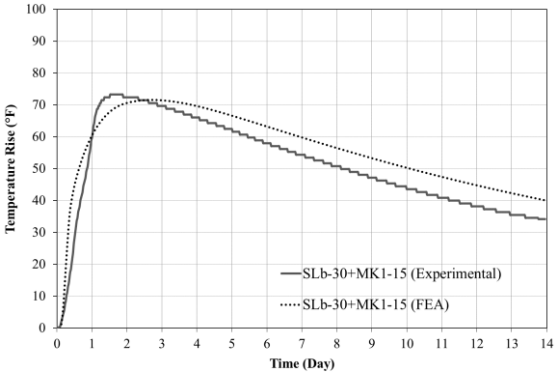

(b) slag-b and MK1 mixture

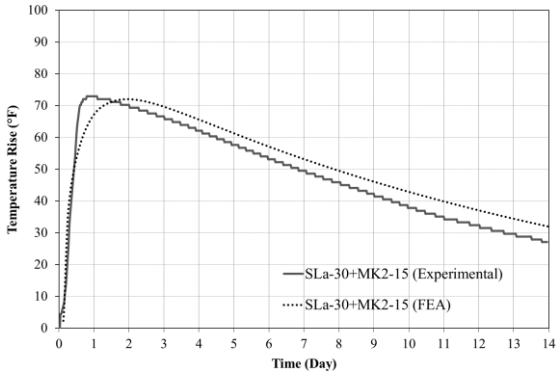

(c) slag-a and MK2 mixture

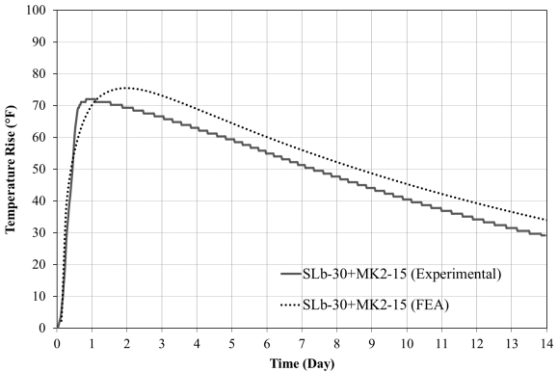

(d) slag-b and MK2 mixture

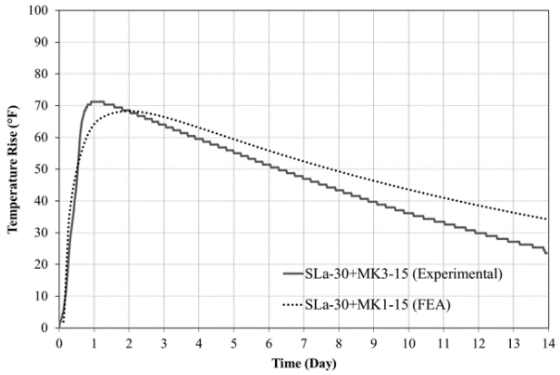

(e) slag-a and MK3 mixture

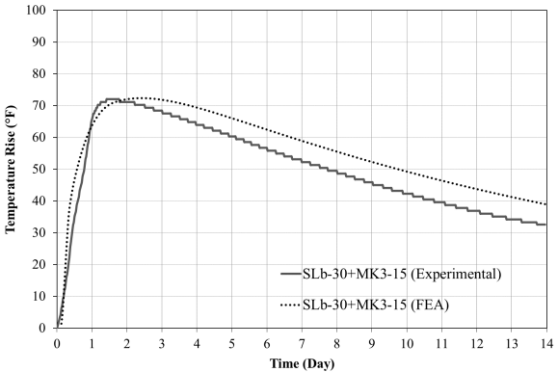

(f) slag-b and MK3 mixture

Figure 70 – Temperature rise development in cube specimens from experimental and FEA studies using 45% ternary mixtures and calculated specific heat values.

The temperature rise results from the FEA analysis overall agree well with the experimental results. The following specific findings are noted:

- The FEA model is able to closely predict temperature development in the cube specimens.
- The predicted maximum temperatures are slightly lower than the experimental maximum temperatures. This is attributed to how the input temperature is evaluated from HoH and specific heat parameters.
- Reductions in the maximum temperature in binary and ternary replacement mixtures are well predicted in the FEA model.
- The time taken to reach the maximum temperature is fairly well predicted by the FEA model.
- The negligible temperature differential across specimens is well predicted by the FEA model. The efficiency of the insulation panels is reasonably demonstrated in the model, as well.

4.7.4 **Adjustment of Specific Heat Capacity**

As described in Section 4.5, specific heat capacities are used to determine a time-temperature history input for analysis. To more accurately predict and avoid underestimating the maximum temperature, specific heat capacities (see Table 33) are slightly adjusted by back-calculating them from the temperature results of the thermal analysis. For each of the 14 cube models, the specific heat parameters presented in Table 34 are used for another round of analysis. This iterative approach results in temperature predictions that closely align with the experimental results. Temperature rises from the second round of the transient thermal analysis are compared to the experimental data in Figure 71 through Figure 74.

Table 34 – Adjusted specific heat capacities used for analysis.

Mixtures	Calculated Specific Heat (W/g°C)	Estimated Specific Heat from FEA (W/g°C)
Control	1.09	1.04
SLa-30	1.12	1.00
SLb-30	1.09	1.04
FA-30	1.11	0.95
SLa-45	1.07	0.9
SLb-45	1.10	1.00
FA-45	1.09	0.94
SLa-30+MK1-15	1.14	1.08
SLa-30+MK2-15	1.13	1.11
SLa-30+MK3-15	1.17	1.11
SLb-30+MK1-15	1.11	1.08
SLb-30+MK2-15	1.11	1.16
SLb-30+MK3-15	1.11	1.12

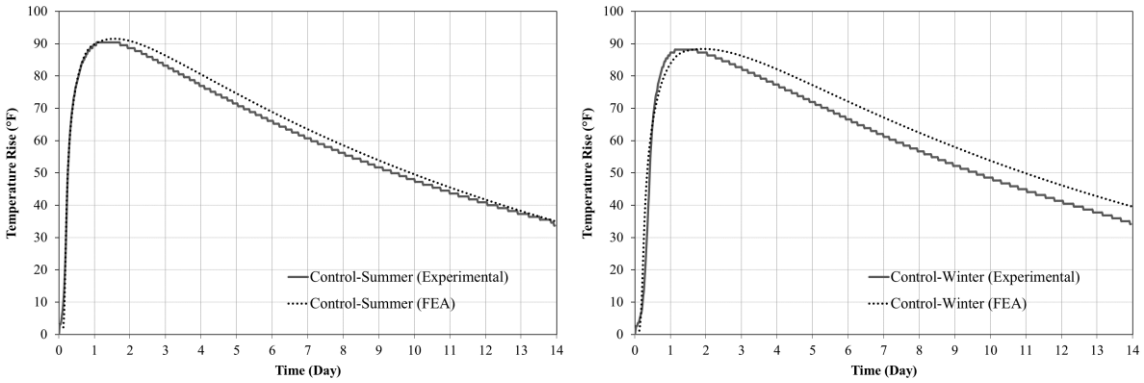

(a) summer placement (b) winter placement

Figure 71 – Temperature rise development in cube specimens from experimental and FEA studies using Control mixtures and estimated specific heat values.

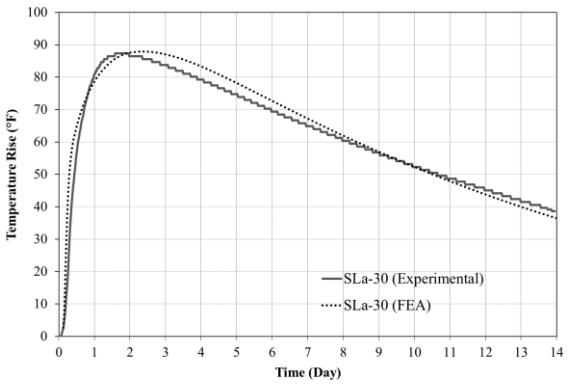

(a) slag-a mixture

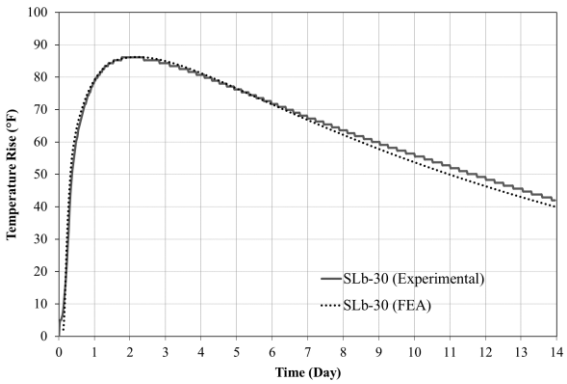

(b) slag-b mixture

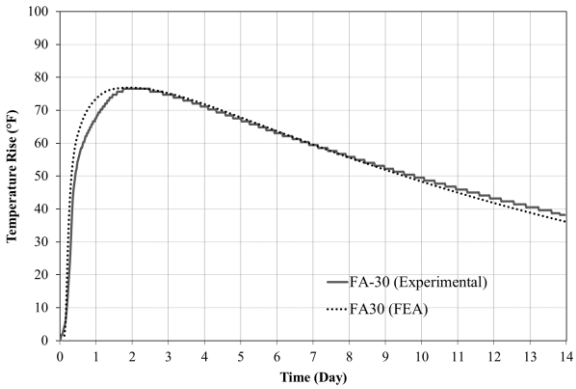

(c) fly ash mixture

Figure 72 – Temperature rise development in cube specimens from experimental and FEA studies using 30% binary mixtures and estimated specific heat values.

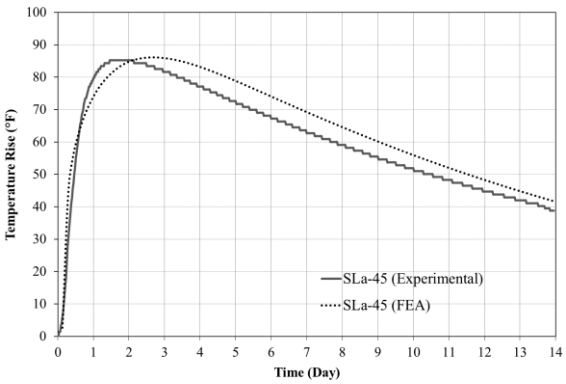

(a) slag-a mixture

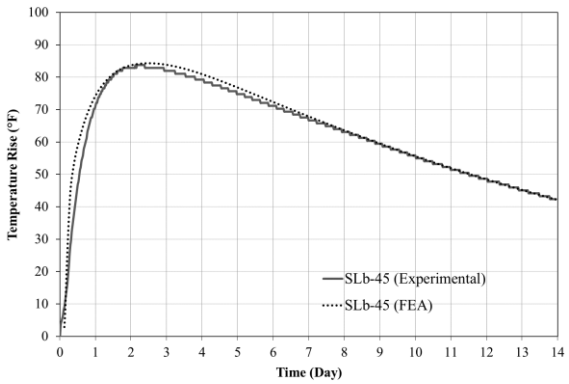

(b) slag-b mixture

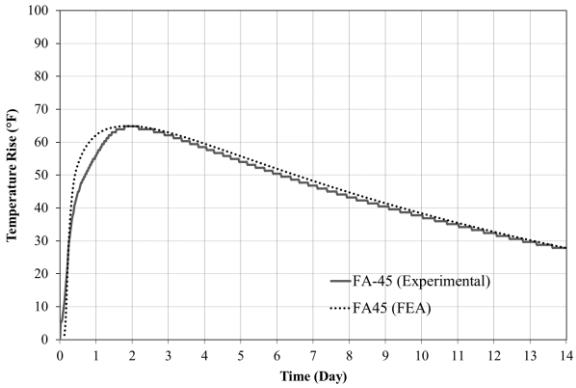

(c) fly ash mixture

Figure 73 – Temperature rise development in cube specimens from experimental and FEA studies using 45% binary mixtures and estimated specific heat values.

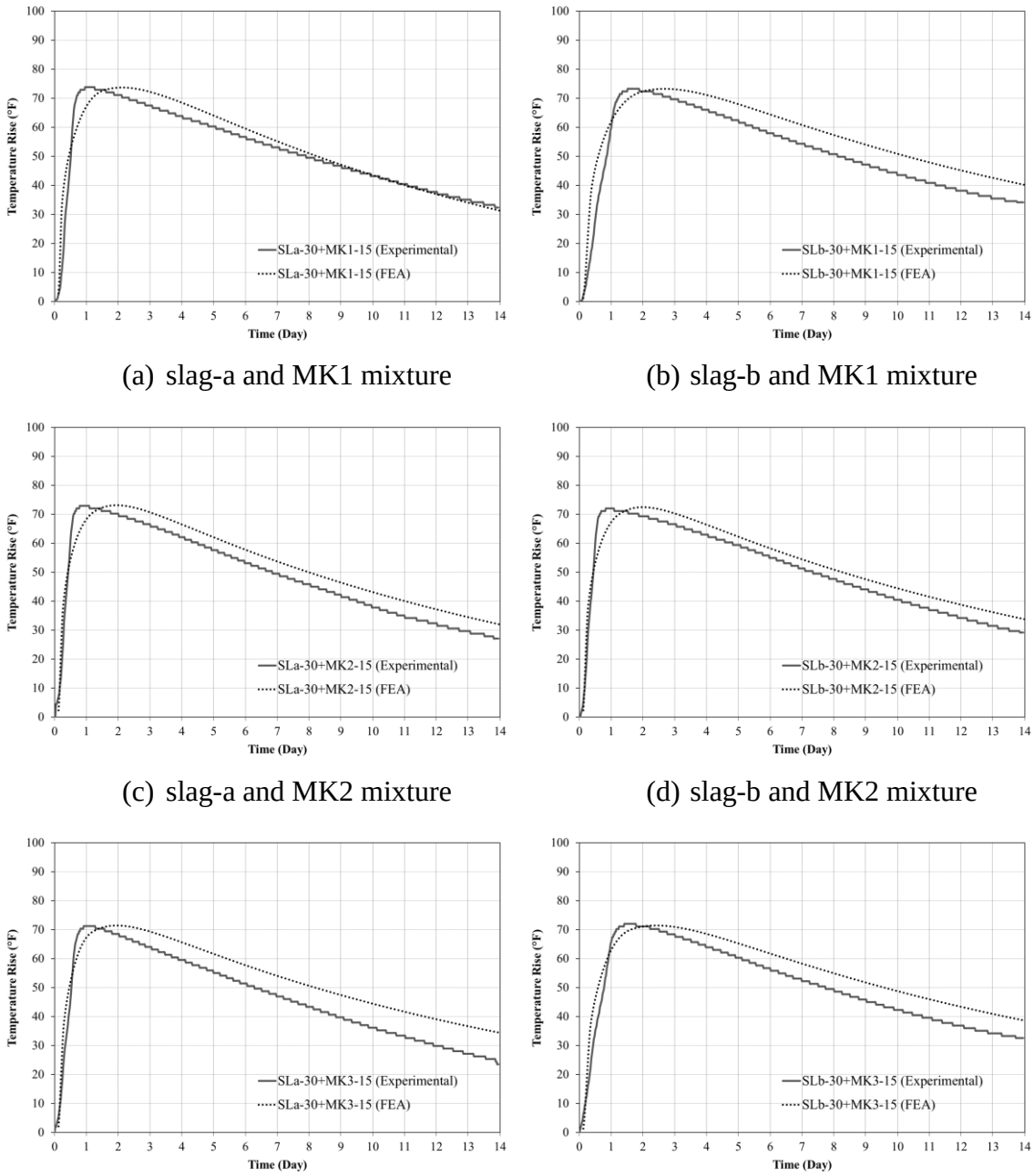

(a) slag-a and MK1 mixture (b) slag-b and MK1 mixture

(c) slag-a and MK2 mixture (d) slag-b and MK2 mixture

(e) slag-a and MK3 mixture (f) slag-b and MK3 mixture

Figure 74 – Temperature rise development in cube specimens from experimental and FEA studies using 45% ternary mixtures and estimated specific heat values.

A comparison between the FEA results and the experimental results shows agreement in the maximum temperature and overall temperature development over time in each of the concrete specimens including different SCMs in binary and ternary replacement

mixtures. Estimated specific heat values are within the general range of specific heat values for mass concrete mixtures specified by ACI 207.2R-07 (2007). From this research methodology and the corresponding analysis of the 14 cube specimens, a reliable FEA model capable of predicting the thermal behavior of mass concrete elements is developed. In addition, specific heat values for concrete mixtures including different SCMs in binary and ternary replacement mixtures are proposed.

4.8 Validation – Experimental Results from a Larger Concrete Specimen

4.8.1 FEA Model Description

The modeling approach is validated by simulating an experimental mass concrete specimen studied by others. In Jung et al.'s (2017) study, the effects of four mixtures, namely high strength concrete, normal strength concrete, low-heat cement, and a ternary mixture on temperatures and strain measurements were studied. Four 13 foot x 13 foot x 13 foot (4.0 m x 4.0 m x 4.0 m) mass concrete specimens, shown in Figure 75, were constructed.

These mass concrete cubes, significantly larger than the cube specimens presented in Section 4.7, were cast on a 32.8 foot x 32.8 foot x 2.0 foot (10.0 m x 10.0 m x 0.6 m) concrete slab. Steel reinforcement was extended from the base slab to the mass concrete cubes for "bonding purpose" (Jung et al., 2017). In this large scale experimental study, multiple temperature and strain sensors were installed at critical locations. Temperature and strain data were collected from the large cube specimens for more than five weeks. Figure 75 shows the casting of the mass concrete cubes, a cube specimen, and the layout of the temperature and strain sensors.

(a) concrete casting in the field (b) mock-up test member in field testing

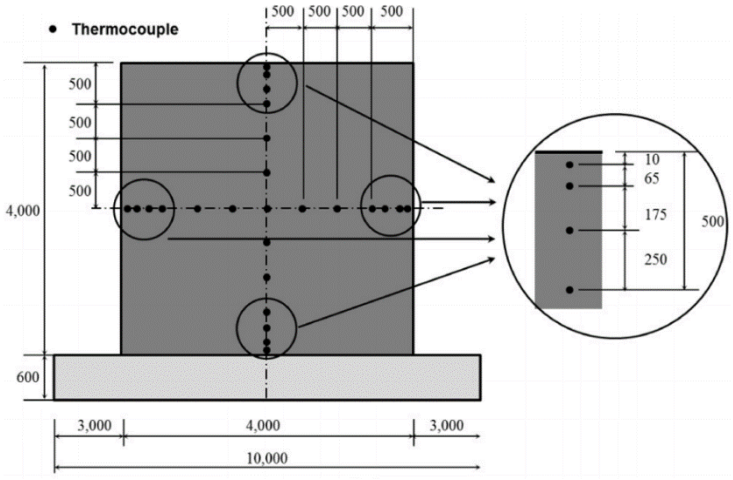

(c) layout of temperature sensors in the member

Figure 75 – Geometry of the 13 foot x 13 foot x 13 foot mass concrete structure (Jung et al., 2017)**.**

Mixture proportions of the four mixtures are shown in Table 35. The mixture proportions used in the normal-strength concrete are very close to the Control mixture design used in the current research project (see Section 3.2.2.2). Therefore, the mass concrete element with the normal-strength concrete mixture is selected to validate the modeling approach and outcomes of this study.

Table 35 – Mixture proportion for the large specimens (Jung et al., 2017)**.**

Member	Water (kg/m³)	Cement (kg/m³)	Fly ash (kg/m³)	GGBFS (kg/m³)	w/b* (–)	Fine aggregate (kg/m³)	Coarse aggregate (kg/m³)	S.P.** (kg/m³)
Normal-strength	170	430 (Type I)	–	–	0.40	770	930	3.01
High-strength	165	585 (Type I)	–	–	0.28	702	874	7.02
Low-heat	180	530 (Type IV)	–	–	0.34	742	881	3.71
Ternary	135	226 (Type IV)	87	134	0.30	820	937	3.58

* w/b: water-to-binder ratio.
** S.P.: superplasticizer.

Figure 76 presents the HoH of the cementitious materials used in the large normal-strength mass concrete specimen studied by Jung et al. (2017). The adiabatic temperature rise for this concrete mixture is calculated from Figure 64 and is presented in Figure 77.

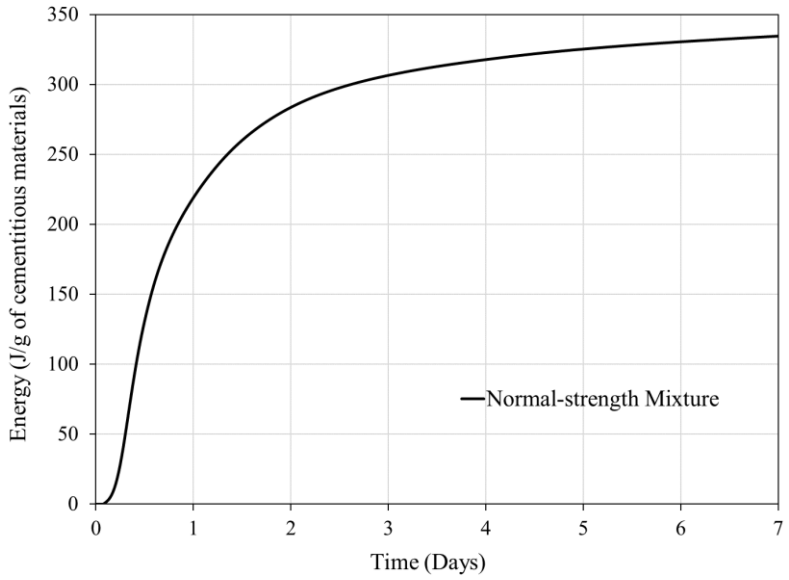

Figure 76 – HoH of the large specimen.

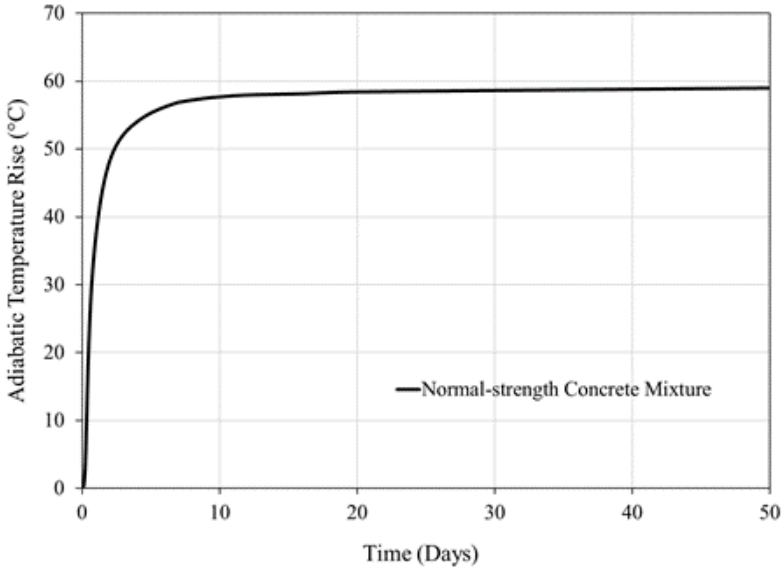

Figure 77 – Adiabatic temperature rise in the large specimen.

A FEA model consisting of a large cube specimen and its base slab is modeled in DIANA (see Figure 78). A transient thermal-structural analysis is performed with nonlinear material models over a period of four weeks. From this analysis, temperature predictions are obtained from the center, side, top, and bottom surfaces of the FEA model. Total strains, including crack strains, and crack widths determined from this analysis are compared to the experimental results to validate the modeling approach used herein.

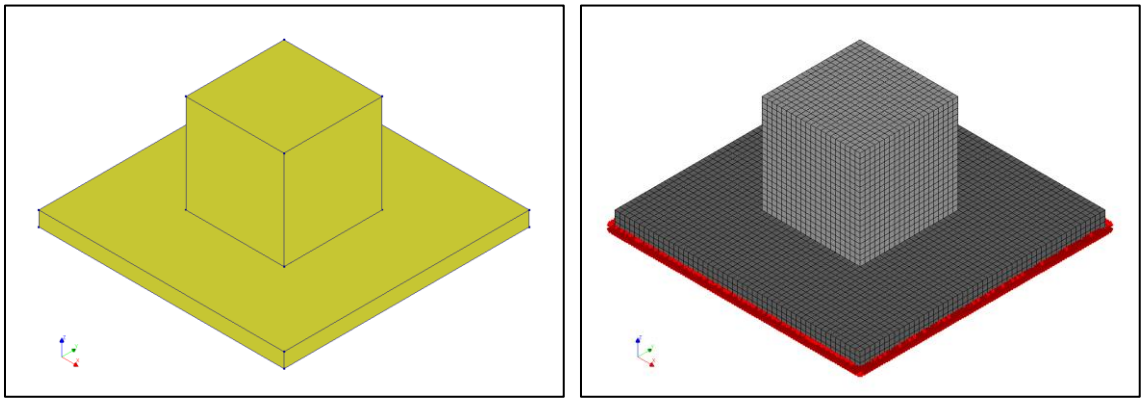

(a) three-dimensional geometry (b) meshing of the model

Figure 78 – The 13 foot x 13 foot x 13 foot mass concrete model in DIANA.

4.8.2 **Boundary Conditions**

For the larger cube specimen investigated in this section, the daily ambient air temperature shown in Figure 79 is applied to the surfaces open to ambient air. A time-dependent heat transfer coefficient is used to reflect the formwork removal time. A value of 1.41 Btu/h·ft^{2}·˚F (8 W/m^{2}·°C) is used with the concrete formwork, and a value of 2.11 Btu/h·ft^{2}·˚F (12 W/m^{2}·˚C) is used once the formwork has been removed. A fixed support boundary condition is applied to the bottom surface of the supporting slab. A concrete placement temperature of 77 °F (25 °C) is used as an initial condition for the large cube model.

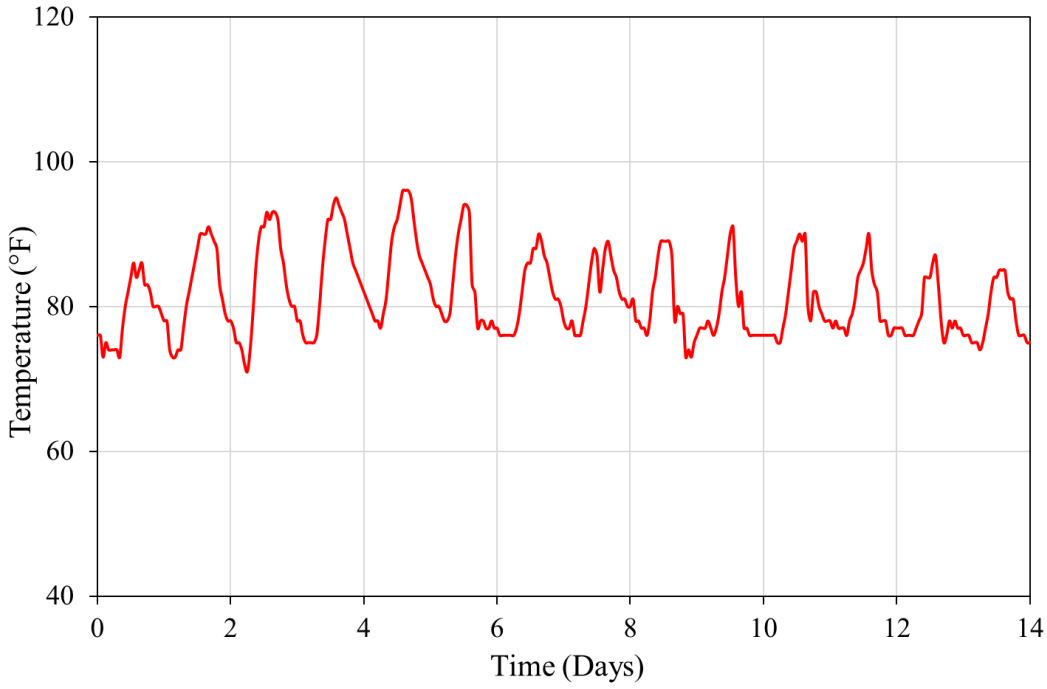

Figure 79 – Daily ambient temperature applied to the large cube model.

Note: (°C x 9/5) + 32 = °F.

4.8.3 **Temperature Results**

Figure 80 presents the temperature distribution from the thermal analysis in a quarter-section view of the 13 foot x 13 foot x 13 foot (4.0 m x 4.0 m x 4.0 m) model. Figure 81 shows temperature-time histories and presents a comparison of experimental and analytical results.

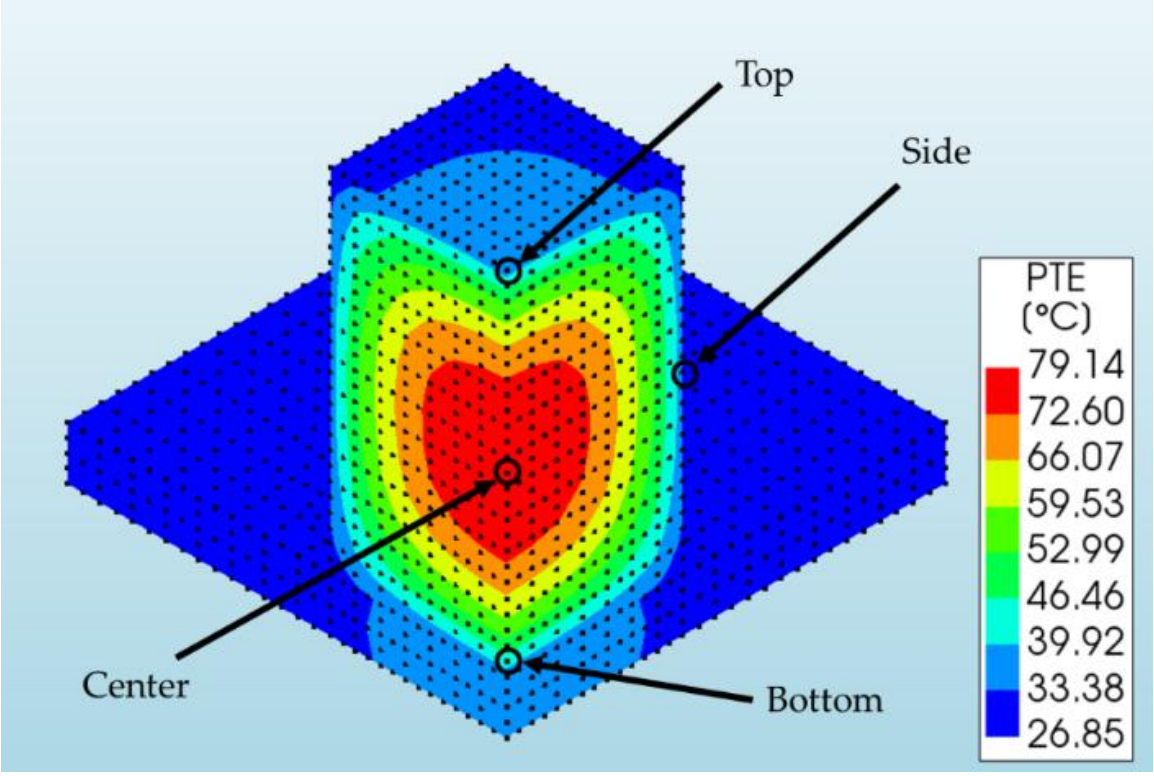

Figure 80 – Temperature distribution in the 13 foot x 13 foot x 13 foot mass concrete structure.

Note: this figure shows a quarter model.

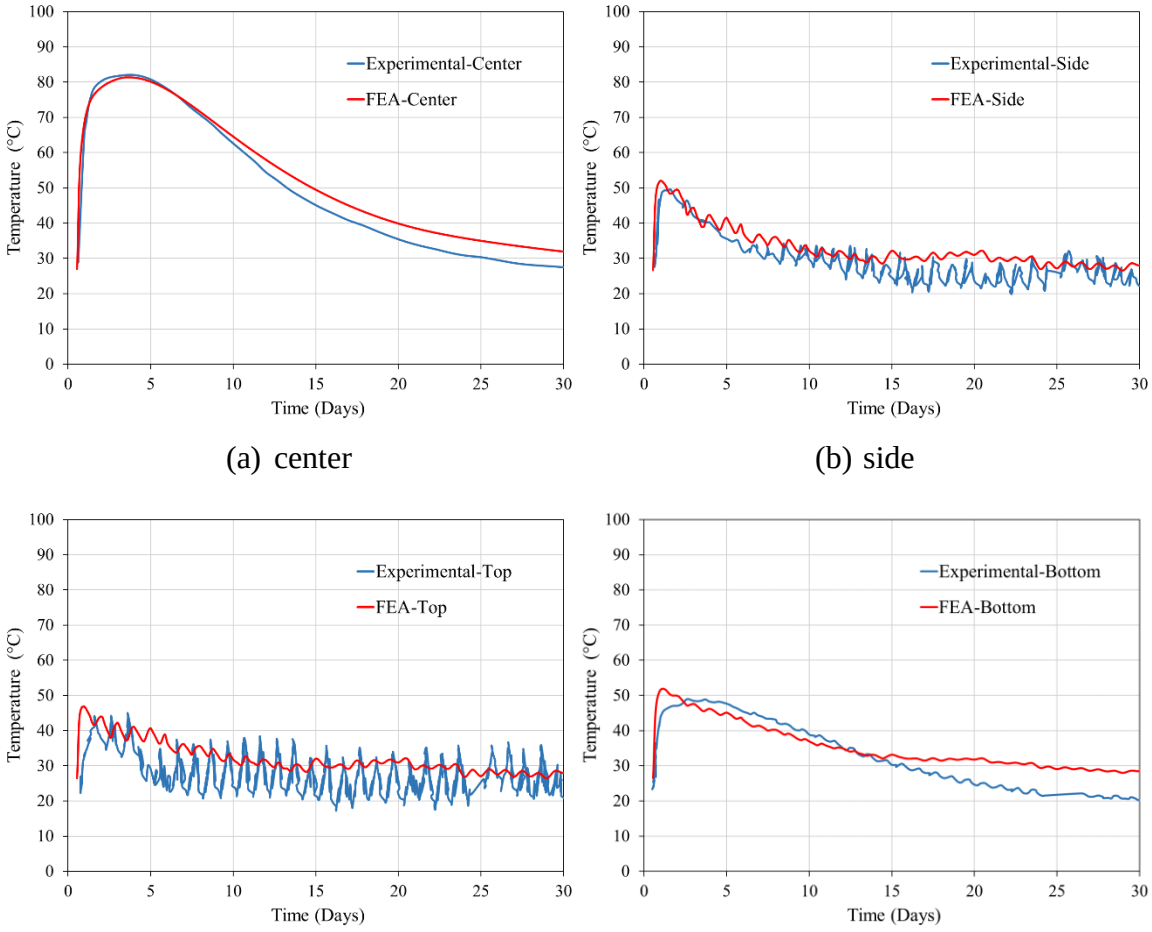

Figure 81 – Temperature development comparison between experimental and FEA results in the 13 foot x 13 foot x 13 foot mass concrete element.

4.8.4 **Strain Results**

Figure 82 presents a comparison of the total strain results at the center of the mass concrete element. Total strain values are bound by the two cases predicted, as shown in Figure 82. The maximum and minimum predicted strains are principal strain E1 and E3, respectively. As a result of a high internal temperature and a significant temperature differential, as Figure 81 illustrates, numerous cracks are observed on all sides of the mass concrete specimen. Cracks on all sides of the mass concrete from the experimental work (see Figure

83) are compared with the cracks predicted by the FEA analysis (see Figure 84). From the experimental results, the lines indicate the pattern of cracking and the values on the lines represent crack widths (in mm). In Figure 84, the lines and their colors drawn on finite elements represent cracks and crack strain intensity, respectively.

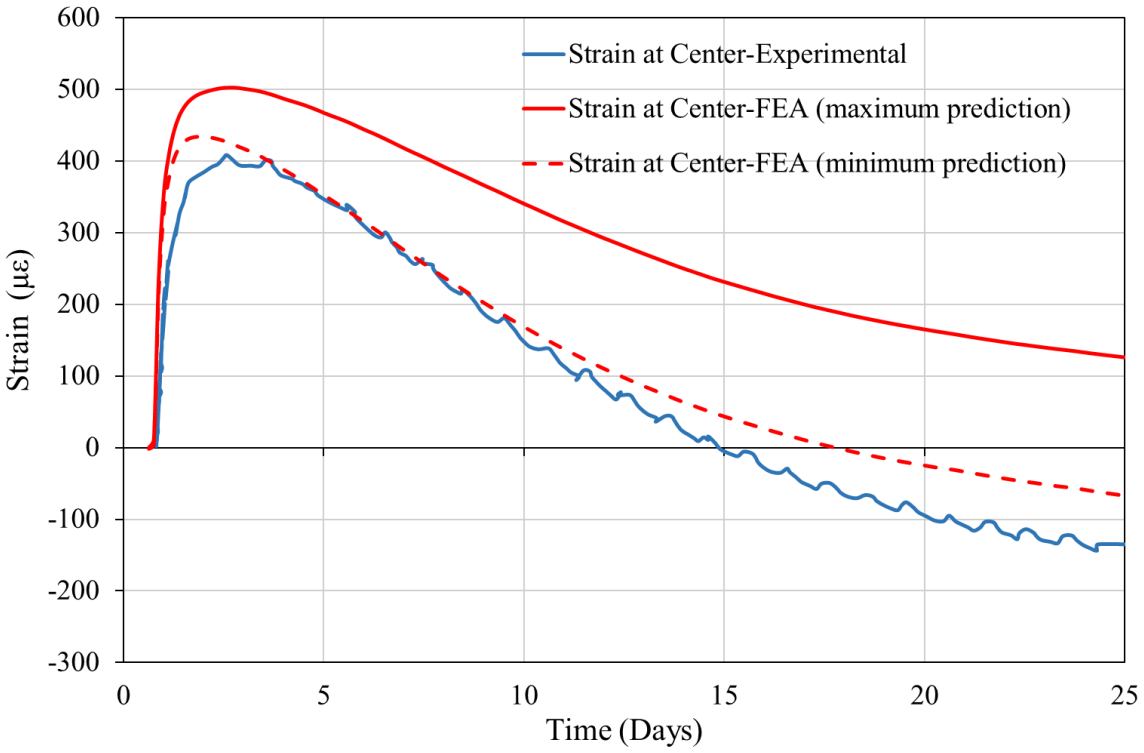

Figure 82 – Total strain development comparison between experimental and FEA results at the center of the large cube specimen.

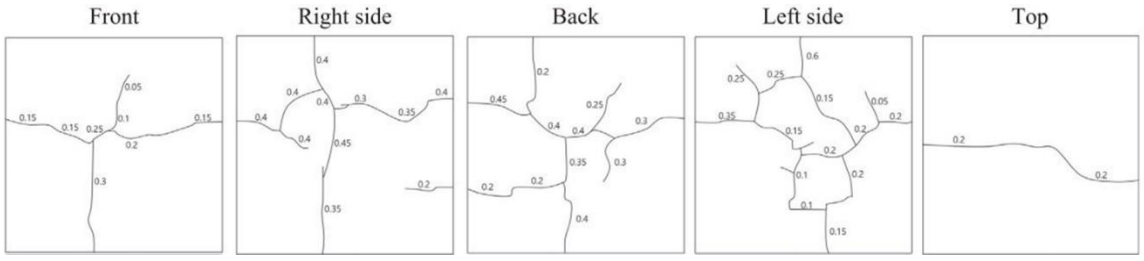

Figure 83 – Experimental crack survey results for the 13 foot x 13 foot x 13 foot mass concrete element.

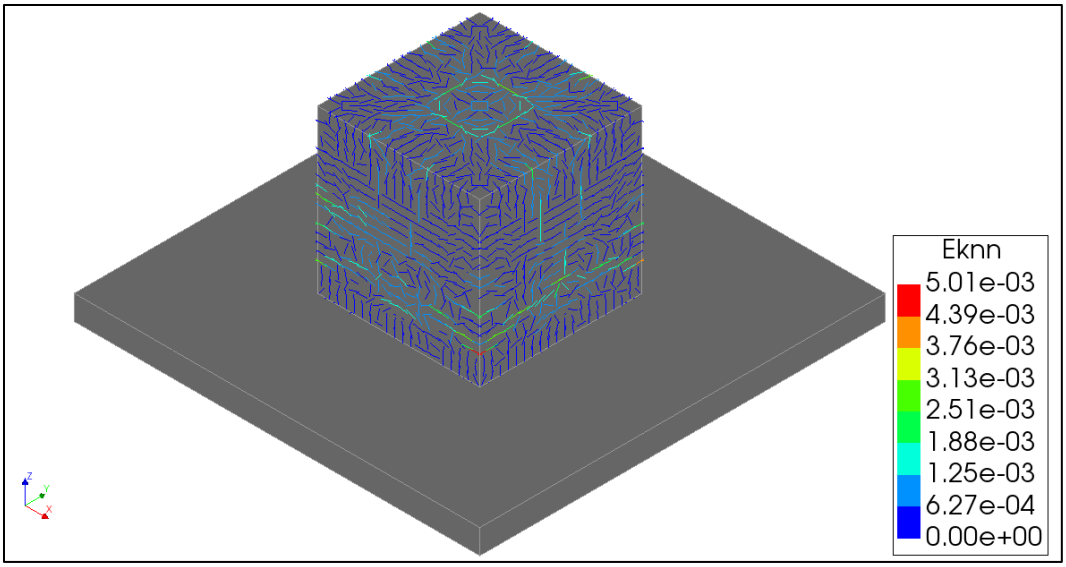

Figure 84 – Crack strain intensity in the large cube specimen on day 7.

4.8.5 **Conclusions**

The following list summarizes conclusions derived from the temperature and strain results:

- Results from the FEA analysis agree with the experimental results.
- The temperature distribution at the center of the mass concrete is particularly well predicted by the FEA model.
- Overall, temperature distribution in the large cube concrete model agrees well with the experimental results.
- A small variation in temperature distribution exists. This arises from potential variation in the daily ambient temperature input adopted in the FEA model. Applying a more precise ambient temperature-time history to the FEA model would have reduced this variation.
- The experimental strain is well predicted by the FEA analysis.

- The FEA model is capable of predicting crack formations on the sides of the mass concrete exposed to ambient air.

Thus, the analysis method employed in this study can be used to effectively predict temperature distribution and strain intensity (or cracking potential) in mass concrete structures.

4.9 Case Study – A Bridge Seal Structure

4.9.1 Background and Model Description

This section presents a numerical simulation of an underwater bridge seal structure. Seals are often used for bridge foundation construction, particularly for bridges over waterways. A large number of cracks in a group of bridge seals were discovered during an underwater inspection. From this investigation, a crack pattern sketch was drawn. The seal selected for this study is a 43.25 foot (13.18 m) long, 19.5 foot (5.94 m) wide, and 22.25 foot (6.78 m) deep mass concrete structure. The bridge runs over the Savannah River, located on the border between Georgia and South Carolina on U.S. 378/Georgia SR 43 as shown in Figure 85. The 2010 construction drawing in Figure 86 shows the layout of the bridge seal.

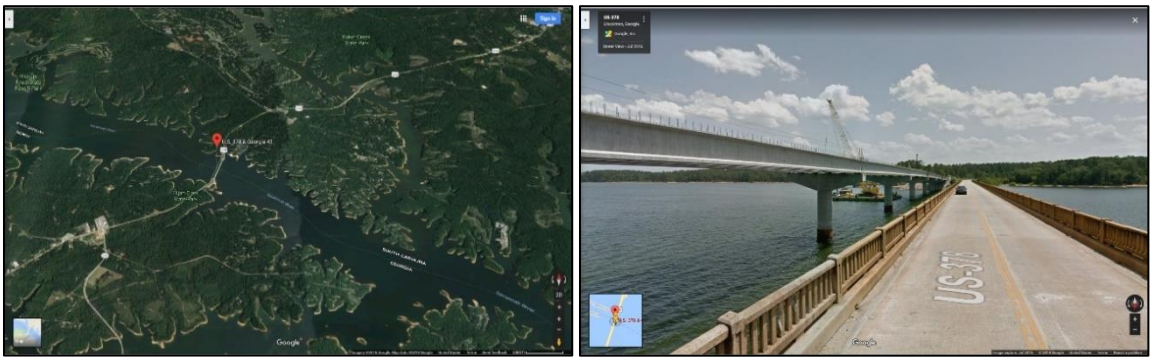

(a) satellite view of the bridge location (b) street view of the bridge bent

Figure 85 – View of the bridge bent (Google Maps, 2018)**.**

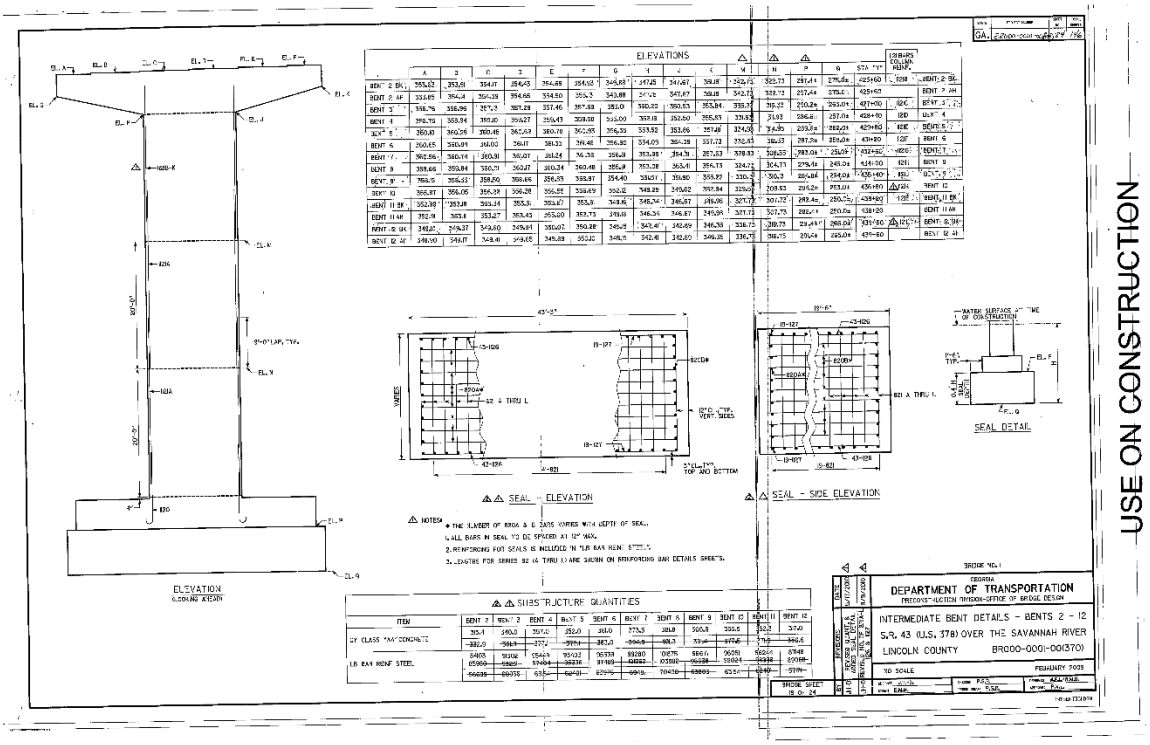

Figure 86 – Construction drawing of the bridge seal (GDOT, 2010)**.**

Based on the latest site photos (Figure 85(b) and Figure 87(b)), at each bent the following elements are constructed on the seal surface: 1) a 39.25 foot (11.96 m) x 15.5 foot (4.72 m) x 5 foot (1.52 m) footing; 2) a column, 66 feet (20.11 m) high with a diameter of 8 feet (2.44 m); and, a 44.5 foot (13.56 m) x 5 foot (1.52 m) x 3.75 foot (1.14 m) trapezoidal cap. These dimensions are illustrated in Figure 88. The circular column here is slightly different from the rectangular pier in the construction drawing (Figures 86 and 87(a)). The thermal analysis results for the rectangular pier are presented in Appendix D. For this case study, the latest design was used because the temperature distributions in the seal structure between that design and the design of the actual structure are found similar. Accordingly, associated crack patterns are similar for the two designs, as well. In summary,

the shape of piers does not affect the temperature and structural analysis results (e.g., the extent of cracking) of the seal structure investigated in this study.

(a) with rectangular piers

(b) with circular piers

Figure 87 – Site photo of the bridge bent.

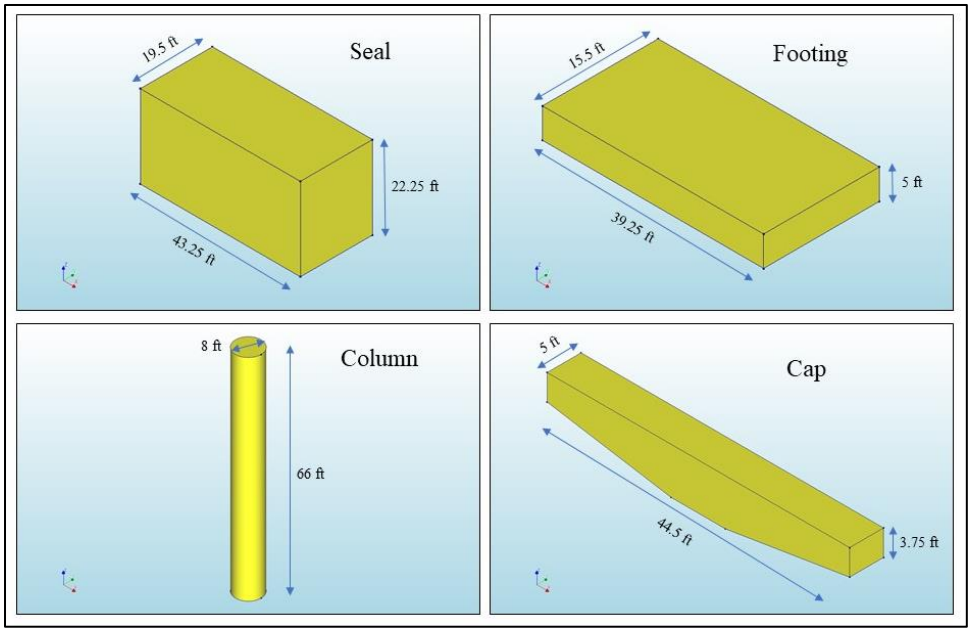

Figure 88 – Dimensions of the seal, footing, column, and cap of the bridge bent structure.

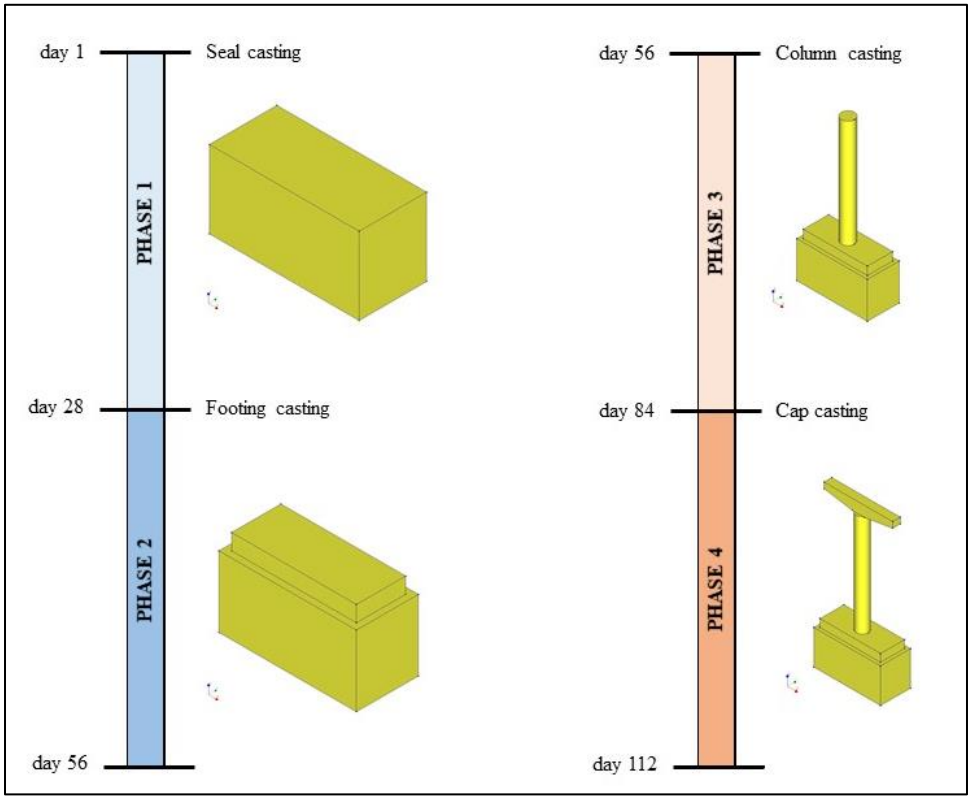

Figure 89 – Construction phases of the bridge bent.

A phased analysis is conducted to simulate a (hypothetical) phased-construction sequence in the bridge seal as shown in Figure 89:

1. Phase 1 consists of seal construction,
2. Phase 2 consists of footing construction after 28 days,
3. Phase 3 is comprised of column construction by 56 days, and
4. Phase 4 consists of cap construction within 84 days.

The results of this analysis are then compared to the site observations. A three-dimensional model of the bridge bent created in DIANA is shown in Figure 90, and Figure 91 presents the rebar arrangement created for the seal model.

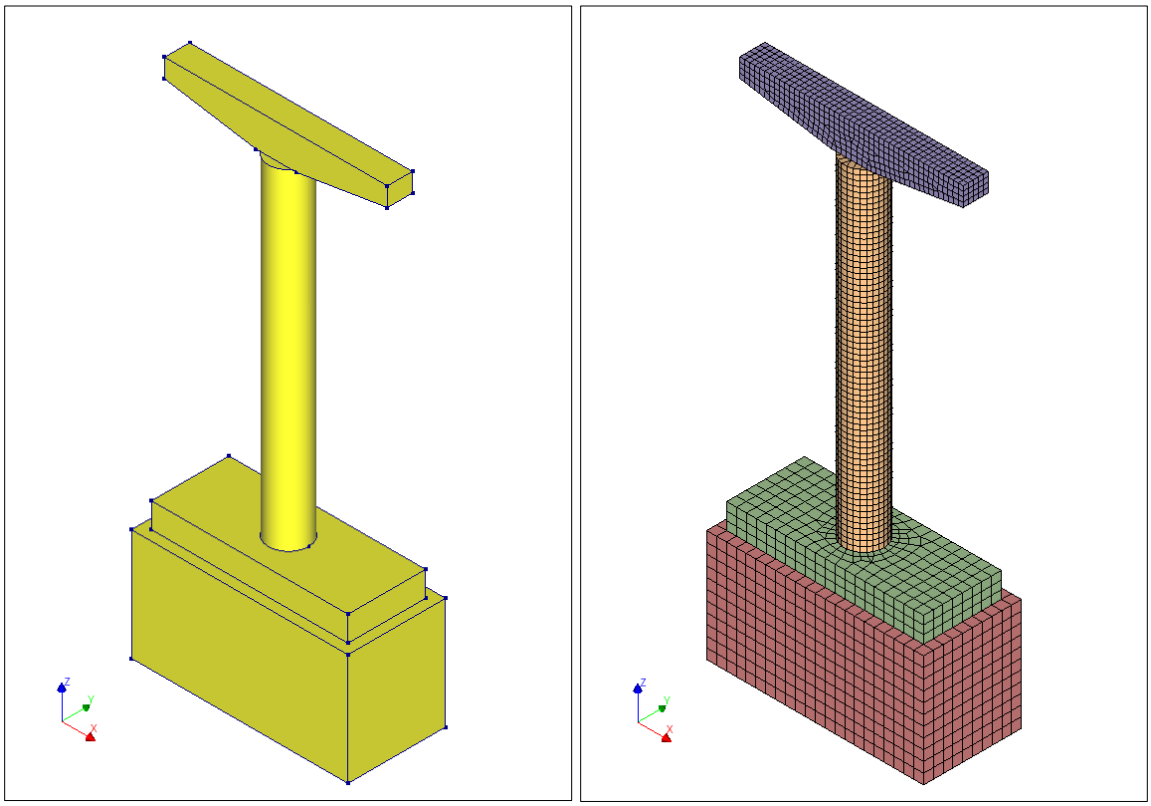

(a) bridge bent model geometry (b) model showing the finite element mesh

Figure 90 – Bridge bent model in DIANA.

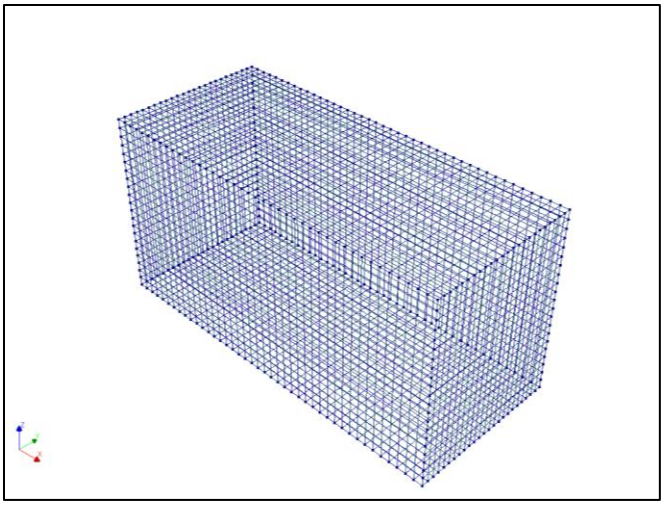

Figure 91 – Rebar arrangement in the bridge seal model.

4.9.2 **Heat of Hydration Input**

Type I/II cement and fly ash are used for the bridge seal concrete placement. By weight, 45% of cement is partially replaced with fly ash. The concrete mixture proportions used for placing the bridge seal are provided in Table 36. The thermal and mechanical properties of this concrete mixture are presented in Table 37.

Table 36 – Mixture proportion used in the bridge seal, lb/yd^3 (kg/m^3).

Cement	Fly ash	Fine Aggregate	Coarse Aggregate	Water
370 (220)	302 (179)	1135 (673)	1735 (1029)	305 (181)

Table 37 – Thermal and mechanical properties of the seal concrete.

Thermal Properties	Conductivity, Btu/hr·ft·°F (W/m·°C)	1.73 (3.0)
	Specific Heat, Btu/lb·°F (J/g·°C)	0.22 (0.94)
	Heat Capacity, Btu/ft^3·°F (J/m^3.°C)	32.83 (2.2x10^6)
Mechanical Properties	Compressive Strength, psi (MPa)	3,500 (24)
	Modulus of Elasticity, psi (MPa)	4,000,000 (27,579)
	Poisson's ratio	0.2
	Coefficient of Thermal Expansion, in/in/°F (mm/mm/°C)	5.2x10^{-6} (9.36x10^{-6})
	Density, lb/ft^3 (kg/m^3)	142.5 (2,283)

Figure 92 presents the HoH of the concrete mixture used in the bridge seal structure. The adiabatic temperature-time history for the concrete mixture is computed for analysis and presented in Figure 93.

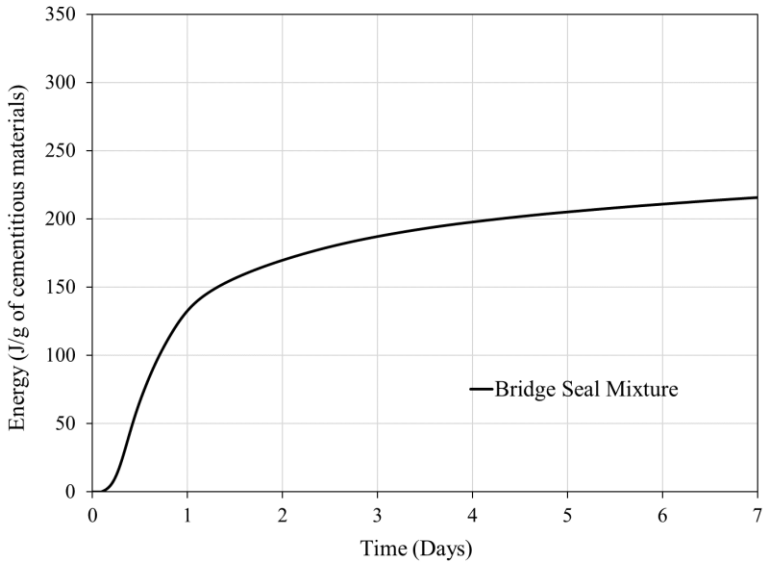

Figure 92 – HoH of the bridge seal mixture.

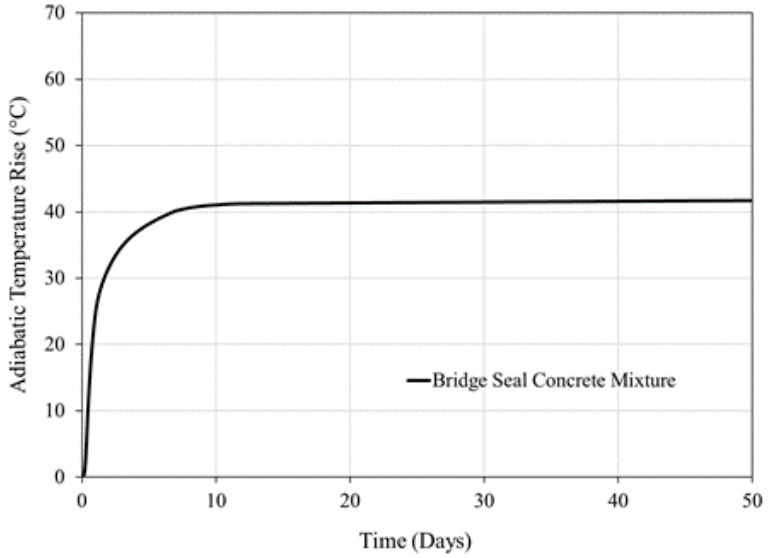

Figure 93 – Adiabatic temperature rise of the bridge seal concrete mixture.

Note: (°F − 32) x 5/9 = °C.

4.9.3 **Boundary Conditions**

For the bridge bent model, the external temperature includes the effect of daily water temperature on the sides and bottom surface of the seal and the effect of daily ambient temperature on the top surface of the seal and the rest of the bent model. Both winter and summer placement conditions are considered in this study. Figure 94 presents the daily ambient and water temperatures (USGS, 2019; Weather Underground, 2019) applied to the bridge seal elements for these two conditions; daily temperatures are obtained for Savannah, Georgia, for the two hottest summer weeks and the two coldest winter weeks (USGS, 2019; Weather Underground, 2019). A cofferdam with 0.25-inch (6.35 mm)-thick steel sheet piles is assumed for enclosing the seal during construction. The following heat transfer coefficients are used for different parts of the bent model:

- 155.7 Btu/h·ft^2·°F (884 W/m^2·°C) applied to the sides and bottom surface of the seal reflecting river water and sheet pile effects.
- 2.47 Btu/h·ft^2·°F (14 W/m^2·°C) applied to the top surface of the seal as it is exposed to ambient air.
- 0.229 Btu/h·ft^2·°F (1.3 W/m^2·°C) applied to the side faces of the footing considering plywood formwork and ambient air temperature effects.
- 2.47 Btu/h·ft^2·°F (14 W/m^2·°C) applied to the top surface of the footing, the column, and the cap as they are in contact with ambient air.

For the structural analysis, the bottom surface of the seal is restrained from vertical movement. An interface element is defined at the bottom surface to reflect the friction between the seal concrete and the underwater terrain in order to allow lateral (thermal) expansions. A friction coefficient of 0.85 is reasonably assumed. For the summer

placement condition, a concrete placement temperature of 85 °F (29.4 °C) is applied to the model as an initial (or reference) condition. For the winter placement condition, a concrete placement temperature of 60 °F (15.6 °C) is applied to the model as an initial condition.

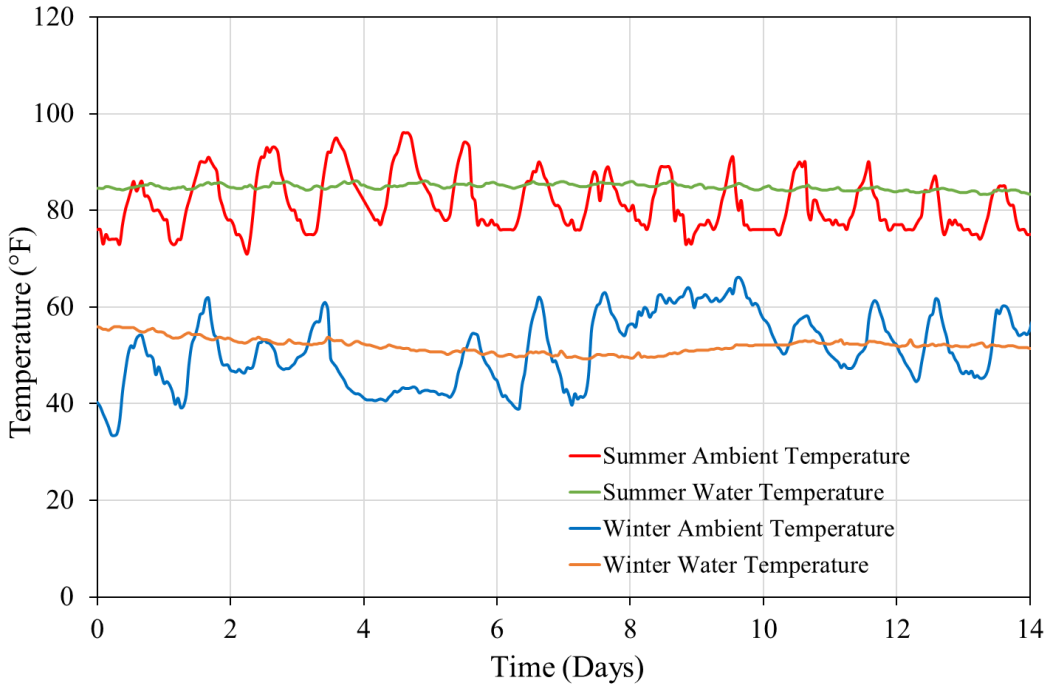

Figure 94 – Summer and winter daily ambient and water temperatures used for analysis.

Note: (°C x 9/5) + 32) = °F.

4.9.4 Temperature Results

Using the bridge bent model described in the previous sections, a coupled thermal-structural analysis is performed with nonlinear material models. The analysis results are presented for both summer and winter placement conditions.

4.9.4.1 Summer placement condition

Temperature distribution in the seal, footing, column, and cap at 1, 3, 7, and 28 days after placing each element is shown in Figure 95 through Figure 98. Figure 95 shows the

temperature distribution in a half section of the seal. Figure 96 shows the temperature distribution in a half section of the seal and footing after the footing is cast at 28 days. Figure 97 shows the temperature distribution in a half section of the seal, footing, and column after the column is cast by 56 days. Figure 98 shows the temperature distribution in a half section of the seal, footing, column, and cap after the cap is cast 84 days after the initial (seal) concrete placement.

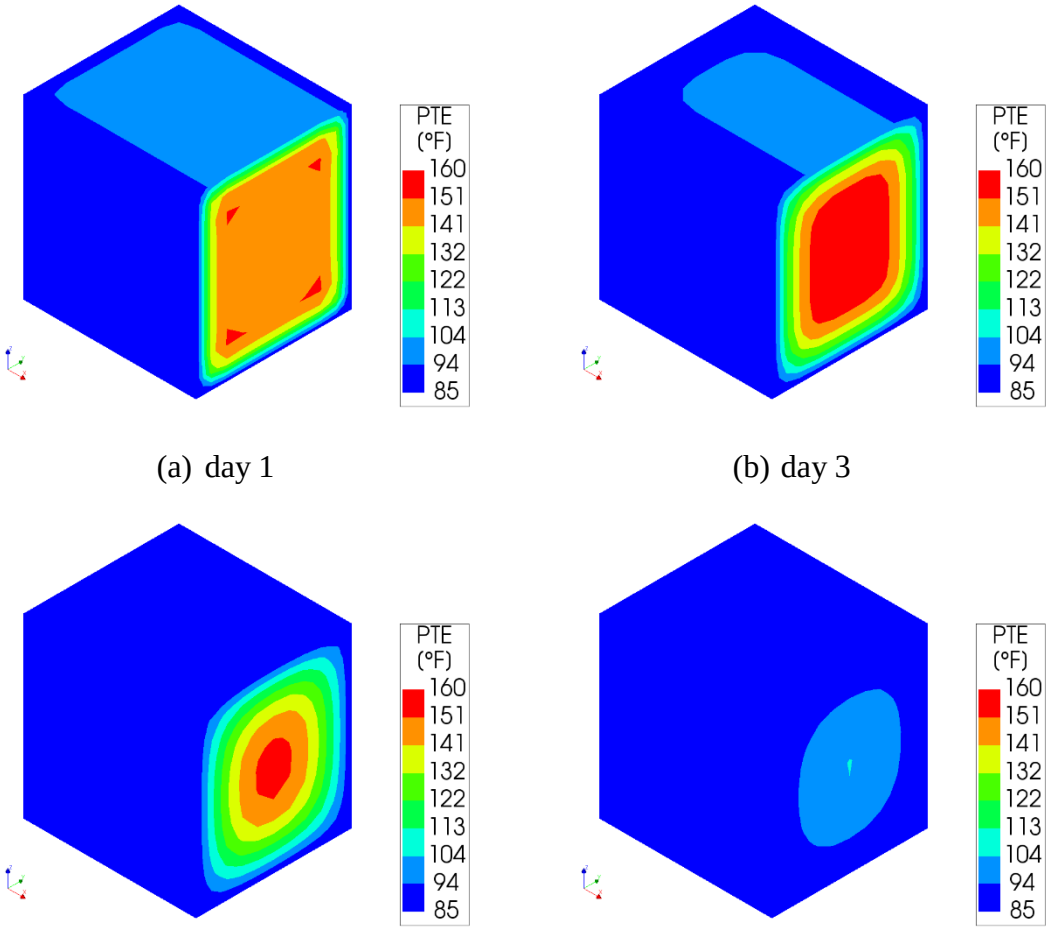

(a) day 1 (b) day 3

(c) day 7 (d) day 28

Figure 95 – Temperature distribution in the bridge seal - 28 days after seal placement (summer).

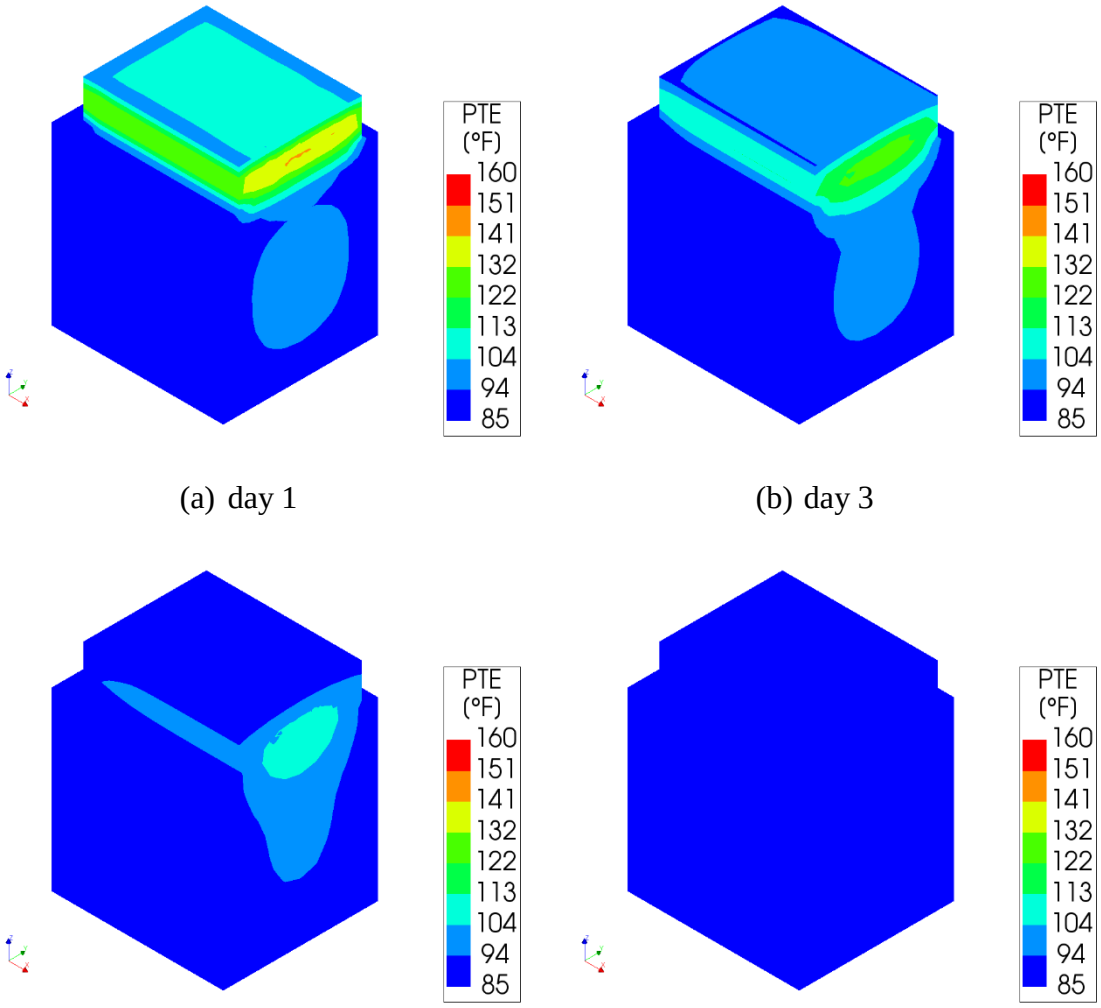

(a) day 1 (b) day 3

(c) day 7 (d) day 28

Figure 96 – Temperature distribution in the bridge seal and footing - 28 days after footing placement (summer).

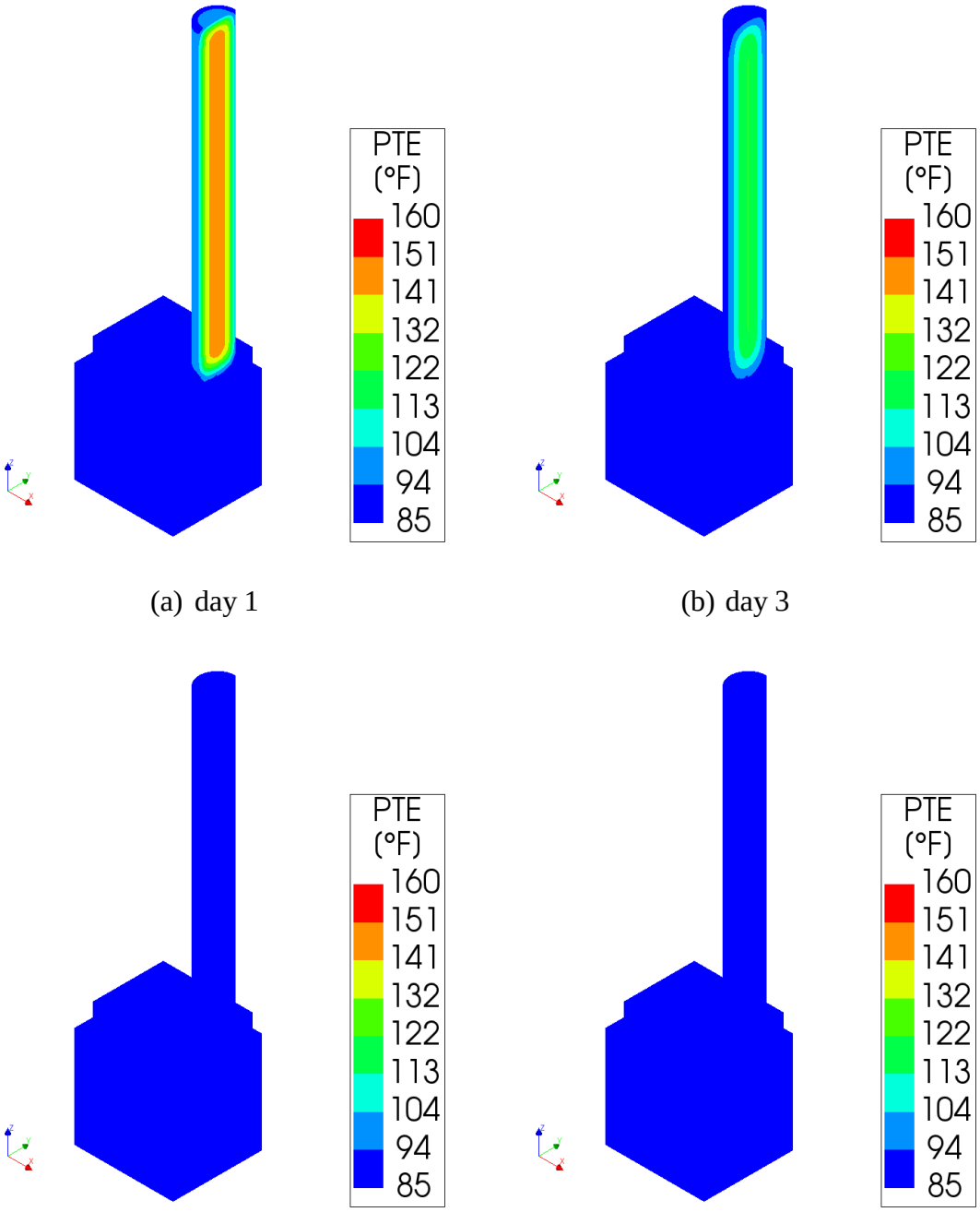

(a) day 1

(b) day 3

(c) day 7

(d) day 28

Figure 97 – Temperature distribution in the bridge seal, footing, and column - 28 days after column placement (summer).

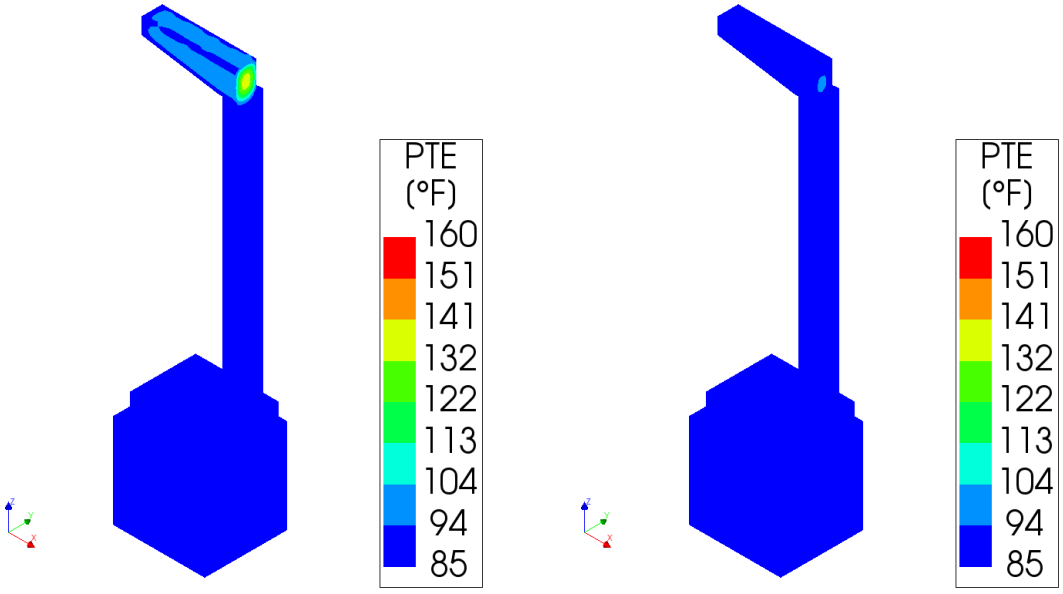

(a) day 1 (b) day 3

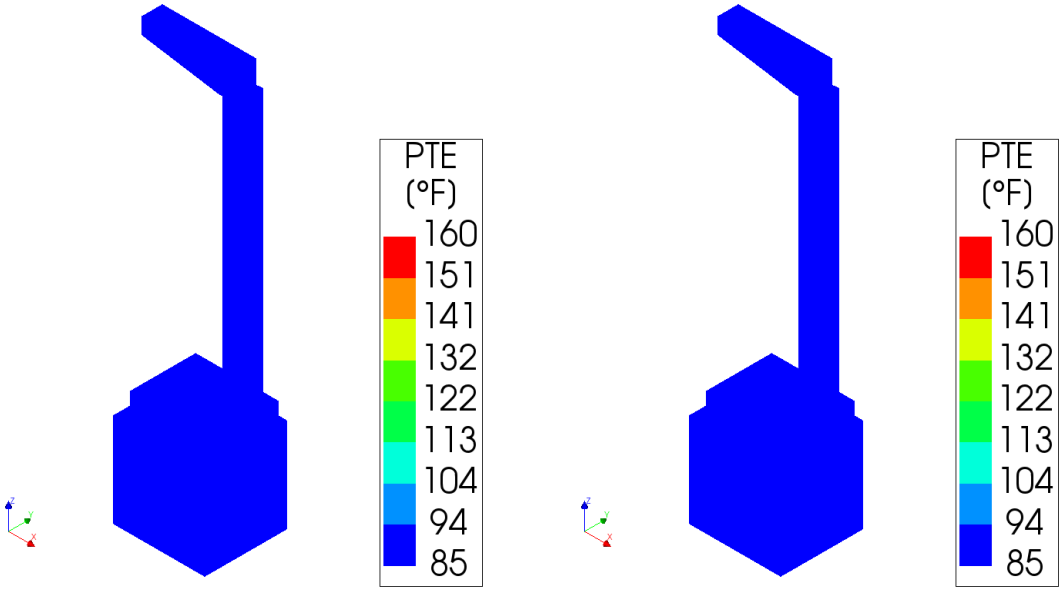

(c) day 21 (d) day 28

Figure 98 – Temperature distribution in the bridge seal, footing, column, and cap - 28 days after cap placement (summer).

Figure 99 through Figure 102 present the temperature-time development at the center, top, bottom, and side surfaces of the seal, footing, column, and cap for the summer placement condition. Figure 99 presents the temperature-time history at the center, top, and side of the seal from after its placement to the end of Phase 4 (cap construction), 112 days after the initial placement. Figure 100 presents the temperature development at the center, top, and side of the footing after its placement at 28 days until the end of Phase 4 (cap construction). Figure 101 presents the temperature history at the center and side of the column after its placement at 56 days until the end of Phase 4. Finally, Figure 102 presents the temperature history at the center and side of the cap. For each element (i.e., seal, footing, column, and cap), the maximum temperature differential developed over time is shown in Figure 103.

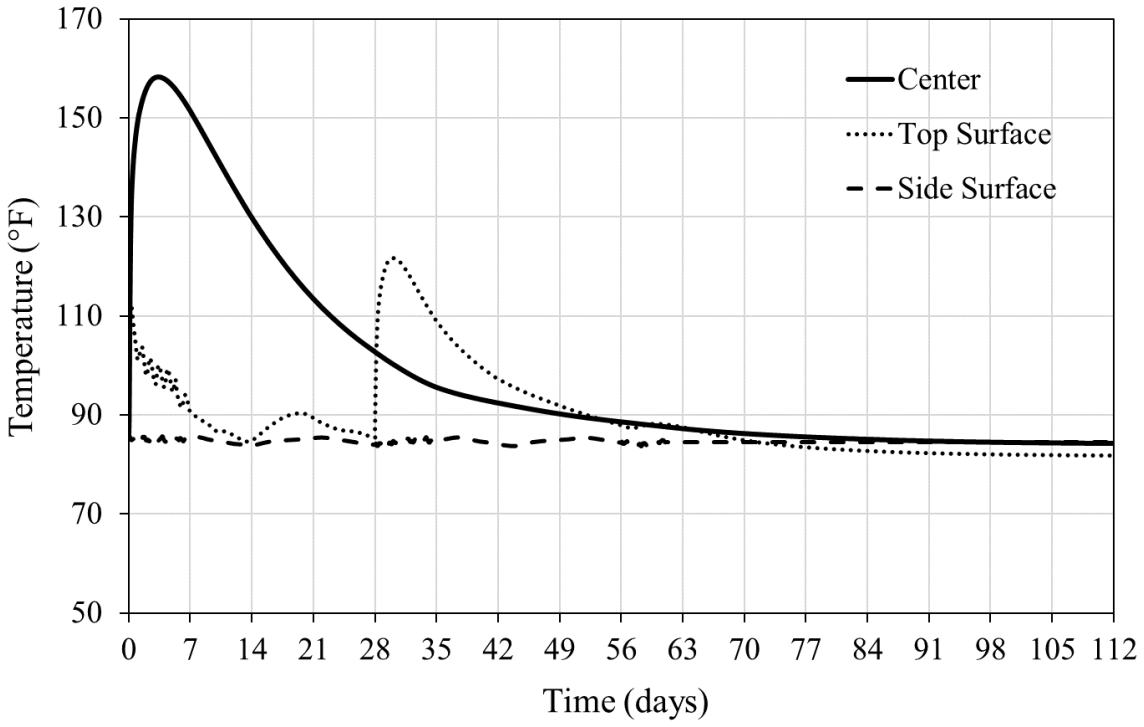

Figure 99 – Temperature development in the bridge seal (summer).

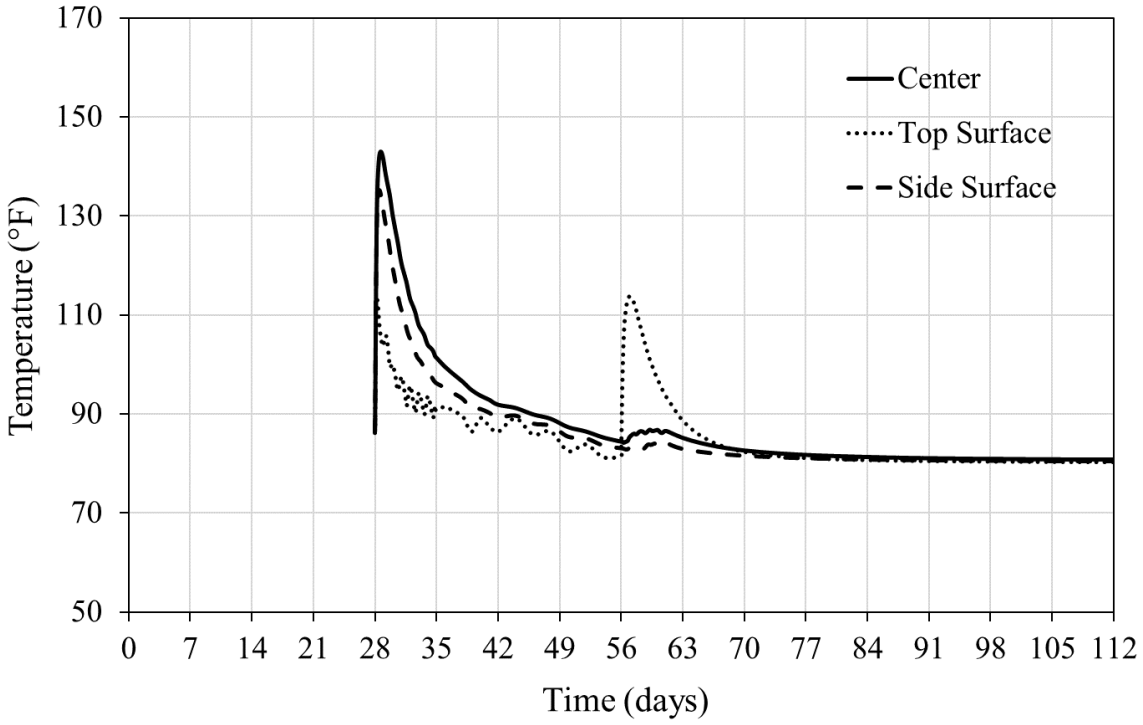

Figure 100 – Temperature development in the footing (summer).

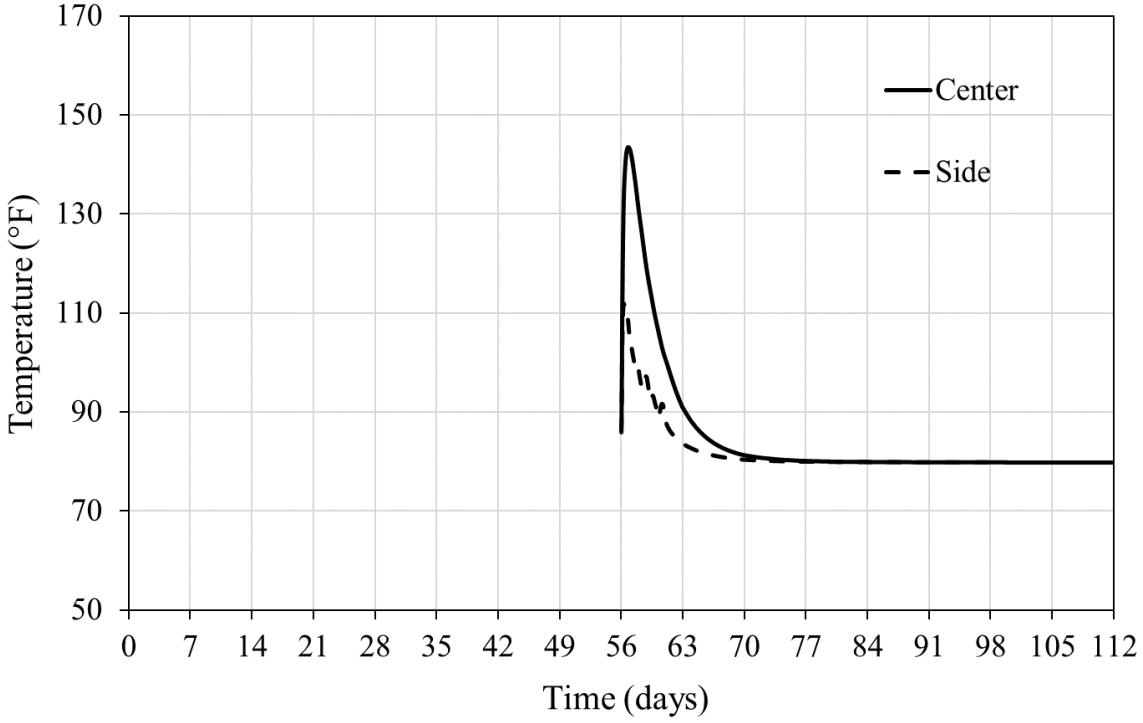

Figure 101 – Temperature development in the column (summer).

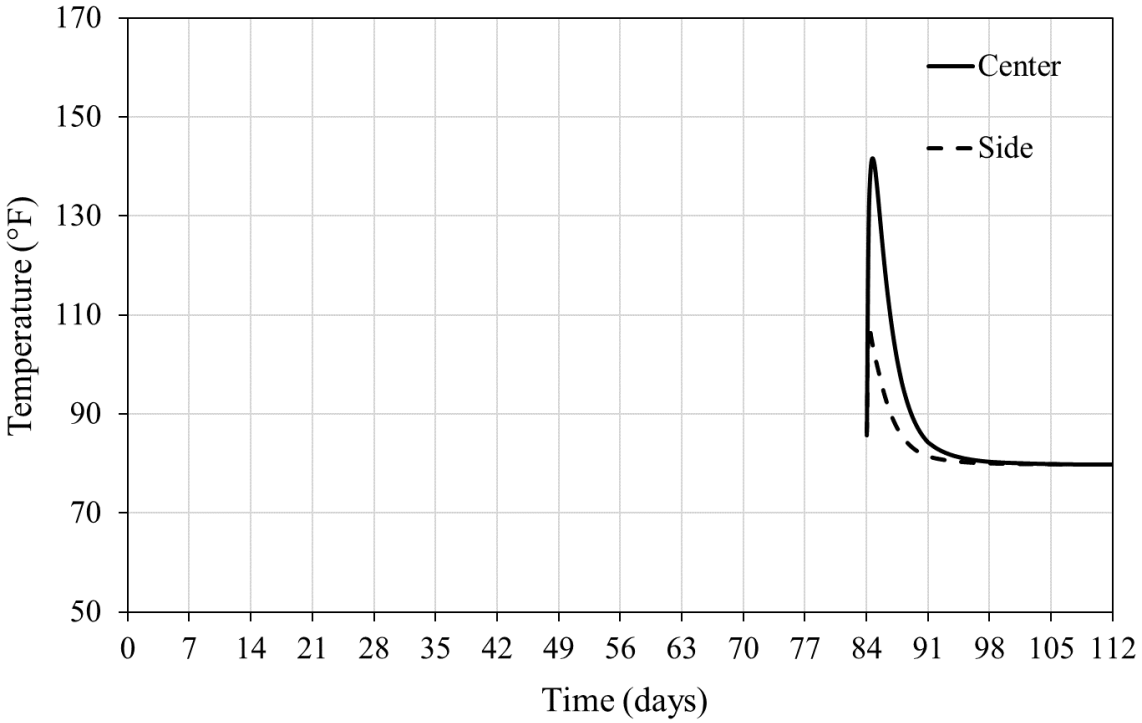

Figure 102 – Temperature development in the cap (summer).

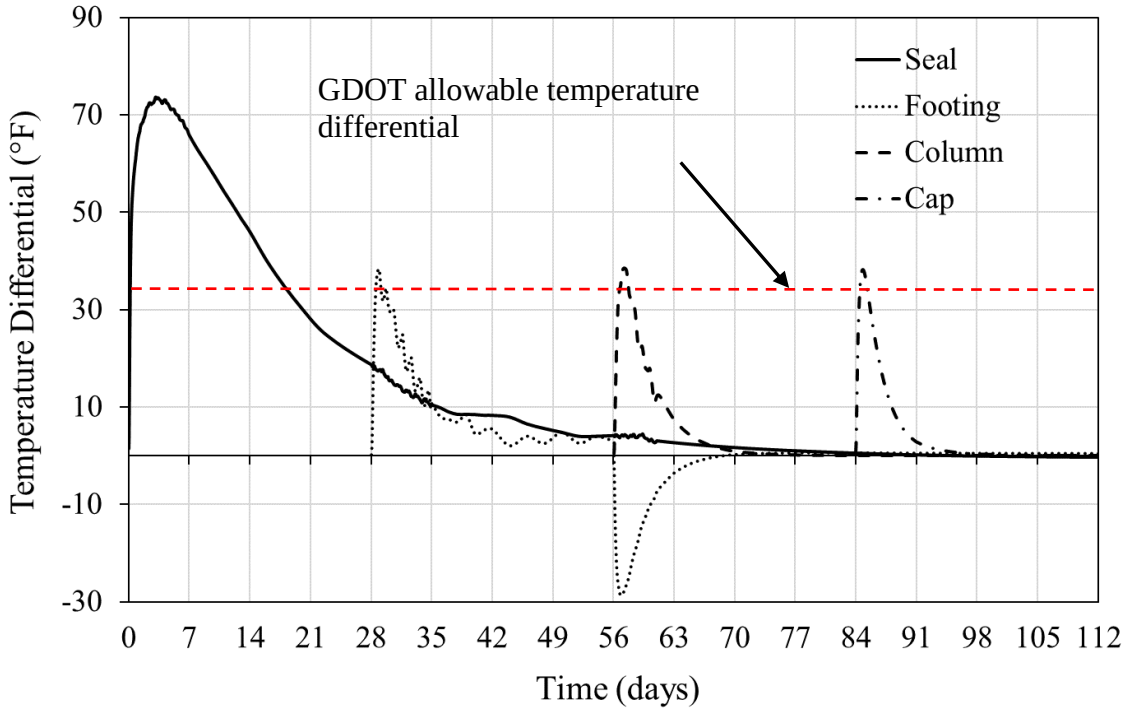

Figure 103 – Temperature differential development in the bridge seal model (summer).

4.9.4.2 Winter placement condition

Temperature distribution in the seal, footing, column, and cap at 1, 3, 7, and 28 days after the initial seal placement in winter is shown in Figure 104 through Figure 107. Figure 104 shows the temperature distribution in a half section of the seal. Figure 105 shows the temperature distribution in a half section of the seal and the footing after the footing is cast at 28 days. Figure 106 shows the temperature distribution in a half section of the seal, footing, and column after the column is cast at 56 days. Figure 107 shows the temperature distribution in a half section of the seal, footing, column, and cap after the cap is cast at 84 days. Similar to the results for the summer placement condition, temperature-time histories are presented in Figure 108 through Figure 111 for the center, top, bottom, and side surfaces of the seal, footing, column, and cap elements.

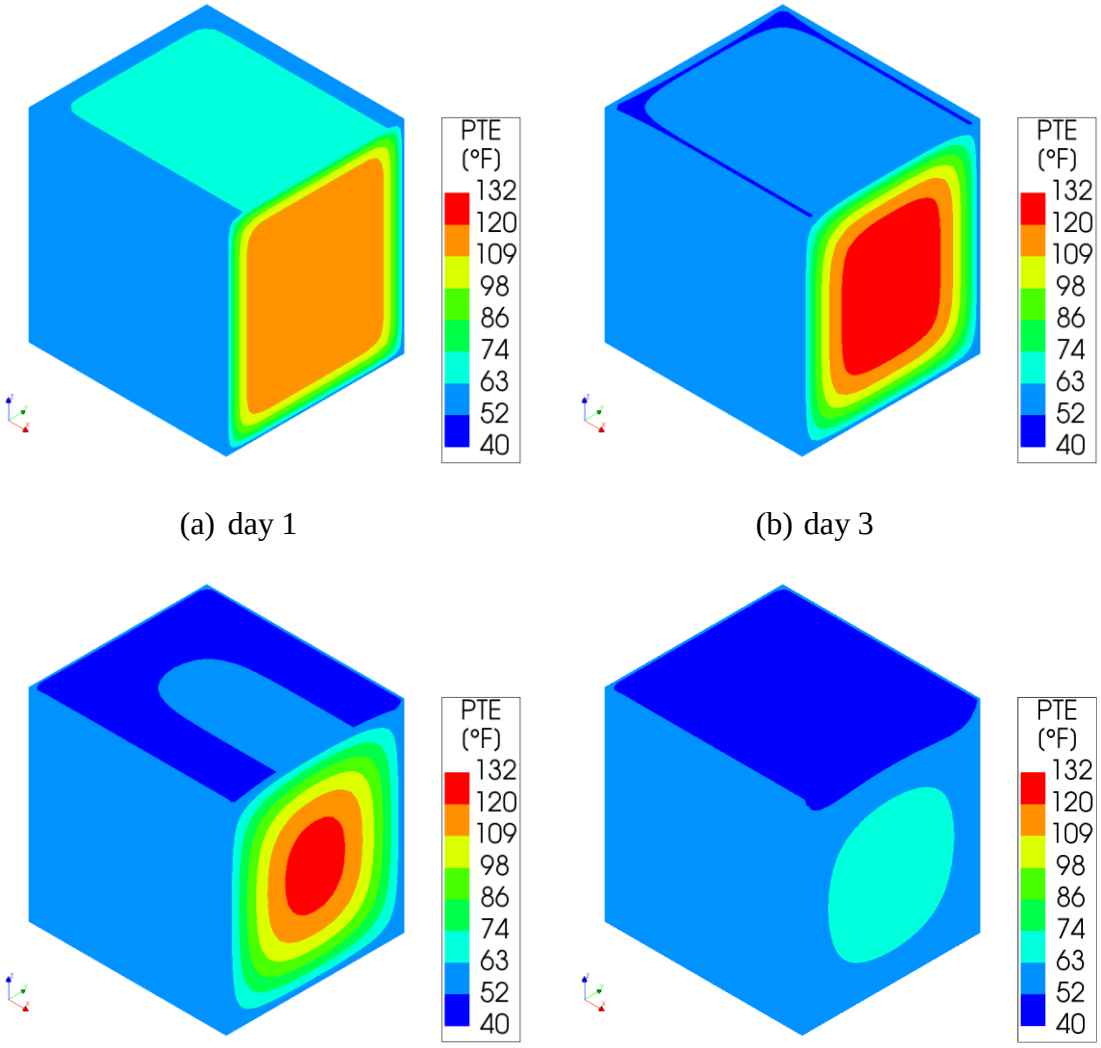

(a) day 1 (b) day 3

(c) day 7 (d) day 28

Figure 104 – Temperature distribution in the bridge seal - 28 days after seal placement (winter).

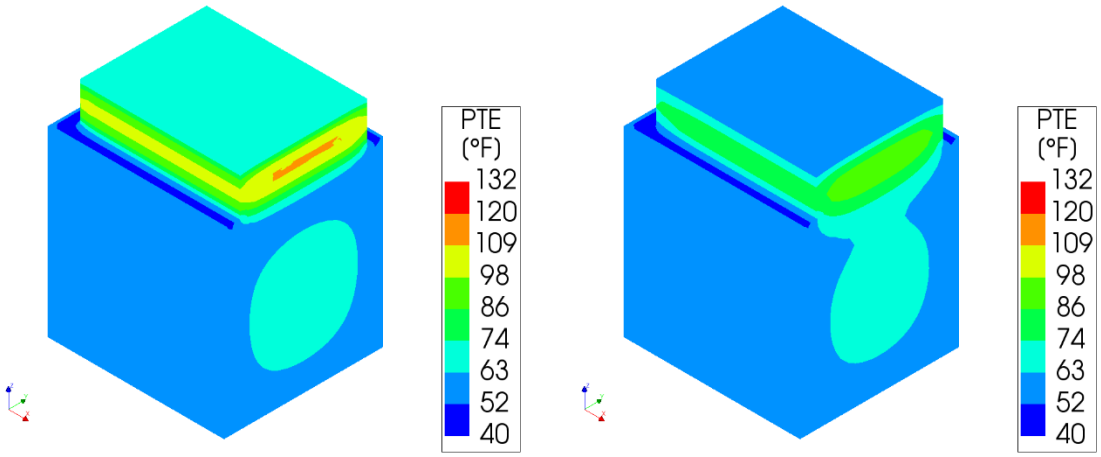

(a) day 1

(b) day 3

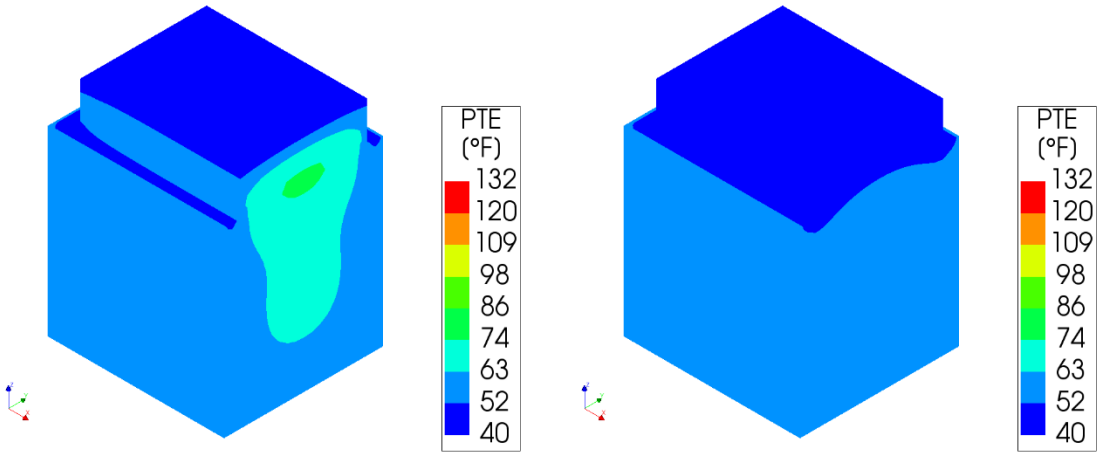

(c) day 7

(d) day 28

Figure 105 – Temperature distribution in the bridge seal and footing - 28 days after footing placement (winter).

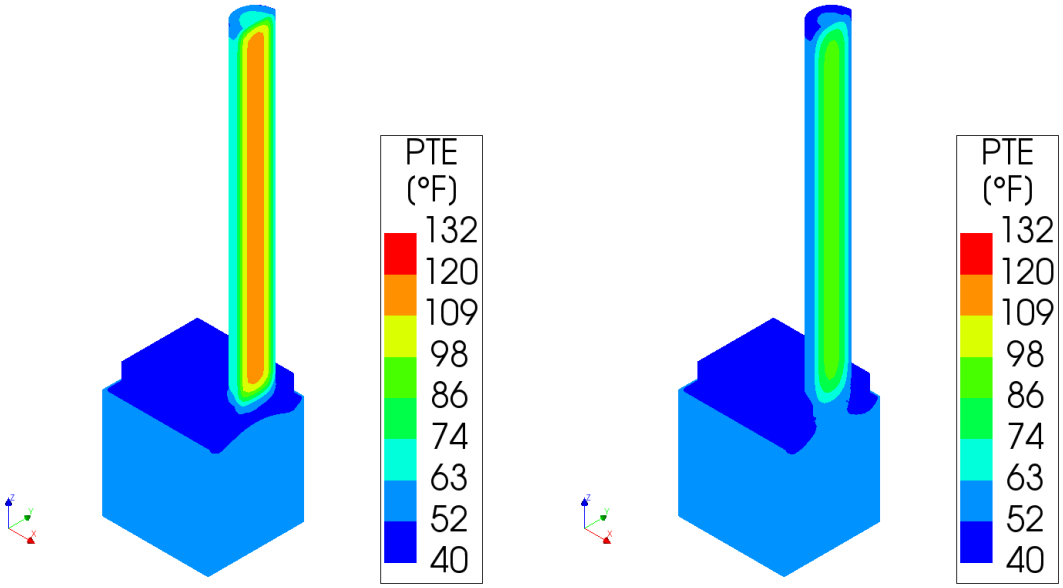

(a) day 1

(b) day 3

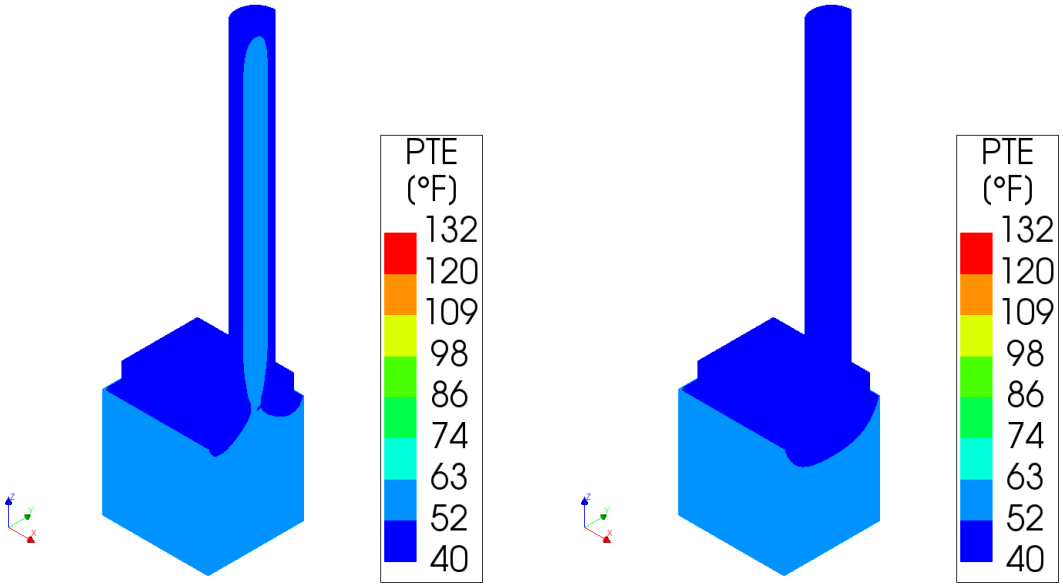

(c) day 7

(d) day 28

Figure 106 – Temperature distribution in the bridge seal, footing, and column - 28 days after column placement (winter).

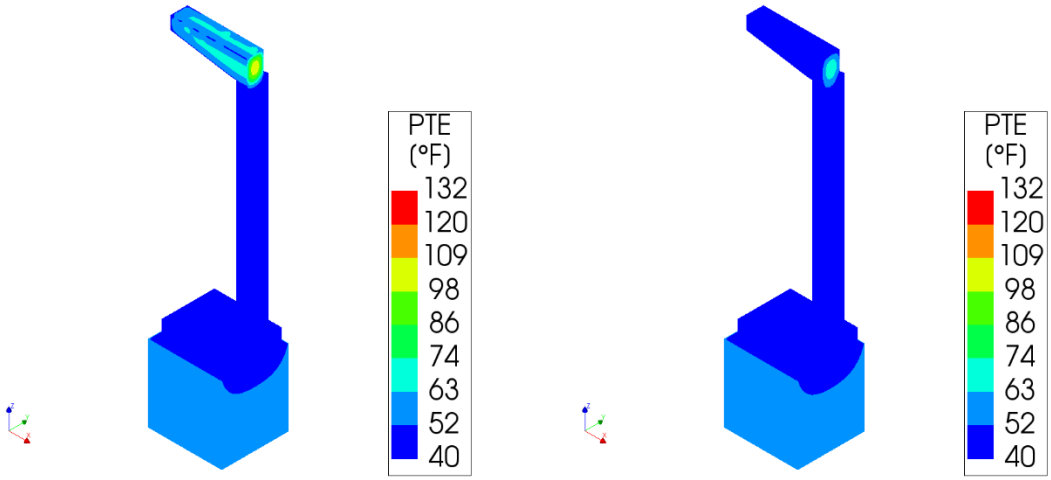

(a) day 1 (b) day 3

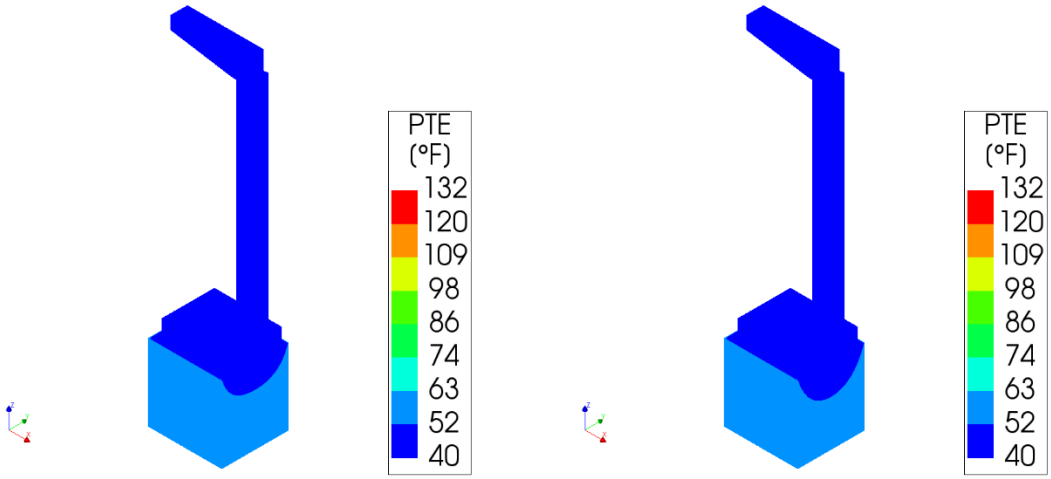

(c) day 7 (d) day 28

Figure 107 – Temperature distribution in the bridge seal, footing, column, and cap - 28 days after cap placement (winter).

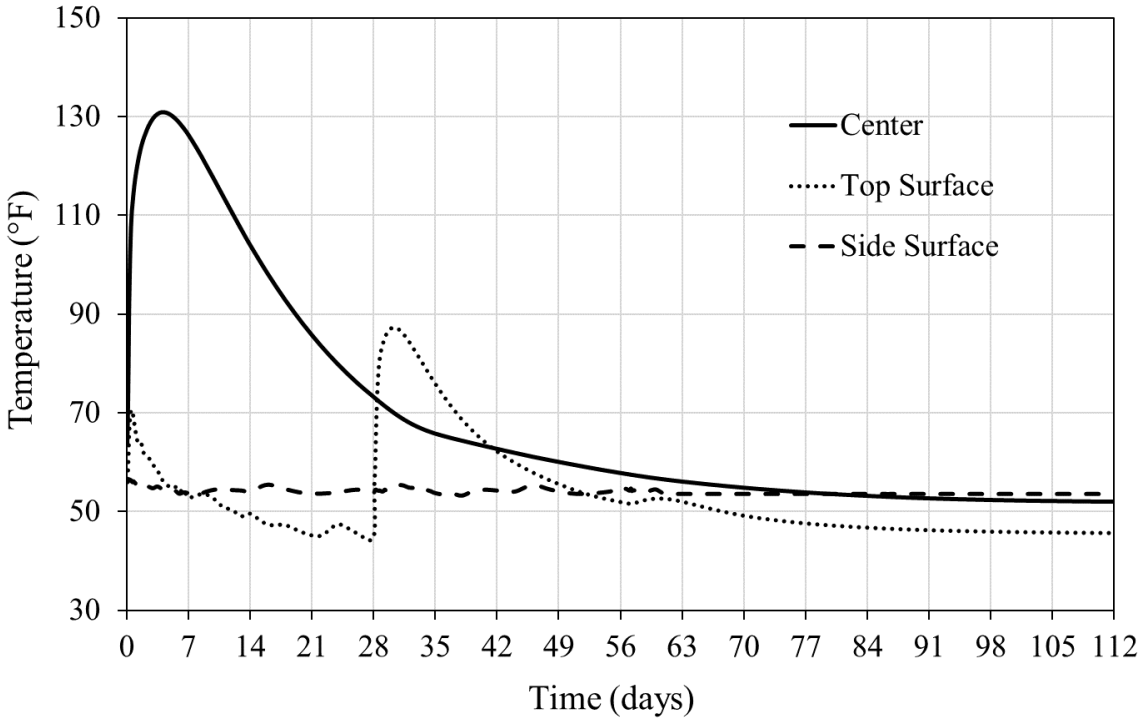

Figure 108 – Temperature development in the bridge seal (winter).

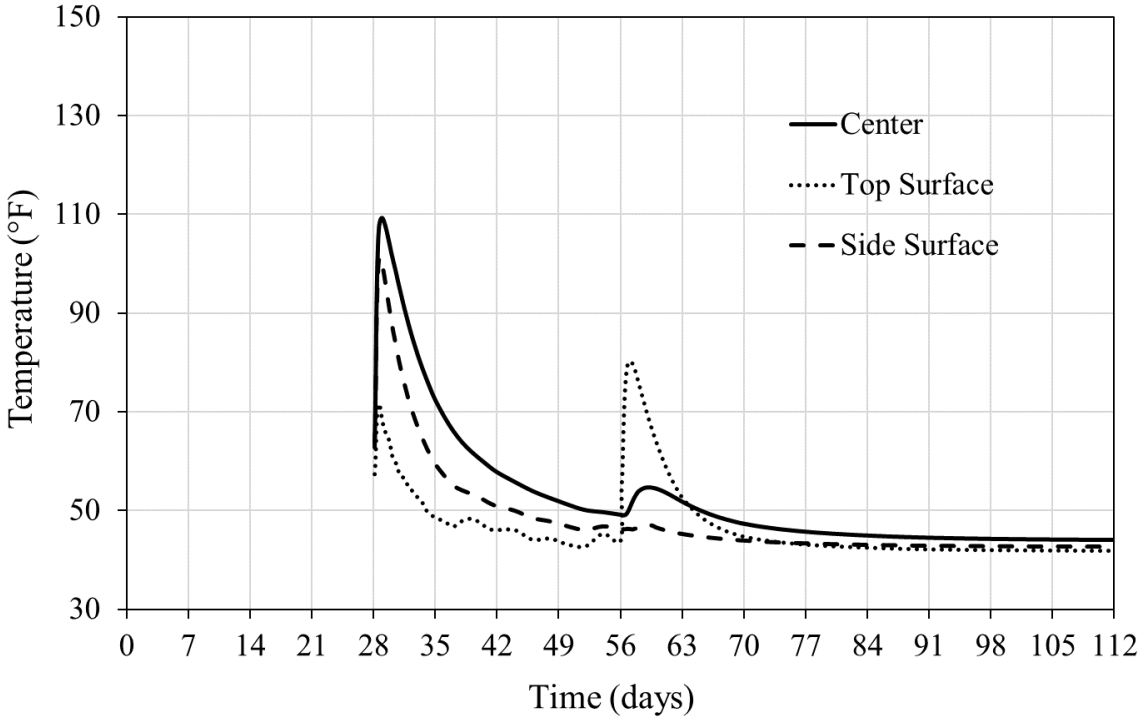

Figure 109 – Temperature development in the footing (winter).

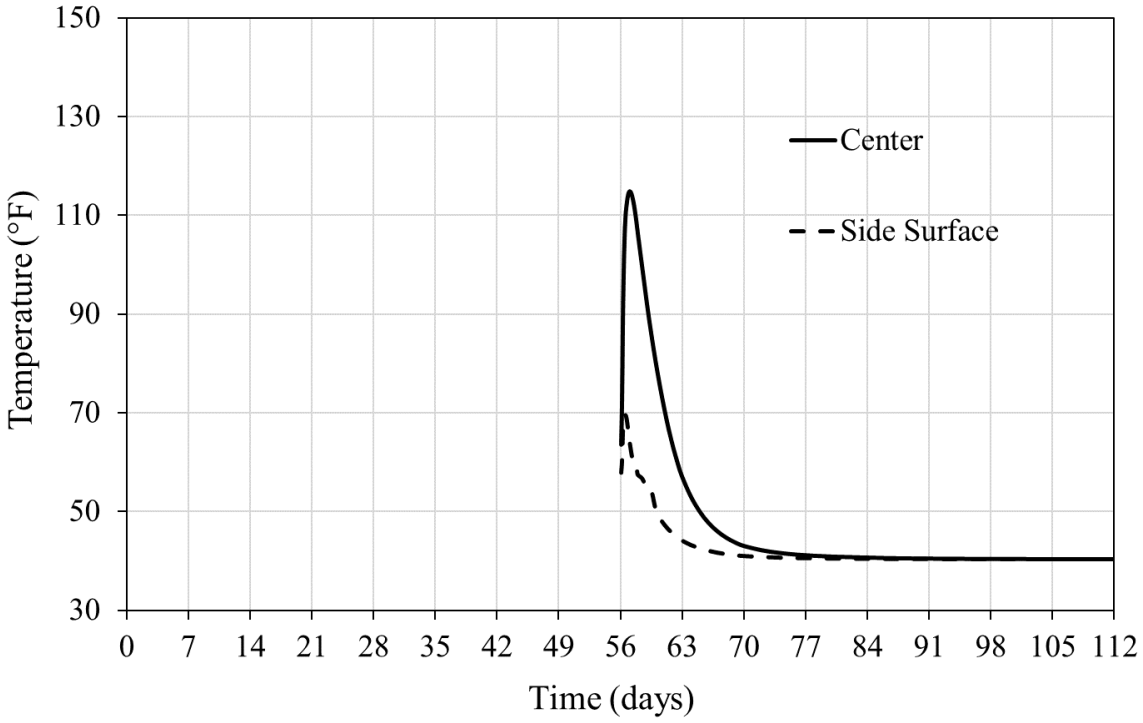

Figure 110 – Temperature development in the column (winter).

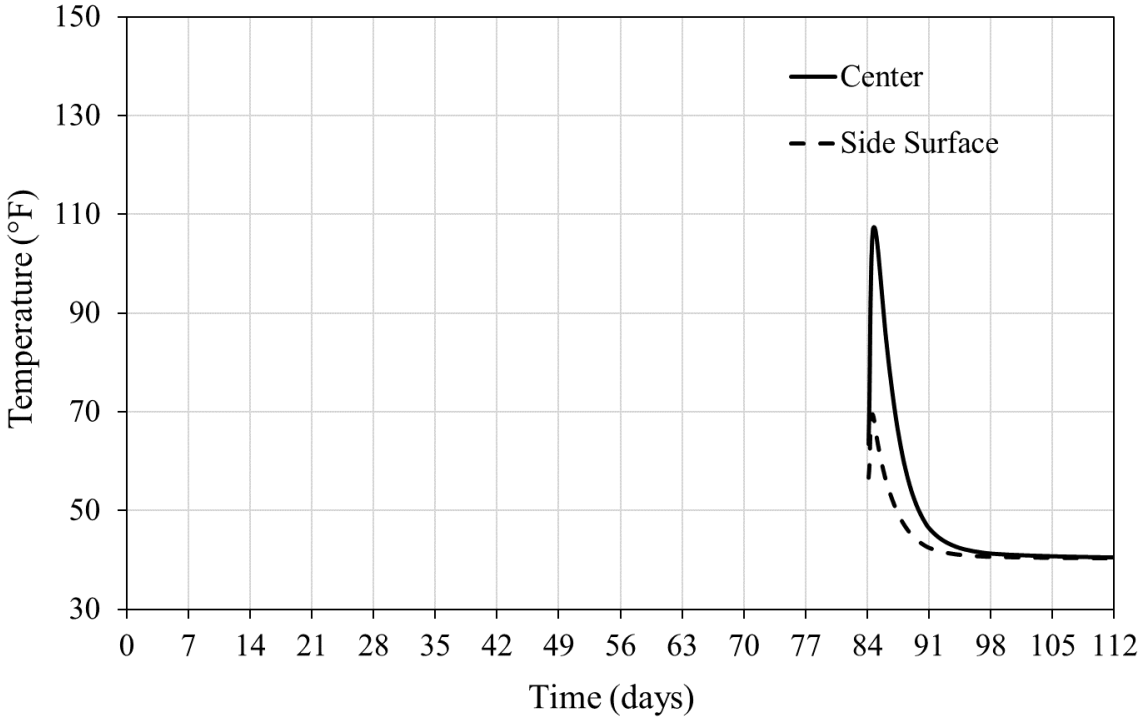

Figure 111 – Temperature development in the cap (winter).

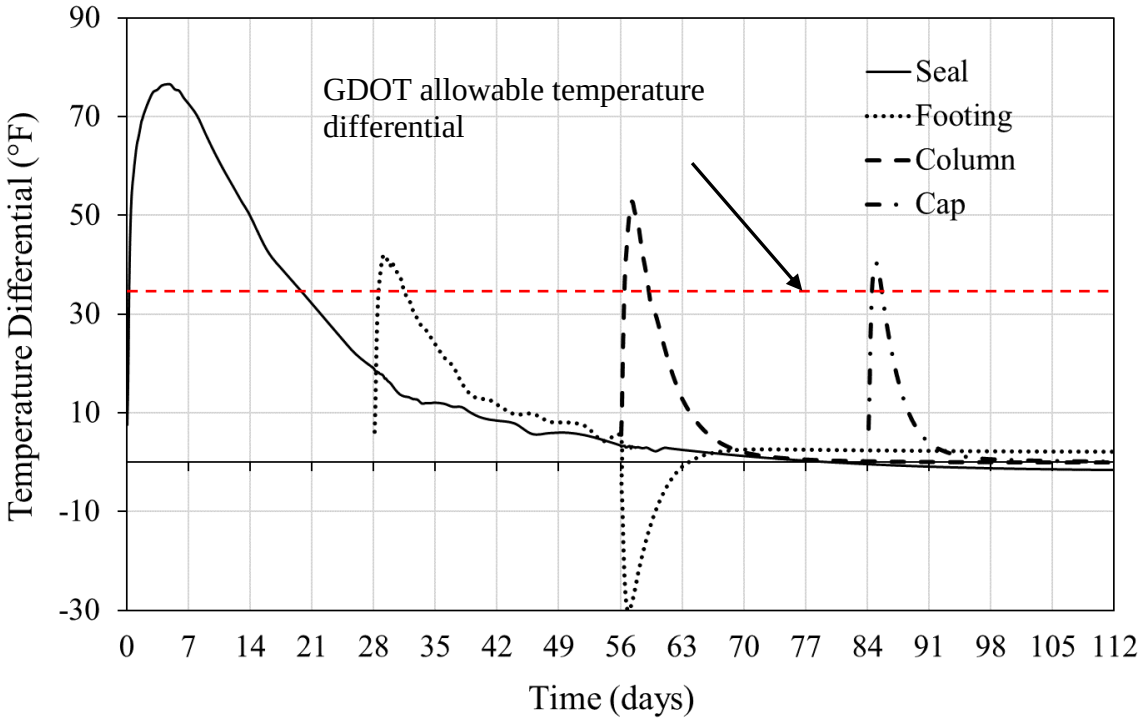

Figure 112 – Temperature differential development in the bridge seal model (winter).

4.9.5 **Strain Results**

4.9.5.1 Summer placement condition

For the structural analysis of the bridge bent structure, two material models are used to obtain strain, total stress, tensile strength, and crack width for the summer placement condition: one using fib requirements and the other using ACI codes.

The results of the structural analysis employing the fib material model are provided in Figure 113 through Figure 116. Figure 113 presents the total strain development in the seal, Figure 114 presents the stress development in the seal, Figure 115 presents the tensile strength development in the seal, and Figure 116 presents elements that are considered cracked. The total strain is an average strain in seal elements and includes the effect of crack strains.

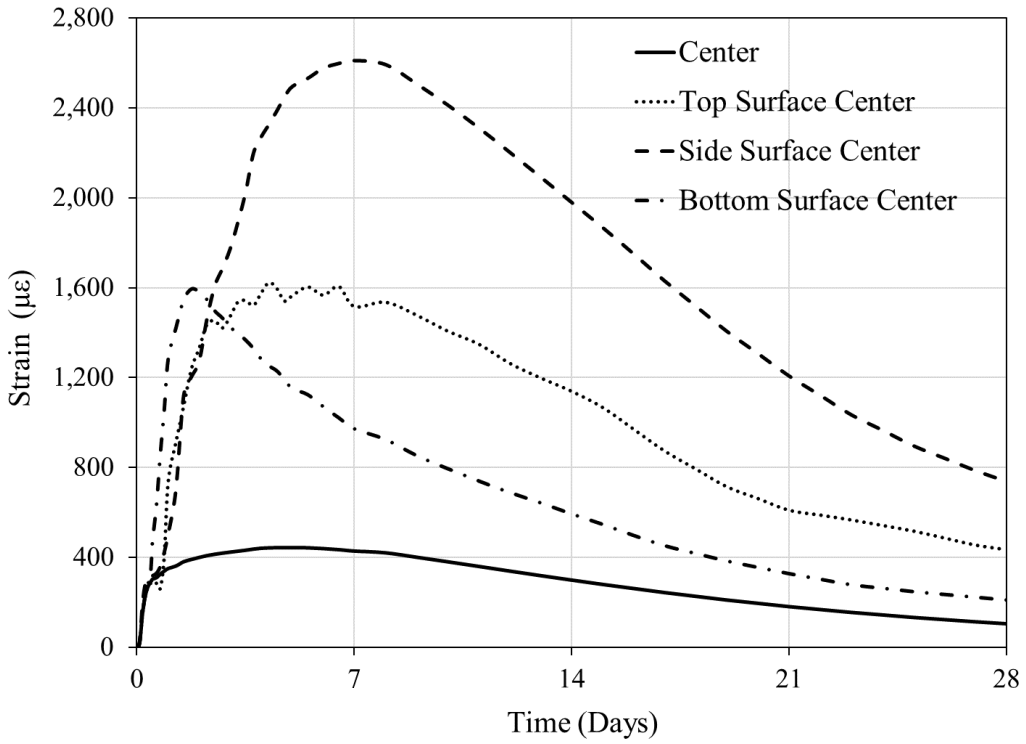

Figure 113 – Total strain development in the bridge seal - fib Model (summer).

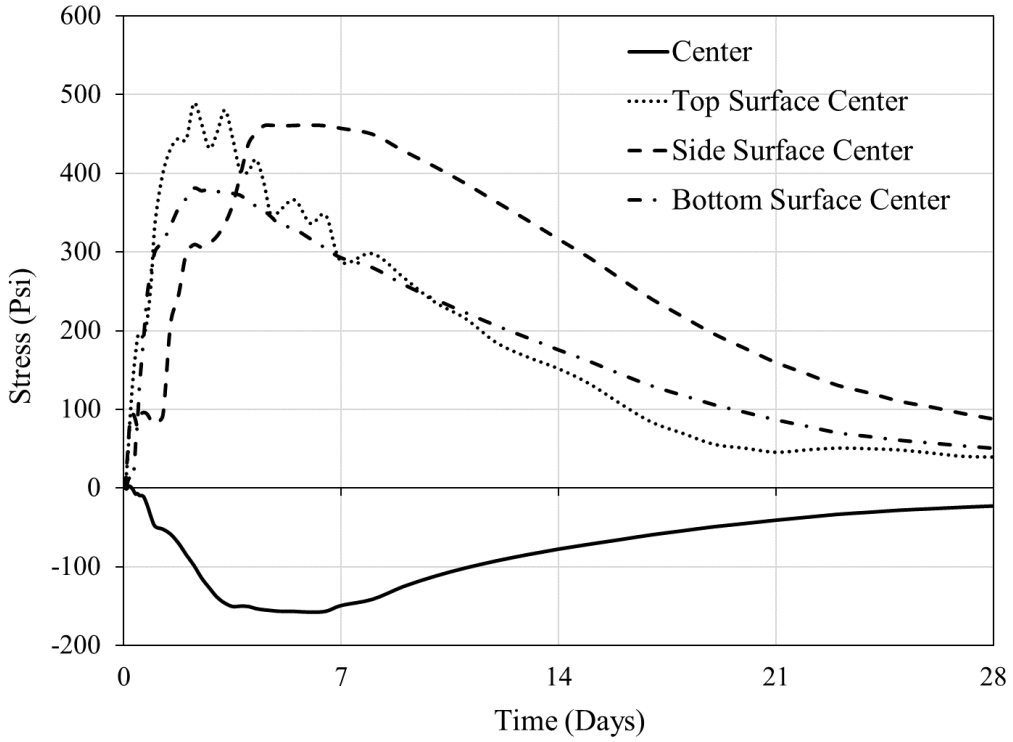

Figure 114 – Stress development in the bridge seal - fib Model (summer).

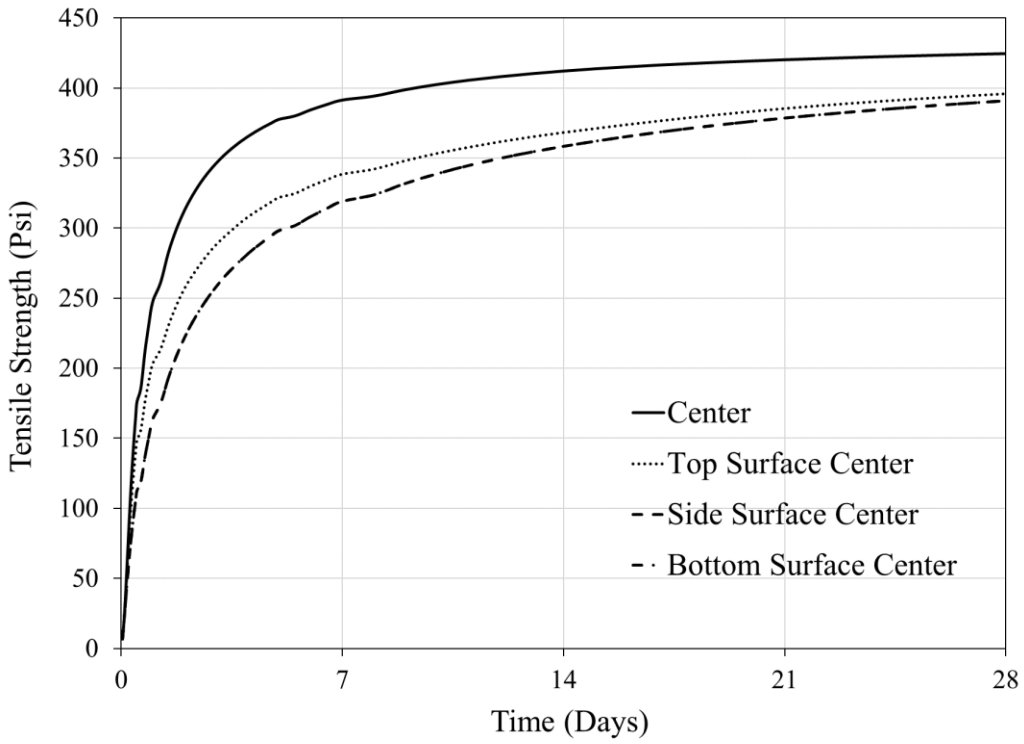

Figure 115 – Tensile strength development in the bridge seal - fib Model (summer).

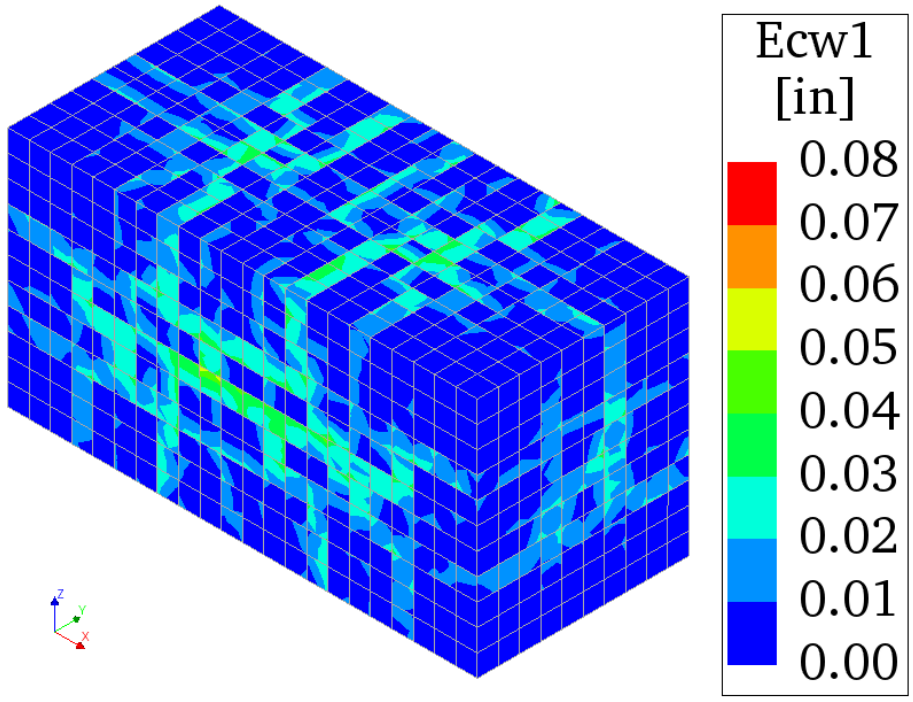

Figure 116 – Crack development in the bridge seal - fib Model (summer).

The results of the structural analysis employing the ACI material model are provided in Figure 117 through Figure 120. Figure 117 presents the total strain development in the seal, Figure 118 presents the stress development in the seal, Figure 119 presents the tensile strength development in the seal, and Figure 120 presents cracked elements.

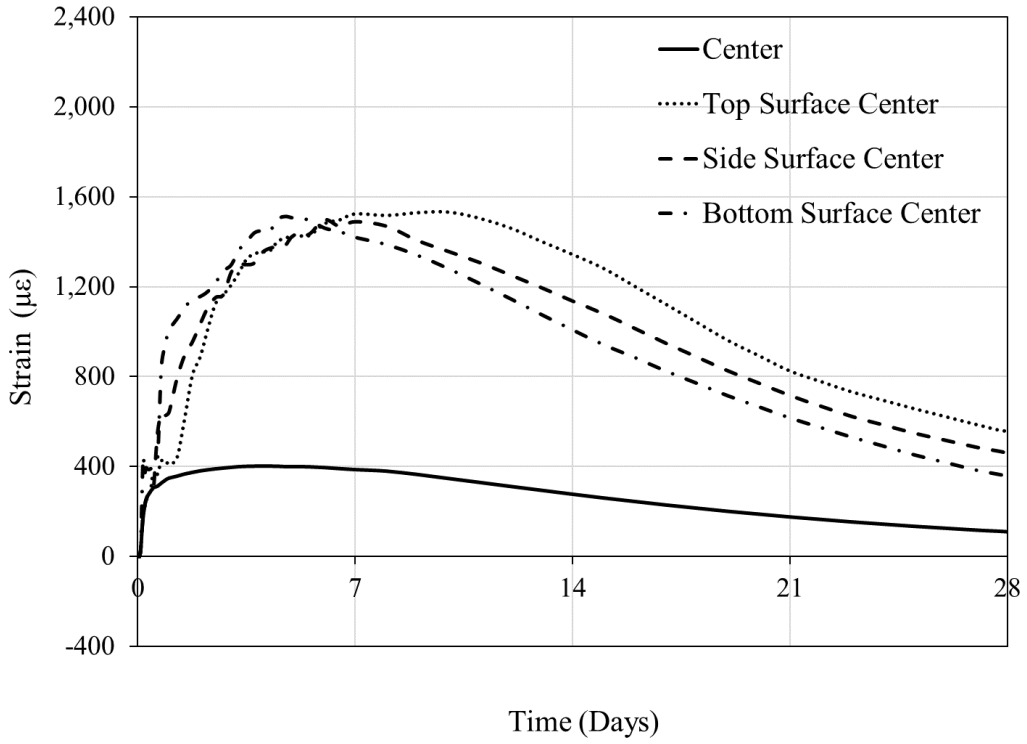

Figure 117 – Total strain development in the bridge seal - ACI Model (summer).

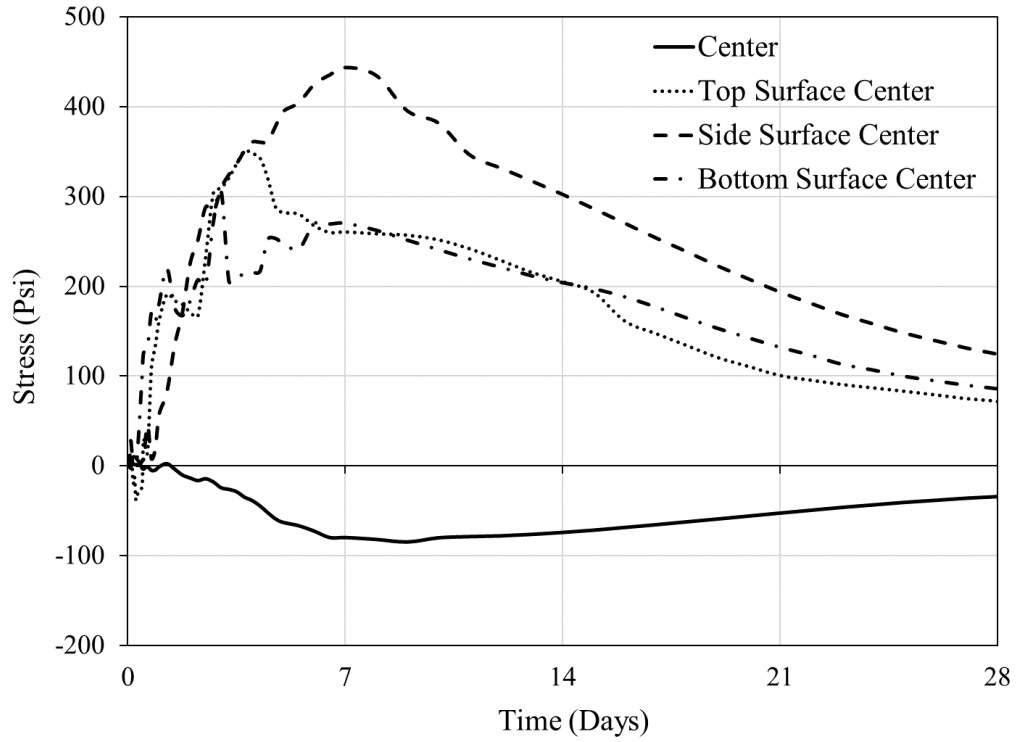

Figure 118 – Stress development in the bridge seal - ACI Model (summer).

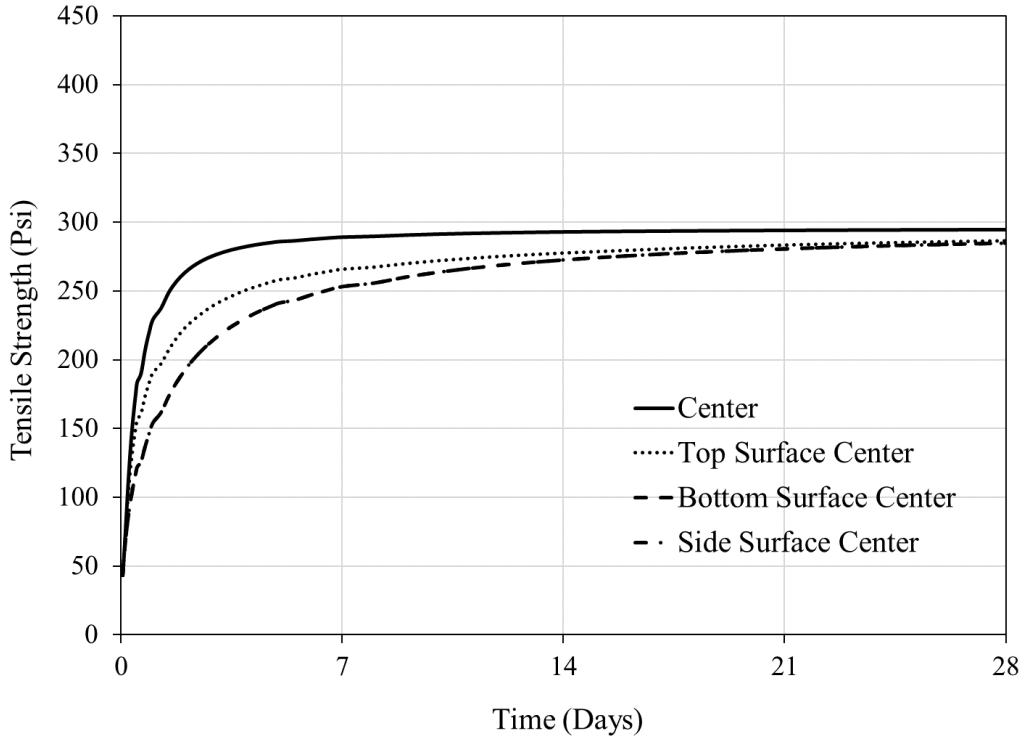

Figure 119 – Tensile strength development in the bridge seal - ACI Model (summer).

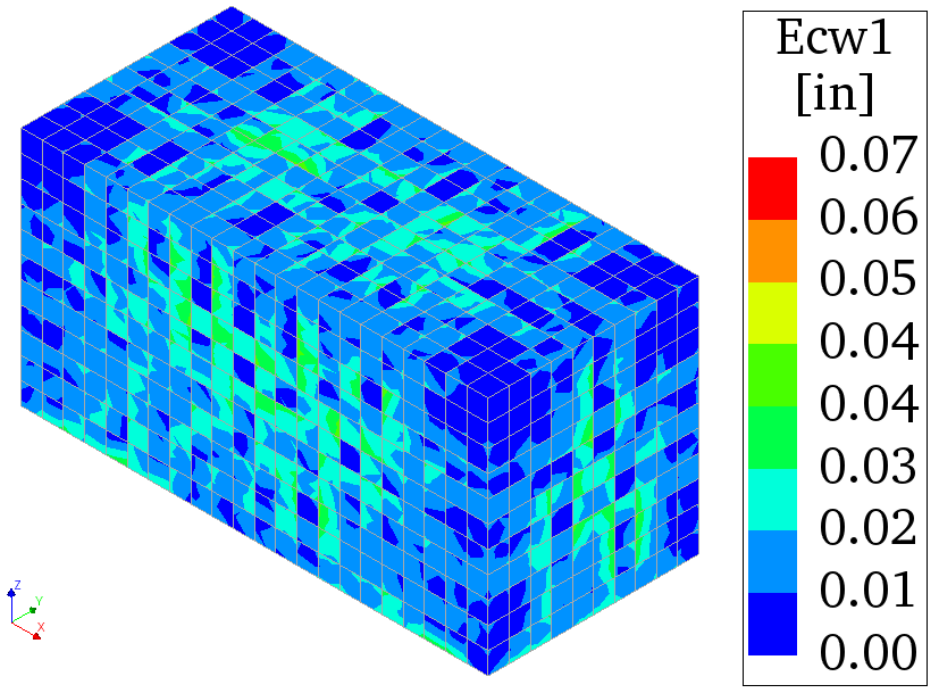

Figure 120 – Crack development in the bridge seal - ACI Model (summer).

4.9.5.2 Winter placement condition

For the winter placement condition, results are presented similarly, starting with those for the structural analysis employing the fib material model. Figure 121 presents the total strain development in the seal, Figure 122 presents the stress development in the seal, Figure 123 presents the tensile strength development in the seal, Figure 124 presents the crack width development in the seal, and Figure 125 presents cracked elements in the seal.

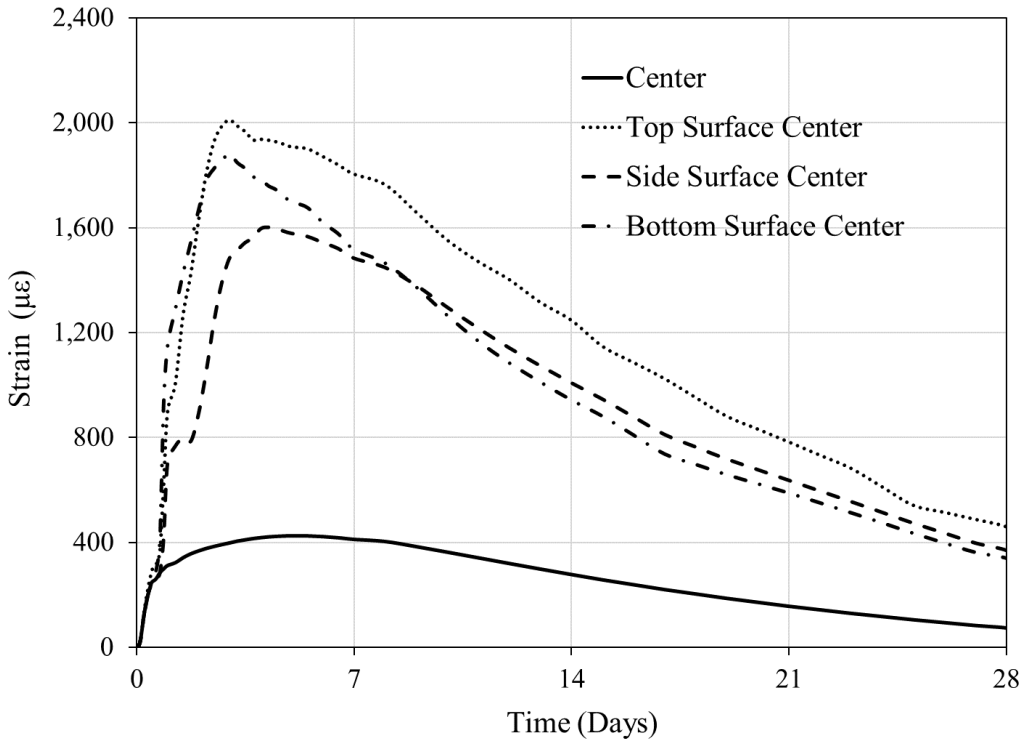

Figure 121 – Total strain development in the bridge seal - fib Model (winter).

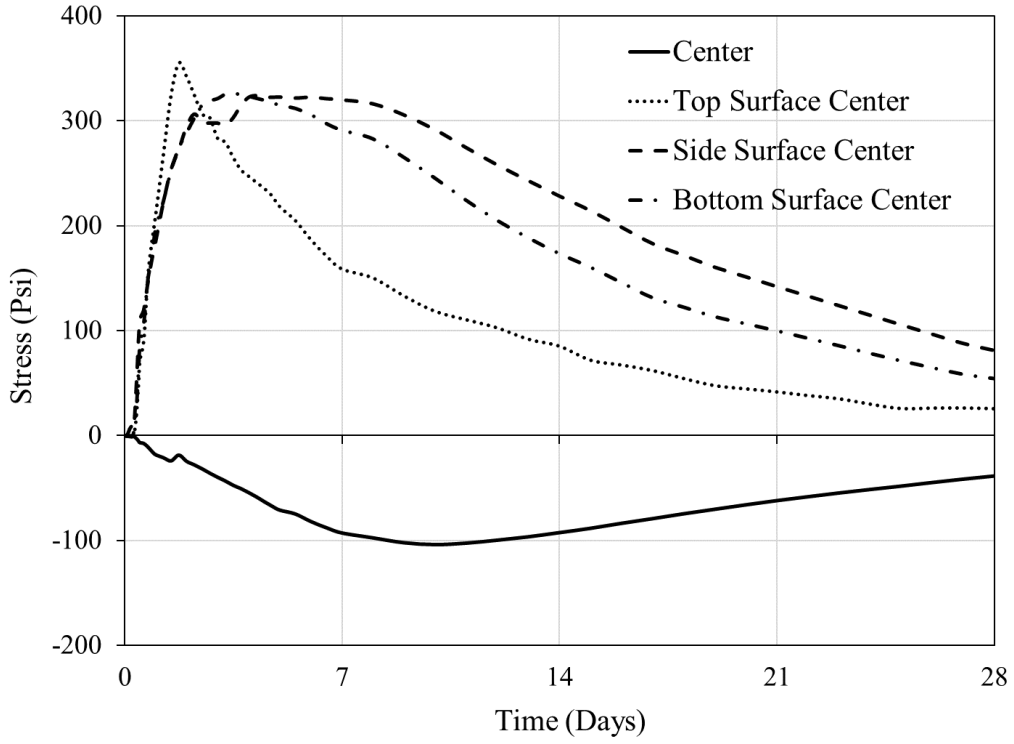

Figure 122 – Stress development in the bridge seal - fib Model (winter).

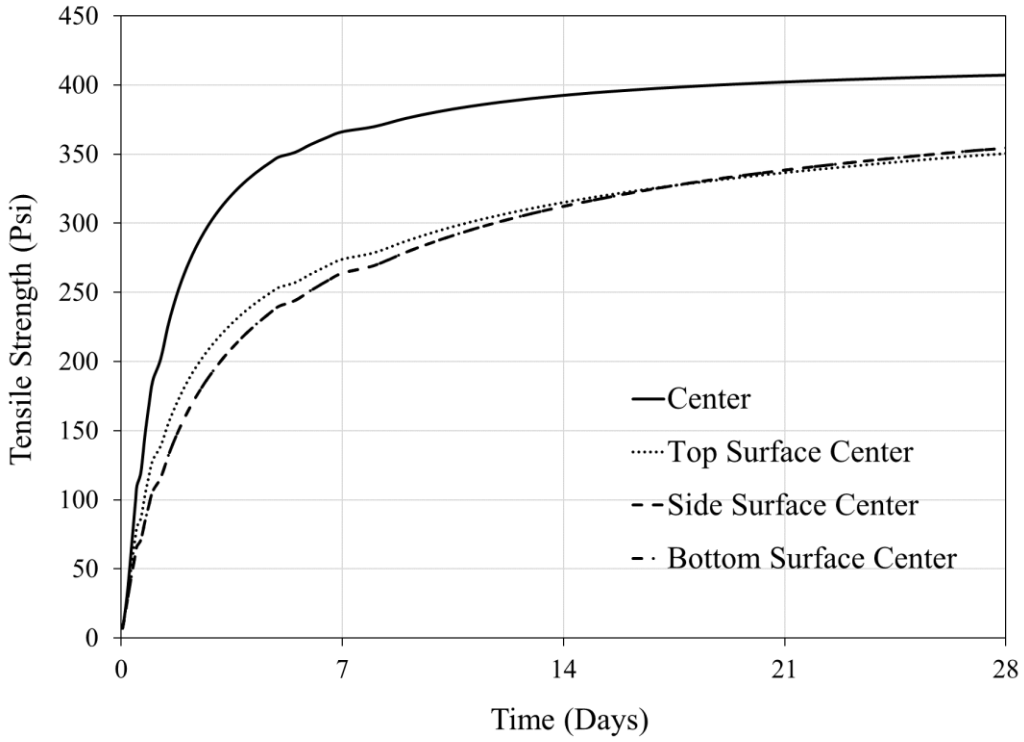

Figure 123 – Tensile strength development in the bridge seal - fib Model (winter).

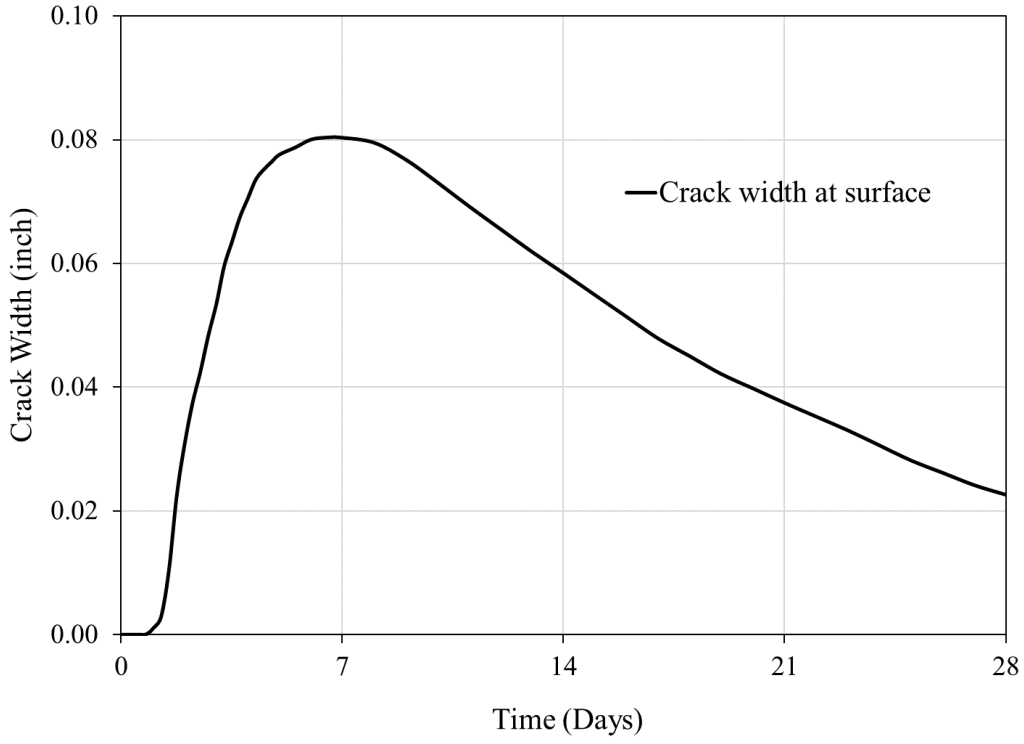

Figure 124 – Crack width development in the bridge seal - fib Model (winter).

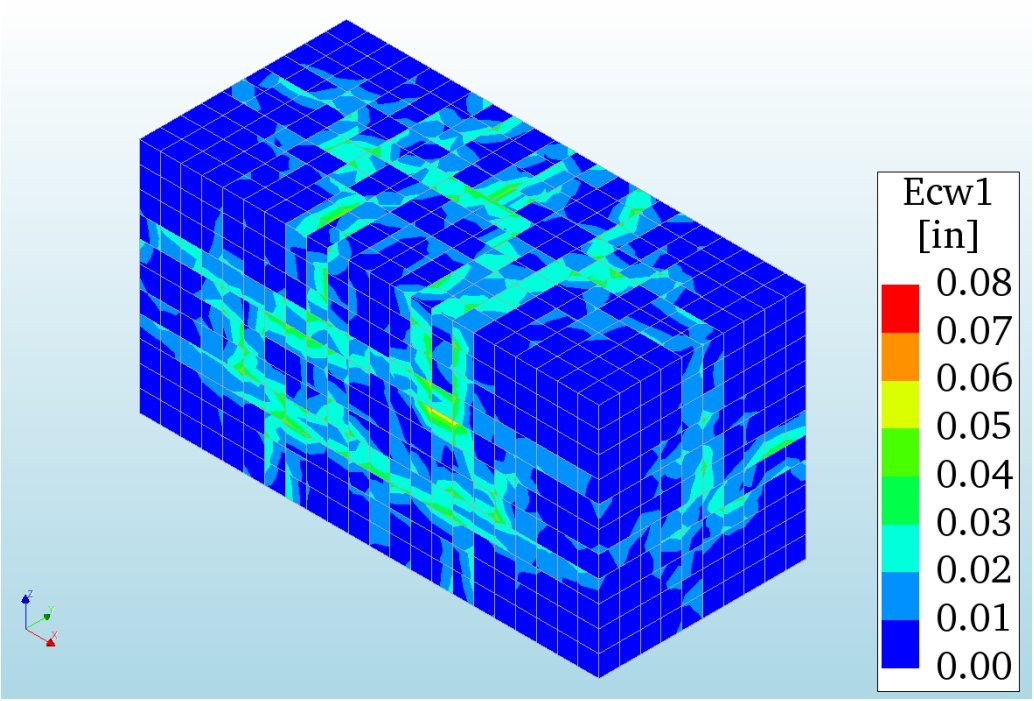

Figure 125 – Crack width in the bridge seal - fib Model (winter).

Below are the results of the analysis using the ACI material model. Figure 126 presents the total strain development in the seal, Figure 127 presents the stress development in the seal, Figure 128 presents the tensile strength development in the seal, and Figure 129 presents crack widths in the seal elements.

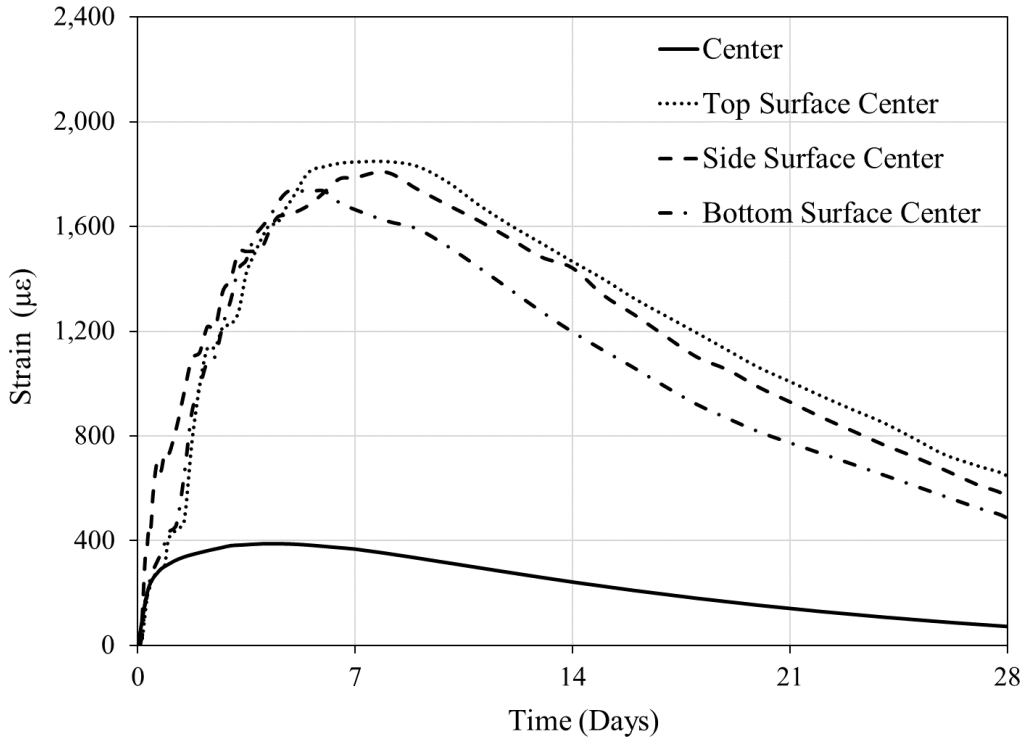

Figure 126 – Total strain development in the bridge seal – ACI Model (winter).

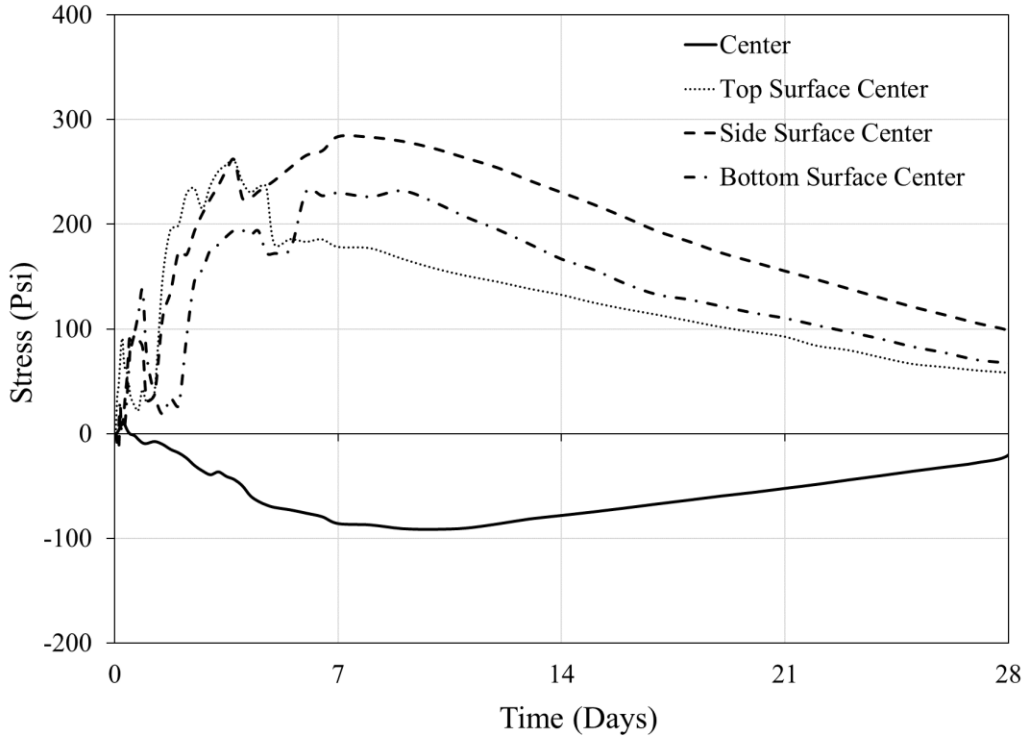

Figure 127 – Stress development in the bridge seal – ACI Model (winter).

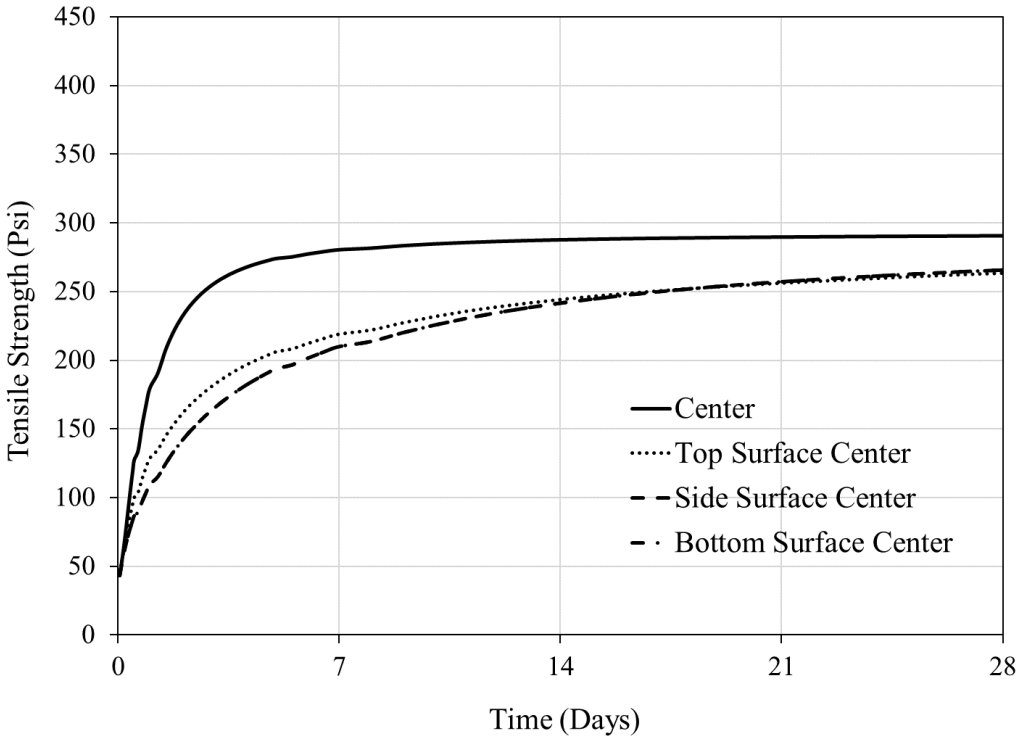

Figure 128 – Tensile strength development in the bridge seal – ACI Model (winter).

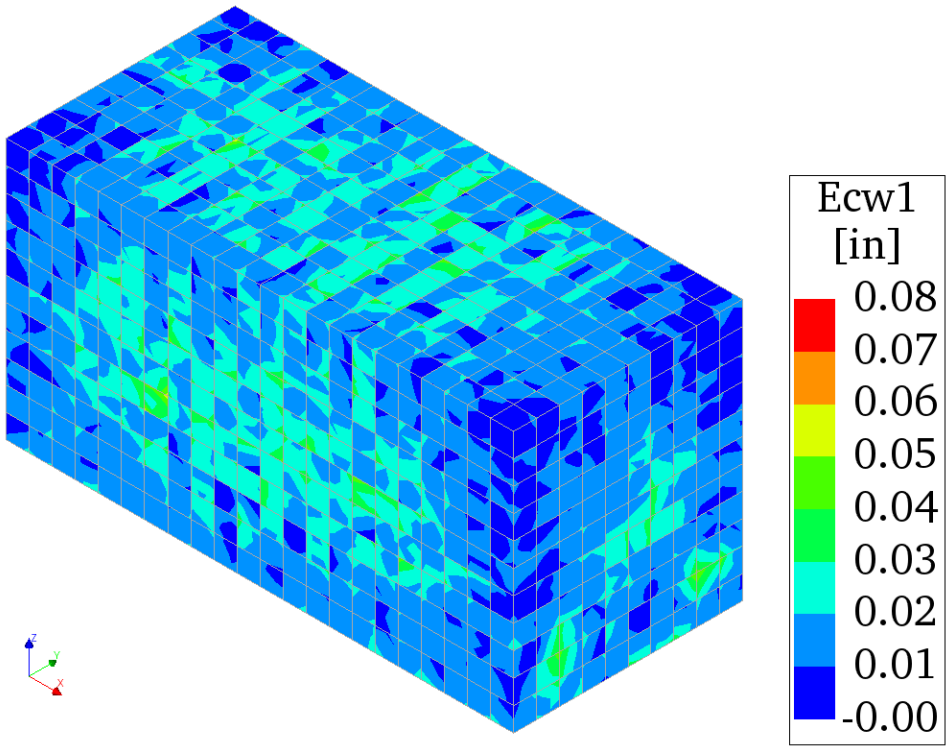

Figure 129 – Crack development in the bridge seal – ACI Model (winter).

4.9.6 **Validation of Bridge Seal Temperature**

A comparison of the temperature rise measurement in the bridge seal is performed between the experimental results, DIANA analysis, prediction equations from Section 3, and ConcreteWork software. The ConcreteWork was developed by the Concrete Durability Center at the University of Texas as part of research funded by the Texas Department of Transportation (TxDOT). Table 38 summarizes temperature predictions made by different methods.

Based on the laboratory test (see Figures 43 and 44), the experimentally measured maximum internal temperature for the seal mixture (FA45) was 151 °F which yielded a maximum temperature rise of 64.8 °F. In our study, the seal analysis results from DIANA indicated a slightly higher maximum temperature of 160 °F, which yielded a maximum temperature rise of 75 °F. This discrepancy was expected due to a small cube specimen and the use of insulation panels. Furthermore, the prediction results from the ConcreteWorks yielded a maximum temperature of 156 °F (see Figure 130), which is in great agreement with the DIANA results from this study. On the other side, the Gadja prediction was slightly higher than the PCA-ACI prediction (see Table 38). The analysis results from this study agree reasonably well with predictions made by the PCA-ACI equation (see Eq. 2) and Texas DOT ConcreteWorks.

Table 38 – Maximum temperature rise comparisons, °F (°C).

Mixture Code	Experimental (see Figs. 43-44) Results	DIANA Analysis Results	PCA-ACI Equation	Gadja Equation (Gadja et al, 2014)	Texas DOT ConcreteWorks Predictions (Fig. 130)
Control	90.5 (50.3)	105 (58.3)	91.0 (50.6)	113.8 (63.2)	101 (56.1)
FA-45	64.8 (36.0)	75 (41.7)	70.5 (39.2)	88.2 (49.2)	71 (39.4)

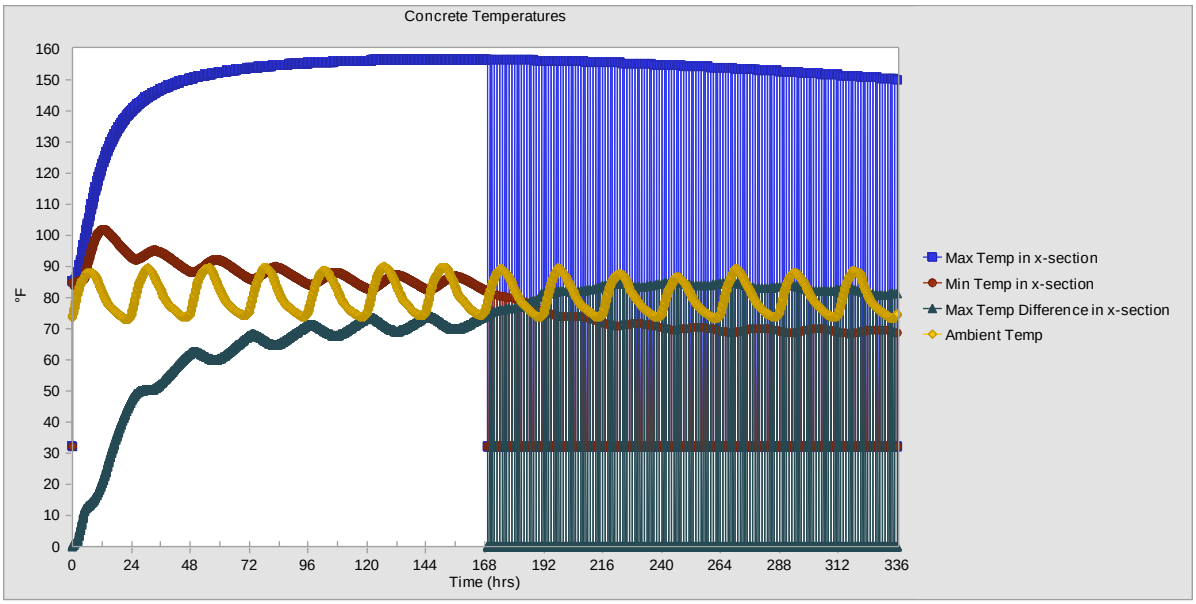

Figure 130 – Texas DOT Concrete Works predictions (TxDOT, 2019)**.**

4.9.7 **Analysis of Results and Discussion**

The temperature results illustrate that the maximum temperature occurs within four days of the reinforced concrete seal placement. As anticipated, the seal model for the summer placement condition results in a higher internal temperature when compared to the model for the winter placement condition; however, the temperature differential in the seal model is slightly higher, up to 10 °F or 5.6 °C, for the winter placement condition. This higher temperature differential between internal and external surfaces is reasonable due to the colder water and ambient temperature surrounding the bridge bent structure in the winter.

The maximum temperature of 158 °F (70 °C) occurs at the core of the seal model with the summer placement condition. According to this result, the seal may be vulnerable to DEF as the maximum temperature approaches the threshold temperature of 160 °F (71.1 °C). In addition, a significant temperature gradient (approximately 74 °F or 41.1 °C) is created in this seal model, one greater than the temperature differential threshold of 35 °F

(19.4 °C) specified in the GDOT Mass Concrete Special Provisions (GDOT, 2013). This significant temperature gradient in the seal is expected to remain unchanged for longer than two weeks. As such, cracks are likely to form on seal structure surfaces. Meanwhile, the temperature differentials in the footing, column, and cap exceed the temperature differential threshold by about 3 °F (1.7 °C) for the summer placement condition and by about 5 °F (2.8 °C) to 20 °F (11°C) for the winter placement condition. At the same time, the maximum internal temperatures in these elements are significantly lower than 158 °F (70 °C).

Overall, results from applying the fib and ACI material models to the bridge bent models show a negligible difference when it comes to crack widths, regardless of placement conditions. The seal model analyzed with the fib material model gives tensile stress 100 psi (0.7 MPa) higher than that given by the ACI model. Concrete cracks when tensile strain reaches approximately 0.0001 inch/inch (0.0001 mm/mm), and tensile strains greater than this threshold are found on the surfaces of the seal model, mainly 7 to 10 days after the initial concrete placement at a time when the tensile strength of concrete is expected to be lower.

A crack width of about 0.08 inch (2 mm) is observed on the surface of the seal model. This width, however, does not correspond to the significantly wider cracks (up to 6 inches or 152 mm) documented by divers. As discussed in Section 1.1.1, tolerable crack widths range between 0.004 inch (0.10 mm) and 0.016 inch (0.40 mm) according to fib (fib, 2013) and ACI (ACI 224R-07, 2007) design guidelines, depending on structures' environmental exposure. For example, for a structure exposed to seawater (or wetting), a crack width of 0.006 inch (0.10 mm) is recommended.

There may be two main reasons for the discrepancy between the crack widths documented by divers and the ones predicted by the model. For one, a combination of DEF cracks and other environmental factors (e.g., exposure to water) might have widened cracks. That is, cracks already formed in the seal structure might have been exacerbated by other factors. In addition, according to the seismic data recorded by the United States Geological Survey (USGS, 2019), the bridge seal structure experienced an earthquake of magnitude ranging between 2.3 and 4.1 (PGA=1%g) in 2012 and 2014. Thus, in addition to water exposure, these earthquakes could have widened crack widths.

CHAPTER 5

SENSITIVITY ANALYSES ON VOLUME-TO-SURFACE AREA RATIOS AND MIXTURE DESIGNS

This study presents a sensitivity analysis on maximum temperature and temperature differential predictions by studying parameters such as volume-to-surface area ratios (V/A), mixture designs, and placement conditions in mass concrete structures. The objective of this analysis is to illustrate how one predicts temperatures for mass concrete mixtures by developing a series of charts. Two mass concrete models are selected: 1) an underwater foundation seal structure, hereafter referred to as "foundation," and 2) a bridge pier/column, hereafter referred to as "column." Drilled shafts are not considered due to a wide range of soil parameters and associated temperature conduction.

The daily water and ambient temperatures surrounding the foundation and column models are considered, respectively. Placement temperatures of 85 °F (29.4 °C) and 60 °F (15.6 °C) are considered for the summer and winter placement conditions, respectively. For the foundation model, the modeling parameters remain unchanged from Chapter 4 unless otherwise indicated. For both models, the total unit weight of cementitious material and the water-to-cementitious material ratio remain constant: 711 lb/yd^3 (422 kg/m^3) and 0.43, respectively. For the foundation and column models, fourteen and fifteen V/A ratios, respectively, are studied with the V/A ratio ranging between 0.1 and 5.0. The following assumptions are made: 1) the rectangular underwater foundation is enclosed by a cofferdam with steel sheet piles and 2) the circular column is constructed with steel formwork. In all

cases, a sensitivity of variables on the maximum internal temperature and differential temperature is studied.

The following variables and analysis cases outlined in Table 39 are considered:

- V/A ratios
- Summer and winter placement conditions
- Mixture designs
    - Cement replacement with varying amounts of slag
    - 70% cement replacement mixtures
    - Water-to-cementitious material ratios
- Insulation materials

Table 39 – Parameters considered in the sensitivity analysis.

Parameters	**Variables**			
	Summer		**Winter**	
Geometry	Foundation	Column	Foundation	Column
Volume-to-surface area ratio (ft)	Up to 5.0		Up to 5.0	
Mixture Design	Control		Control	
	SL30+MK15		SL30+MK15	
	FA45		FA45	
	SL55+MK15		SL55+MK15	
	SL40+FA30		SL40+FA30	
Water-to-cementitious material ratio (w/c)	Control with w/c=0.36		Control with w/c=0.36	
	Control with w/c=0.43		Control with w/c=0.43	
	Control with w/c=0.48		Control with w/c=0.48	
Insulation Materials	No insulation		No insulation	
	Insulation with R-value of 1 ($ft^2 \cdot °F \cdot h/BTU$)		Insulation with R-value of 1 ($ft^2 \cdot °F \cdot h/BTU$)	
	Insulation with R-value of 2 ($ft^2 \cdot °F \cdot h/BTU$)		Insulation with R-value of 2 ($ft^2 \cdot °F \cdot h/BTU$)	
	Insulation with R-value of 3 ($ft^2 \cdot °F \cdot h/BTU$)		Insulation with R-value of 3 ($ft^2 \cdot °F \cdot h/BTU$)	

Note: For 1 inch (=25.4 mm) thick panel, 1 $ft^2 \cdot °F \cdot h/BTU$ = 0.18 $m^2 \cdot °C/W$; 1ft = 0.30 meter.

5.1 Foundation Model

5.1.1 Sensitivity of Volume-to-Surface Area Ratios

Figure 131 presents fourteen underwater foundation models representing various V/A ratios. As a point of reference, the V/A ratio is 4.16 in the bridge seal structure presented in Chapter 4. Figure 132 and Figure 133 present the maximum temperature and temperature differential in the foundation model for varying V/A ratios. Both summer and winter placement conditions are studied using the Control mixture, in order to study the effect of one variable at a time. Figure 134 and Figure 135 present the effect of V/A on the time elapsed to reach the maximum temperature in the foundation during summer and winter placement conditions, respectively. Figure 136 shows the temperature-time history.

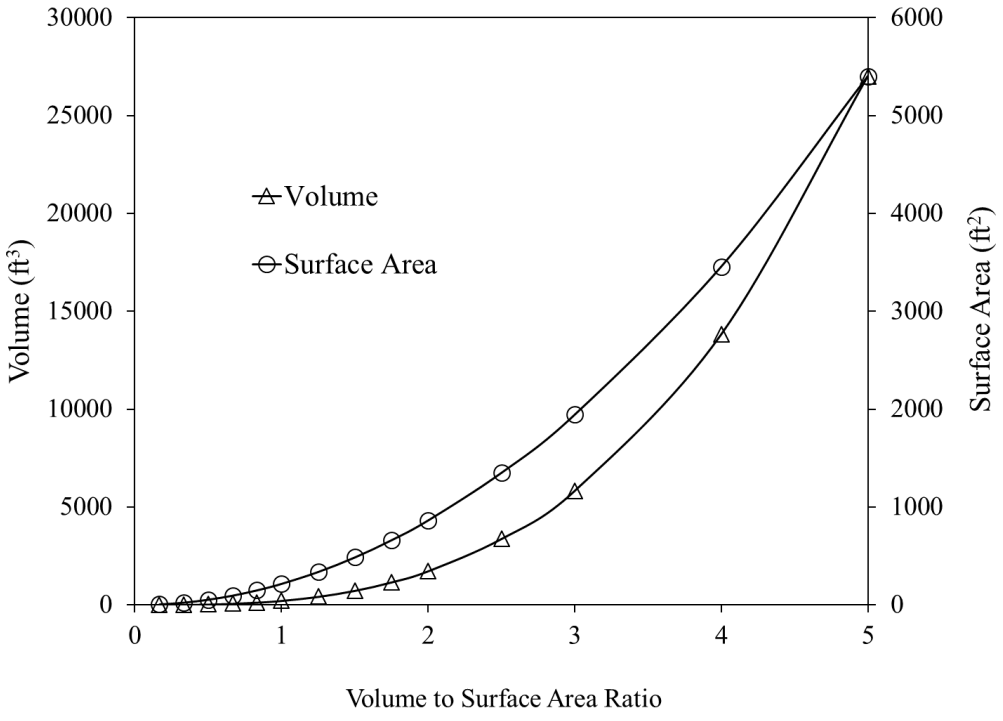

Figure 131 – Volume and surface area corresponding to V/A ratio – foundation.

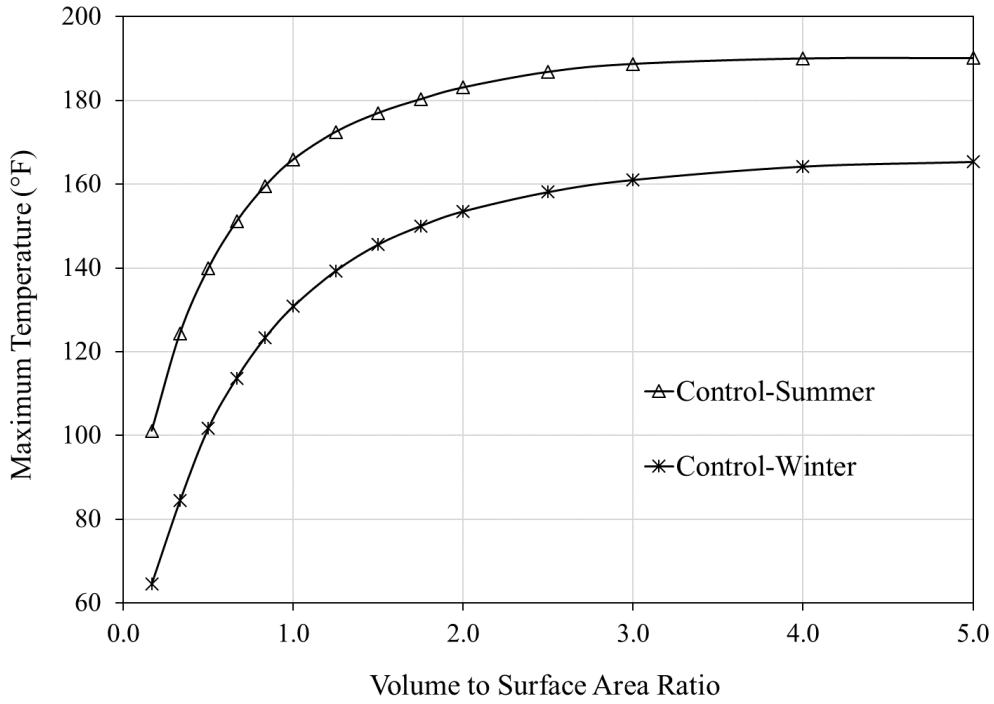

Figure 132 – Effect of V/A ratio on maximum temperature – foundation.

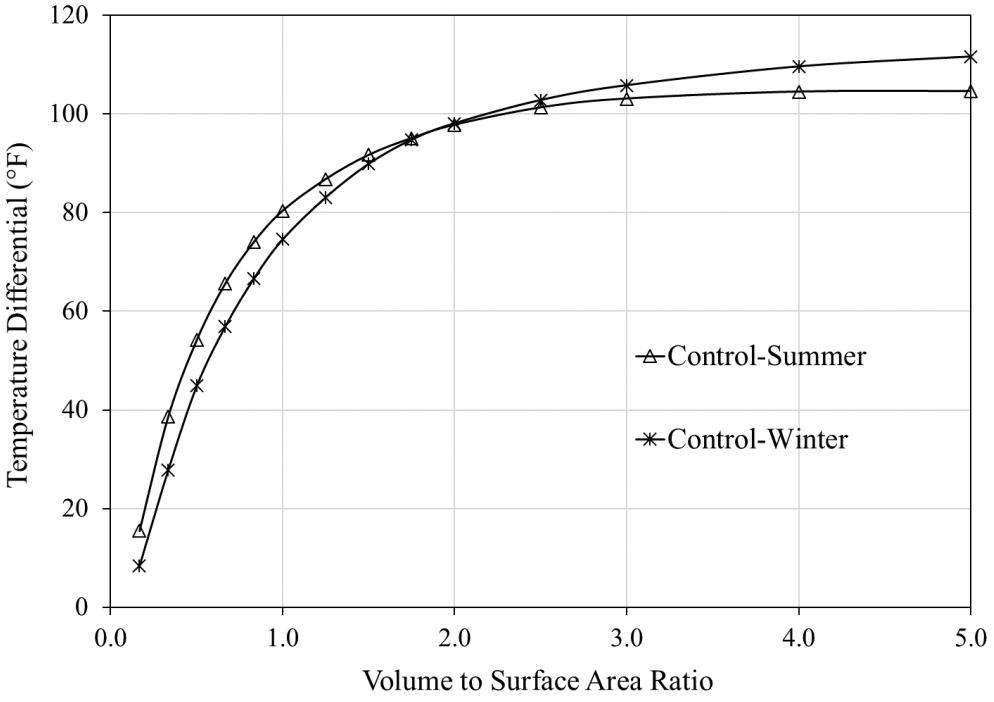

Figure 133 – Effect of V/A on maximum temperature differential – foundation.

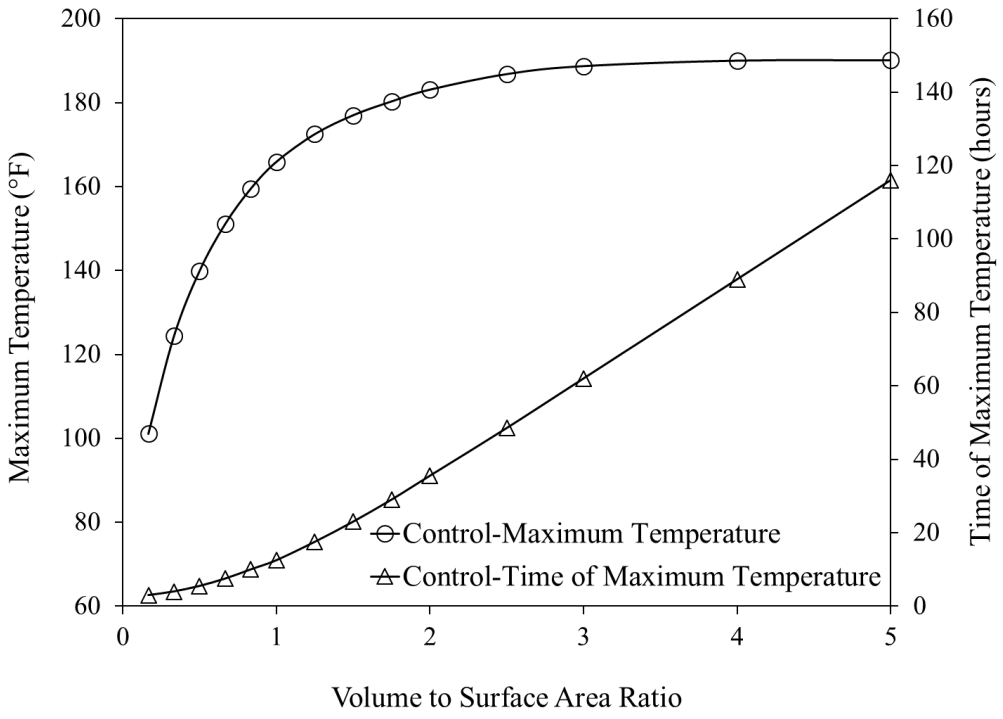

Figure 134 – V/A, time elapsed, and maximum temperature – foundation (summer).

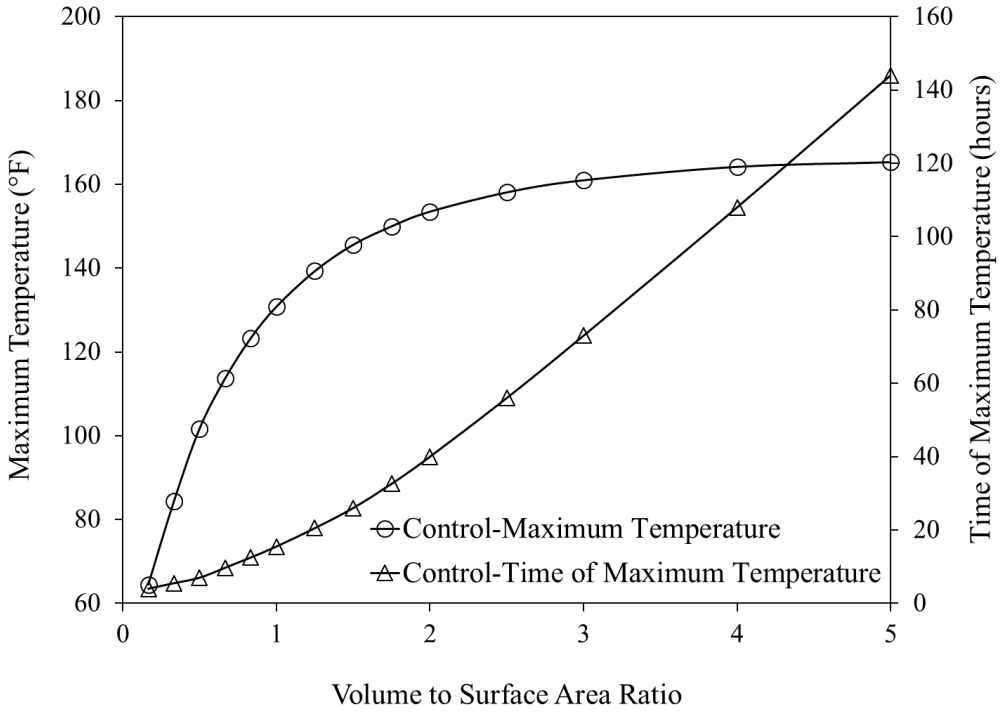

Figure 135 – V/A, time elapsed, and maximum temperature – foundation (winter).

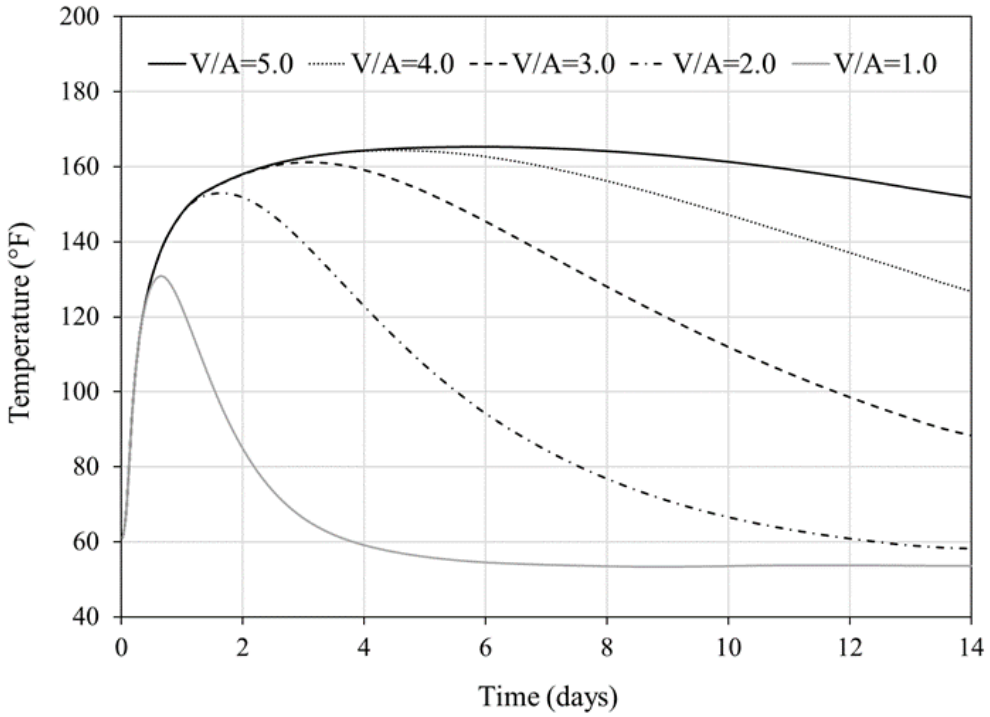

Figure 136 – Temperature-time history for different V/A – foundation (winter).

Overall, an increase in the V/A ratio for both summer and winter placement conditions yields increased maximum temperature and temperature differential. However, the maximum temperature and temperature differential predictions appear more sensitive to the V/A ratio when it is less than 3.0. For the V/A ratio exceeding 3.0, it is important to recognize that the time elapsed to reach the maximum temperature (Figure 134 and Figure 135) significantly increases. Furthermore, the structure is exposed to the elevated temperature for a longer period as the V/A increases beyond 3.0 (see Figure 136). In other words, although the maximum temperature slightly increases at V/A ratios exceeding 3.0, the exposure time significantly increases as the V/A ratio increases. The effect of long-term exposure of concrete to elevated temperatures can cause aggregate expansion and affect the thermal properties such as conductivity and specific heat, as well as the compressive strength of concrete. As it approaches the boiling temperature 212 °F (100

°C), the cement paste dehydrates and the paste-aggregate bond weakens. Therefore, it is anticipated that thermal expansion continues with the extended exposure to elevated temperature. Depending on the temperature range, thermal cracks develop and grow in width and/or spalling could occur as the V/A ratio increases beyond 3.0. Therefore, the effect of V/A ratio must be reviewed in conjunction with the heat of hydration of concrete mixtures, which is presented in the following sections.

5.1.2 **Sensitivity of Mixture Designs**

The effect of 45% cement replacement containing 30% slag and 15% MK (SL30+MK15 mixture) on the maximum temperature and temperature differential is investigated in this section. The results are compared with two reference mixtures: the Control mixture and a mixture containing 45% cement replacement with fly ash (FA45). Figure 137 through Figure 140 present the effect of each mixture design for both placement conditions on the maximum temperature and temperature differential predictions.

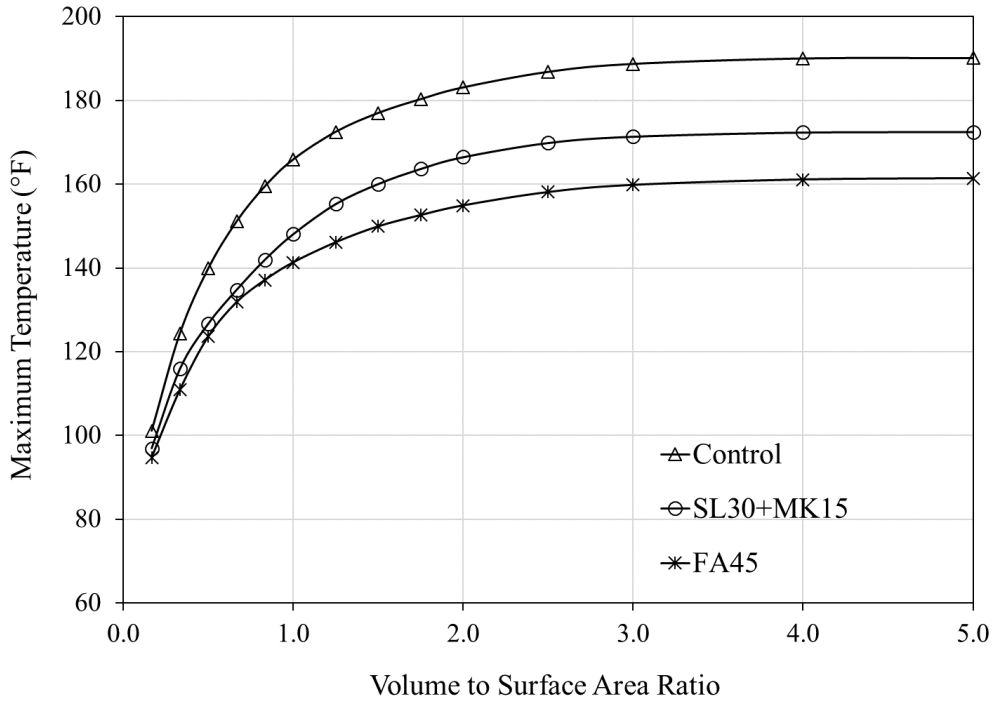

Figure 137 – Effect of 45% replacement mixtures on maximum temperature – foundation (summer).

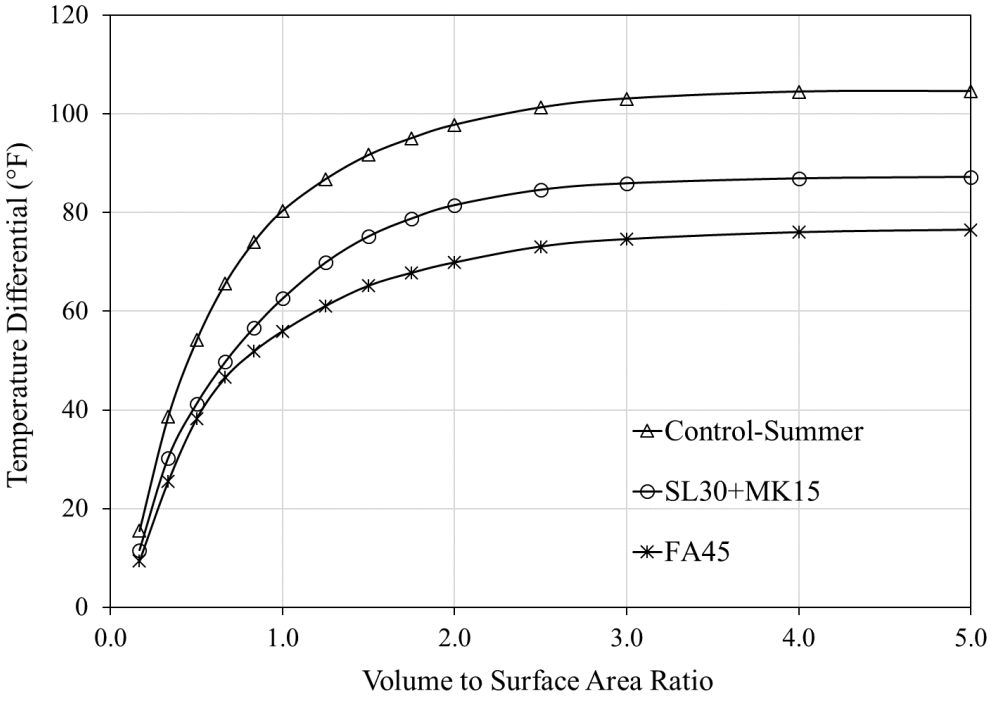

Figure 138 – Effect of 45% replacement mixtures on temperature differential – foundation (summer).

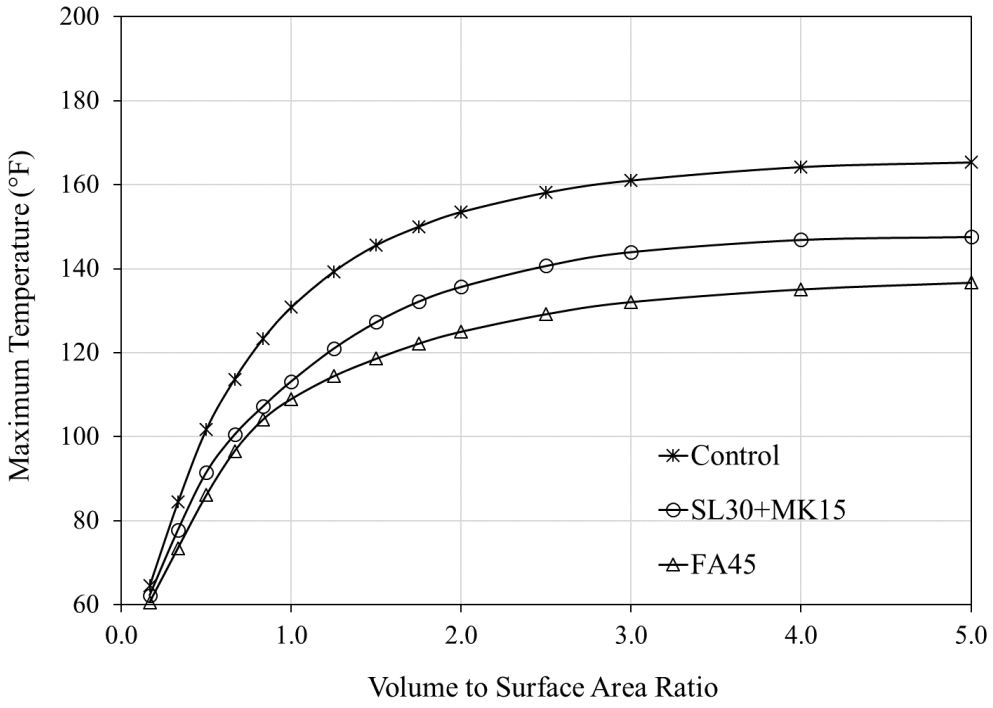

Figure 139 – Effect of 45% replacement mixtures on maximum temperature – foundation (winter).

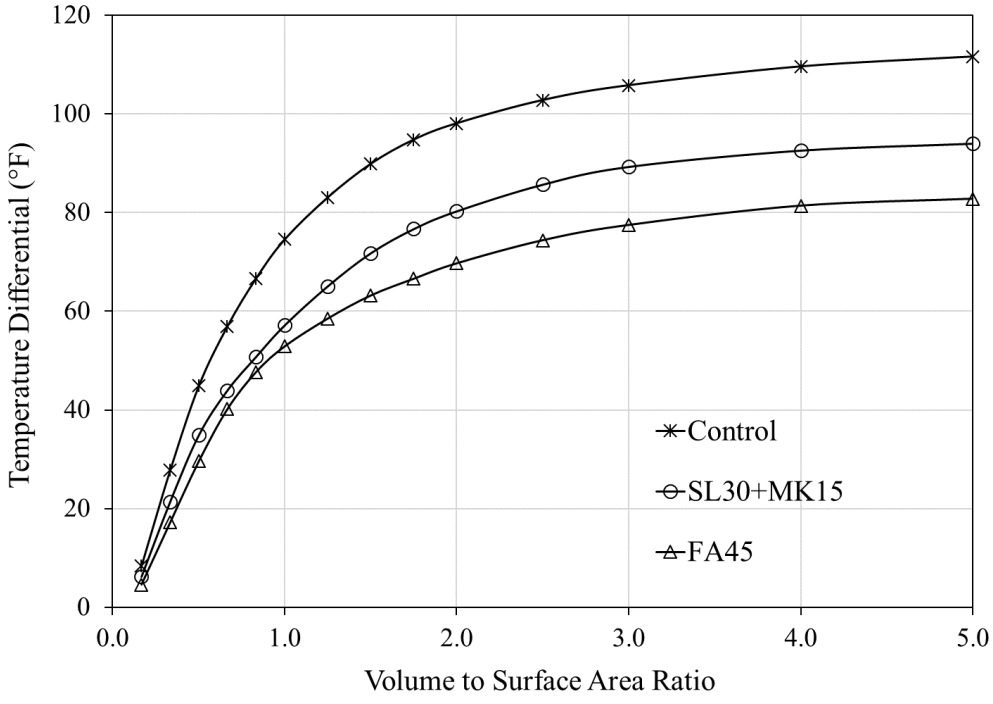

Figure 140 – Effect of 45% replacement mixtures on temperature differential – foundation (winter).

The use of a ternary (SL30+MK15) mixture significantly reduces the maximum temperature and temperature differential predictions. This reduction is, however, not as significant as it is for the FA45 mixture, particularly when the V/A ratio is greater than 1.0.

5.1.3 **Total Strain versus V/A ratio**

A sensitivity analysis is conducted to study the effect of V/A ratios on total strains which include the effect of crack widening. Figure 141 below presents the predicted strains in the foundation model for three different mixture designs (Control, SL30+MK15, and FA45). The strain predictions from the sensitivity analysis follow the same trend as the temperature prediction results; the increase in V/A ratio results in a linear increase in the maximum strain. However, the tensile strain continues to increase as the V/A ratio increases beyond 3.0 due to the extended exposure to elevated temperature although the temperature plateaus for V/A ratios exceeding 3.0 (see Section 5.1.1).

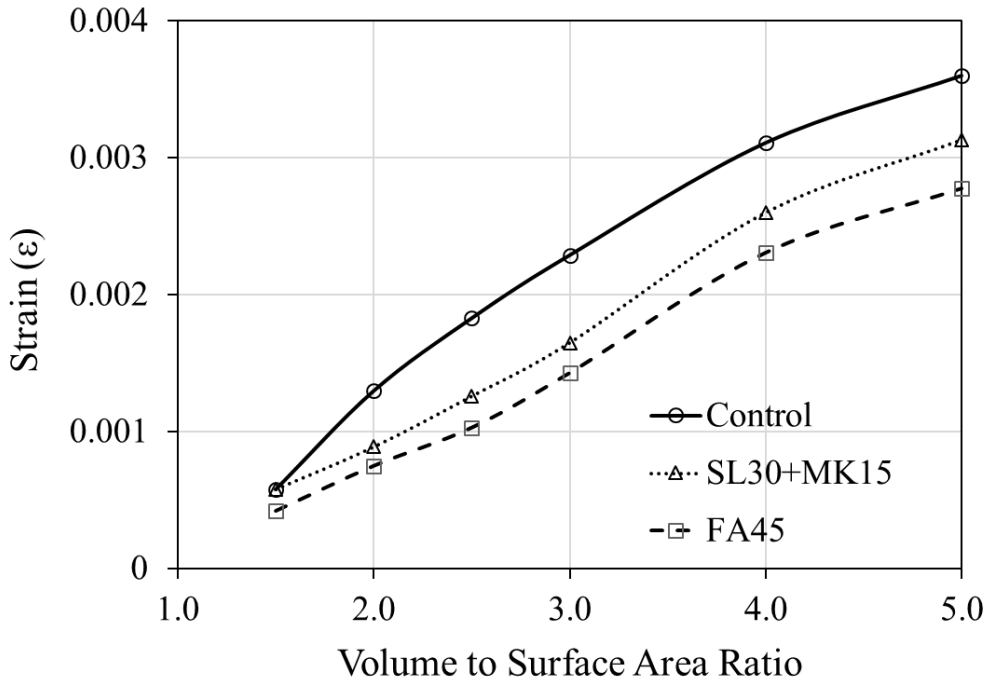

Figure 141 – Total Tensile Strain vs. V/A ratio.

5.1.4 **Sensitivity of Slag Replacement Level**

To investigate the effect of increased slag replacement levels on the maximum temperature and temperature differential, two ternary mixtures are considered: 1) SL30+MK15 and 2) SL55+MK15. Similar to the previous section, these mixtures are studied for both summer and winter placement conditions. Figure 142 through Figure 145 present the influence of increased slag replacement levels (SL30+MK15 and SL55+MK15).

The results indicate that a significant reduction in the maximum temperature and temperature differential occurs when the slag replacement level is increased from 30% to 55% in combination with 15% MK in a ternary replacement mixture. The maximum temperature is well under 158 °F (70 °C) for all V/A ratios when the SL55+MK15 mixture is used. In addition, the maximum temperature differential for this mixture is 10% lower than those of the FA45 mixture.

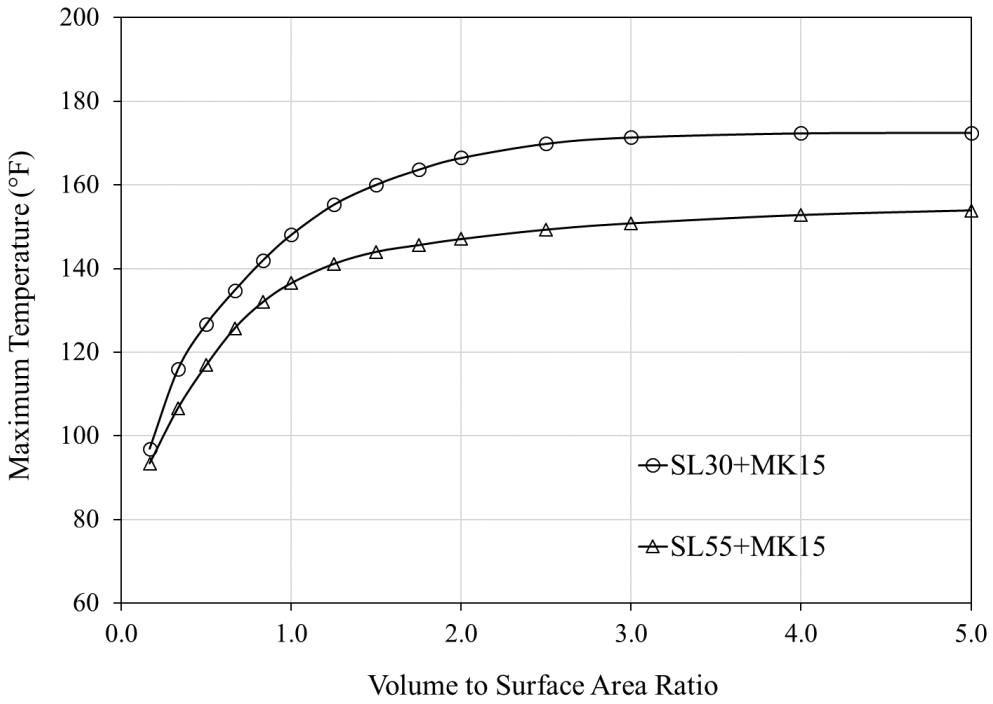

Figure 142 – Effect of increased slag content on maximum temperature in ternary mixtures – foundation (summer).

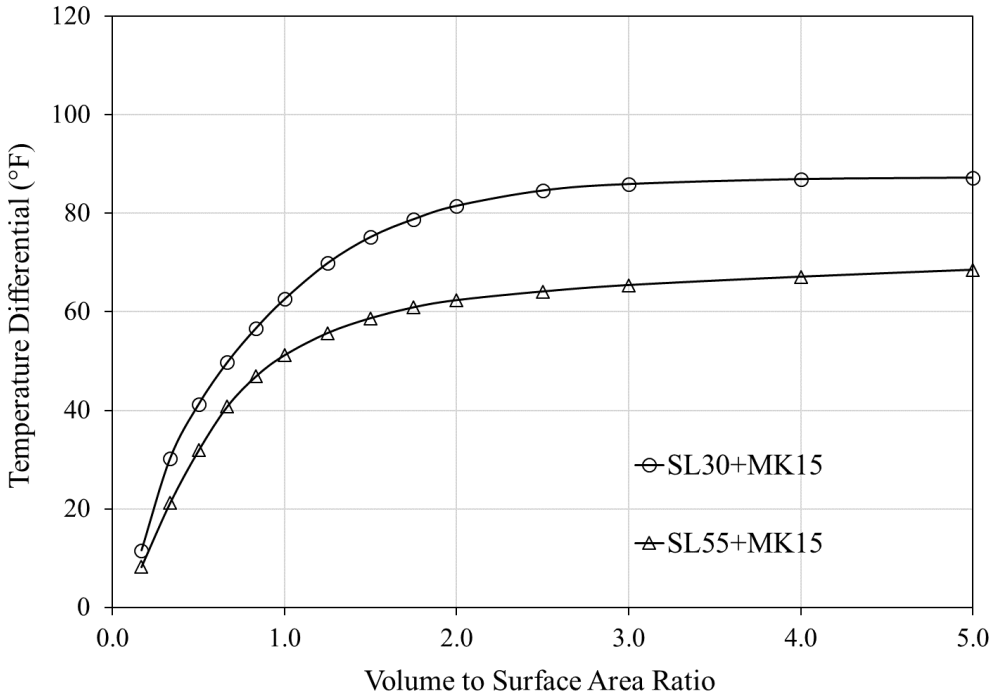

Figure 143 – Effect of increased slag content on temperature differential in ternary mixtures – foundation (summer).

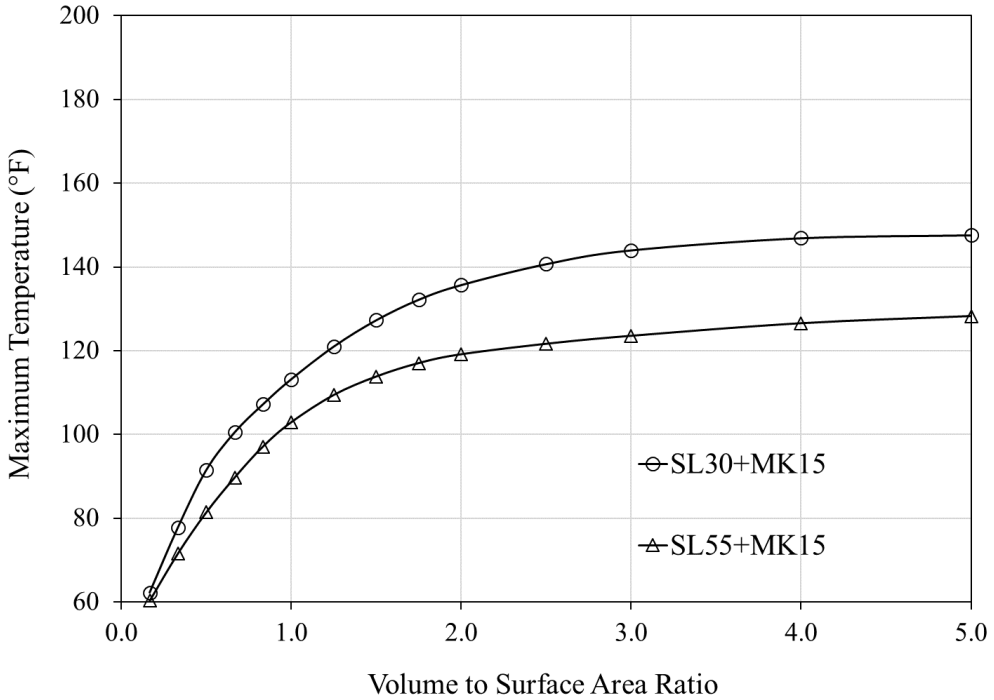

Figure 144 – Effect of increased slag content on maximum temperature in ternary mixtures –foundation (winter).

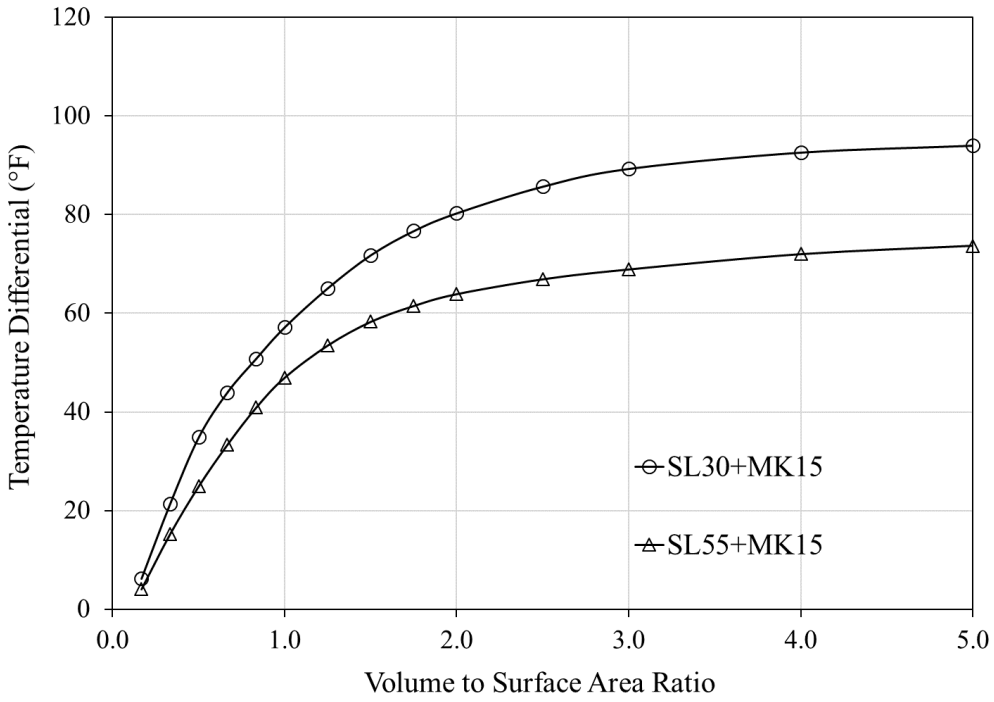

Figure 145 – Effect of increased slag content on temperature differential in ternary mixtures – foundation (winter).

5.1.5 Sensitivity of Ternary Mixtures at 70% Replacement Level

In addition to the SL55+MK15 mixture, a combination of fly ash and slag is considered in a ternary mixture. The reduction in temperature observed in the SL55+MK15 mixture at the 70% replacement level is compared with a mixture containing 40% slag and 30% fly ash (SL40+FA30) replacements. Figure 146 through Figure 149 present the maximum temperature and temperature differential predictions in the foundation model for the SL55+MK15 and SL40+FA30 mixtures. Overall, the maximum temperature and temperature differential predictions agree well, although the SL40+FA30 mixture yields slightly lower predictions.

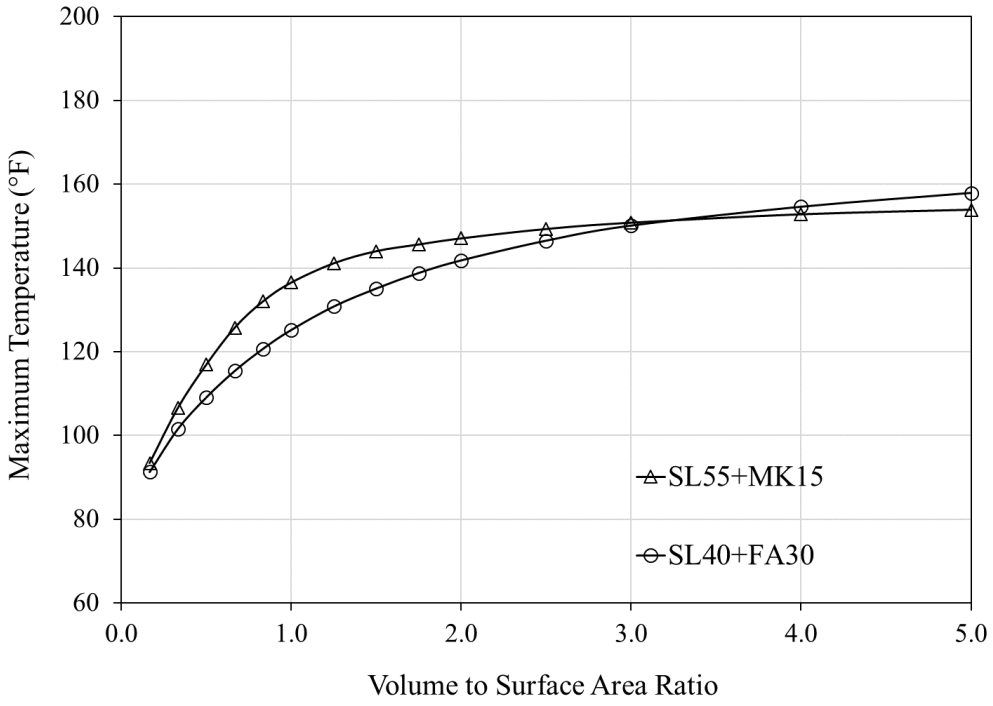

Figure 146 – Effect of ternary mixtures with 70% replacement level on maximum temperature – foundation (summer).

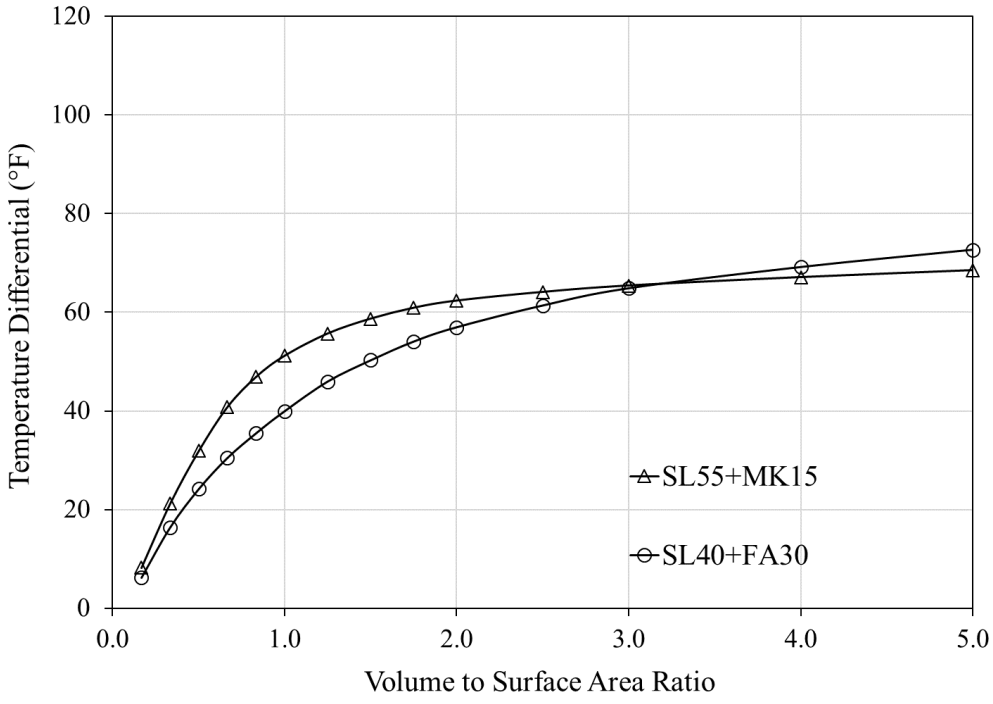

Figure 147 – Effect of ternary mixtures with 70% replacement level on temperature differential – foundation (summer).

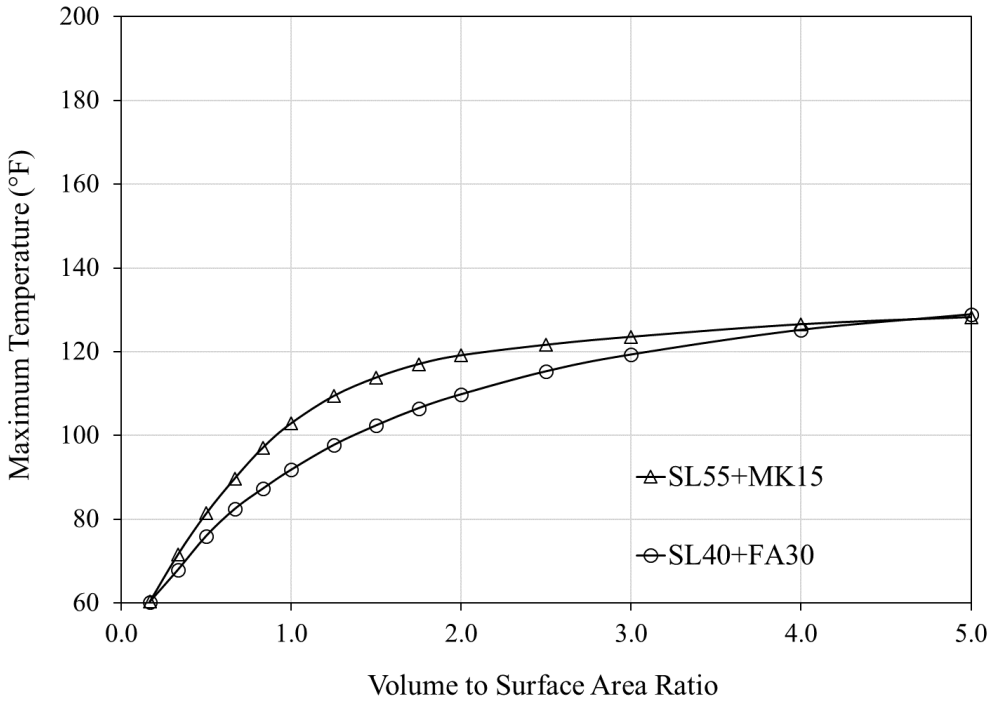

Figure 148 – Effect of ternary mixtures with 70% replacement on maximum temperature – foundation (winter).

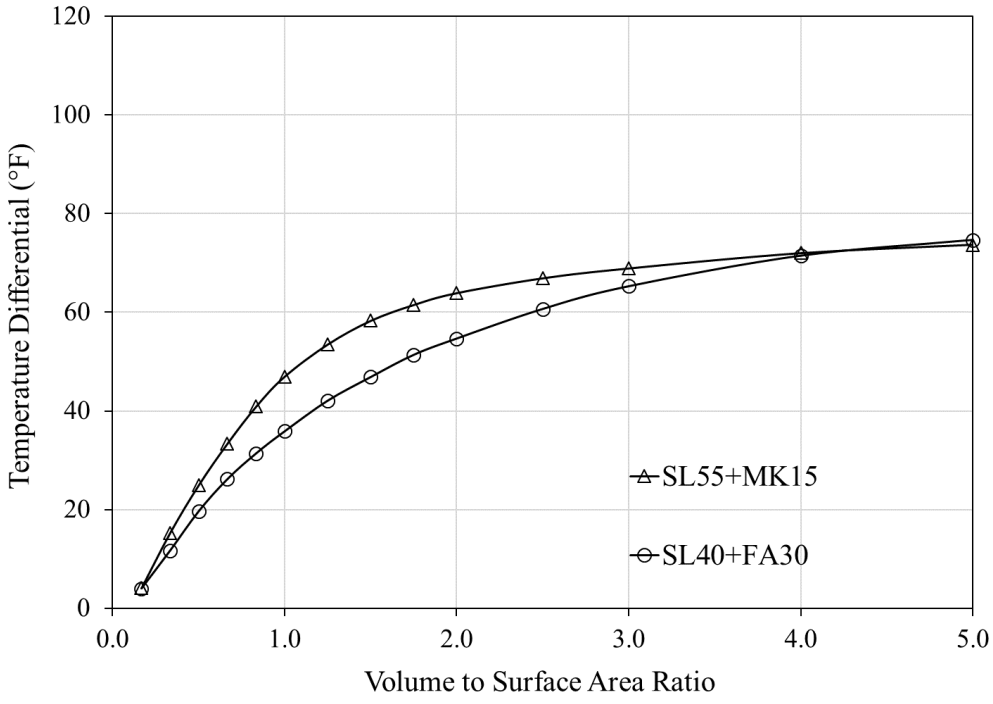

Figure 149 – Effect of ternary mixtures with 70% replacement on temperature differential – foundation (winter).

5.1.6 **Sensitivity of Water-to-Cementitious Material Ratios**

The effects of three water-to-cementitious material (w/c) ratios, 0.36, 0.43, and 0.48, on the maximum temperature and temperature differential are investigated using the Control mixture with summer and winter placement conditions. The selected w/c ratios are based on the common range of w/c ratios used by state DOTs in mass concrete placements (see Section 3.1.2). Figure 150 through Figure 153 present the maximum temperature and temperature differential predictions for the foundation model with varying w/c ratios. As the figures below show, the increase in w/c ratio from 0.36 to 0.48 in the Control mixture results in an increase in both maximum temperature and temperature differential.

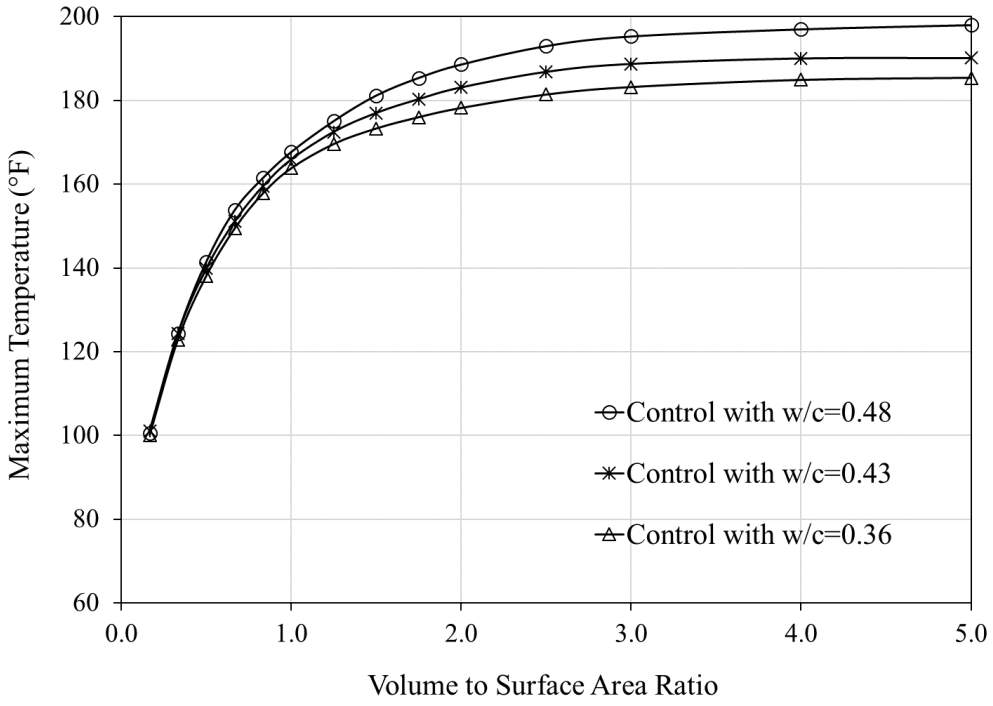

Figure 150 – Effect of w/c on maximum temperature – foundation (summer).

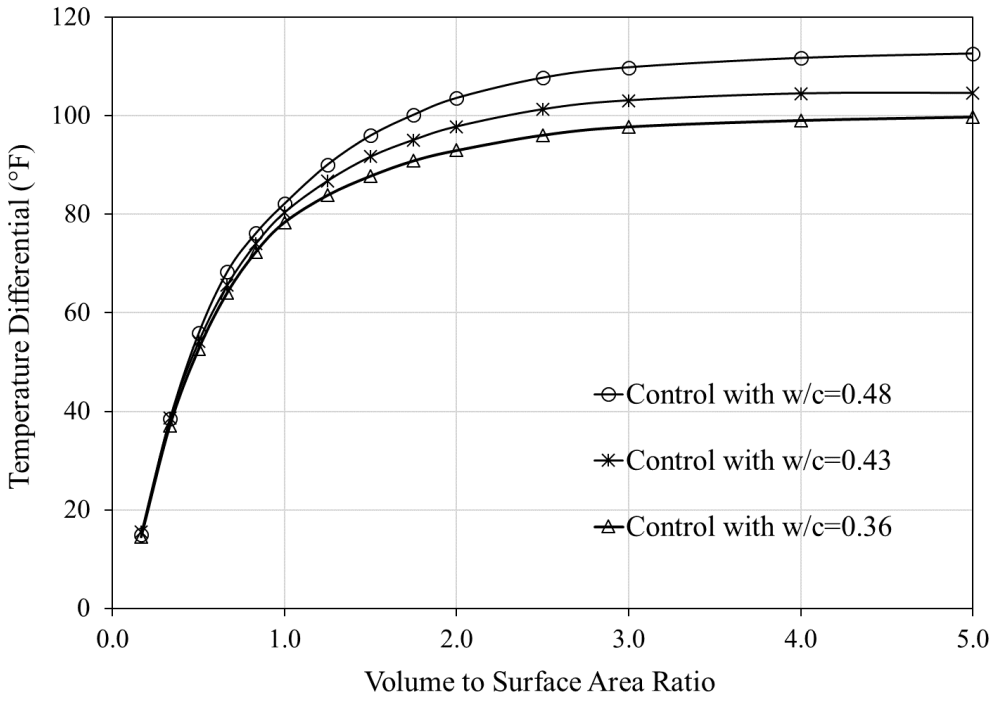

Figure 151 – Effect of w/c on temperature differential – foundation (summer).

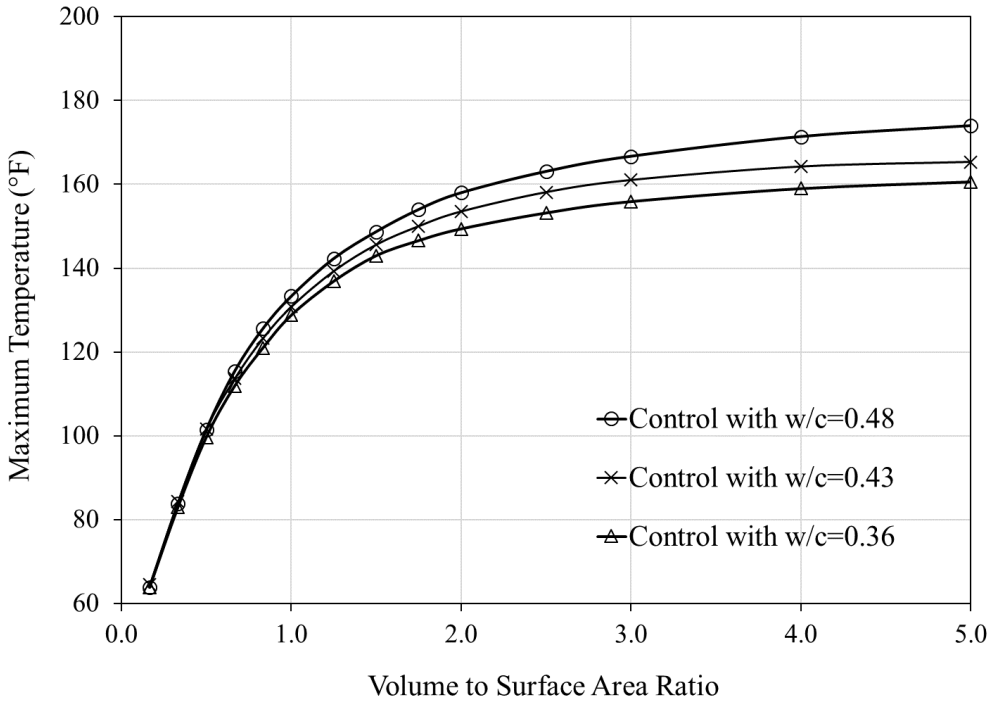

Figure 152 – Effect of w/c on maximum temperature – foundation (winter).

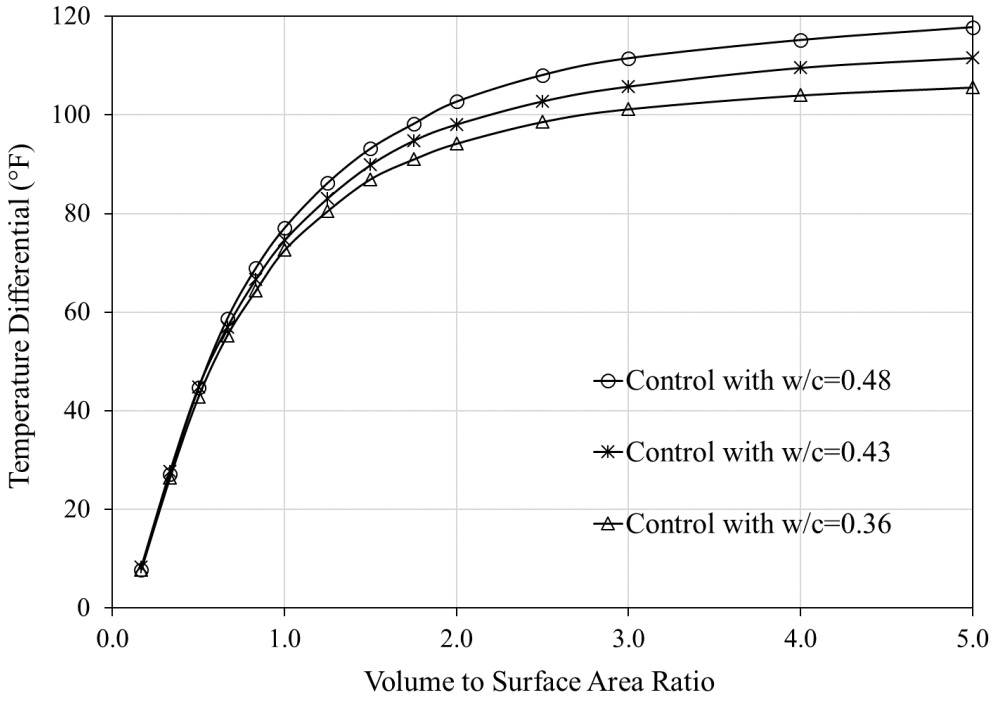

Figure 153 – Effect of w/c on temperature differential – foundation (winter).

5.1.7 Sensitivity of Insulation Material R-value

The effect of insulation materials (or R-values) on the maximum temperature and temperature differential is investigated. The foundation model is considered with 1) no insulation, 2) an insulation panel with an R-value of 1 $ft^2 \cdot °F \cdot h/BTU$ (0.18 $m^2 \cdot °C/W$), 3) and an insulation panel with an R-value of 3 $ft^2 \cdot °F \cdot h/BTU$ (0.52 $m^2 \cdot °C/W$). Both summer and winter placement conditions are considered with the Control mixture in order to show the effect, noting that it is not practical to use insulated cofferdam. Figure 154 through Figure 157 present the maximum temperature and temperature differential predictions corresponding to the criteria outlined above.

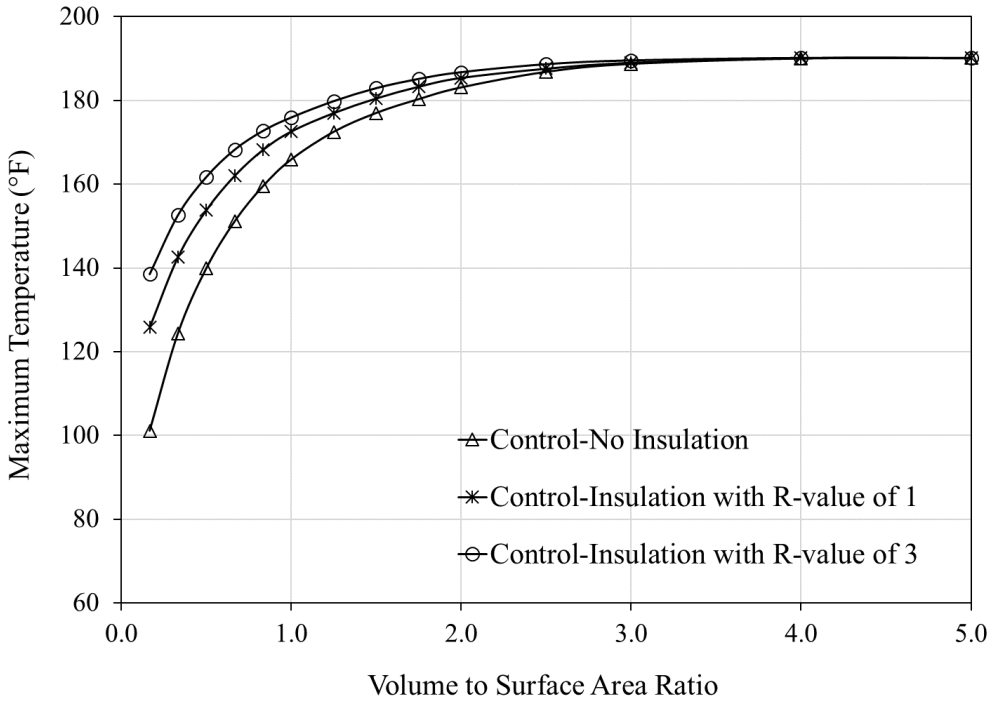

Figure 154 – Effect of insulation on maximum temperature – foundation (summer).

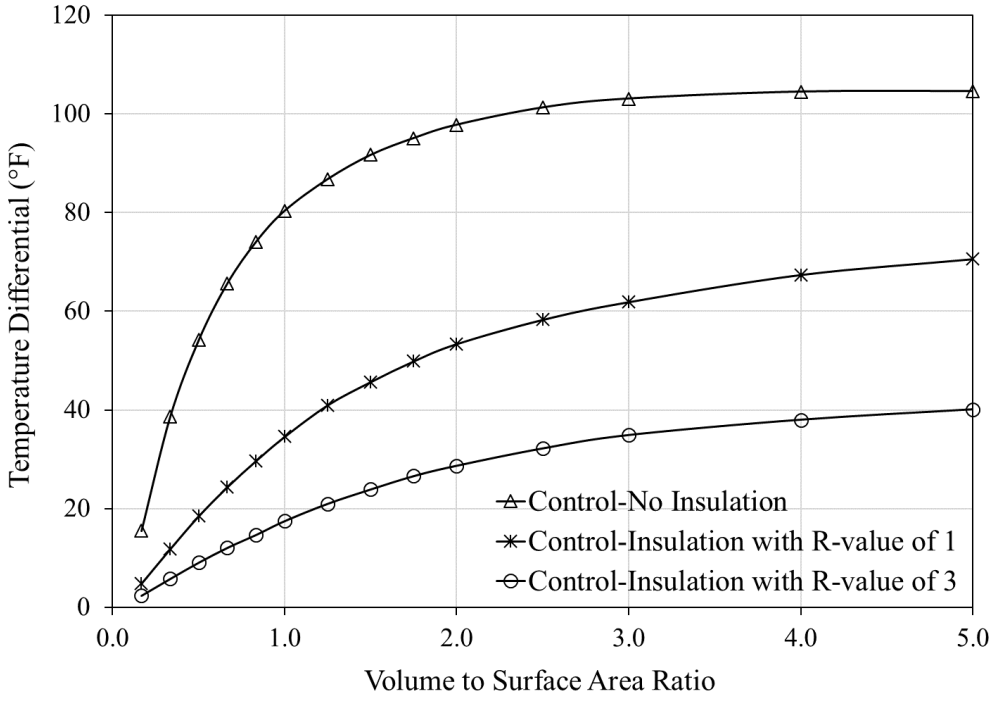

Figure 155 – Effect of insulation on temperature differential – foundation (summer).

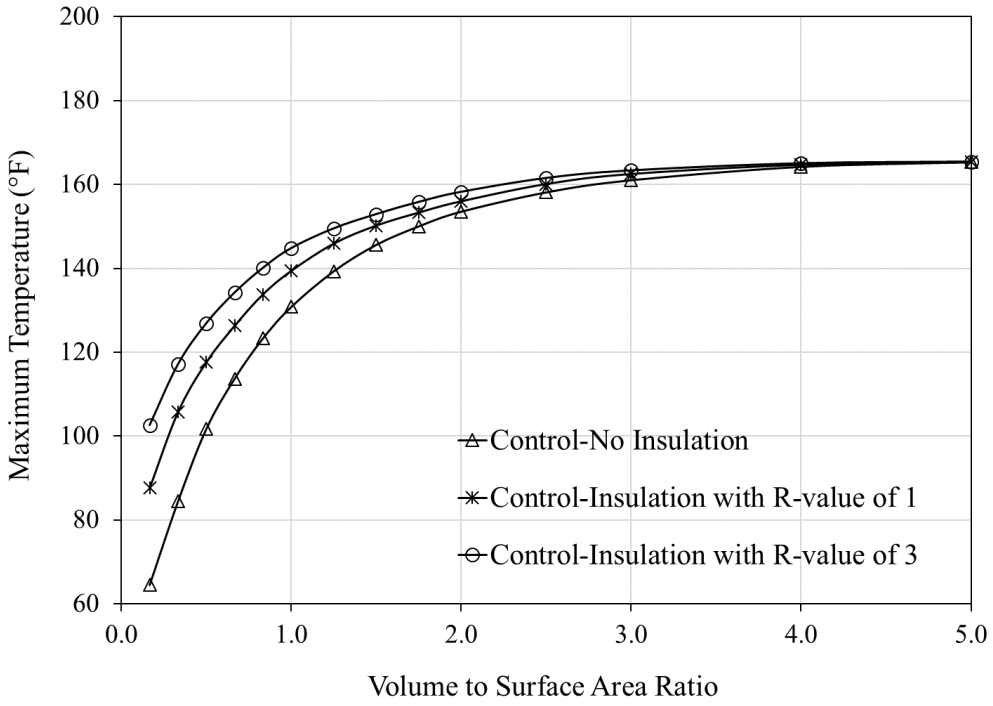

Figure 156 – Effect of insulation on maximum temperature – foundation (winter).

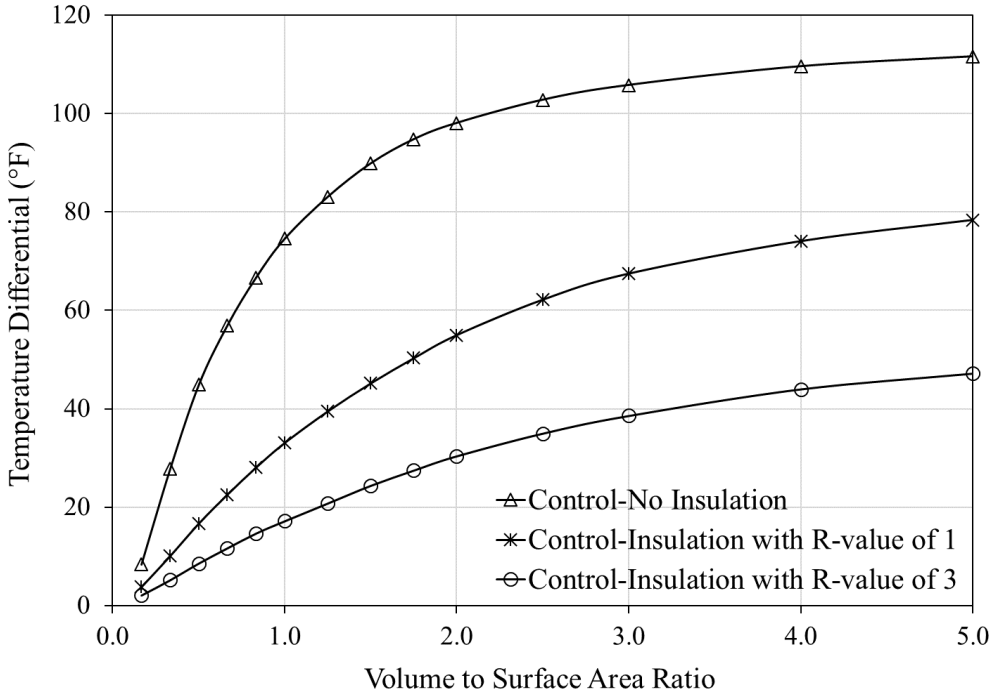

Figure 157 – Effect of insulation on temperature differential – foundation (winter).

The efficiency of insulation materials has a significant effect on the temperature differential. Using insulation material with an R-value of 1 significantly reduces temperature differential, and this effect is even more pronounced when the R-value is increased from 1 to 3. The maximum temperature, meanwhile, is not affected by the presence of insulating materials.

5.1.8 Summary of Sensitivity Analysis for Foundation

Prediction results for all parameters considered in the sensitivity analysis of the mass concrete foundation are summarized here. Specifically, prediction results at a V/A ratio of 3.0 are shown in Table 40 and Table 41 for the summer and winter placement conditions, respectively.

Table 40 – Summary of results for the foundation at V/A=3.0 (summer).

Parameters	Variables	W/C	Maximum Temperature, °F (°C)	Maximum Temperature Differential, °F (°C)
Mixture Design	Control	0.43	188.7 (87.1)	103.1 (57.3)
	SL30+MK15	0.43	171.4 (77.4)	85.9 (47.7)
	FA45	0.43	159.8 (71.0)	74.6 (41.4)
	SL55+MK15	0.43	150.8 (66.0)	65.4 (36.3)
	SL40+FA30	0.43	150.1(65.6)	64.9 (36.1)
W/C	Control	0.36	183.2 (84.0)	97.8 (54.3)
	Control	0.43	188.7 (87.1)	103.1 (57.3)
	Control	0.48	195.3 (90.7)	109.8 (61.0)
Insulation	Control-No Insulation	0.43	188.7 (87.1)	103.1 (57.3)
	Control-Insulation with R=1	0.43	189.0 (87.2)	61.9 (34.4)
	Control-Insulation with R=3	0.43	189.5 (87.5)	34.9 (19.4)

Table 41 – Summary of results for the foundation at V/A=3.0 (winter).

Parameters	Variables	W/C	Maximum Temperature, °F (°C)	Maximum Temperature Differential, °F (°C)
Mixture Design	Control	0.43	161.0 (71.7)	105.8 (58.8)
	SL30+MK15	0.43	144.0 (62.2)	89.3 (49.6)
	FA45	0.43	132.1 (55.6)	77.5 (43.1)
	SL55+MK15	0.43	123.5 (50.8)	68.9 (38.3)
	SL40+FA30	0.43	119.3 (48.5)	65.3 (36.3)
W/C	Control	0.36	155.9 (68.8)	101.2 (56.2)
	Control	0.43	161.0 (71.7)	105.8 (58.8)
	Control	0.48	166.7 (74.8)	111.5 (61.9)
Insulation	Control-No Insulation	0.43	161.0 (71.7)	105.8 (58.8)
	Control-Insulation with R=1	0.43	162.5 (72.5)	67.5 (37.5)
	Control-Insulation with R=3	0.43	163.3 (72.9)	38.6 (21.4)

GDOT's Special Provision for mass concrete limits the maximum temperature in a mass concrete placement to 158 °F (70 °C) and the temperature differential to 35 °F (19.4 °C). The results presented in Table 40 and Table 41 are evaluated based on these limits. Any placement temperature exceeding a GDOT threshold is highlighted in gray. These results indicate the benefit of using ternary replacement mixtures at a higher replacement level as the maximum temperature is significantly lower for the SL55+MK15 and SL40+FA30 mixtures. However, the placement condition significantly affects the maximum temperature. For the winter placement condition, almost all mixtures meet the maximum temperature requirement. The temperature differential, however, exceeds the 35 °F (19.4 °C) limit in all mixtures except the Control mixture with an insulation panel with an R-value of 3 $ft^2 \cdot °F \cdot h/BTU$ (0.52 $m^2 \cdot °C/W$) in the summer placement condition.

Therefore, insulation material with high R-values must be provided for mass concrete placements to meet the temperature differential limit.

In conclusion, the use of ternary replacement mixtures is promising in controlling the maximum temperature in mass concrete placements. Further, when it is possible to use insulated formwork with an adequate R-value, the temperature differential can be maintained under the specified limit of 35 °F.

5.2 Column Model

5.2.1 Sensitivity of Volume-to-Surface Area Ratios

Figure 158 presents the volume and surface area of the 15 column models corresponding to their V/A ratios used in the sensitivity analysis. Figure 159 and Figure 160 present the maximum temperature and temperature differential for a column with varying V/A ratios when the Control mixture is used. Figure 161 and Figure 162 present the effect of V/A on the elapsed time to reach maximum temperature in the column model during summer and winter conditions, respectively. Figure 163 shows the temperature-time history over two weeks with the winter placement condition.

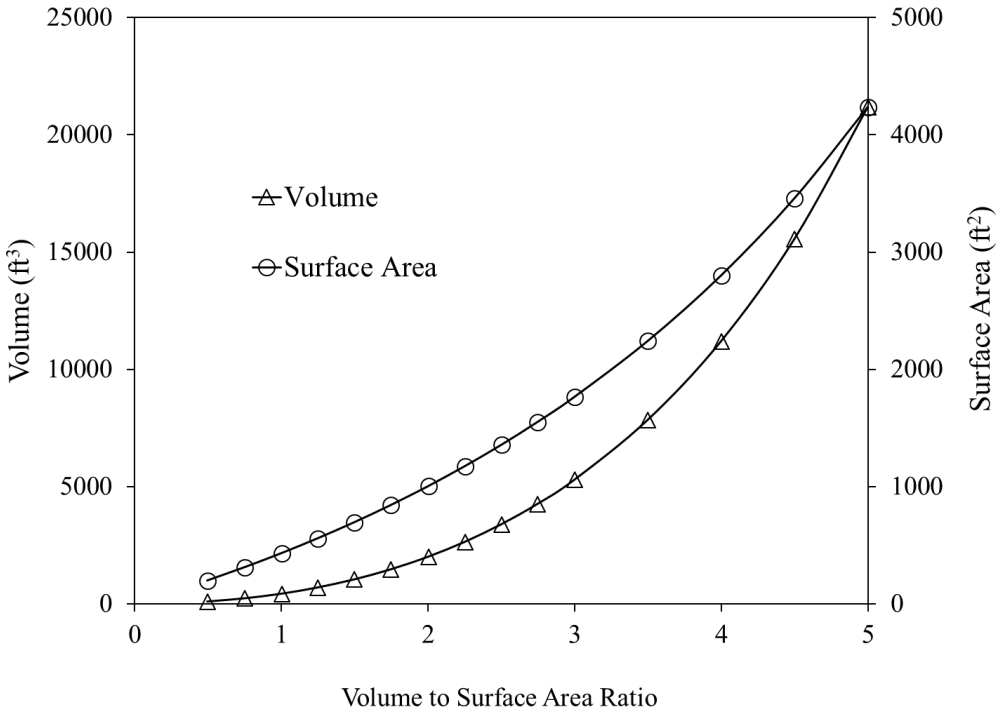

Figure 158 – Volume and surface area corresponding to V/A ratio – column.

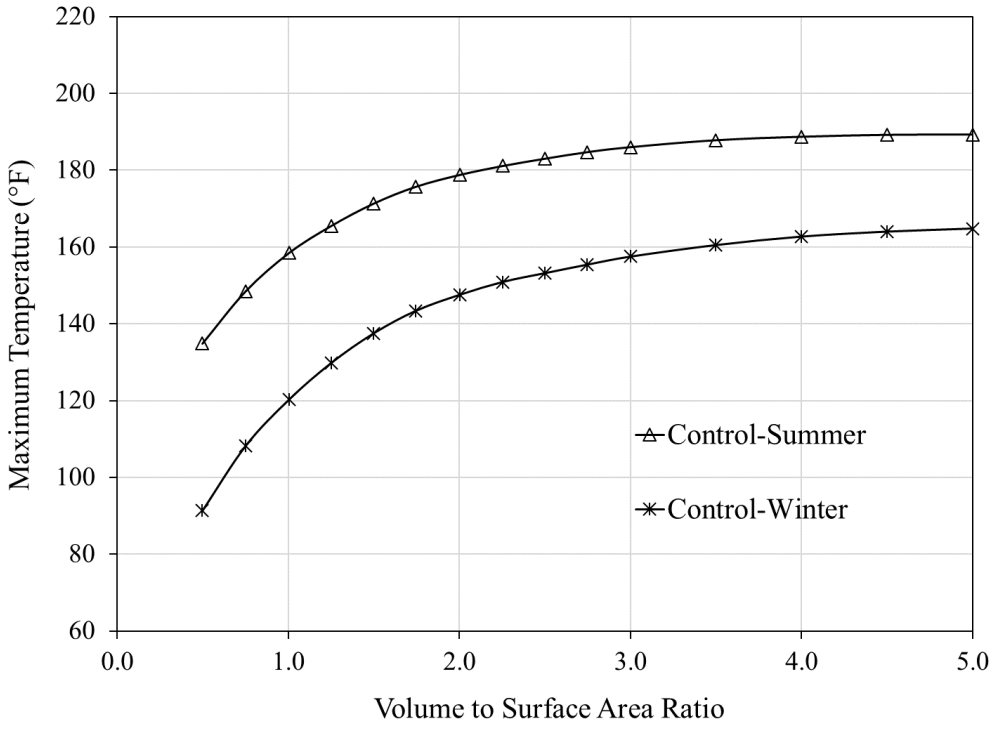

Figure 159 – Effect of V/A ratio on maximum temperature – column.

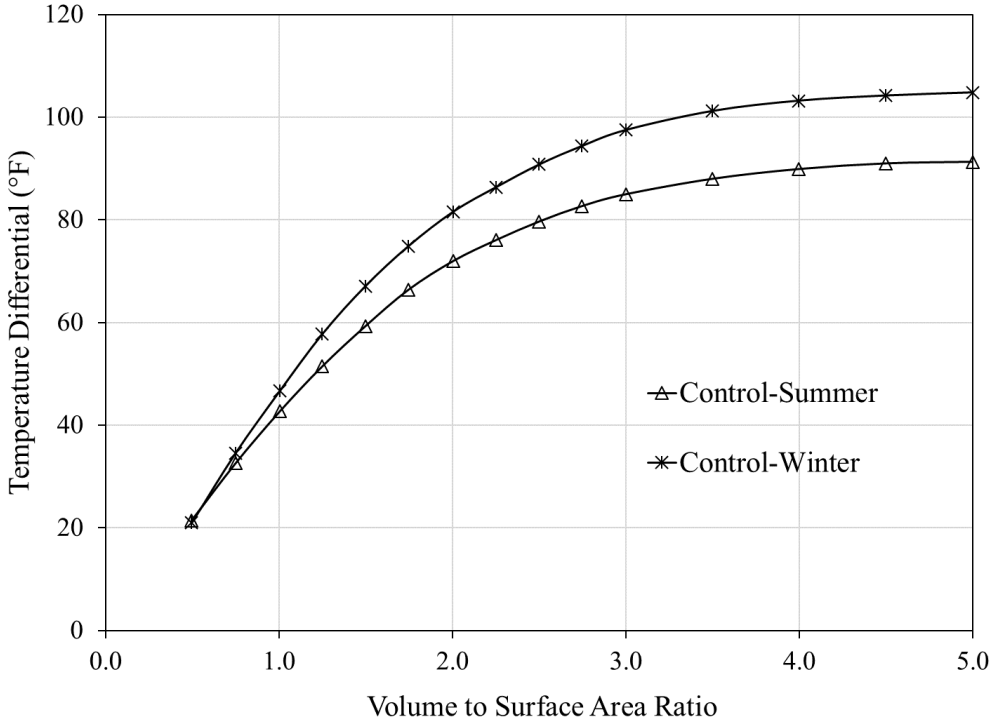

Figure 160 – Effect of V/A ratio on temperature differential – column.

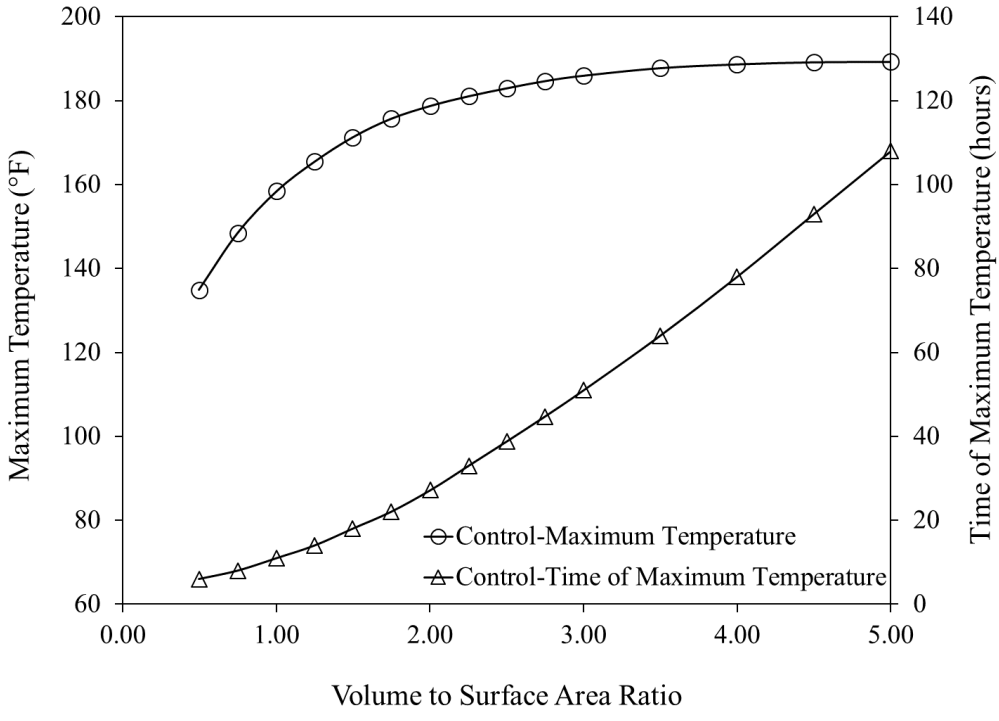

Figure 161 – Effect of V/A on time of maximum temperature – column (summer).

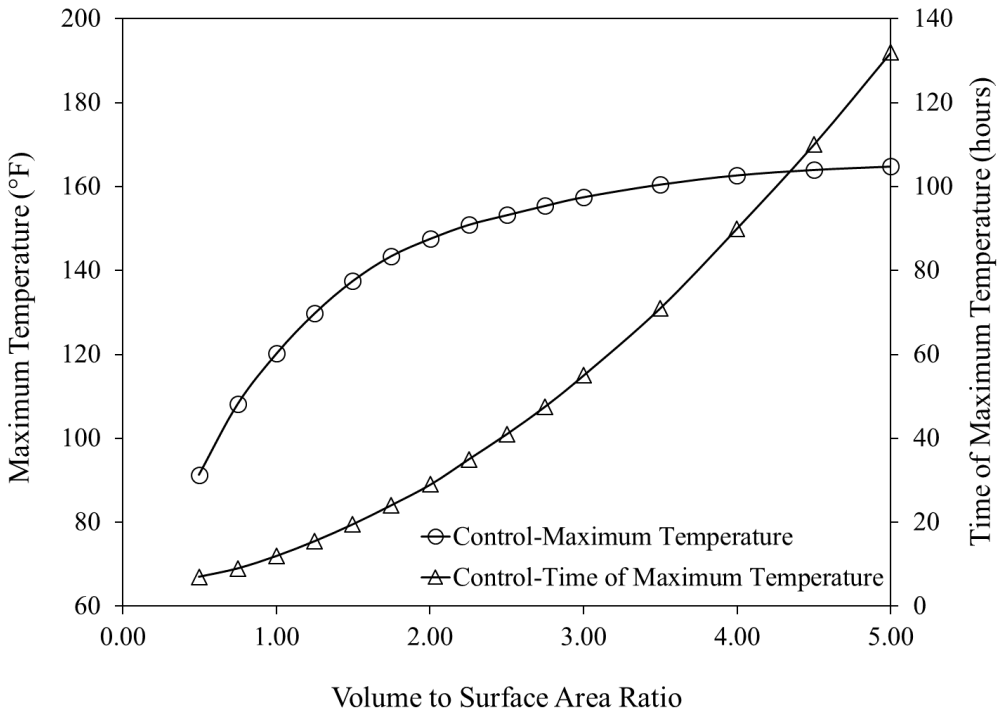

Figure 162 – Effect of V/A on time of maximum temperature – column (winter).

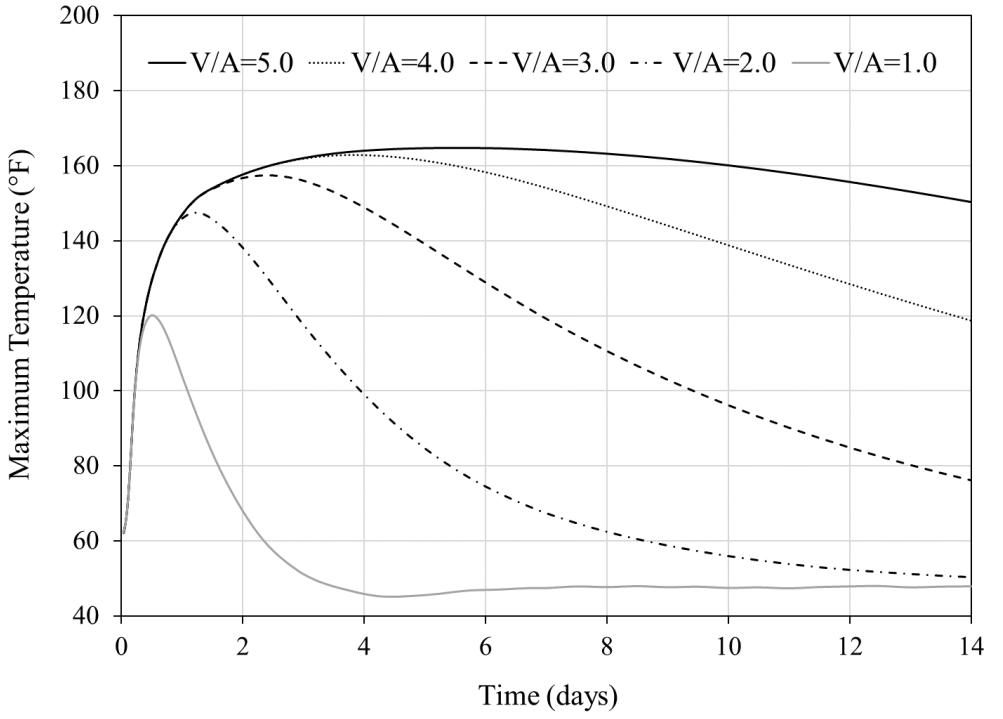

Figure 163 – Temperature-time history for different V/A – column (winter).

As the V/A ratio increases, both the maximum temperature and temperature differential increase for both summer and winter placement conditions. As anticipated, the maximum temperature is significantly higher in summer, while the temperature differential is higher in winter due to much colder ambient temperatures surrounding the column. The summary charts (see Figure 159 and Figure 160) only show the maximum temperature and maximum temperature differential and thus are not adequate to evaluate the effect of the V/A ratio on the extent of cracking, as concluded with the foundation model. The maximum temperature and temperature differential predictions in the column model may appear more sensitive to the V/A ratio when it is less than 3.0. However, it is important to understand that the increase in the V/A ratio results in a significant increase in the elapsed time to reach the maximum temperature (Figure 161 and Figure 162), and the exposure time to elevated temperature increases as the V/A ratio increases (see Figure 163).

5.2.2 **Sensitivity of Mixture Designs**

Figure 164 through Figure 167 present the effect of each mixture design on the maximum temperature and temperature differential predictions. Consistent with the findings from the foundation model (see Section 5.1.2), the use of a ternary (SL30+MK15) mixture shows a significant reduction in the maximum temperature and temperature differential predictions. The reduction, however, is not as significant as in the FA45 mixture.

5.2.3 **Sensitivity of Slag Replacement Level**

Two ternary mixtures are investigated: 1) SL30+MK15 and 2) SL55+MK15. Figure 168 through Figure 171 present the influence of increased slag replacement levels on the maximum temperature and temperature differential. The temperature prediction results indicate that significant reductions in the maximum temperature and temperature

differential occurs when the slag replacement level increases from 30% to 55% in a ternary mixture. When the SL55+MK15 mixture is used, the maximum temperature is well under 158 °F (70 °C) for all V/A ratios. Overall, the results from the column model are consistent with the results of the foundation model.

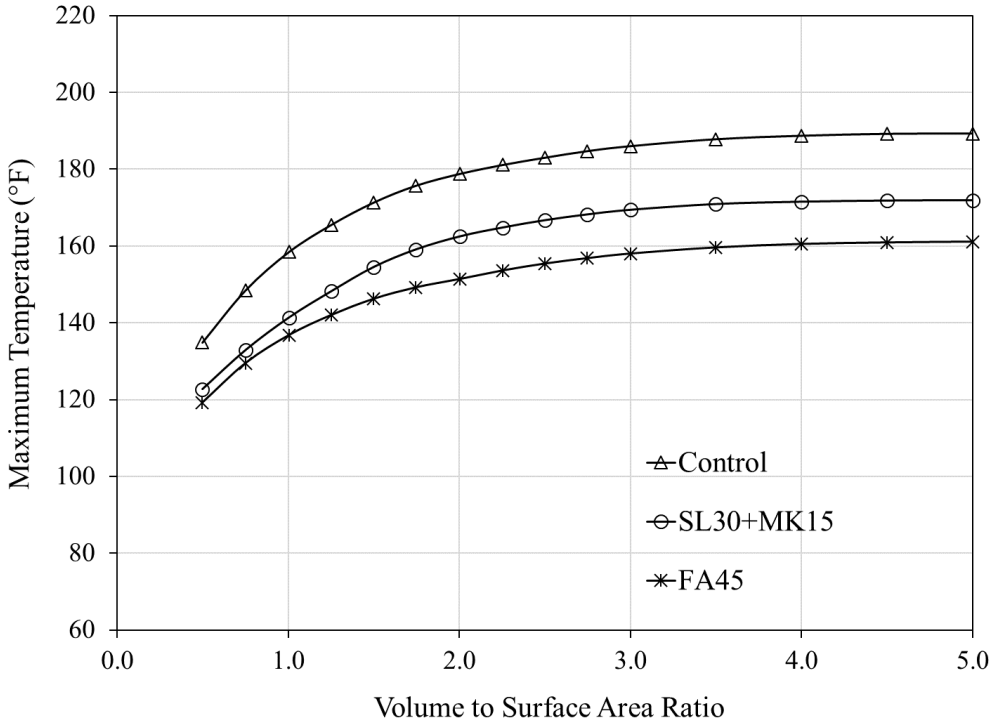

Figure 164 – Effect of 45% replacement mixtures on maximum temperature – column (summer).

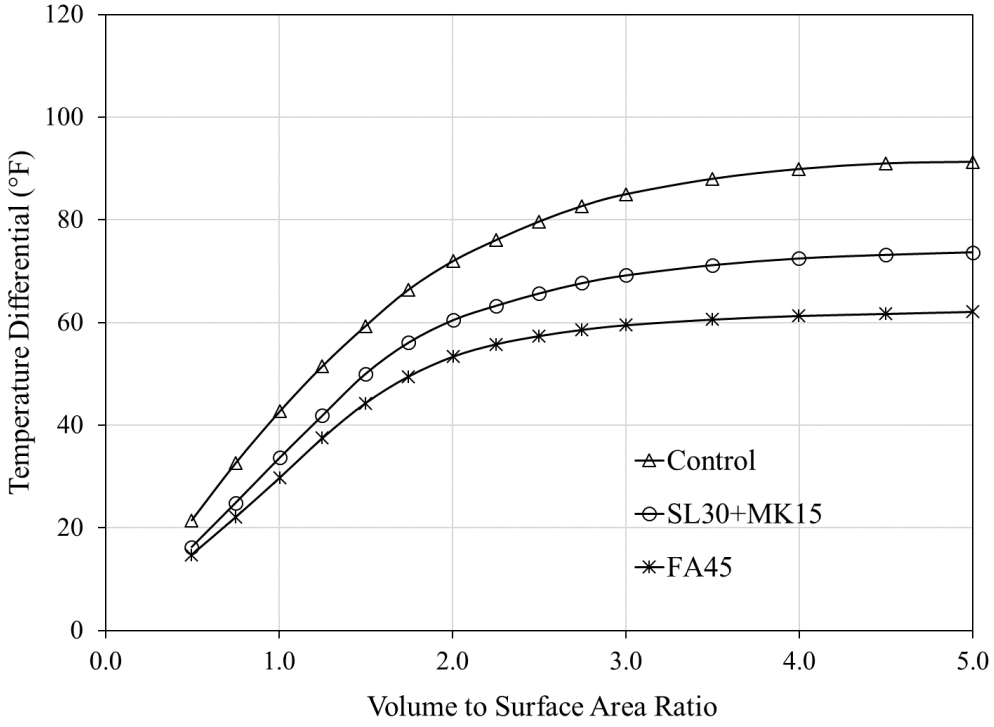

Figure 165 – Effect of 45% replacement mixtures on temperature differential – column (summer).

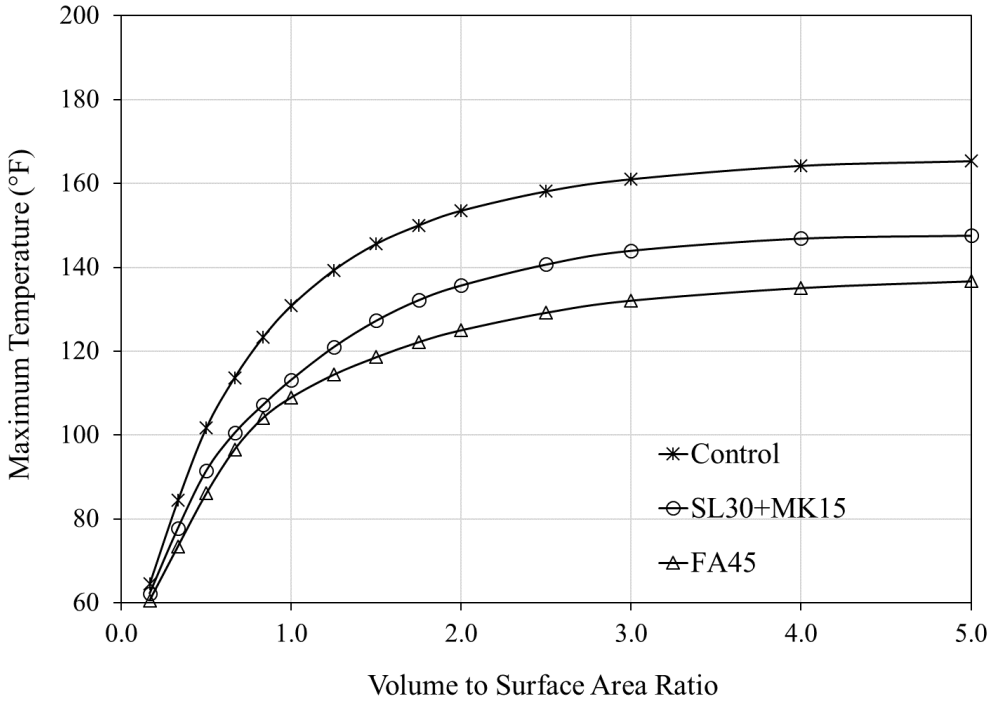

Figure 166 – Effect of 45% replacement mixtures on maximum temperature – column (winter).

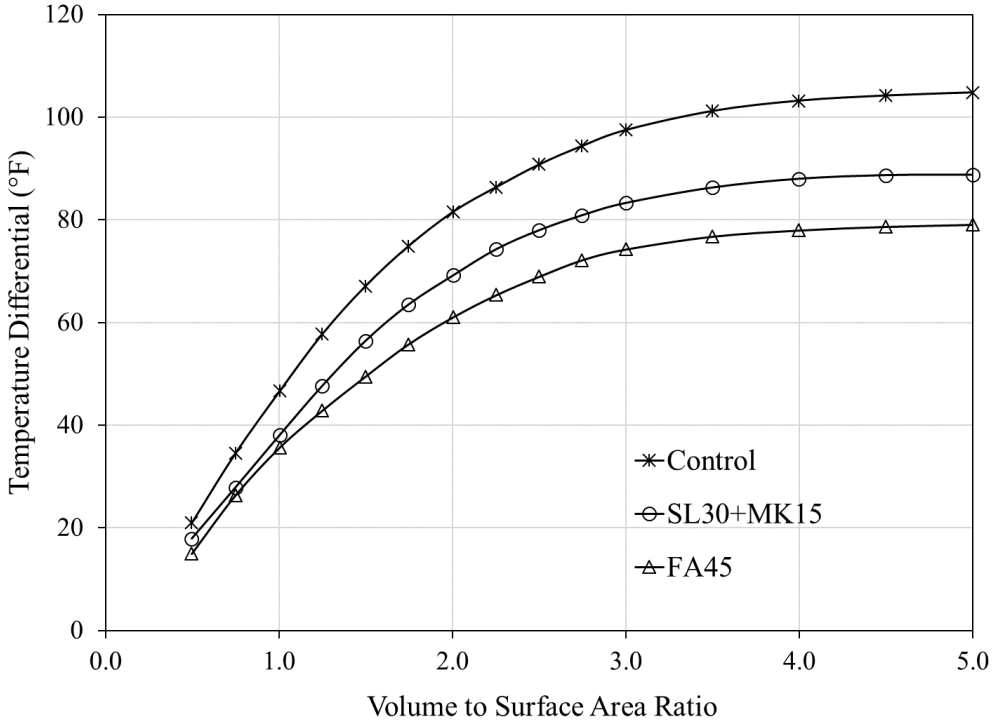

Figure 167 – Effect of 45% replacement mixtures on temperature differential – column (winter).

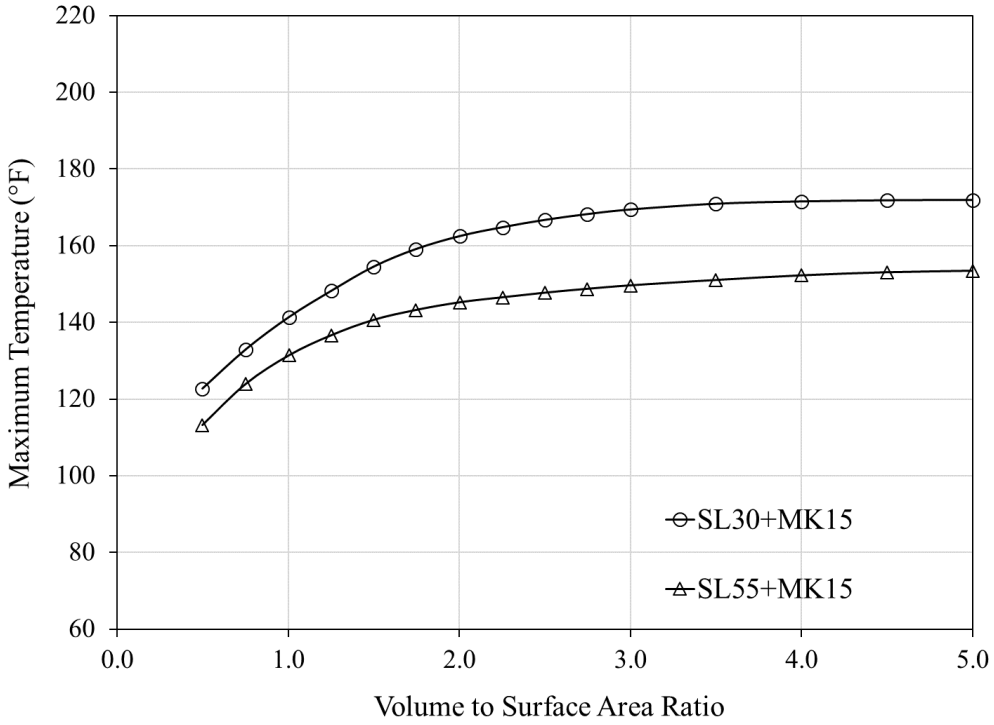

Figure 168 – Effect of increased slag content on maximum temperature – column (summer).

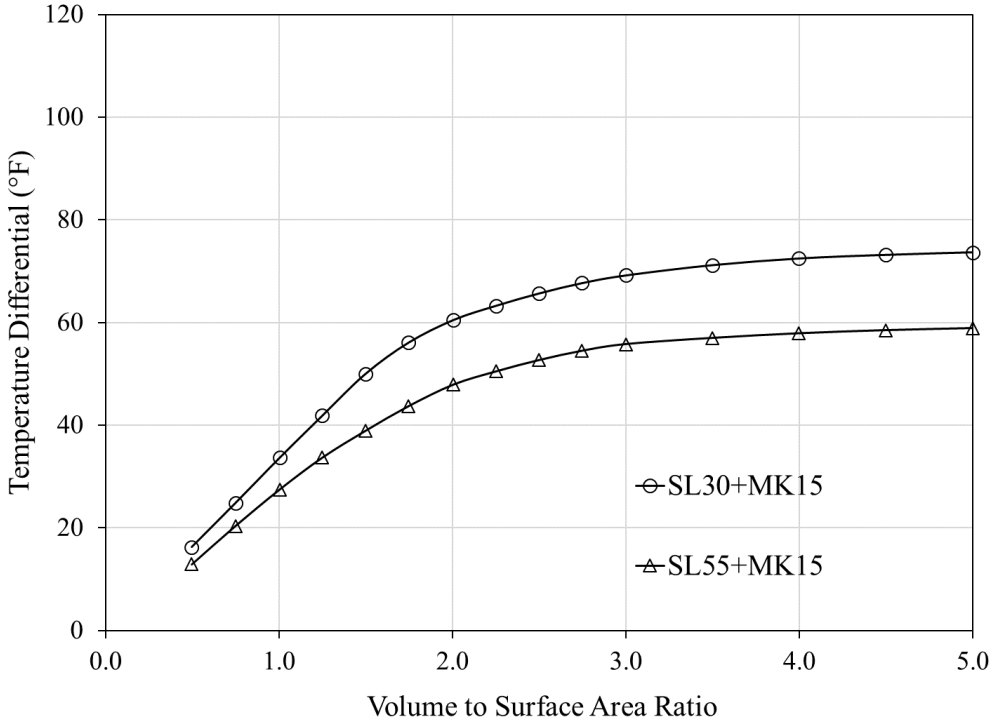

Figure 169 – Effect of increased slag content on temperature differential – column (summer).

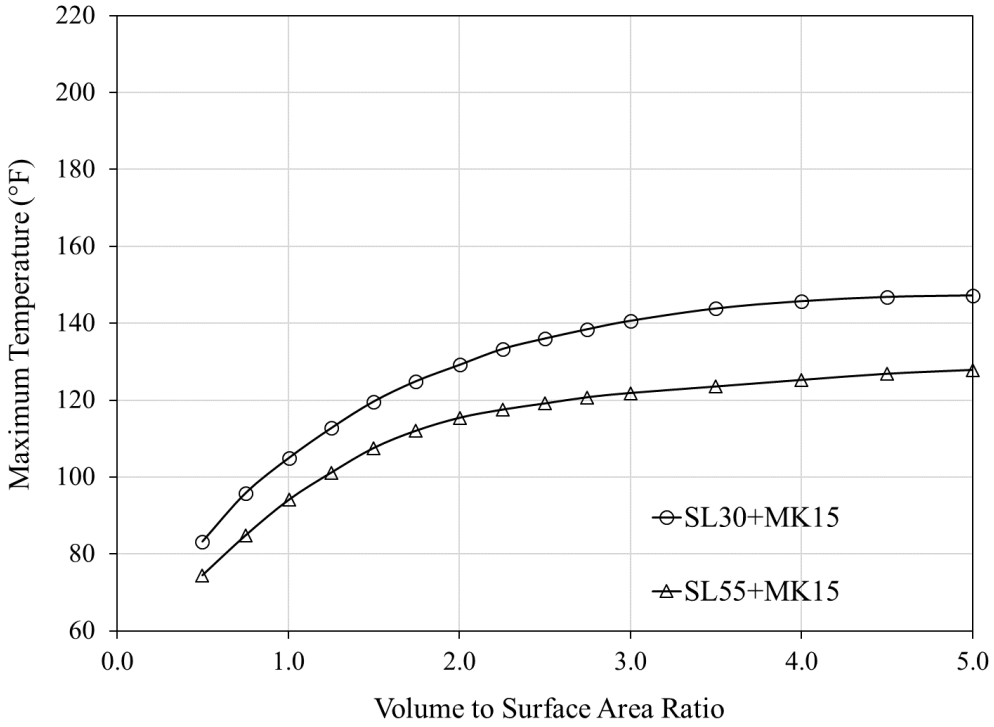

Figure 170 – Effect of increased slag content on maximum temperature in ternary mixtures – column (winter).

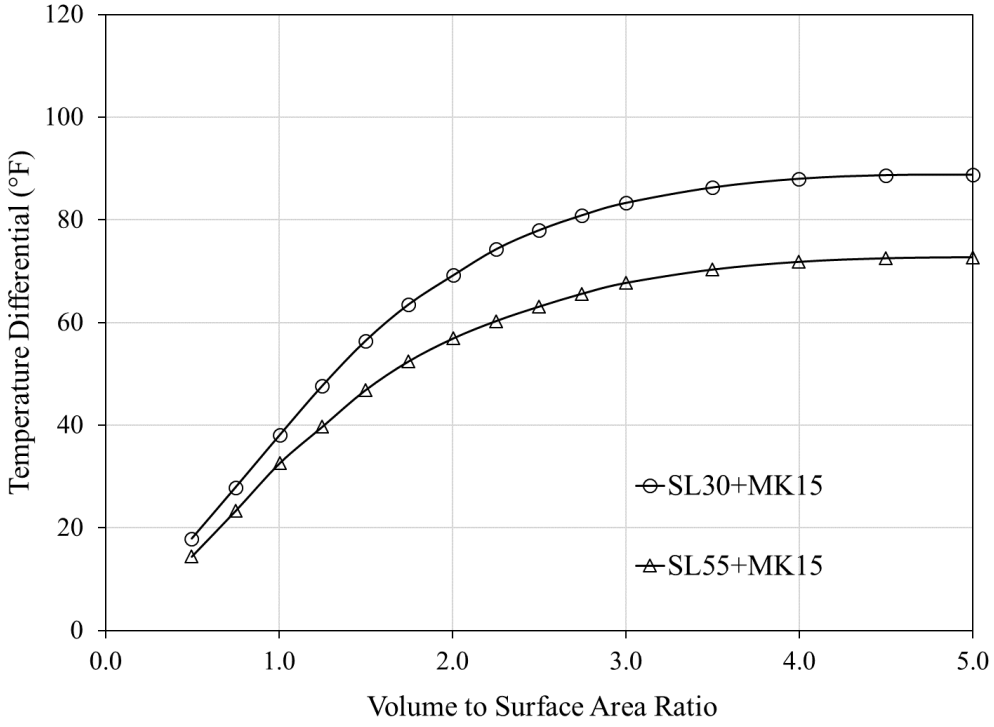

Figure 171 – Effect of increased slag content on temperature differential in ternary mixtures – column (winter).

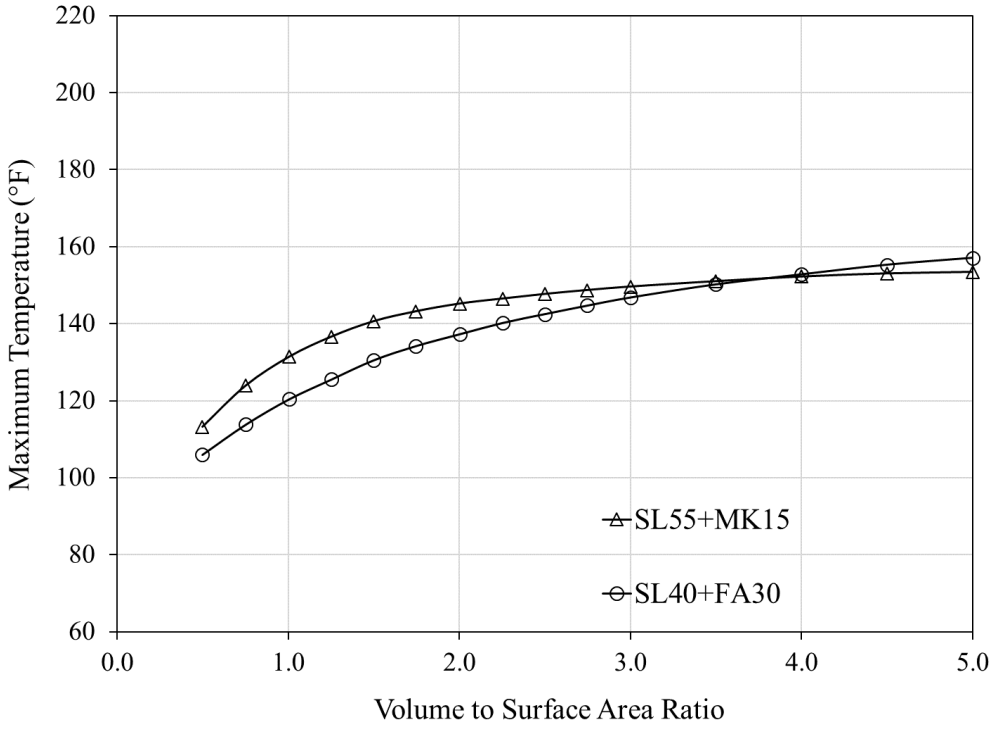

Figure 172 – Effect of ternary mixtures at 70% replacement level on maximum temperature – column (summer).

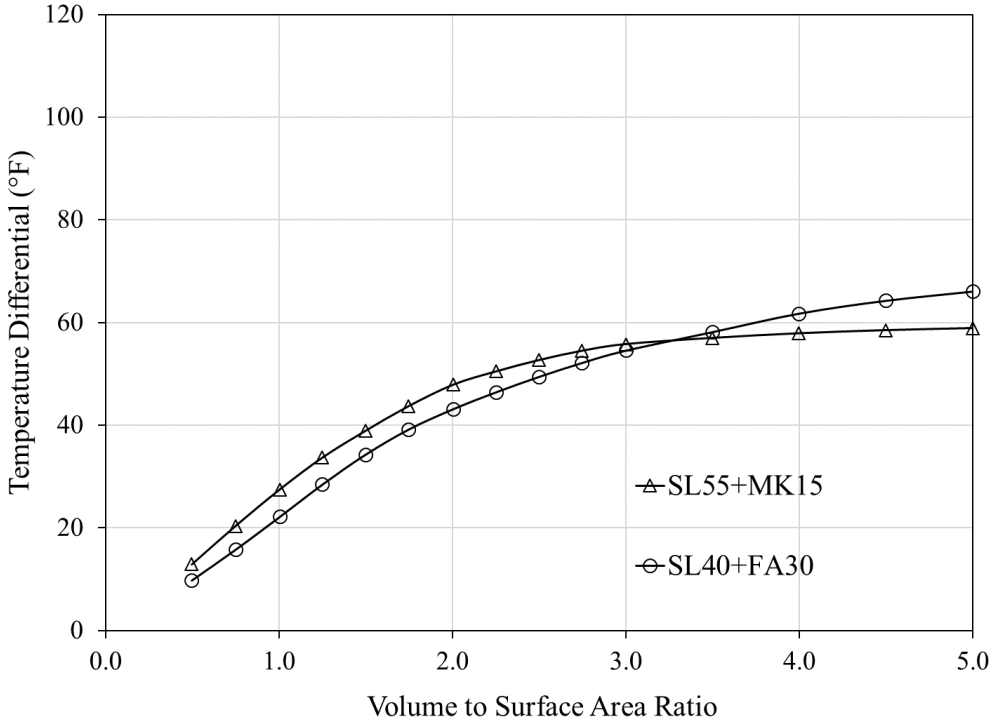

Figure 173 – Effect of ternary mixtures at 70% replacement level on temperature differential – column (summer).

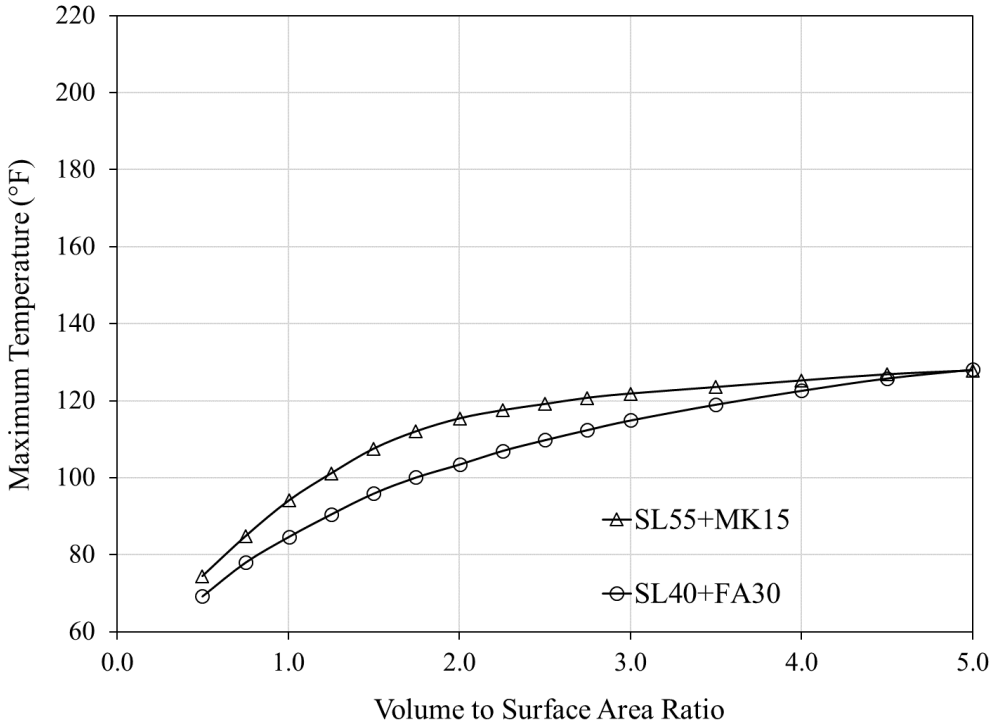

Figure 174 – Effect of ternary mixtures at 70% replacement level on maximum temperature – column (winter).

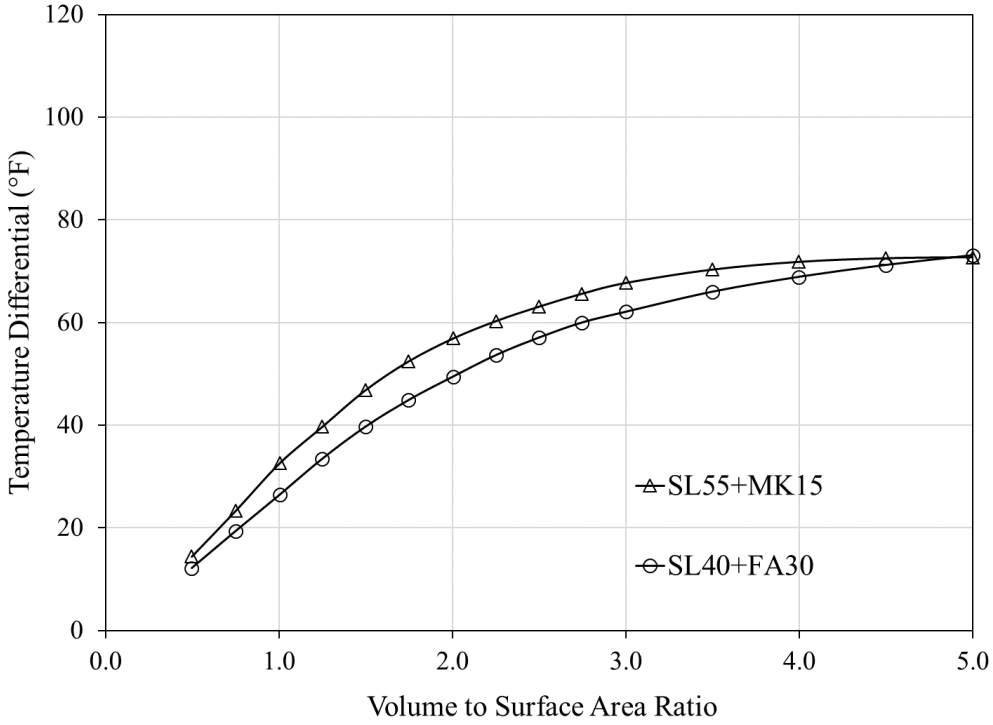

Figure 175 – Effect of ternary mixtures at 70% replacement level on temperature differential – column (winter).

5.2.4 Sensitivity of Ternary Mixtures at 70% Replacement Level

Figure 172 through Figure 175 present the maximum temperature and temperature differential predictions for the column model to compare the performance of two ternary mixtures: SL55+MK15 and SL40+FA30. Results indicate adequate performance across predictions.

5.2.5 Sensitivity of Water-to-Cementitious Material Ratios

Figure 176 through Figure 179 present the maximum temperature and temperature differential predictions in the column model using the heat of hydration from the Control mixture. As anticipated, the results show that an increase in the w/c ratio from 0.36 to 0.48 results in increased maximum temperature and temperature differential.

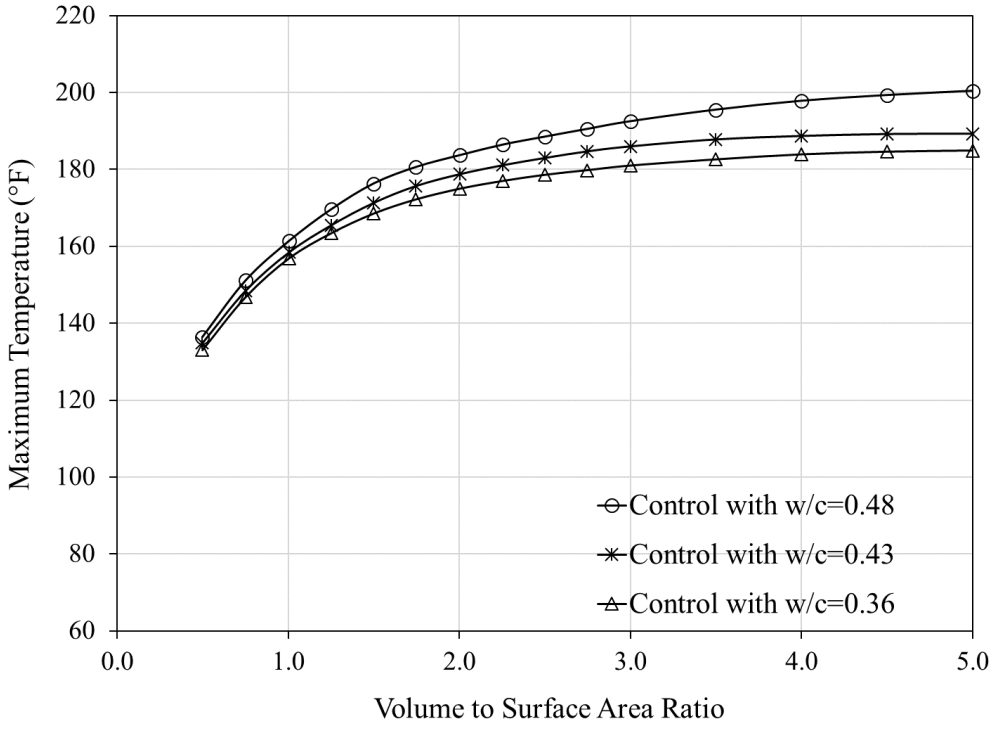

Figure 176 – Effect of w/c on maximum temperature – column (summer).

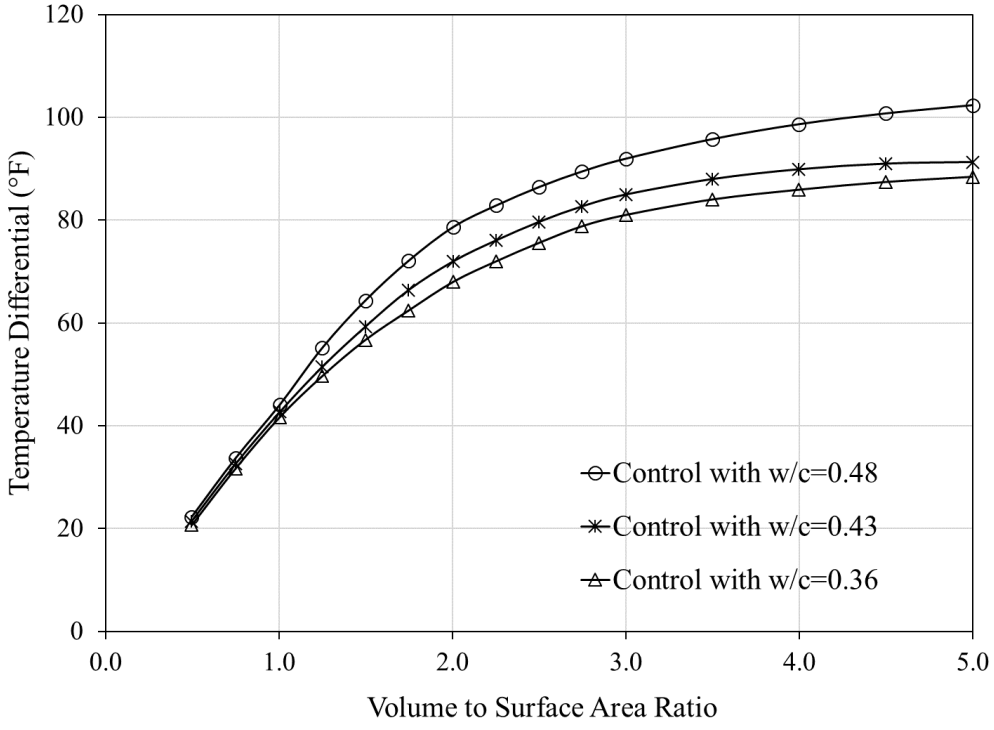

Figure 177 – Effect of w/c on temperature differential – column (summer).

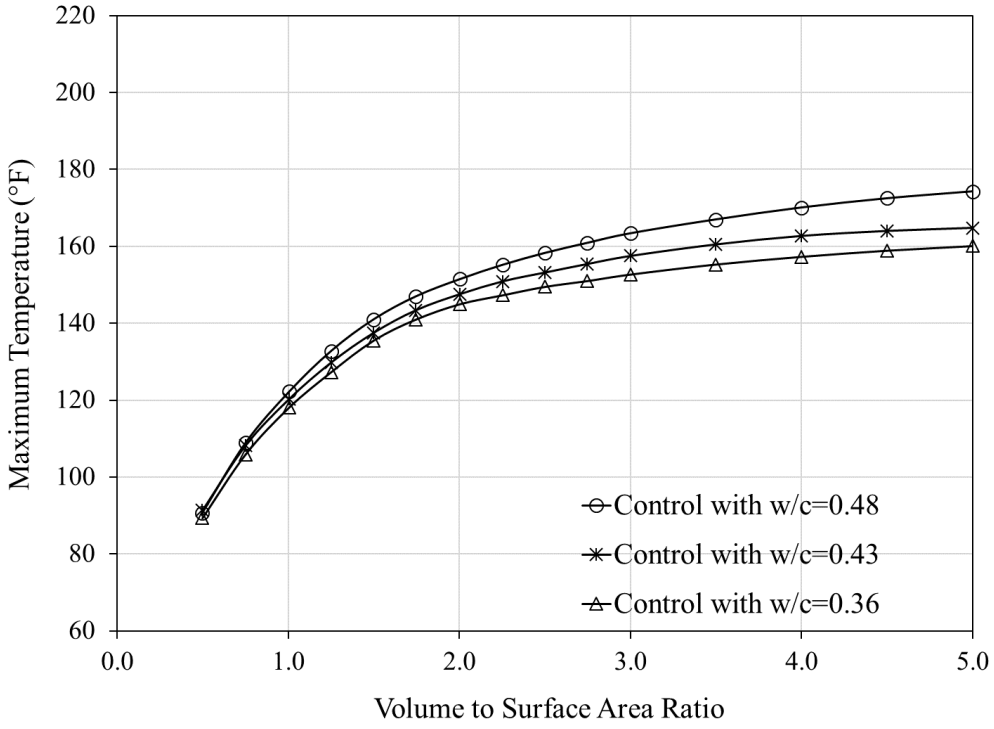

Figure 178 – Effect of w/c on maximum temperature – column (winter).

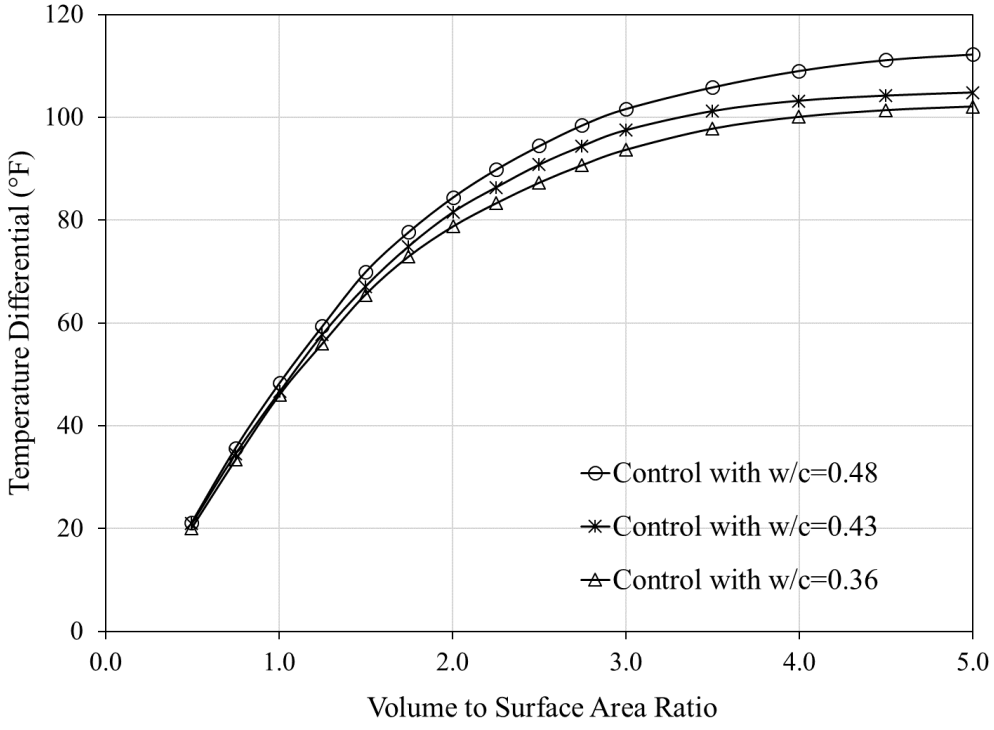

Figure 179 – Effect of w/c on temperature differential – column (winter).

5.2.6 **Sensitivity of Insulation Materials by R-value**

The effect of insulated formwork on the maximum temperature and temperature differential is studied. As a point of reference, the Control mixture is first studied with insulated formwork with the R-value of 1, 2, and 3 $ft^2 \cdot °F \cdot h/BTU$. Subsequently, the FA45 mixture is studied. Figure 180 through 187 show the outcome.

The maximum temperature in the column model is not significantly affected by the presence of insulated formwork whereas an increase in the R-value considerably affects the temperature differential. In the column model with the FA45 mixture, R-value of 2 and 3 $ft^2 \cdot °F \cdot h/BTU$ is required for columns with a V/A ratio less than 2.5 and greater than 3.0, respectively, in order to meet the maximum temperature differential limit of 35 °F (19.4 °C). A higher R-value is required when the V/A ratio exceeds 3.5.

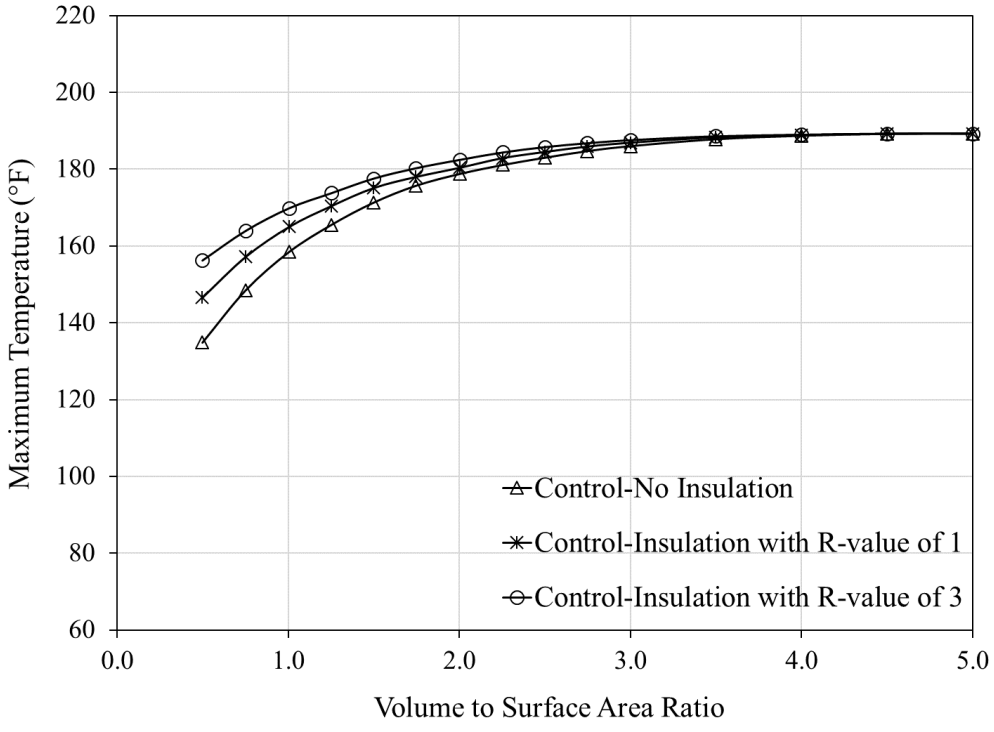

Figure 180 – Effect of insulation on maximum temperature with Control mixture – column (summer).

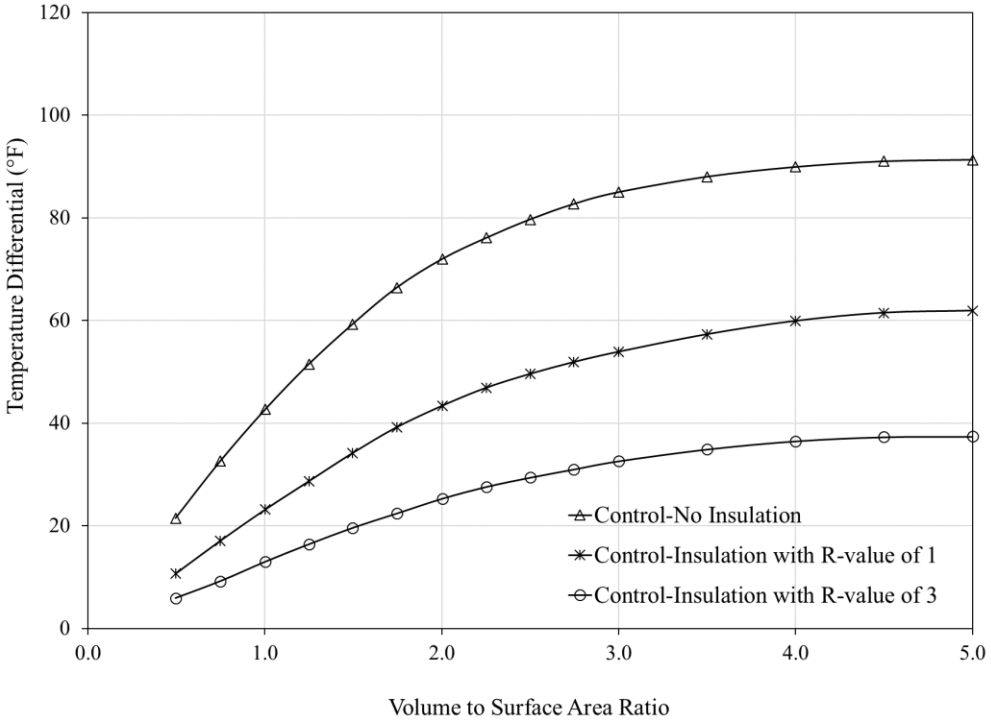

Figure 181 – Effect of insulation on temperature differential with Control mixture – column (summer).

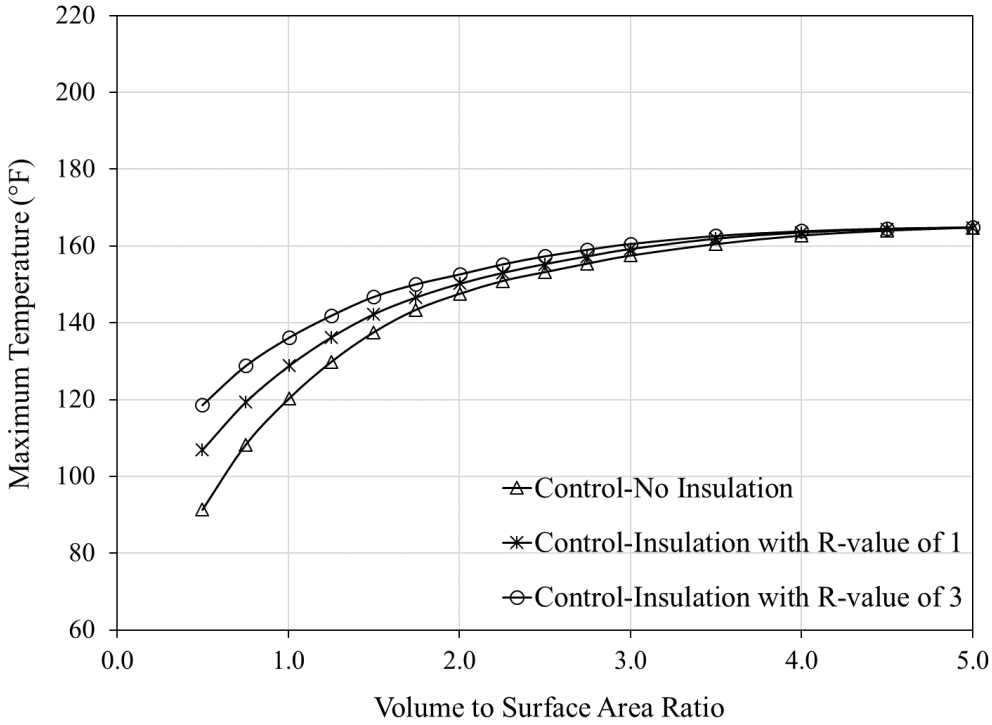

Figure 182 – Effect of insulation on maximum temperature with Control mixture – column (winter).

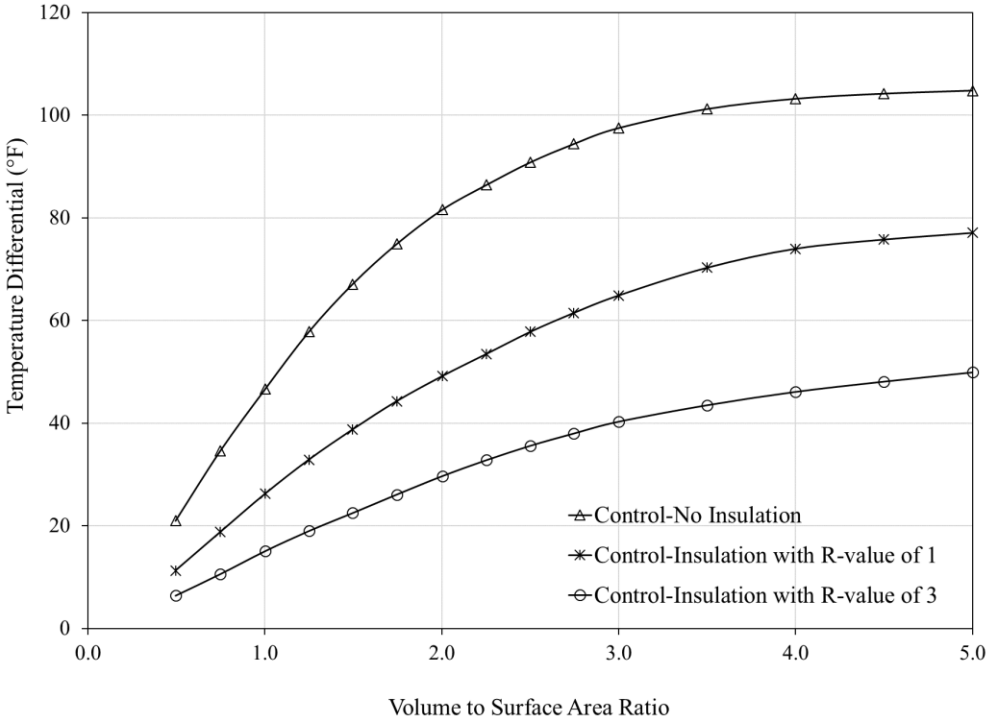

Figure 183 – Effect of insulation on temperature differential with Control mixture – column (winter).

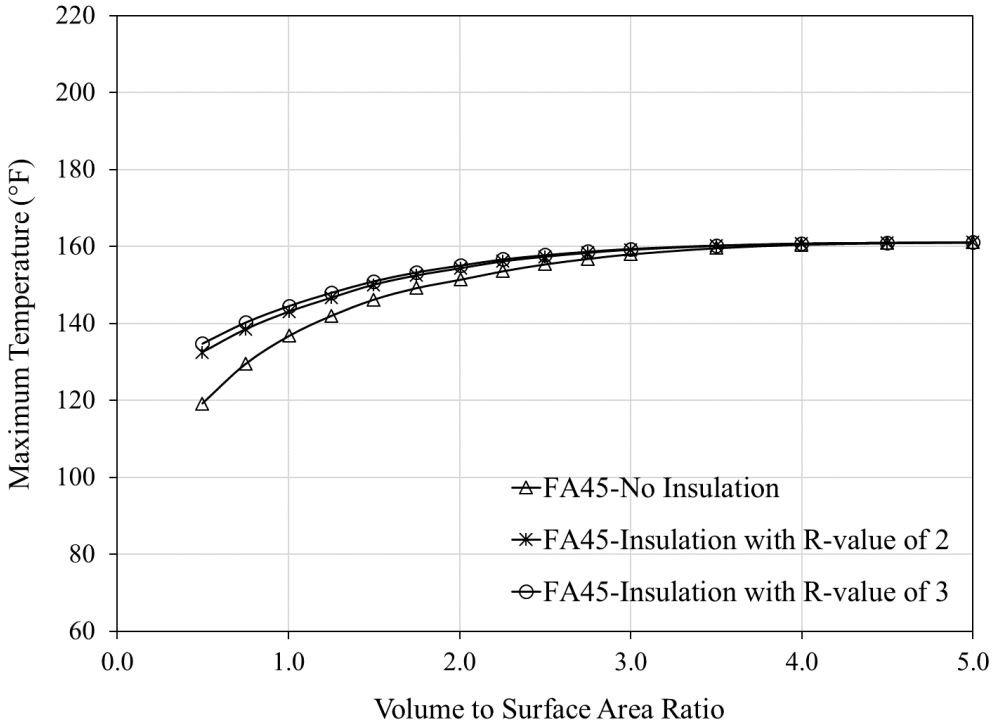

Figure 184 – Effect of insulation on maximum temperature with FA45 mixture – column (summer).

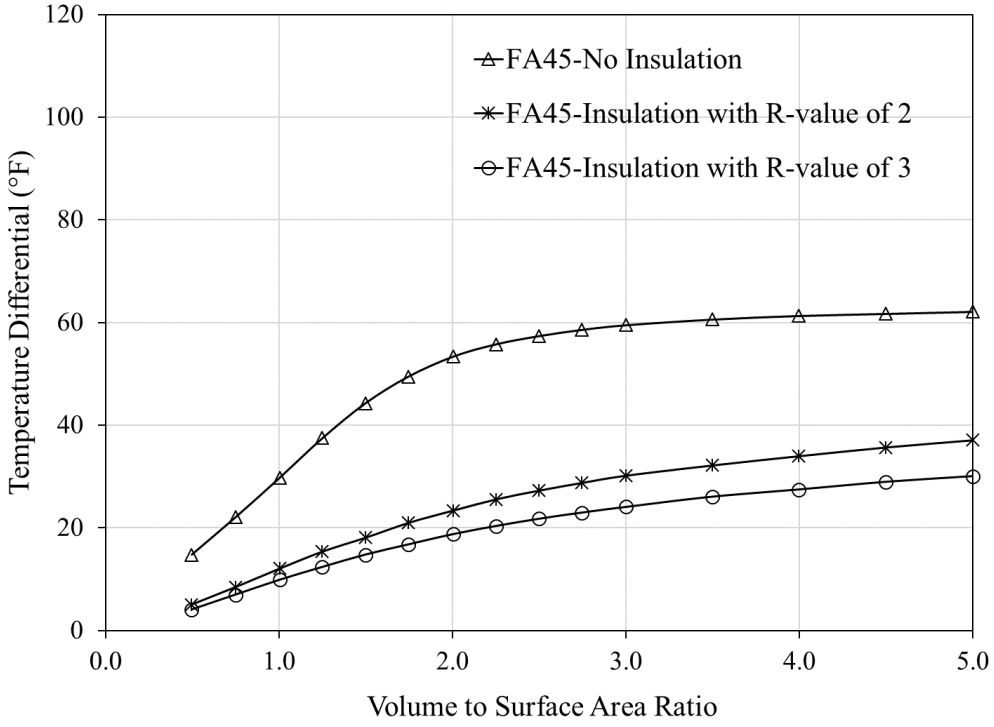

Figure 185 – Effect of insulation on temperature differential with FA45 mixture – column (summer).

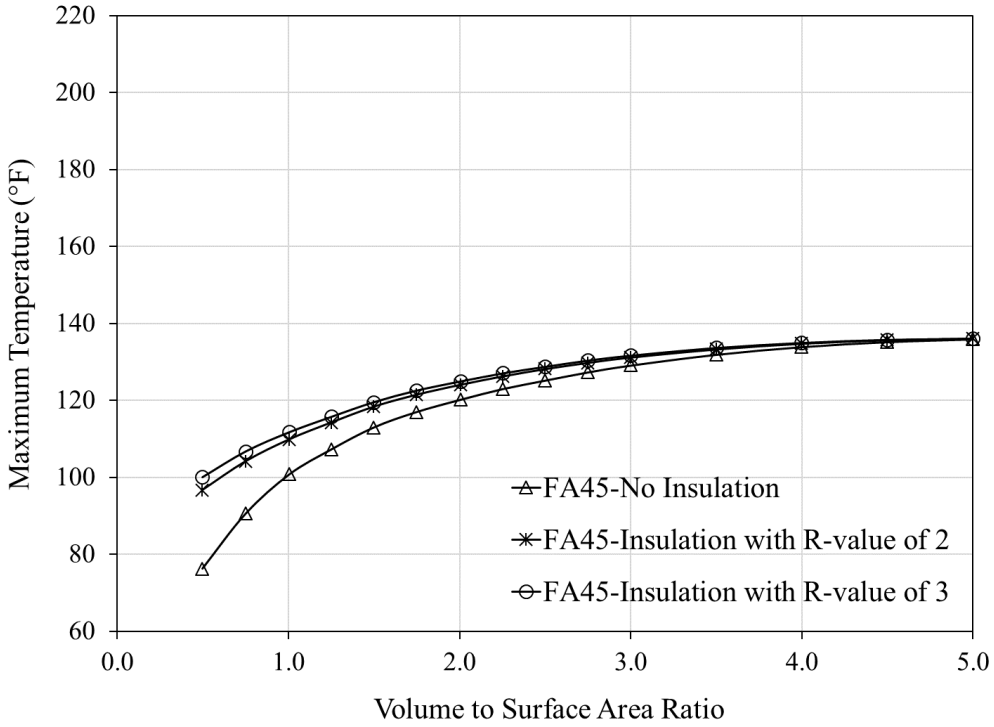

Figure 186 – Effect of insulation on maximum temperature with FA45 mixture – column (winter).

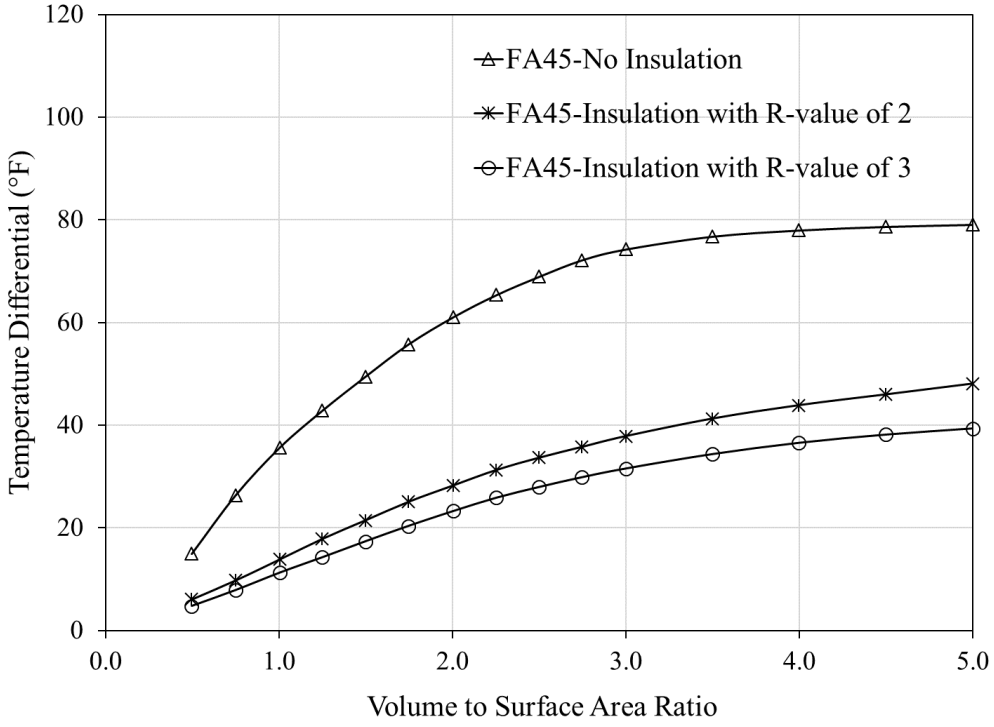

Figure 187 – Effect of insulation on temperature differential with FA45 mixture – column (winter).

5.2.7 Summary of Sensitivity Analysis for Column

Similar to the foundation model, the temperature predictions results of the column model are summarized below in Table 42 and Table 43, for a V/A ratio of 3.0 for both summer and winter placement conditions. Any temperature exceeding the allowable temperature limits appears in gray. As with the foundation model, the placement condition plays a critical role in controlling the maximum temperature; for the winter placement condition specifically, almost all mixtures studied meet the maximum temperature requirement. In columns with a V/A ratio greater than 3.0, the FA45 mixture must be placed with insulated (R>3) formwork. For example, a column with V/A of 3.0 has a height of 30 ft (9.1 m) and a diameter of 15 ft (4.6 m). Columns with a V/A ratio of 2.0 (height=30 ft (9.1 m) and diameter = 9.25 ft (2.8 m)) requires a R-value of 1.

Table 42 – Summary of results for the column at V/A=3.0 (summer).

Parameters	Variables	W/C	Maximum Temperature, °F (°C)	Maximum Temperature Differential, °F (°C)
Mixture Design	Control	0.43	186 (85.6)	85.0 (47.2)
	SL30+MK15	0.43	169.4 (76.3)	69.2 (38.4)
	FA45	0.43	158.0 (70.0)	59.5 (33.1)
	SL55+MK15	0.43	149.6 (65.3)	55.8 (31)
	SL40+FA30	0.43	146.8 (63.8)	54.6 (30.3)
W/C	Control	0.36	181.0 (82.8)	81.0 (45.0)
	Control	0.43	186.0 (85.6)	85.0 (47.2)
	Control	0.48	192.5 (89.2)	92.0 (51.1)
Insulation	Control-No Insulation	0.43	186.0 (85.6)	85.0 (47.2)
	Control-Insulation with R=1	0.43	186.9 (86.1)	53.9 (29.9)
	Control-Insulation with R=3	0.43	187.6 (86.4)	32.6 (18.1)
	FA45-No Insulation	0.43	158.0 (70.0)	59.5 (33.1)
	FA45-Insulation with R=2	0.43	159.2 (70.7)	30.2 (16.8)
	FA45-Insulation with R=3	0.43	159.4 (70.8)	24.1 (13.4)

Table 43 – Summary of results for the column at V/A=3.0 (winter).

Parameters	Variables	W/C	Maximum Temperature, °F (°C)	Maximum Temperature Differential, °F (°C)
Mixture Design	Control	0.43	157.5 (69.7)	97.5 (54.2)
	SL30+MK15	0.43	140.6 (60.3)	83.3 (46.3)
	FA45	0.43	129.1 (53.9)	74.3 (41.3)
	SL55+MK15	0.43	121.8 (49.9)	67.7 (37.6)
	SL40+FA30	0.43	114.9 (46.1)	62.1 (34.5)
W/C	Control	0.36	152.7 (67.1)	93.7 (52.1)
	Control	0.43	157.5 (69.7)	97.5 (54.2)
	Control	0.48	163.4 (73.0)	101.7 (56.5)
Insulation	Control-No Insulation	0.43	157.5 (69.7)	97.5 (54.2)
	Control-Insulation with R=1	0.43	159.2 (70.7)	64.9 (36.1)
	Control-Insulation with R=3	0.43	160.6 (71.4)	40.3 (22.4)
	FA45-No Insulation	0.43	129.1 (53.9)	74.3 (41.3)
	FA45-Insulation with R=2	0.43	131.2 (55.1)	37.9 (21.1)
	FA45-Insulation with R=3 *	0.43	131.7 (55.4)	31.6 (17.6)

* meets both the internal and differential temperature requirements.

5.3 Discussion on the Bridge Seal Model

The sensitivity analysis of the foundation model (Section 5.1) showed that the ternary replacement mixtures (SL55+MK15 and SL40+FA30) meet the maximum temperature requirement. On the contrary, they fail to meet the maximum temperature differential requirement. Therefore, an insulated formwork with a R-value of 3 $ft^2 \cdot °F \cdot h/BTU$ (0.52 $m^2 \cdot °C/W$) was hypothetically provided to meet the requirement. In this section, the bridge seal model (see Section 4.9) is discussed in conjunction with the two ternary replacement mixtures (SL55+MK15 and SL40+FA30) and insulated formwork with a R-value of 3 $ft^2 \cdot °F \cdot h/BTU$ (0.52 $m^2 \cdot °C/W$) for summer and winter placement conditions. For the summer and winter placement conditions, a concrete placement temperature of 85 °F (29.4 °C) and 60 °F (15.6 °C) is considered, respectively.

Figure 188 through Figure 191 present the effect of insulation on the maximum temperature and temperature differential in the bridge seal including the SL55+MK15 mixture in summer and winter placement conditions. Figure 192 through Figure 195 present the effect of insulation on the maximum temperature and temperature differential in the bridge seal including the SL40+FA30 mixture. The bridge seal structure has a volume-to-surface area ratio of 4.16 as indicated by the dashed red line in the figures. The prediction results for all parameters considered in the sensitivity analysis of the bridge seal are summarized in Table 44 and Table 45 for the V/A ratio of 4.16.

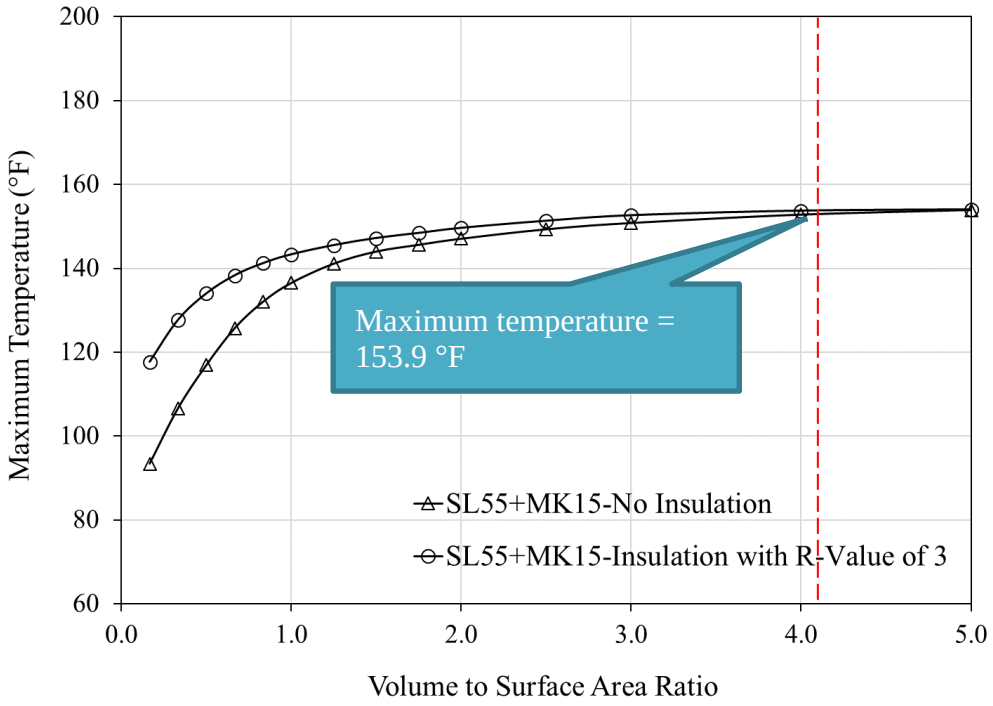

Figure 188 – Effect of insulation on maximum temperature of SL55+MK15 mixture – seal (summer).

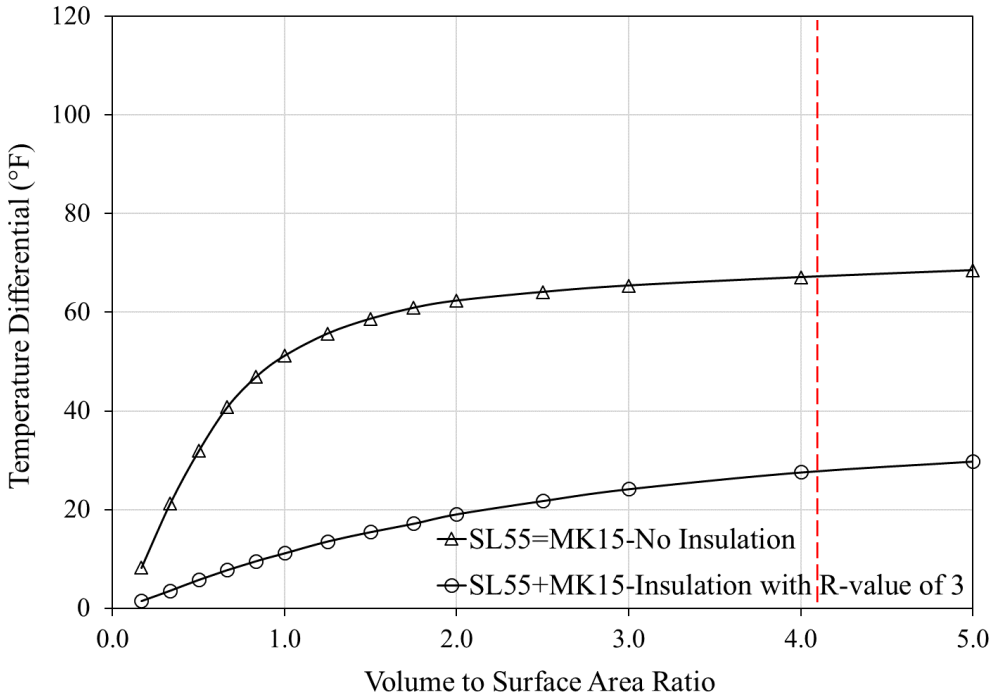

Figure 189 – Effect of insulation on temperature differential of SL55+MK15 mixture – seal (summer).

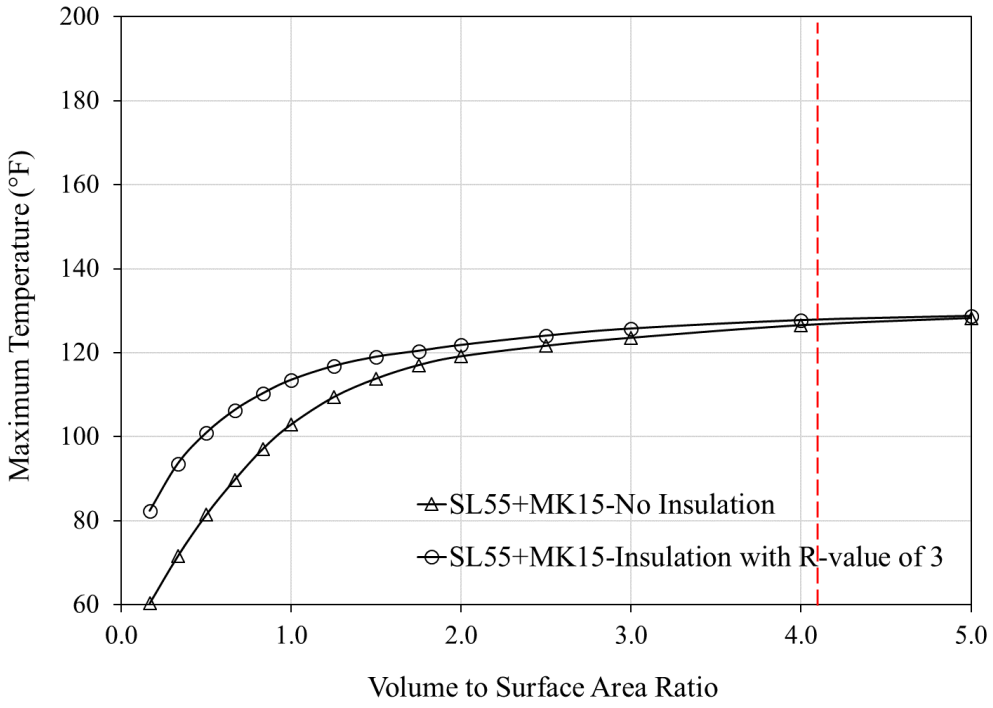

Figure 190 – Effect of insulation on maximum temperature of SL55+MK15 mixture – seal (winter).

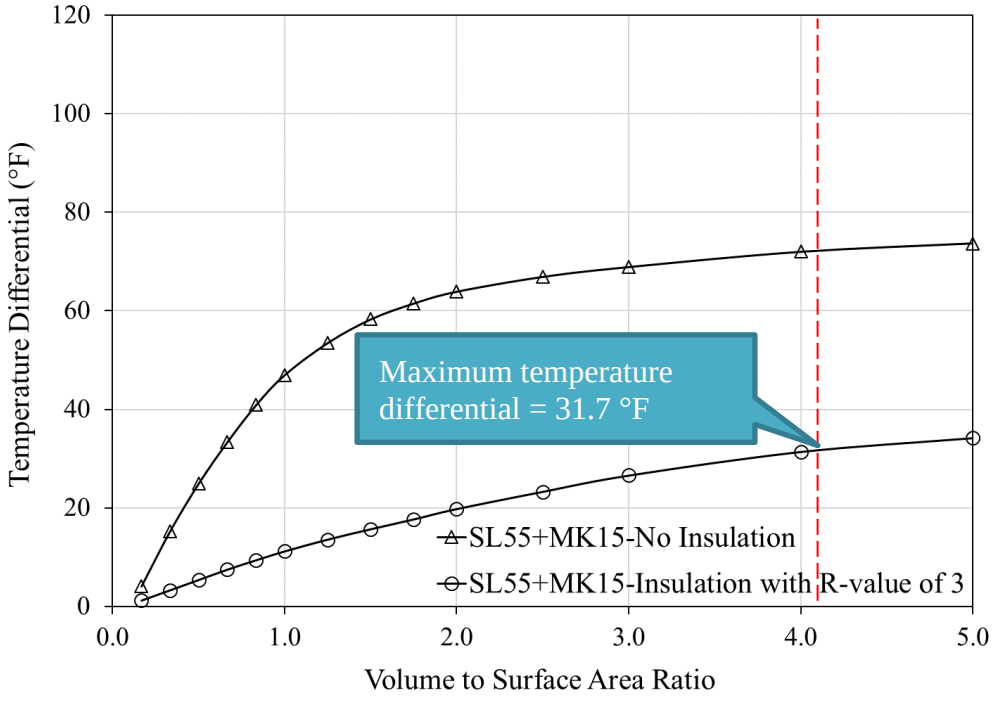

Figure 191 – Effect of insulation on temperature differential of SL55+MK15 mixture – seal (winter).

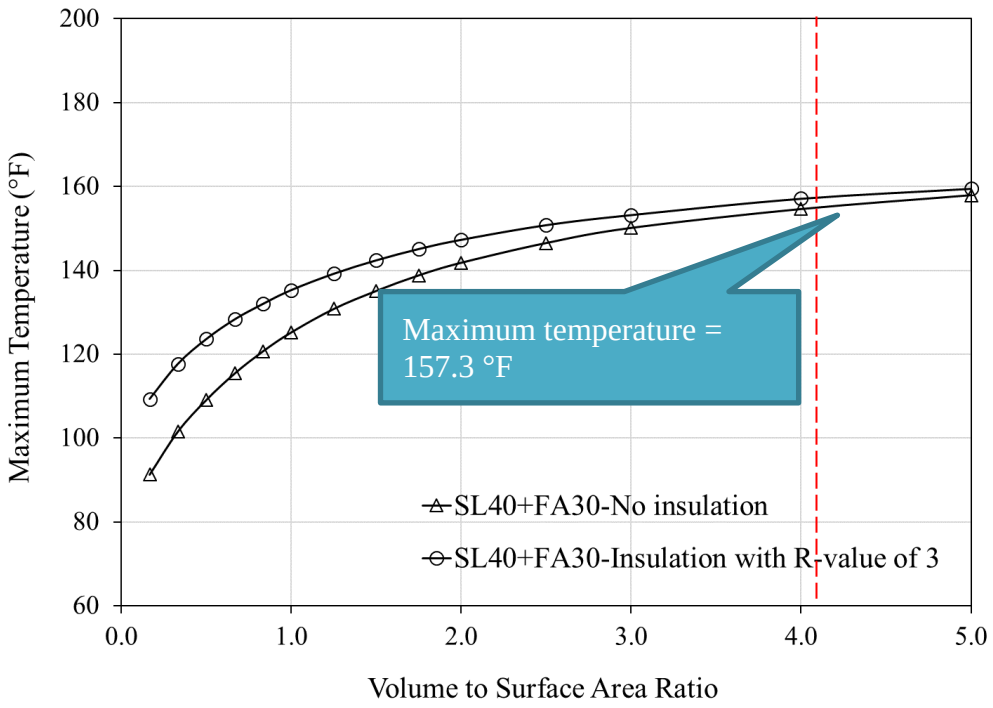

Figure 192 – Effect of insulation on maximum temperature of SL40+FA30 mixture – seal (summer).

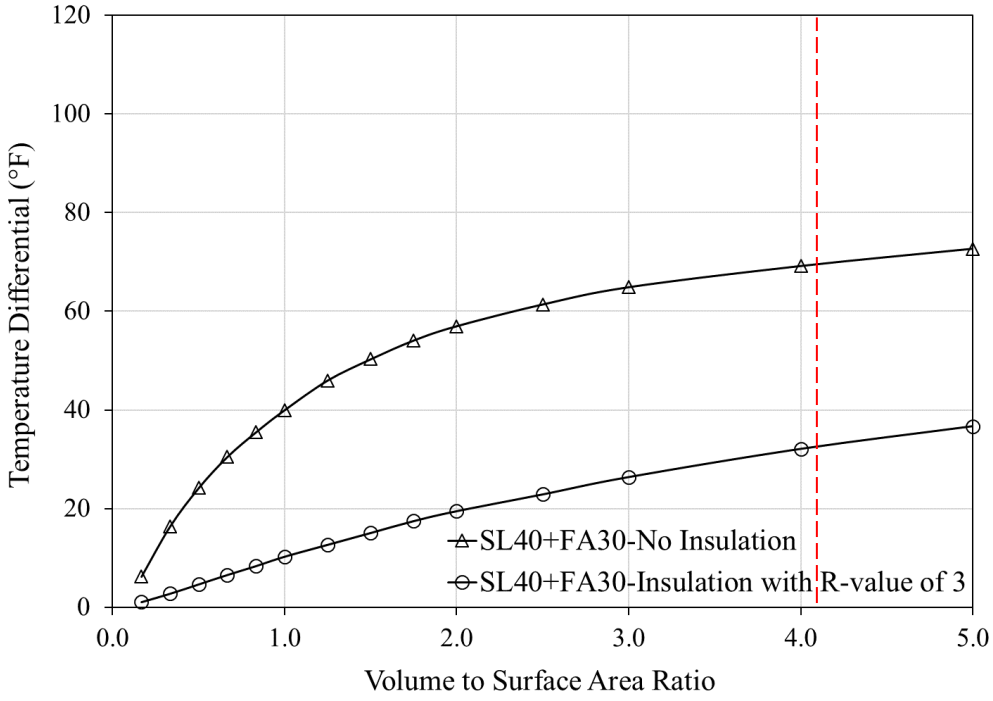

Figure 193 – Effect of insulation on temperature differential of SL40+FA30 mixture – seal (summer).

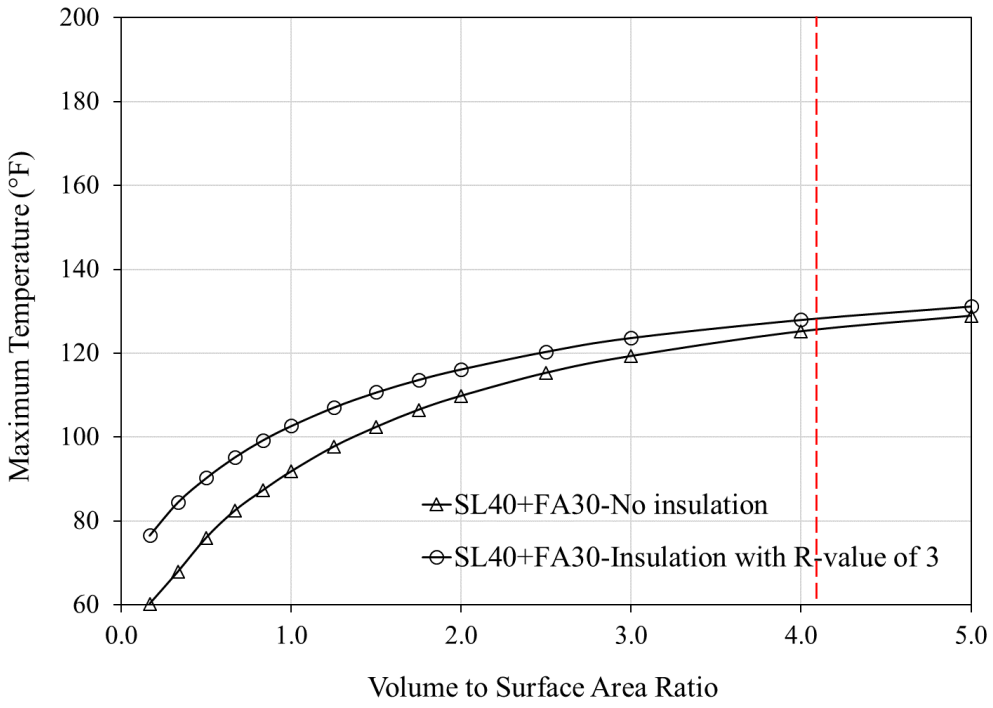

Figure 194 – Effect of insulation on maximum temperature of SL40+FA30 mixture – seal (winter).

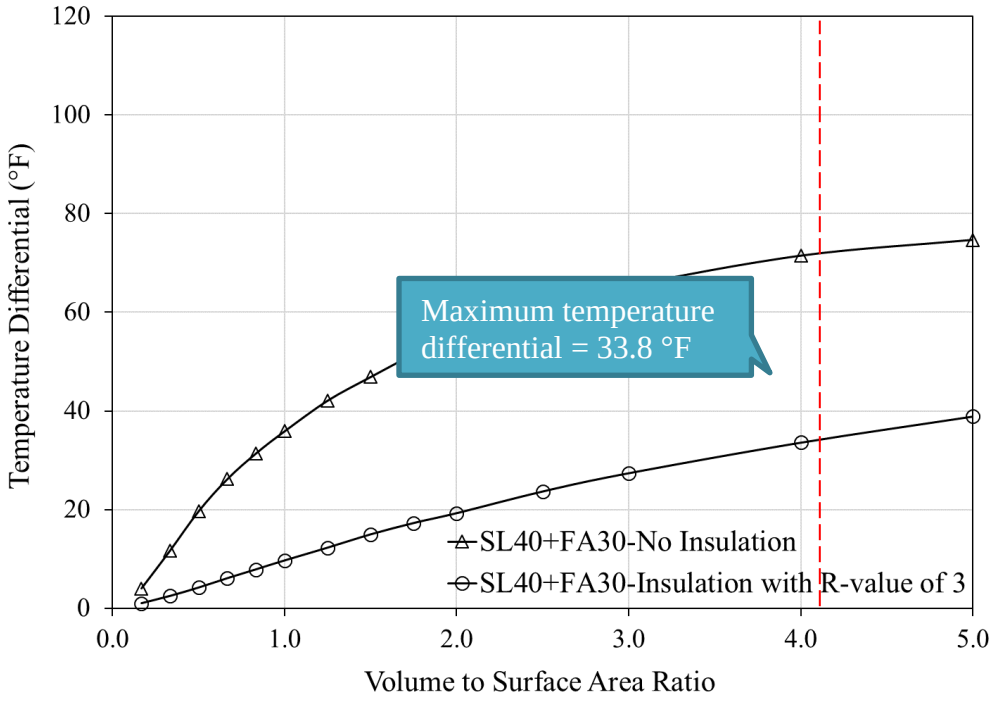

Figure 195 – Effect of insulation on temperature differential of SL40+FA30 mixture – seal (winter).

Table 44 – Summary of Analysis Results - Bridge Seal (summer placement).

Parameters	Variables	W/C	Maximum Temperature, °F (°C)	Maximum Temperature Differential, °F (°C)
Mixture Design	Control (the seal mixture w/o FA)	0.43	190.0 (87.8)	104.5 (58.1)
	SL30+MK15	0.43	172.4 (78.0)	86.9 (48.3)
	FA45 (the seal mixture)	0.43	161.1 (71.7)	76 .0 (42.2)
	SL55+MK15	0.43	152.8 (67.1)	67.1 (37.3)
	SL40+FA30	0.43	155.0 (68.3)	69.5 (38.6)
W/C	Control	0.36	184.9 (84.9)	99.3 (55.2)
	Control	0.43	190.0 (87.8)	104.5 (58.1)
	Control	0.48	197.3 (91.8)	111.2 (61.8)
Insulation Provided	Control-No Insulation	0.43	190.0 (87.8)	104.5 (58.1)
	Control-Insulation with R=1	0.43	190.1 (87.8)	67.6 (37.6)
	Control-Insulation with R=3	0.43	190.1 (87.8)	38.3 (21.3)
	SL55+MK15 with R=3 *	0.43	153.9 (67.7)	27.8 (15.4)
	SL40+FA30 with R=3 *	0.43	157.3 (69.6)	32.3 (17.9)

* meets both the internal and differential temperature requirements.

Table 45 – Summary of Analysis Results - Bridge Seal (winter placement).

Parameters	Variables	W/C	Maximum Temperature, °F (°C)	Maximum Temperature Differential, °F (°C)
Mixture Design	Control (the seal mixture w/o FA)	0.43	164.4 (73.6)	110.0 (61.1)
	SL30+MK15	0.43	147.0 (63.9)	92.8 (51.6)
	FA45 (the seal mixture)	0.43	135.3 (57.4)	81.6 (45.3)
	SL55+MK15	0.43	126.7 (52.6)	72.2 (40.1)
	SL40+FA30	0.43	125.5 (51.9)	71.7 (39.8)
W/C	Control	0.36	159.3 (70.7)	104.2 (57.9)
	Control	0.43	164.4 (73.6)	110.0 (61.1)
	Control	0.48	171.6 (77.6)	115.4 (64.1)
Insulation	Control-No Insulation	0.43	164.4 (73.6)	110.0 (61.1)
	Control-Insulation with R=1	0.43	164.9 (73.8)	74.3 (41.3)
	Control-Insulation with R=3	0.43	165.1 (73.9)	44.3 (24.6)
	SL55+MK15 with R=3 *	0.43	127.9 (53.3)	31.7 (17.6)
	SL40+FA30 with R=3 *	0.43	128.0 (53.3)	33.8 (18.8)

* meets both the internal and differential temperature requirements.

Among the mixtures investigated, the bridge seal analysis indicates that two mixtures (SL55+MK15 and SL40+FA30) meet the maximum internal temperature requirement (158 °F). However, they do not meet the differential requirement (35 °F). Insulated formwork with a R-value (per inch) of 3 $ft^2 \cdot °F \cdot h/Btu$ (0.52 $m^2 \cdot °C/W$) or higher must be provided to meet the requirement. The analysis assumes there is no gap/seam (perfectly bonded) between insulated formwork/sheets. It is fairly easy to find a 1-inch (25.4 mm) thick insulation panel with a R-value of 3 in the market although insulated cofferdam may not be practical. For a 0.5 inch (12.7 mm) thick insulation panel, this means that a R-value of 6 is required. It is concluded that the internal temperature is controlled by the summer placement condition, whereas the gradient temperature is controlled by the winter placement condition.

5.4 Findings and Discussion

The charts and tables developed in this section may be used to predict the maximum internal temperature and temperature differential in mass concrete structures. For a given V/A ratio, they inform GDOT which mixture design meets the temperature requirements conforming to a placement condition. Here, mixture design is based on the cement content of 711 lb/yd^3 (422 kg/m^3). A temperature prediction for any mixture with a different cement content may be adjusted by 10-12.8 °F for every 100 lb/yd^3 (9.4-12 °C for every 100 kg/m^3) of cement increased (or decreased) from the base mixture. The placement conditions of 85 °F (29.4 °C) and 60 °F (15.6 °C) for summer and winter, respectively, may need to be adjusted for more severe placement conditions and mixture designs significantly deviating from the mixtures studied herein. Based on this study, the first two temperature threshold combinations shown in Table 46 are not feasible. This is because mixtures with the total

temperature of 200 °F (93.3 °C) yield crack widths ranging between 0.02 in (0.51 mm) and 0.06 in (1.52 mm), which are not acceptable for its exposure type (see Section 4.9.7). The third option with the maximum allowable internal temperature of 158 °F (70 °C) and maximum temperature differential of 35 °F (19.4 °C) is achievable because the crack width remains less than 0.006 inch (0.1 mm). These limits are consistent with current limits specified by GDOT.

Table 46 – Maximum Allowable Internal and Differential Temperature.

Temperature Limits	
Maximum Allowable Temperature, °F (°C)	Maximum Temperature Differential, °F (°C)
158 (70)	50 (27.8)
170 (76.7)	35 (19.4)
158 (70)	35 (19.4)

Appendix F presents detailed procedures for testing methodology and selecting suitable mixtures for mass concrete placements. This section also provides design examples which illustrate how to use the design charts, presented in this chapter, and identify a mixture in order to meet the required temperature allowables in mass concrete placements.

CHAPTER 6

CONCLUSIONS

The research team recognizes the challenges posed by increasingly scarce Class F fly ash resources available for construction in the United States and thus presents key findings and recommendations in the following sections to address these challenges. The team also recognizes technical challenges in measuring crack strains and quantifying maximum temperature and temperature gradients, challenges contractors face as they strive to deliver structures free of thermal cracks for GDOT under the specified temperature limits (GDOT, 2013). The research team also understands that the most conservative interpretation of existing standards (e.g., ACI 301) could be costly for both GDOT and contractors. Meanwhile, the study team acknowledges the long-term financial impact of thermal cracks in a transportation structure as they affect structure durability and are likely to result in full or partial replacement of the structure.

This chapter concludes the dissertation with an overview of its findings and discussion in terms of three components: (1) supplementary cementitious materials, (2) heat of hydration and temperature, and (3) analytical investigation. In the following section, the dissertation concludes by offering recommendations on how the Georgia Department of Transportation should approach supplementary and/or innovative materials with a performance-based and practical design mindset.

6.1 Supplementary Cementitious Materials

The use of SCMs in concrete mixtures is recommended to mitigate the temperature rise resulting from the heat of cement hydration. Other specific recommendations are as follows:

- Pozzolanic materials, such as slag and metakaolin (MK), are recommended as alternatives to Class F fly ash.
- In particular, more slag in mass concrete mixtures results in a linear decrease in the heat of hydration and temperature increase. On the other hand, partial replacements (up to 45%) of cement with two different slag products in binary replacement mixtures result only in a slight reduction (≤ 6.7 °F or 3.7 °C) in the maximum temperature. Thus, higher replacement levels (> 50%) of cement by slag are recommended.
- When slag is considered as a sole supplementary material in mass concrete structures, the durability of such structures must be investigated. A 30% replacement level shows that the resistance to ASR and sulfate attack drops significantly (see Figure 30).
- The use of MK in concrete mixtures enhances the mechanical properties and durability characteristics. Furthermore, when combined with slag, MK has the potential to significantly reduce the heat of hydration (HoH) (see Figure 45).
- Binary usage of MK results in increased mechanical strengths, although the most significant increases are in compressive strength. Increases up to 44% at 28 days of age are observed (see Figures 17 through 19 and Table 5).

- Binary usage of MK also results in increased chloride-ion penetrability and resistance to sulfate and ASR chemical attacks. A replacement level of 15% will ensure adequate resistance (see Figures 20 through 22 and Table 5).
- Partial replacements (15%) of cement with three different MK products in binary replacement mixtures do not adversely affect the maximum temperature. When MK is used in ternary replacement mixtures in combination with slag (additional 30% cement replacement), the maximum temperature rise reduces by 20% (see Figure 50).
- Ternary replacement mixtures using MK (15%) and slag (30%) products exhibit very high resistance to ASR and sulfate attacks as well as very low chloride-ion penetrability (see Figures 28 through 30).
- These mixtures also result in CTE values near the threshold value of 5.55×10^{-6} in./in./˚F (10×10^{-6} mm/mm/˚C), which is slightly higher than normal-strength concrete (see Figure 32). Drying shrinkage, however, is reduced from that of Control mixture (see Figure 31).
- At high replacement levels of cement with slag, it is recommended that GDOT utilize up to 15% MK in supplementary cement replacement (ternary) mixtures.
- The ternary replacement mixtures using 15% MK and 30% slag result in HoH and temperature reduction similar to those obtained by the cement replacement mixture using 30% Class F fly ash (see Figures 45 and 50).
- HoH and its corresponding temperature rise in a ternary mixture of 55% slag and 15% MK are considerably lower (approximately 5%) than those of a binary

replacement mixture containing 45% Class F fly ash (see Tables 40 through 45), although the durability of the former mixture has not been investigated.

- In addition, the ternary replacement mixture of 55% slag and 15% MK yields similar results (i.e., hydration heat and temperature rise) to those associated with a ternary replacement mixture containing 40% slag and 30% Class F fly ash (see Tables 40 through 45).
- Contrary to the literature, additive materials such as PVA and BaO contribute little to hydration heat control. The 10% by weight addition of PVA paste to cementitious mixtures results in a negligible reduction in HoH. The addition of 3.5% BaO powder (97% BaO) to cementitious mixtures results in a 3-hour delay in HoH peak and setting time in the early period after concrete placement; yet, only a slight reduction in HoH (by 3%) is achieved over a week period (see Figures 46 and 47).
- In binary mixtures, the rate of heat evolution is consistent with strength development; however, in ternary mixtures including 30% slag and 15% MK replacements, strength development is not consistent with the rate of heat evolution (see Figures 13,14, and 25 and Tables 3 and 6).

6.2 Heat of Hydration in Cementitious Materials and Temperature

Experimental results show that it is possible to measure HoH for cementitious materials by conducting a simple laboratory calorimeter test for seven days (or longer) in accordance with ASTM C1702 procedures using a small paste mixture prepared in a laboratory. In addition, the specific heat capacity of each mixture, whether experimentally measured in a cube specimen or reasonably assumed, may be used to convert a heat energy-time history to an adiabatic-temperature-rise versus time history. The latter temperature-time history

can then be used in a coupled thermal-structural finite element analysis to predict the maximum temperature and temperature differential for a structure and evaluate its potential for cracking. The following lists major findings:

- HoH results from paste and mortar mixture samples (e.g., a sieved sample from a cube mixture in this study) including different SCMs correspond well. Thus, a more practical calorimeter test on paste samples should be used to study temperature rise in a concrete mixture. On the contrary, mortar mixture results may be used for a relative comparison among mixtures containing various SCMs and a mixture containing a 45% cement replacement with Class F fly ash.
- HoH results from small mixtures provide an effective tool to predict the relative reduction or increase in maximum temperature rise measurements for the cube specimens (see Section 3.2).
- Small mock-up (e.g., 2 foot or 0.61 m cube) specimens are sufficient to quantify the temperature rise when it is well insulated on all six sides. It is strongly recommended that insulation materials with an R-value (per inch) of approximately 50 $ft^2 \cdot °F \cdot h/BTU$ (8.8 $m^2 \cdot °C/W$) be used.
- Existing maximum temperature prediction methods from the literature sufficiently estimate the maximum temperature rise in binary mixtures, yet they fail to predict the maximum temperature rise in ternary replacement mixtures containing slag and MK. Both slag and MK combined in a ternary mixture result in a significant reduction in maximum temperature rise, and the existing equations are not designed to predict this reduction.

- Additional tests are needed to establish a temperature prediction equation for ternary replacement mixtures.

6.3 Analytical Investigation

It is concluded from the analysis results that the maximum temperature differential limit of 35 °F (19.4 °C) specified in the current GDOT's Special Provision for mass concrete is adequate for limiting the crack width within 0.006 inch (0.1 mm) (see Section 5.4). It is also concluded that the maximum internal temperature limit of 158 °F (70 °C) will only be met in 70% cement replacement mixtures (SL55+MK15 and SL40+FA30). Finally, the 70% replacement mixtures will not meet the temperature differential requirement in the bridge seal model. Nonetheless, placement conditions including environmental conditions significantly affect the maximum temperature and temperature differential.

The sensitivity analysis of the foundation model (Section 5.1) showed that the two ternary replacement mixtures (SL55+MK15 and SL40+FA30) meet the maximum internal temperature requirement. On the contrary, they fail to meet the maximum temperature differential requirement. Therefore, an insulated formwork with a R-value of 3 $ft^2 \cdot °F \cdot h/BTU$ (0.52 $m^2 \cdot °C/W$) was hypothetically provided to meet the requirement. For the V/A ratio of 4.16., i.e., in the bridge seal model studied in Section 5.3, the internal and differential temperature requirements will be met only if the ternary replacement mixtures were used with an insulated formwork/cofferdam. The insulation materials require a R-value greater than 3 $ft^2 \cdot °F \cdot h/BTU$ (0.52 $m^2 \cdot °C/W$).

Similar to the foundation model, for a V/A ratio of 3.0 for both summer and winter placement conditions, the FA45 mixture must be placed with insulated (R>3) formwork. For example, a column with V/A of 3.0 has a height of 30 ft (9.1 m) and a diameter of 15

ft (4.6 m). Columns with a V/A ratio of 2.0 (height=30 ft (9.1 m) and diameter = 9.25 ft (2.8 m)) requires a R-value of 1.

For a given volume-to-surface area ratio (V/A) in a mass concrete structure, the charts and tables developed in Chapter 5 should inform GDOT which mixture design meets the temperature requirements conforming to a placement condition. Based on the analytical investigation presented in Chapters 4 and 5, the two temperature threshold combinations (158+50 °F and 170+35 °F shown in Tables 1 and 46) are not feasible (see Section 5.4). The combination including the maximum allowable internal temperature of 158 °F (70 °C) and maximum temperature differential of 35 °F (19.4 °C) is achievable (see Section 5.4).

CHAPTER 7

RECOMMENDATIONS AND FUTURE WORK

7.1 Recommendations from the Phase-I and Phase-II tests involving MK

It is strongly recommended that the following requirements be met when using MK. The MK products (#1 and #3) locally sourced for this research meet the requirements:

- Conforms to ASTM C618 (Standard Specification for Coal Fly Ash and Raw or Calcined Natural Pozzolan for Use in Concrete)
- $Al_2O_3 + SiO_2 + Fe_2O_3 \geq 90\%$

  This ensures that the vast majority of the kaolin base material was kaolinite and not kaolin converted to glassy alumina and silica.
- LOI $\leq 3\%$ by mass
- At least 99% pass through No. 325 sieve
- Strength activity index (ASTM C311) at 7 days of age $\geq 100\%$
- Replaces a maximum of 20% cement by weight
    - Minimum of 15% if used for ASR or sulfate resistance.

7.2 Recommendation from the Phase-II mass concrete study

Two temperature components, maximum internal temperature and temperature differential, are critical to mass concrete structures. A temperature differential occurs when the hydration heat produced in a mass concrete element is dissipated to the surrounding environment (e.g., water or air) and thus significantly lowers the surface temperature

relative to the heat contained at the concrete core. When this happens, the internal temperature increases and causes an expansion of concrete at the core, whereas the surface temperature drop results in a significant contraction. A substantial temperature differential, one exceeding 35 °F (19.4 °C), inevitably results in thermal cracking which undermines durability in a newly placed mass concrete structure. An internal temperature exceeding 158 °F (70 °C) could yield another outcome detrimental to durability: thermal cracking from delayed ettringite formation.

Based on the literature review presented in Chapter 3, in addition to the use of SCMs and cooling systems, the following measures are recommended to lower the maximum temperature and temperature differential:

- Lower the placement temperature of concrete.
- Use a lower w/c material ratio, if possible.
- Consider more effective insulation materials.
- Internal cooling (pipe) systems, if possible, should be considered to further lower the maximum internal temperature as well as the temperature differential in mass concrete. Additionally, insulation materials with a high R-value (possibly greater than 3 $ft^2 \cdot °F \cdot h/BTU$ (0.52 $m^2 \cdot °C/W$)) should be considered to minimize the temperature gradient.

Based on the analytical investigation presented in Chapters 4 and 5, it is strongly recommended that an FEA should be conducted by using a heat energy-time history of concrete mixtures particularly for mass concrete structures with complex geometry and severe environmental conditions. In addition to the HoH, thermal boundary conditions and

convection/solar radiation significantly affect FEA results. The FEA should be able to evaluate a temperature distribution and predict the extent of thermal cracking.

Based on this study, the following recommendations are made:

1. The research team recommends that the allowable temperature limits, the maximum internal temperature of 158 °F (70 °C) and the maximum temperature differential of 35 °F (19.4 °C), in current Special Provisions to Section 500, should remain as they are.
2. Through this study, the research team has identified ternary replacement mixtures potentially suitable for mass concrete placements. Among the 45% cement replacement mixtures considered in this study, the ternary mixture composed of 30% slag and 15% metakaolin replacements achieves superior performance in terms of mechanical properties, durability, and reducing thermal cracking potential from heat of hydration. In a case study involving a bridge seal including a 45% fly ash replacement, however, the research team finds that circumventing substantial temperature differentials is extremely challenging, particularly for underwater concrete placements. Therefore, and especially in this context, the study team recommends that GDOT consider an increased cement replacement level (from 45% to 70%) and the use of insulating formwork, if possible.
3. It is strongly recommended that GDOT further study the performance of two ternary mixtures containing a 70% cement replacement with 1) 40% slag + 30% fly ash and 2) 55% slag + 15% metakaolin in order to reduce the potential for thermal cracking and thus optimize the long-term performance of mass concrete structures in Georgia. The durability of these two mixtures and the kinetics of deteriorations must be studied.

4. Research on establishing a slag limit is highly recommended. The current provision states, “Slag may comprise no more than 75% by mass of total cementitious and pozzolanous materials.” As a result, there is a room for replacing cement with slag exceeding 30% in binary and ternary replacement mixtures. This study indicates cement replacement with slag equaling to and over 30% could pose a durability problem in binary mixtures. For this reason, a few state transportation agencies specify a limit on slag as low as 25-35% for mass concrete placements. For Georgia, a more strategic approach is recommended: GDOT should sustain current limit but consider requiring a durability test (see Item 2 in Appendix A).
5. Due to inherent variations in concrete properties and material heterogeneity, it is recommended that future research considers statistical approaches for measuring thermal cracks facing imperfect conditions that are more reflective of real life.
6. Finally, the study team has developed temperature prediction models based on a coupled thermal-structural analysis and corresponding charts (see Chapter 5) to facilitate maximum temperature and temperature differential predictions. It is highly recommended that GDOT study typical mass concrete structures and environmental conditions.
7. Future work should include identifying other sustainable and/or innovative alternatives to fly ash and performing coupled thermal-structural analyses to autonomously design mass concrete structures free of thermal cracks. A parametric design/analysis enables such a process.

7.3 Towards Performance-based Specifications

The research team recommends that GDOT considers a shift from prescriptive specifications to performance-based specifications. Specific recommendations include allowing higher internal temperature limits, over 158 °F (70 °C), for mixtures consisting of SCMs when empirical studies show a low risk of DEF occurring in such mixtures. It is also recommended that GDOT allows a variable temperature differential and time-dependent strength development when an analysis indicates a low- to no-potential for cracking. Such performance-based approaches are expected to allow the use of innovative materials and temperature control methods.

7.4 Implementable Recommendations

The research team recommends that GDOT consider changes to the Special Provisions to Section 500 (see Appendix A). Appendix B provides reasons for the changes.

REFERENCES

AASHTO LRFD. (2017). *Bridge Construction Specifications, 4th Edition.* American Assocciation of State Highway and Transportation Officials.

ACI 207.1R-05. (2012). *Guide to Mass Concrete.* American Concrete Institute.

ACI 207.2R-07. (2007). *Report on Thermal and Volume Change Effects on Cracking of Mass Concrete.* American Concrete Institute.

ACI 211.1-91. (2009). *Standard Practice for Selecting Proportions for Normal, Heavyweight, and Mass Concrete.* American Concrete Institute.

ACI 224R-07. (2007). *Causes, Evaluation, and Repair of Cracks in Concrete Structures.* American Concrete Institute.

ACI 301-16. (2016). *Specifications for Structural Concrete.* American Concrete Institute.

ACI 349. (2013). *Code Requirements for Nuclear Safety-Related Concrete Structures and Commentary.* American Concrete Institute.

Alshamsi, A. (1997). Microsilica and ground granulated blast furnace slag effects on hydration temperature. Vol. 27. 1851-1859.

ArDOT. (2014). *Standard Specifications for Highway Construction.* Little Rock, AR: Arkansas Department of Transportation,.

Arora, A., Sant, G., & Neithalath, N. (2016). Ternary blends containing slag and interground/blended limestone: Hydration, strength, and pore structure. *Construction and Building Materials*, 102, 113-124.

ASTM C1679-17. (2017). *Standard practice for measuring hydration kinetics of hydraulic cementitious mixtures using isothermal calorimetry*. West Conshohocken, PA: American Society for Testing and Materials (ASTM). ASTM International. doi:10.1520/C1679-17

ASTM C1702. (2017). *Standard Test Method for Measurement of Heat of Hydration of Hydraulic Cementitious Materials Using Isothermal Conduction Calorimetry.* West Conshohocken, PA: ASTM International. American Society for Testing and Materials. doi:10.1520/C1702-17

ASTM C192/C192M. (2018). *Standard Practice for Making and Curing Concrete Test Specimens in the Laboratory*. West Conshohocken, PA: ASTM International. American Society for Testing and Materials. doi:10.1520/C0192_C0192M-18

Badogiannis, E., Aggeli, E., Papadakis, V. G., & Tsivilis, S. (2015). Evaluation of chloride-penetration resistance of metakaolin concrete by means of a diffusion–Binding model and of the k-value concept. *Cement and Concrete Composites*, 63, 1-7. doi:10.1016/j.cemconcomp.2015.07.012

Bamforth, P. (2007). *Early-age thermal crack control in concrete.* London: CIRIA.

Bažant, Z. P., Kaplan, M. F., & Bazant, Z. P. (1996). *Concrete at high temperatures: material properties and mathematical models.* London: Addison-Wesley.

Berodier, E. (2015). Impact of the supplementary cementitious materials on the kinetics and microstructural development of cement hydration. Retrieved from Infoscience: EPFL Scientific Publications. doi:10.5075/epfl-thesis-6417

Bofang, Z. (2014). *Thermal Stresses and Temperature Control of Mass Concrete.* New York: Elsevier.

Boháč, M., Palou, M., Novotný, R., Másilko, J., Všianský, D., & Staněk, T. (2014). Investigation on early hydration of ternary portland cement-blast-furnace slag–metakaolin blends. *Construction and Building Materials*, 64, 333-341. doi:10.1016/j.conbuildmat.2014.04.018

Bouzoubaâ, N., Lachemi, M., Miao, B., & Aïtcin, P. C. (1997). Thermal damage of mass concrete: experimental and numerical studies on the effect of external temperature variations. *Canadian Journal of Civil Engineering,* 24(4), 649-657.

Brindley, G., & Nakahira, M. (1957). The Role of Water Vapour In The Dehydroxylation of Clay Minerals. *Clay Minerals 3(17), 114-119*. doi:10.1180/claymin.1957.003.17.01

Brooks, J., & Johari, M. (2001). Effect of metakaolin on creep and shrinkage of concrete. *Cement & Concrete Composites*, 23(6): p. 495-502.

Brown, T. D., & Javaid, M. Y. (1970). The thermal conductivity of fresh concrete. *Matériaux et Construction*, 3(6), 411-416.

Brykov, A. S. (2015). Hydration of Portland Cement in the Presence of Highly Reactive Metakaolin. *Materials Sciences and Applications*, Vol. 6, 391-400. doi:0.4236/msa.2015.65044

Caldarone, M. A., Gruber, K. A., & Burg, R. G. (1994). High reactivity metakaolin (HRM): a new generation mineral admixture for high performance concrete. *Concrete International,*, 16(11), 37-41.

Caltrans. (2015). *Standard Specifications.* Sacramento, CA: California Department of Transportation.

Choi, W. C., Khil, B. S., Chae, Y. S., Liang, Q. B., & Yun, H. D. (2014). Feasibility of using phase change materials to control the heat of hydration in massive concrete structures. *The Scientific World Journal*. doi:10.1155/2014/781393

Chorzepa, M., Durham, S., & Sullivan, M. (2017). Evaluation of Metakaolin and Slag for GDOT Concrete Specifications and Mass Concrete Provision – Phase I: final report, (Report No.: FHWA-GA-17-1616). Atlanta, GA: Georgia Department of Transportation.

Curcio, F., DeAngelis, B., & Pagliolico, S. (1998). Metakaolin as a pozzolanic microfiller for high-performance mortars. *Cement and Concrete Research*, 28, 803-809.

Day, R. L. (1992). The effect of secondary ettringite formation on the durability of concrete: a literature analysis (No. RD108T).

De Schutter, G., & Taerwe, L. (1995). Specific heat and thermal diffusivity of hardening concrete. *Magazine of Concrete Research*, 47(172), 203-208.

DelDOT. (2016). *Standard Specifications for Road and Bridge Construction.* Dover, DE: The State of Delaware Department of Transportation.

Diamond, S. (1996). Delayed ettringite formation—processes and problems. *Cement and concrete Composites*, 18(3) 205-215.

DIANA. (2017). Theory Manual. Retrieved from https://dianafea.com/manuals/d102/Theory/Theory.html

DIANA. (2019). Users Manual. Retrieved from https://dianafea.com/diana-manuals

DIANA FEA. (Version 10.2). Retrieved from https://dianafea.com/index.php/

DOTD. (2016). *Standard Specifications for Roads and Bridges.* Baton Rouge, LA: Louisiana Department of Transportation and Development.

Duan, P., Shui, Z., Chen, W., & Shen, C. (2013). Effects of metakaolin, silica fume and slag on pore structure, interfacial transition zone and compressive strength of concrete. *Construction and Building Materials*, 44, 1-6. doi:https://doi.org/10.1016/j.conbuildmat.2013.02.075

FDOT. (2017). *Standard Specifications for Road and Bridge Construction.* Tallahassee, FL: Florida Department of Transportation.

Ferreira, R. M., Castro-Gomes, J. P., Costa, P., & Malheiro, R. (2015). Effect of metakaolin on the chloride ingress properties of concrete. 2015. *KSCE Journal of Civil Engineering*, 1-10.

FHWA. (2017). *Start-up Guide: Performance-Based Practical Design. Publication No. FHWA-HIF-17-026.* Retrieved from https://www.fhwa.dot.gov/design/pbpd/documents/hif17026.pdf

FHWA FP-14. (2014). *The Standard Specifications for Construction of Roads and Bridges on Federal Highway Projects.* USDOT Federal Highway Administration.

fib. (2013). *fib Model Code for Concrete Structures 2010.* doi:10.1002/9783433604090.

Gadja, J., & Alsamsam, E. (2006). *Engineering Mass Concrete Structures.* [Professional Development Series]. Skokie, IL: Portland Cement Association.

Gajda, J., Weber, M., & Diaz-Loya, I. (2014). A Low Temperature Rise Mixture for Mass Concrete. *Concrete international*.

Gallucci, E., Mathur, P., & Scrivener, K. (2010). Microstructural development of early age hydration shells around cement grains. *Cement and Concrete Research*, 40, 4-13.

GDOT. (2013). *State of Georgia. Special Provision. Section 500-Concrete Structures.* Atlanta, GA: Georgia Department of Transportation.

Georgia Mining Association. (2016). *Georgia's Kaolin Industry: Employment, Economic & Environmental Impact.* Retrieved from https://www.georgiamining.org/GMA-georgia-kaolin-industry.php

Gleize, P. J., Cyr, M., & Escadeillas, G. (2007). Effects of metakaolin on autogenous shrinkage of cement pastes. *Cement and Concrete Composites*, 29(2), 80-87.

Google Maps. (2018). Retrieved from https://www.google.com/maps/

Gruyaert, E., Robeyst, N., & De Belie, N. (2010). Study of the hydration of portland cement blended with blast-furnace slag by calorimetry and thermogravimetry. *Journal of Thermal Analysis and Calorimetry*, 102, 941-951.

Güneyisi, E., Gesoğlu, M., & Mermerdaş, K. (2008). Improving strength, drying shrinkage, and pore structure of concrete using metakaolin. *Materials and Structures*, 41(5), 937-949. doi:https://doi.org/10.1617/s11527-007-9296-z

Güneyisi, E., Gesoğlu, M., Karaoğlu, S., & Mermerdaş, K. (2012). Strength, permeability and shrinkage cracking of silica fume and metakaolin concretes. *Construction and Building Materials*, 34, 120-130. doi:https://doi.org/10.1016/j.conbuildmat.2012.02.017

Hamid, H., Chorzepa, M., Sullivan, M., Durham, S., & Kim, S. (2018). Novelties in Material Development for Massive Concrete Structures: Reduction in Heat of Hydration Observed in Ternary Replacement Mixtures. *Infrastructures*, 3(2), 8. doi:10.3390/infrastructures3020008

Hansen, P. F., Hansen, J., Hougaard, K., & Pedersen, E. J. (1982). Thermal properties of hardening cement paste. *Proceedings of RILEM international conference on concrete at early ages* (pp. Vol. 1982, pp. 23-36). Paris: RILEM.

Heinz, D., Ludwig, U., & Rüdiger, I. (1989). Delayed ettringite formation in heat treated mortars and concretes. *Concrete Precasting Plant and Technology*, 11, 56-61.

IDOT. (2016). *Standard Specifications for Road and Bridge Construction.* Springfield, IL: Illinois Department of Transportation.

IDT. (2017). *Standard Specifications for Highway Construction.* Boise, Idaho: Idaho Transportation Department.

Iowa DOT. (2015). *Developmental Specifications for Mass Concrete.* Ames, IA: Iowa Department of Transportation.

Ismail, M., Noruzman, A. H., Bhutta, M. A., Yusuf, T. O., & Ogiri, I. H. (2016). Effect of vinyl acetate effluent in reducing heat of hydration of concrete. KSCE Journal of Civil Engineering. 20(1), 145-151.

Jiang, G., Rong, Z., & Sun, W. (2015). Effects of metakaolin on mechanical properties, pore structure and hydration heat of mortars at 0.17 w/b ratio. Construction and Building Materials. 93: p. 564-572.

JSCE. (2007). *Guidlines for Concrete No.15-Standard Specifications for Concrete Structures.* Japan Society of Civil Engineers.

Jung, S. H., Choi, Y. C., & Choi, S. (2017). Use of ternary blended concrete to mitigate thermal cracking in massive concrete structures—A field feasibility and monitoring case study. *Construction and Building Materials*, 137, 208-215.

Justice, J., & Kurtis, K. (2007). Influence of metakaolin surface area on properties of cement-based materials. *Journal of Materials in Civil Engineering*, 19(9): p. 762-771.

Kang, S., Kim, J., Moon, C., & Song, M. (2015). Early hydration-retarding mechanism of polymer-modified cement. *Materials Research Innovations*, 19(sup8), S8-22.

Khatib, J. M., Kayali, O., & Siddique, R. (2009). Dimensional Change and Strength of Mortars Containing Fly Ash and Metakaolin. Vol. 21. *Journal of Materials in Civil Engineering. Vol. 21, Issue 9. American Society of Civil Engineers*.

Khatib, J., & Hibbert, J. (2005). Selected engineering properties of concrete incorporating slag and metakaolin. *Construction and Building Materials*, 19(6): p. 460-472.

Kim, Y. R., Khil, B. S., Jang, S. J., Choi, W. C., & Yun, H. D. (2015). Effect of barium-based phase change material (PCM) to control the heat of hydration on the mechanical properties of mass concrete. *Thermochimica acta*, 613, 100-107.

Kingspan USA. (2019). Retrieved from https://www.kingspan.com/us/en-us

KYTC. (2012). *Standard Specifications for Road and Bridge Construction.* Frankfort, KY: Kentucky transportation Cabinet.

Lagier, F., & Kurtis, K. (2007). Influence of Portland cement composition on early age reactions with metakaolin. *Cement and Concrete Research*, 37(10): p. 1411-1417.

Lawrence, A. M. (2009). *A finite element model for the prediction of thermal stresses in mass concrete.* Vol. 71, No. 03.

Li, C., Sun, H., & Li, L. (2010). A review: The comparison between alkali-activated slag (Si+ Ca) and metakaolin (Si+ Al) cements. *Cement and Concrete Research*, 40(9), 1341-1349.

Maia, L., Azenha, M., Faria, R., & Figueiras, J. (2011). Influence of the cementitious paste composition on the e-modulus and heat of hydration evolutions. *Cement and Concrete Research*, 41, 799-807.

Marikunte, S. S., & Phelps, R. J. (2012). *Strength and Permeability of Concrete with Metakaolin: Statistical Study, in Transportation Research Board 91st Annual Meeting TRB:*. Washington DC, United States.

MassDOT. (2015). *Suppplemental Specifications.* Boston, MA: Massachusetts Department of Transportation.

MDOT. (2017). *Standard Specifications for Road and Bridge Construction.* Jackson, MS: Mississippi Department of Transportation.

Meinhard, K., & Lackner, R. (2008). Multi-phase hydration model for prediction of hydration-heat release of blended cements. *Cement and Concrete Research*, 38, 794-802.

Meland, I. (1983). Fly ash, Silica Fume, Slag and other Mineral Bt-Products in Concrete. *ACI Special Publication SP-79*, 665-676.

Mindess, S., Young, J., & Darwin, D. (2003). *Concrete. Second ed.* Upper Saddle River, New Jersey: 2003: Pearson Education, Inc.

MnDOT. (2018). *Standard Specifications for Construction.* Saint Paul, MN: Minnesota Department of Transportation.

Murray, H., & Lyons, S. (1955). Correlation of Paper-Coating Quality With Degree of Crystal Perfection of Kaolinite. *Department of Geology. Indiana University.*

NCDOT. (2018). *Standard Specifications for Roads and Structures.* Raleigh, NC: North Carolina Department of Transportation.

NHDOT. (2016). *Standard Specifications.* Concord, NH: New Hampshire Department of Transportation.

NJDOT. (2007). *Standard Specifications for Road and bridge Construction.* Ewing Township, NJ: New Jersey Department of Transportation.

NYSDOT. (2019). *Standard Specifications.* Albany, NY: New York State Department of Transportation.

ODOT. (2016). *Construction and Material Specifications.* Columbus, OH: Ohio Department of Transportation.

PCA. (2011). *Design and Control of Concrete Mixtures-The guide to applications, methods, and materials. 15th edition. EB001.15.* Portland Cement Association.

Poon, C., Kou, S., & Lam, L. (2006). Compressive strength, chloride diffusivity and pore structure of high performance metakaolin and silica fume concrete. *Construction and Building Materials*, 20(10): p. 858-865.

Ramezanianpour, A. A. (2014). Cement Replacement Materials. Springer Berlin Heidelberg.

Ramezanianpour, A., & Jovein, H. B. (2012). Influence of metakaolin as supplementary cementing material on strength and durability of concretes. *Construction and Building Materials, 2012. 30: p. 470-479.*, 30: p. 470-479.

Reinhardt, H. W., Blaauwendraad, J., & Jongedijk, J. (1982). Temperature development in concrete structures taking account of state dependent properties. *International Conference on concrete at early ages (Vol. 1).* Paris: RILEM.

RIDOT. (2016). *Standard Specifications for Road and Bridge Construction.* Rhode Island Department of Transportation.

Sabih, G., & Tarefder, R. (2016). Impact of variability of mechanical and thermal properties of concrete on predicted performance of jointed plain concrete

pavements. *International Journal of Pavement Research and Technology*, 9(6): p. 436-444.

San Nicolas, R., Cyr, M., & Escadeillas, G. (2014). Performance-based approach to durability of concrete containing flash-calcined metakaolin as cement replacement. *Construction and Building Materials*, 313-322.

SCDOT. (2007). *Standard Specifications for Highway Construction.* Columbia, SC: South Carolina Department of Transportation.

SFA. (2019). Retrieved from Silica Fume Association: https://www.silicafume.org/

Shui, Z. H., Zhang, R., Chen, W., & Xuan, D. X. (2010). Effects of mineral admixtures on the thermal expansion properties of hardened cement paste. *Construction and Building Materials*, 24(9), 1761-1767.

Siang, G. C. (2017). Determination of Temperature Rise and Temperature Differentials of CEMII/BV Cement for 20MPa Mass Concrete using Adiabatic Temperature Rise Data. *IOP Conference Series: Materials Science and Engineering*, (Vol. 217, No. 1, p. 0.

Snelson, D. G., Wild, S., & O'Farrell, M. (2008). Heat of hydration of Portland Cement–Metakaolin–Fly ash (PC–MK–PFA) blends. *Cement and Concrete Research*, 38(6), 832-840.

Taylor, H. F., Famy, C., & Scrivener, K. L. (2001). Delayed ettringite formation. *Cement and concrete research*, 31(5), 683-693.

Tia, M., Ferraro, C. C., Lawrence, A., Smith, S., & Ochiai, F. (2010). *Development of design parameters for mass concrete using finite element analysis: final report, (No. UF Project No. 00054863).* Florida. Department of Transportation.

Torres Agredo, J., Mejia de Gutiérrez, R., & Gutiérrez, C. (2008). The performance of mortar containing added metakaolin regarding sulfate action. *Ingeniería e Investigación*, 28(1): p. 117-122.

TxDOT. (2014). *Standard Specifications for Construction and Maintenance of Highways, Streets, and Bridges.* Austin, TX: Texas Department of Transportation.

TxDOT. (2019). Retrieved from https://www.txdot.gov/inside-txdot/division/information-technology/engineering-software.external.html

USGS. (2013). *2012-2013 Minerals Yearbook: Georgia.*

USGS. (2019). *Earthquake Hazards Program*. Retrieved from The United States Geological Survey: https://earthquake.usgs.gov/

USGS. (2019). *National Water Information System: Web Interface*. Retrieved from The United States Geographical Survey: https://nwis.waterdata.usgs.gov/nwis/

VDOT. (2016). *Road and Bridge Specifications.* Richmond, VA: Virginia Department of Transportation.

Wang, G. M., Kong, Y., Shui, Z. H., Li, Q., & Han, J. L. (2014). Experimental investigation on chloride diffusion and binding in concrete containing metakaolin. *Corrosion Engineering, Science and Technology*, 49(4), 282-286.

Weather Underground. (2019). Retrieved from Weather Underground: https://www.wunderground.com/

Wild, S., Khatib, J. M., & Roose, L. J. (1998). Chemical shrinkage and autogenous shrinkage of Portland cement—metakaolin pastes. *Advances in cement research*, 10(3), 109-119.

Wild, S., Khatib, J., & Jones, A. (1996). Relative strength, pozzolanic activity and cement hydration in superplasticised metakaolin concrete. *Cement and Concrete Research*, 26(10): p. 1537-1544.

Wu, X., Roy, D., & Langton, C. (1983). Early stage hydration of slag-cement. *Cement and Concrete Research*, 13, 277-286.

WVDOT. (2010). *Special Provision.* Charleston, WV: West Virginia Department of Transportation.

Zhao, D., Qian, X., Gu, X., Jajja, S. A., & Yang, R. (2016). Measurement techniques for thermal conductivity and interfacial thermal conductance of bulk and thin film materials. *Journal of Electronic Packaging*, 138(4), 040802.

APPENDIX A

CHANGES RECOMMENDED TO CURRENT SPECIAL PROVISION

In Appendix A, changes to GDOT Special Provision to Section 500 (GDOT, 2013) are recommended based on this study as well as the literature review (see Section 3.1). Appendix B provides the reason for the recommendations.

September 11, 2013

DEPARTMENT OF TRANSPORTATION

STATE OF GEORGIA

SPECIAL PROVISION

Section 500─Concrete Structures

Add the following to Subsection 500.1.02:

B. Referenced Documents

"Guide to Mass Concrete", ACI 207.1R-05.

"Report on Thermal and Volume Change Effects on Cracking of Mass Concrete", ACI 207.2R-07.

"Cooling and Insulating Systems for Mass Concrete", ACI 207.4R-05.

"Standard Practice for Selecting Proportions for Normal, Heavyweight, and Mass Concrete", ACI 211.1-91.

"Control of Cracking Concrete Structures", ACI 224R-01. "Specification of Structural Concrete", Section 8, ACI 301-10.

"Compressive Strength of Cylindrical Concrete Specimens", AASHTO T 22-10

"Making and Curing Concrete Test Specimens in the Laboratory", ASTM C192

Add the following to Subsection 500.3.05:

AM. Mass Concrete

Mass concrete is defined as "Any large volume of concrete with dimensions large enough to require that measures be taken to cope with the generation of heat and attendant volume change to minimize cracking". Any concrete element with a least dimension greater than 5ft (or greater than 6 ft diameter for a drilled shaft) shall be designated as mass concrete and will use this specification. [1-option A] Mass concrete elements shall be free of thermal cracks, which result from heat of hydration during the curing of the mass concrete. [1-option B] Mass concrete elements shall not

crack as a result of heat of hydration during the curing of the mass concrete. The introduction of a construction joint at a dimension less than 5 ft does not ensure that the maximum temperature attained by or the differential temperature in concrete is adequately controlled. Proposals for large volume concrete shall thus be evaluated based on the heat development and a Thermal Control Plan.

a. Temperature Specifications for Mass Concrete

Mass concrete shall conform to the concrete acceptance criteria and the following temperature requirements to prevent delayed ettringite formation (DEF) and thermally induced stress cracks:

1. The maximum allowable internal temperature of mass concrete meeting the requirements of Subsection 500.3.05.AM.b.1, shall not exceed 158 °F.
2. The maximum temperature differential between interior and exterior portions of the designated mass concrete element shall not exceed 35 °F.
3. The maximum temperature of the concrete when delivered and prior to placement shall be 85 °F.

b. Materials Selection and Mix Design Development

Materials used for mass concrete shall conform to the provisions in Section 500-Concrete Structures of GDOT Standard Specifications-Construction of Transportation Systems and the following requirements. When in conflict, materials shall conform to the special provisions below rather than those in Section 500.

1. Use Class F fly ash (no Class C fly ash is allowed), granulated iron blast-furnace slag or other pozzolans, if approved by the Department in all mass concrete. Slag may comprise no more than 75% by mass of total cementitious and pozzolanous materials. [2] If the slag is a sole cement replacement material or is used in combination with silica fume, fly ash and/or metakaolin, test the concrete mixture for durability (for example, complying with ASTM C1012 and/or C1567). Class F fly ash may comprise no more than 40% by mass of total cementitious and pozzolanous materials. When a combination of multiple different pozzolans is used, the total amount may be no more than 75% by mass of total cementitious and pozzolanous materials.
2. High-early-strength (ASTM C150 Type III or ASTM C1157 HE) cement, metakaolin, silica fume, calcium chloride and accelerating type admixtures shall not be used unless an adiabatic temperature study is completed showing temperature rise significantly less than that of plain unmodified concrete.
3. A retarding admixture, pretested with the job materials under job conditions, may be permitted to prevent cold joints due to the quantity of concrete placed, as approved by the Engineer.

4. Coarse aggregate larger than #5 stone maximum size aggregate is permitted to be used for mass concrete, if approved by the Engineer.
5. Other materials and/or mix designs may be proposed to the Engineer for approval, with documentation that the proposed mix designs meet temperature specifications from Subsection 500.3.05.AM.a for mass concrete.
6. Laboratory-designed mix proportions of materials are permitted for commonly used combinations of materials. Request these mixes in writing from the State Materials Engineer specifying the class of concrete and the source of ingredients.
7. Degree of Alkali-Silica Reactivity (ASR) of either fine or coarse aggregate is determined by testing the aggregates in ASTM C1260, or ASTM C1567 (either expansion shall be less than 0.10% after 14 days immersion). Unless the results of petrography indicate a significant change in the composition of materials in quarries, ASTM 1293 (expansion <0.04% at 1 year) is not required to be conducted, before a mix design can be approved by the Engineer. Alternatively obtain low ARS risk aggregate materials from certified suppliers.
8. The mixture will be capable of demonstrating a laboratory compressive strength at 28 [3] or 56 days meeting the requirements of Table 1 – Concrete Mix Table, Subsection 500.1.03.A. Compressive strength will be determined based upon result of six cylinders prepared and tested in accordance with AASHTO T 22 and ASTM C192.

c. Thermal Control Plan

At least 30 calendar days prior to placing any concrete defined as mass concrete, the contractor shall submit to the Engineer for approval a Thermal Control Plan (TCP). [4] Develop the TCP in accordance with Section 207 of the ACI Manual of Concrete Practice to meet the maximum allowable temperature and temperature differential limits. The TCP shall show complete analysis of the anticipated thermal developments in the mass concrete elements for all expected project temperature ranges using the proposed mix design, casting procedures and materials. A primary focus of the TCP is actions to take when any of the temperature controls noted in Subsection 500.3.05.AM are exceeded or are anticipated to be exceeded. As a minimum, the TCP shall include details about the following:

1. Concrete mix design showing composition, proportions, and sources for all components.
2. Proposed methods to control concrete temperature at time of placement, such as pre- cooling of raw materials or concrete.
3. Duration and method of curing.
4. Calculations of maximum concrete temperatures for the range of expected air, water (for underwater construction) and concrete temperatures.

5. Proposed methods to control maximum temperature during curing. A mechanical cooling system may be used to control the internal temperature of mass concrete during curing but shall be designed in conformance with the Thermal Control Plan. If a mechanical cooling system is used, the plans for the cooling system operation and final grouting after cooling shall be submitted to the Engineer for approval.

6. When the maximum concrete temperature nears 140 °F, notify the Engineer and take corrective measures immediately to retard further increase in the temperature to limit it to the 158 °F maximum. Utilize the mechanical cooling system, if installed, to lower the overall temperature. Other active measures may include, but not limited to for any further pours: chilled water for mixing, precooling aggregate stockpiles, ice for mixing water, nitrogen gas, and shade for aggregate stockpiles. Cease placement of concrete until the maximum temperature has been lowered.

7. Proposed methods to control temperature differentials during curing that could include insulation for the forms and exposed portions of concrete. Contractor must take actions that prevent the exterior surfaces of the concrete from getting too cool, too quickly such as using insulation or heater or by preventing the core from getting too hot.

8. When the internal concrete temperature differential between interior and exterior concrete nears 30 °F, notify the Engineer and take corrective measures immediately to retard further increase in the temperature differential to limit it to the 35 °F maximum. Utilize the mechanical cooling system, if being use, to lower the internal temperature. Other active measures may include, but not limited to: chilled water for mixing, precooling aggregate stockpiles, ice for mixing water, nitrogen gas, and shade for aggregate stockpiles. Cease placement of concrete until the temperature differential has been lowered.

9. Calculations of maximum temperature gradients within each concrete element during curing. Calculations shall include maximum possible temperature induced tensile stress in the concrete in addition to tensile stresses at 1 day, 3 days, 7 days, 28 days, and 56 days after placement. [5] Calculations shall include the time when the maximum concrete temperature and maximum temperature differential occur. The thermal calculation model and/or computational software shall be submitted to the Engineer for approval.

10. Temperature monitoring and recording system, that shall consist of temperature sensors connected to a data acquisition system. The temperature sensor types and locations shall be specified.

11. Results of strength tests of sample cylinders. The concrete shall attain the specified strength at an age (28 or 56 days) as specified by the Engineer. Match curing of concrete is required. Match curing shall be conducted according to temperature history obtained using thermocouples typically 2 to [6] 3 ~~6~~ inches from surface and at the centroid of the concrete pour. The depth of the thermocouple may need to be established by the depth of rebar or other anchoring structure (See Subsection 500.3.05.AM.d.3 and Subsection

500.3.05.AM.d.5).

12. For all mass concrete construction, the TCP shall be developed by a Professional Engineer, licensed in the State of Georgia, who shall be competent in the modeling, design, and temperature control of mass concrete with at least three mass concrete projects experience that can be verified by the Department.

Place no concrete until the mass concrete mix design and the proposed TCP is reviewed and approved by the Engineer. If concrete design mixture is changed, the TCP must be updated and approved by the Engineer.

d. Temperature Monitoring and Recording System

1. Install within the concrete placed in each mass pour and in the surrounding environment of the concrete, temperature sensing devices (thermocouples) of a type approved by and at locations based on the plan approved by the Engineer.
2. The sensing system will contain as a minimum two independent sets of sensing devices in order to assure readings if one of the systems fail. The sensing devices shall be accurate to within 2 °F range.
3. Thermocouples shall be placed at the centroid of the pour, or wherever the point of expected maximum temperature is anticipated. Additional thermocouples shall be placed on the exterior to monitor the maximum temperature differential. Ensure the thermocouples are placed at a depth of 2 to [7] 3 ~~6~~ inches below the surface.
4. The temperature monitoring and recording system for mass concrete shall consist of temperature sensors connected to a data acquisition system capable of printing, storing, and downloading data to a computer. Data shall be printed and submitted to the Engineer daily with a copy sent to Office of Materials and Testing.
5. Two independent sets of sensing devices shall be placed at each of the following locations and readings to be taken hourly [8] for the duration of the mass concrete temperature monitoring period (see item e.2 below): (1) center of the mass pour; (2) midpoint of the side which is the shortest distance from the center; (3) midpoint of the top surface; (4) midpoint of the bottom surface; and (5) corner of the mass pour which is furthest distance from the center. Ensure the thermocouples are placed at a depth of 2 to [9] 3 ~~6~~ inches below the surface.

e. Placing and Curing Mass Concrete

When placing and curing mass concrete do the following:

1. Maintain a temperature differential of 35 °F or less between the interior and exterior portions of the designated mass elements.
2. Monitor and maintain records of the concrete temperature, beginning with casting and continuing until the maximum temperature is reached and begins decreasing to a differential of no more than 35 °F from the mean [10-option

A] ~~annual~~ ambient temperature of the surrounding environment, for three consecutive days. [10-option B] from the average outside air temperature. The average outside air temperature shall be determined by averaging the daily high and low temperatures over the preceding three calendar days. [10-option C] from the average outside air temperature. The average outside air temperature shall be determined by averaging the daily low temperatures over the preceding three calendar days.

3. The contractor shall suggest consolidation techniques based on the placement technique to be used for mass concrete. The consolidation technique shall be reviewed and approved by the Engineer before start of placement of mass concrete. Slump tests or slump-flow (ASTM C 1611) tests, as applicable, shall be used to provide quality control from batch to batch.
4. Maintain a minimum concrete placement rate of 30 cubic yards per hour or as designated on the plans or in the Special Provisions. Any requested change from this placement rate is to be approved by the Engineer.

f. Acceptance

Mass concrete shall conform to the concrete acceptance criteria and the temperature requirements as stated earlier to prevent delayed ettringite formation (DEF) and thermally induced stress cracks.

If the Contractor fails to conform to any of the above temperature requirements in any one pour, any additional mass concrete pours will cease. The Engineer may, at its sole discretion, direct that the concrete be removed or otherwise mitigated, at no cost to the Department. The contractor shall revise the Thermal Control Plan and design calculations to correct the problem and resubmit the revised Thermal Control Plan. Mass concrete placement shall not begin until the Engineer has approved the revised Thermal Control Plan. No extension of time or compensation will be made for any rejected mass concrete element or revisions of the Thermal Control Plan.

APPENDIX B

BASIS FOR RECOMMENDATIONS SHOWN IN APPENDIX A

Recommended Item [1] - Addition

"[1-option A] Mass concrete elements shall be free of thermal cracks, which result from heat of hydration during the curing of the mass concrete."

OR

"[1-option B] Mass concrete elements shall not crack as a result of heat of hydration during the curing of the mass concrete."

Reason for the Recommendation [1]:

Four state DOTs include a similar statement (see below). Based on their recommendations, [1-option A] or [1-option B] is recommended. Option A is more stringent. Having such a specific statement ensures that the contractor delivers a mass concrete structure free of thermal cracking (i.e., a structure that does not develop thermal cracks).

- "Assume the responsibility to produce a structure free of cracks, which result from unnecessary heat of hydration during the curing of the mass concrete." (MnDOT, 2018)
- "Produce a structure free of shrinkage cracks that would be a result of heat of hydration during the curing of large concrete cross-sections." (Iowa DOT, 2015)
- "It is the Design-Builder's responsibility to determine which elements will be considered as Mass Concrete based on the temperature requirements of this specification and to ensure that elements do not crack as a result of temperature differentials." (DelDOT, 2016)

- “Produce a structure free from thermal cracks.” (DOTD, 2016)

Recommended Item [2] - Addition

“[2] If the slag is a sole cement replacement material or is used in combination with silica fume, fly ash and/or metakaolin, test the concrete mixture for durability (for example, complying with ASTM C1012 and/or C1567)."

Reason for the Recommendation [2]:

The change was recommended based on six state DOT specifications (see below) and the research findings presented in this dissertation. Please review Table 14 (see Page 100) for allowable slag limits specified by other state DOTs. They are as low as 25-35%. The existing statement, “Slag may comprise no more than 75% by mass of total cementitious and pozzolanous materials” could be interpreted as a 75% cement replacement by slag alone is allowed, in the absence of other SCMs. In this study, it is found that ternary replacement mixtures including slag such as SL40+FA30 and SL55+MK15 is promising for reducing heat of hydration, however, the durability must be further investigated.

- “Slag or fly ash may be used as a cementitious replacement material for cement up to a maximum limit of 75% by weight of total cementitious material in the mix.” (DelDOT, 2016)
- “Fly Ash - Ensure that the quantity of cement replaced with fly ash is 18% to 50% by weight, except where the core temperature is expected to rise above 165 °F. In that case, ensure that the percentage of fly ash is 35% to 50% by weight. Slag - Ensure that the quantity of cement replaced with slag is 50% to 70% by weight. Ensure that slag is 50% to 55% of total cementitious content by weight when used in combination with silica fume, ultrafine fly ash and/or metakaolin.” (FDOT, 2017)

- "Replace portland cement with fly ash at 20 percent to 50 percent by weight or replace with slag cement at 50 percent to 70 percent by weight or a ternary mix meeting specification requirement. Certify that the cementitious combination generates a heat of hydration of not more than 70 calories/gram at 7 days as determined by ASTM C186 or ASTM C1702." (DOTD, 2016)
- "Ternary mixes are defined as Portland cement and two other supplementary cementitious materials, or blended cement and one other supplementary cementitious material with a maximum replacement of 40% by weight." (MnDOT, 2018)
- "The Contractor may use slag as a replacement for cement as specified in 903.01, up to a maximum replacement level of 50 percent by weight of the total cementitious material. If more than 30 percent of cement is replaced, test the concrete mix design for scaling as specified in ASTM C 672, and ensure that it complies with a visual rating less than 3." (NJDOT, 2007)
- "The designed concrete mixture shall meet the following requirements: Strength: 56 day minimum compressive strength of 6,000 psi. Slump: 7" to 9". Entrained Air: 5 to 8%. • Water/Total Cementitious Material Ratio: 0.40 maximum. Class F Fly Ash – 20% to 50% by weight of cementitious materials or 30% to 70% GGBFS by weight of cementitious materials. Cement – Type I or II only • Total cementitious content: 700-lb/cy maximum." (NYSDOT, 2019)

Recommended Item [3] – Addition

In the following statement, it was recommended to add "or 56".

"Cementitious material content shall be the minimum required to meet the target strength. The mixture will be capable of demonstrating a laboratory compressive strength at 28 or

56 days meeting the requirements of Table 1 – Concrete Mix Table, Subsection 500.1.03.A. Compressive strength will be determined based upon result of six cylinders prepared and tested in accordance with AASHTO T 22 and ASTM C192."

Reason for the Recommendation [3]:

The recommended change is consistent with the existing Special Provision (Section C.11).

Recommended Item [4] - Addition

"[4] Develop the TCP in accordance with Section 207 of the ACI Manual of Concrete Practice to meet the maximum allowable temperature and temperature differential limits."

Reason for the Recommendation [4]:

Three state DOTs including FDOT recommend developing a temperature thermal control plan per ACI. This statement ensures that contractors follow the standard procedures.

- "Develop the MCCP in accordance with Section 207 of the ACI Manual of Concrete Practice to ensure concrete core temperatures for any mass concrete element do not exceed the maximum allowable core temperature of 180 °F and that the temperature differential between the element core and surface do not exceed the maximum allowable temperature differential of 35 °F." (FDOT, 2017)
- "Provide temperature control of these elements in accordance with ACI 207.1R-05, "Guide to Mass Concrete," ACI 207.2R-07, "Report on Thermal and Volume Change Effects on Cracking of Mass Concrete," and ACI 207.4R-05, "Cooling and Insulating Systems for Mass Concrete." (MnDOT, 2018)
- "The Thermal Control Plan shall at a minimum include a Heat Dissipation Study (Reference ACI 207 or thermal modeling software) as well as to describe the measures

and procedures the Contractor intends to use to satisfy the Temperature Control Requirements for each mass concrete element." (NYSDOT, 2019)

Recommended Item [5] - Addition

"[5] Calculations shall include the time when the maximum concrete temperature and maximum temperature differential occur."

Reason for the Recommendation [5]:

Understanding the time when the maximum internal temperature and differential temperature occur helps the department and its contractor with a thermal control plan and curing mass concrete elements. Iowa DOT recommends a similar statement.

- "The thermal control plan should include the selected mathematical method for evaluating heat of hydration thermal effects, which shall include the calculated adiabatic temperature rise, calculated maximum concrete temperature, and calculated maximum temperature differential between the internal concrete core and concrete 2 to 3 in. (50 to 75 mm) from the exposed surface. The time when the maximum concrete temperature and maximum temperature differential will occur is required." (IDOT, 2016)
- The results from this study show that the time of maximum temperature and temperature differential changes significantly with the type of cementitious materials used in the concrete. Additionally, the time of maximum temperature differential is significantly affected by the type of formwork and insulation materials as well as the time of formwork removal.

Recommended Item [6 and 7] - Replacement

In the following statements, it is recommended to replace "6" with "3".

“Match curing shall be conducted according to temperature history obtained using thermocouples typically 2 to 3 ~~6~~ inches from surface and at the centroid of the concrete pour.”

“Additional thermocouples shall be placed on the exterior to monitor the maximum temperature differential. Ensure the thermocouples are placed at a depth of 2 to 3 ~~6~~ inches below the surface.”

Reason for the Recommendation [6 and 7]:

Based on the review of other state DOT specifications, 2 to 3 inches are recommended. Measuring temperature at a depth of 6 inches reduces the maximum temperature differential. In case of the bridge seal structure studied herein, a 5% reduction was observed.

- “The maximum temperature differential between the internal concrete core and concrete 2 to 3 in. (50 to 75 mm) from the exposed surface shall not exceed 35 °F (19 °C).” (IDOT, 2016)
- “For each placement of structural mass concrete, two temperature sensors shall be installed at each of the following locations (for a total of eight temperature sensors): Center of the placement, midpoint of the side which is the shortest distance from the center (2 inch to 4 inch cover), midpoint of the top surface (2 inch to 4 inch cover), and air temperature.” (Iowa DOT, 2015)
- “Generally, use one monitoring point in the center of the largest mass of concrete and a second point approximately 2 inches inside the face nearest to the first monitoring point.” (SCDOT, 2007)

- "Install devices to measure the surface temperature no more than 3 in. from the surface." (TxDOT, 2014)
- "Thermocouples shall be installed so that one is located 2 inches (50 mm) from the top of flat placements or side of vertical placements, one is located 2 inches (50 mm) from the bottom of flat placements or other side of vertical placements, and the third is located midway between the first and second thermocouples." (MassDOT, 2015)

Recommended Item [8] - Addition

"Two independent sets of sensing devices shall be placed at each of the following locations and readings to be taken hourly [8] for the duration of the mass concrete temperature monitoring period (see item e.2 below):"

Reason for the Recommendation [8]:

The phrase is added to the item from the GDOT Special Provision to clearly specify the duration of temperature monitoring.

- "Temperatures shall be electronically recorded automatically by an approved recorder furnished by the Contractor and shall be capable of continuously recording a minimum of one reading per hour for the duration of the mass concrete temperature monitoring period." (Iowa DOT, 2015)

Recommended Item [9] - Replacement

In the following statements, it is recommended to replace "6" with "3".

"Ensure the thermocouples are placed at a depth of 2 to [9] 3 ~~6~~ inches below the surface."

Reason for the Recommendation [9]:

See the reason for items 6 and 7.

Recommended Item [10] - Revision

"Monitor and maintain records of the concrete temperature, beginning with casting and continuing until the maximum temperature is reached and begins decreasing to a differential of no more than 35 °F from the mean annual ambient temperature of the surrounding environment, for three consecutive days."

In the above statement, three options are given:

- [option-A] to eliminate "annual"
- [option-B] replace "from the mean annual ambient temperature of the surrounding environment, for three consecutive days" with "from the average outside air temperature. The average outside air temperature shall be determined by averaging the daily high and low temperatures over the preceding three calendar days."
- [option-C] replace "from the mean annual ambient temperature of the surrounding environment, for three consecutive days" with "from the average outside air temperature. The average outside air temperature shall be determined by averaging the daily low temperatures over the preceding three calendar days."

Reason for the Recommendation [10]:

Option A: Using the "mean annual ambient temperature" could yield less conservative measurements than using the mean daily ambient temperature.

Option B: the revised statement clearly communicates how to determine the average outside air temperature.

Option C: yields the most conservative ambient temperature for mitigating thermal cracks.

The following list five state DOTs' recommendations associated with the revision listed above:

- “Thermal control of each placement shall be maintained until the temperature of the interior is within 50ºF of the average outside air temperature. The average outside air temperature shall be determined by averaging the daily high and low temperatures over the preceding seven calendar days.” (Iowa DOT, 2015)
- “Maintain thermal control of each placement until the temperature at the center is within 35 °F of the average outside air temperature. Determine the average outside air temperature by averaging the daily high and low temperatures over the preceding 7 calendar days.” (KYTC, 2012)
- “Mass concrete should remain covered and monitored until the difference between the core temperature and the average daily ambient temperature is below 35 °F.” (NCDOT, 2018)
- “Mass concrete temperature control procedures shall remain in effect until the temperature differential between the average peak temperature and the 3-day mean ambient low temperature is less than 35 °F.” (RIDOT, 2016)
- “The data logger shall record the temperatures at each thermocouple at least once every hour from the time the thermocouple is covered with concrete until 3 days after the peak temperature is reached, or as directed by the Engineer.” (VDOT, 2016)

APPENDIX C

OTHER RECOMMENDATIONS FROM STATE DOT REVIEW

In this section, a summary of the literature review from the mass concrete standard specifications per ACI and state DOTs (Sections 3.1.1 and 3.1.2) is presented.

1. Summary of Literature Review:

The summary of the literature review ranges from mass concrete definition to temperature limits, material selection, and thermal control plan.

Mass Concrete Definition

The definition of mass concrete is specified by three criteria: minimum dimension, volume-to-surface-area ratio, and minimizing of cracking due to heat generation.

- The minimum dimension criteria needed to specify an element as a mass concrete placement ranges from 3 ft to 7 ft. The most specified limit is 4 and 5 ft among the DOTs.
- The volume-to-surface area ratios of 1 ft and 0.6 ft are used in connection with the minimum dimension requirement of 3 ft by Florida and Rhode Island DOTs, respectively.
- In addition to the minimum dimension criteria, a number of state DOTs (California, Georgia, and Massachusetts) define the mass concrete per the ACI definition of mass concrete: “Any large volume of cast in place concrete with dimensions large

enough to require that measures be taken to cope with generation of heat and attendant volume change to minimize cracking."

Maximum temperature and temperature differential limits

- Maximum Temperature:

  In the majority of the state DOTs, the maximum temperature limit in mass concrete is specified at 158 to 160 °F, which is similar to the maximum temperature specified by ACI. Two state DOTs allow a higher maximum temperature: Florida and Virginia DOTs. Florida DOT allows the maximum temperature of 180 °F when fly ash is used, and Virginia DOT allows the maximum temperature of 170 °F when slag is used. On the other hand, Massachusetts and Rhode Island DOTs allow a maximum temperature of only 154 °F and 155 °F, respectively.

- Maximum Temperature Differential:

  In most of the state DOTs, the maximum temperature differential is limited at 35 °F regardless of the age or strength of the concrete, which is again similar to the limit specified by ACI. A slightly higher temperature differential is allowed by few DOTs: Arkansas and Ohio allow 36 °F, Massachusetts allows 38 °F, and West Virginia allows 40 °F. Few state DOTs (Delaware, Illinois, Iowa, and Minnesota) allow a variable maximum temperature differential vs time based on the strength and maturity of the concrete. The variable maximum temperature differential limits per each state is as follow: 30-60 °F per Delaware, up to 50 °F per Illinois, 20-50 °F per Iowa, and 45-60 °F per Minnesota.

Maximum placement temperature

The limit on maximum placement temperature varies between 70 °F and 90 °F. Delaware, Iowa, and Kentucky DOTs are on the lower end of that range, whereas Mississippi, Ohio, and Virginia DOTs are on the higher end.

Maximum and minimum total SCM content

A few state DOTs specify minimum cementitious material content required to meet the target strength.

- Maximum Total SCM Content:

  Most of the state DOTs do not have a limit on the maximum total SCM content in the mass concrete mixture. Only four DOTs specify the maximum limit: 720-750 lb/cy for pile per California DOT, 700 lb/cy per New York and Texas DOTs, and 600 lb/cy per North Carolina and Rhode Island DOTs.

- Minimum Total SCM Content:

  A range of minimum total SCM content (470 to 680 lb/cy) is specified among the DOTs, generally based on the type of cement, placement geometry and condition.

Percentage of SCMs replacement allowed

- Fly Ash (Class F):

  The maximum cement replacement with fly ash varies between 20 and 50%. Among the state DOTs, 10 DOTs allow a maximum replacement level less than 30%, and 8 DOTs allow a maximum replacement level more than 30%.

- Slag:

  The maximum replacement level with slag varies between 25 to 75%, with a 50% replacement being most common among the state DOTs. Nine state DOTs allow maximum replacement level lower than 50%, and 10 DOTs allow maximum replacement level ≥ 50%.

- Ternary replacement mixture:

  Among the state DOTs, 12 of them allow the use of ternary replacement mixtures (generally fly ash and slag) in mass concrete placements. The individual limit on each SCM is commonly applied to their limits in the ternary mixtures as well. The use of metakaolin in ternary replacement mixtures is prescribed only in Florida, Illinois, and Texas DOTs, and only Illinois DOT has specified its maximum limit at 5%. Meanwhile, six DOTs have allowed the use of silica fume at a maximum replacement level ranging between 5 and 10%.

<u>Compressive strength and/or heat of hydration requirements</u>

- Compressive Strength

  The minimum 28 days compressive strength ranges between 2500 and 4500 psi among the state DOTs. Most of the DOTs also allow the 56 days compressive strength criteria due to the use of SCMS, which have a higher rate of strength development at later ages**.**

- Heat of Hydration

  Only two state DOTs have specified the limit on the heat of hydration or maximum adiabatic temperature rise: Louisiana DOT limits the heat of hydration at 70

calories/gm at 7 days, and Rhode Island DOT limits the maximum adiabatic temperature rise at 75 °F.

Water to cementitious material ratio and slump requirements

- Water-to-cementitious material ratio (w/c)

  The maximum water to cementitious ratio (w/c) changes among the state DOTs, ranging between 0.4 and 0.58. Nine state DOTs have the maximum w/c limit of 0.45 or lower, and six state DOTs have the maximum w/c > 0.45.

- Slump

  Two ranges of slump are observed among the state DOTS: six state DOTs specify slump around 4", and seven state DOTs specify slump up to 8".

Curing and formwork requirements

- Curing

  The curing period of mass concrete changes between 3 to 14 days among the state DOTs, with 14 days being observed the most. Burlap blanket is commonly suggested for curing.

- Formwork

  The time of formwork removal is about 4 to 7 days. The formwork shall be kept until the temperature differential is under 35 °F and continue decreasing. The concrete should have sufficient strength to withstand the anticipated thermal gradient before the formwork is stripped.

Methods to cool down concrete temperature

The methods to cool down concrete temperature consist of pre-cooling of the concrete ingredients and post-cooling of the concrete placement. The common pre-cooling practices include: using ice in the mixing water (no frozen pieces of ice after mixing), storing cement and aggregates in cool or shaded locations, sprinkle coarse aggregate with water or wet the stockpile, controlling rate of concrete placement, placing concrete at times of day when the ambient temperature is lowest (in summer) or highest (in winter), and use of liquid nitrogen system to cool the concrete mass before placement. The most common post-cooling practice includes the use of mechanical cooling pipes in the concrete to control the internal temperature of mass concrete during curing and conformance with the Thermal Control Plan.

The methods to control temperature differential, in addition to the practices with lowering internal temperature, include: insulating the forms and the surface of the concrete, providing supplemental external heat at the concrete surface to prevent heat loss.

Temperature monitoring requirements

The temperature monitoring period begins when the casting is complete and continuing until the temperature at the center is within 35 °F of the 3-day or 7-day average daily ambient temperature. A monitoring period of 7 to 14 days is commonly specified among the state DOTs.

2. Additional Recommendations:

From state DOT specifications, the research team has selected nine items and statements worth considering.

Recommendation [1]:

"Instead of the temperature differential limit of 35 °F, the contractor may propose, for consideration by the Engineer, a plan to use a performance-based criteria for a variable temperature differential limit, based on the concrete strength as determined by the maturity at any given time. Based on strength gain of the concrete, multiple maximum temperature differentials at different times may be proposed. The proposed temperature differential, however, shall not exceed 50 °F (28 °C). The proposed value shall be justified through a finite element analysis or a mathematical method. Use test data from the actual concrete placed in the element to define any specific input properties of the concrete used in the model. The calculated thermal stresses developed within the concrete shall not exceed the tensile strength of the concrete, and a safety factor of at least two (2) shall be applied to all stress calculations. At least 60 calendar days prior to casting a mass concrete element that utilizes differential temperature vs. concrete strength curves, submit the finite element analysis or the mathematical model as part of the Mass Concrete Placement and Temperature Plan."

Reason for the Recommendation [1]:

- "The Contractor may propose, for consideration by the Engineer, differential temperature vs. concrete strength curves based upon the following:

  1. A finite element analysis revealing the calculated thermal stresses developed within the concrete will not exceed the tensile strength of the concrete,

  2. Use test data from the actual concrete placed in the element to define any specific input properties of the concrete used in the model,

  3. Apply a safety factor of at least two (2) to all stress calculations,

4. At least 60 calendar days prior to casting a mass concrete element that utilizes differential temperature vs. concrete strength curves, submit the finite element analysis as part of the Mass Concrete Placement and Temperature Plan,

5. The Engineer reserves the right to allow and discontinue use of the strength curves based on cracking observed on previous concrete elements, and

6. On concrete placements where differential temperature vs. concrete strength curves are allowed for use by the Engineer, the allowable differential temperature referenced in Table MC-11 will be determined from the curves." (MnDOT, 2018)

- "After the Contractor has established, to the satisfaction of the Engineer, that proper control can be maintained of the concrete mix properties, including curing temperatures, the Contractor shall have the option of submitting a plan to use a performance-based criteria for a variable differential limit, based on the concrete strength as determined by the maturity at any given time. This will supersede the 35 °F limit. Failure to maintain proper temperature control under this plan will result in reversion to the 35 °F limit for subsequent placements until such time that the Contractor demonstrates to the Engineer that causes for the loss of control have been identified and corrected." (RIDOT, 2016)
- "The Contractor has the option to propose a higher maximum temperature differential between the internal concrete core and concrete 2 to 3 in. (50 to 75 mm) from the exposed surface, but the proposed temperature differential shall not exceed 50 °F (27.8 °C). In addition, based on strength gain of the concrete, multiple maximum temperature differentials at different times may be proposed. The proposed value shall be justified through a mathematical method." (IDOT, 2016)

Recommendation [2]:

"The use of special cements or additives that will reduce heat of hydration is permitted meeting the minimum strength and durability requirements."

Reason for the Recommendation [2]:

"The Department will allow the inclusion of the following items in the Thermal Control Plan: Use of special cements or additives that will reduce heat of hydration without affecting strength or durability." (KYTC, 2012)

Recommendation [3]:

"Ternary mixtures are defined as Portland cement and two other supplementary cementitious materials, or blended cement and one other supplementary cementitious material. The ternary replacement mixtures of class F fly ash and slag or slag and metakaolin is permitted. The individual limits of each SCM shall apply to ternary mixtures and the total amount shall not exceed 75% by weight of total cementitious materials in the mixture."

Reason for the Recommendation [3]:

- The results of this study illustrate the significance of ternary replacement mixtures of both (fly ash and slag) and (slag and metakaolin) in controlling the heat of hydration and temperature rise in mass concrete placements.
- "Ternary mixes are defined as Portland cement and two other supplementary cementitious materials, or blended cement and one other supplementary cementitious material with a maximum replacement of 40% by weight. The maximum %SCM

(FA/SL/SF/ternary) of (30/70/5/70) for mass concrete pier and foundation. The individual limits of each SCM shall apply to ternary mixtures." (MnDOT, 2018)

Recommendation [4]:

"Cementitious material content shall be the minimum required to meet the target strength. The mixture design shall produce a workable and durable concrete meeting the 28 or 56 days compressive strength requirements."

Reason for the Recommendation [4]:

- The total cementitious content shall be the minimum to lower the heat generation. The results of this study also show that the use of supplementary cementitious materials at certain replacement levels can compromise strength or durability.
- "Concrete used in mass concrete pours shall not exceed Class A4. Cementitious material content shall be the minimum required to meet the target strength. Water/Cementitious material ratio shall be limited to 0.4 maximum." (VDOT, 2016)
- "The mix design shall produce a workable and durable concrete meeting the minimum strength requirements specified in Table 802-1 and shall have a low heat of hydration when placed in large quantities." (ArDOT, 2014)

Recommendation [5]:

"Mass concrete elements exposed to water shall have reached at least 28 days compressive strength as indicated by the approved Maturity Curve and shall have a peak temperature-to-water temperature differential less than 35 °F prior to exposure." (RIDOT, 2016)

Recommendation [6]:

"Form and insulation removal shall be done in a manner to prevent cracking and ensure the maximum temperature differential is maintained. Insulation shall be in good condition as determined by the Engineer and properly attached. In no event will form stripping be allowed before the surface concrete reaches at least 80 percent of its design strength. After form striping, concrete shall be protected from freezing temperatures for 48 hours by of insulating blankets or other methods approved by the Engineer."

Reason for the Recommendation [6]:

- "Form and insulation removal shall be done in a manner to prevent cracking and ensure the maximum temperature differential is maintained. Insulation shall be in good condition as determined by the Engineer and properly attached." (IDOT, 2016)
- "For mass concrete placements with a least dimension of less than or equal to 6.5 feet the TCP procedures may include, but are not limited to, the following: Insulating the forms and the surface of the concrete to prevent temperature differential." (Iowa DOT, 2015)
- "The forms may be stripped when the concrete strength is high enough (as determined by the maturity curves or match-cast cylinders) to withstand the anticipated thermal gradient between the core temperature and the 48-hour average air temperature. In no event will form stripping be allowed before the surface concrete reaches at least 80 percent of its design strength. After form striping, concrete shall be protected from freezing temperatures for 48 hours by of insulating blankets or other methods approved by the Engineer." (VDOT, 2016)

Recommendation [7]:

"All mass concrete elements shall be kept completely and continuously moist by means of moisture retention. White polyethylene sheeting meeting the requirements of 707.10 shall be used. The sheeting shall be installed, and joints shall be sealed, so as to prevent as much moisture loss as possible. Water curing shall not be permitted. Curing shall be continued for a period of at least 7 calendar days." (WVDOT, 2010)

Recommendation [8]:

"The temperature of any water used for moist curing of mass concrete shall be controlled to within 30 °F of the peak concrete temperature." (RIDOT, 2016)

Recommendation [9]:

"[24] A crack may require repair by the Contractor as determined by the Engineer. The Contractor shall be responsible for the repair of all cracks. Protective coat or a concrete sealer shall be applied to a crack less than 0.007 in. (0.18 mm) in width. A crack that is 0.007 in. (0.18 mm) or greater shall be pressure injected with epoxy at no additional cost to the Department."

Reason for the Recommendation [9]:

- "(d) Inspection and Repair of Cracks. The Engineer will inspect the concrete for cracks after the temperature monitoring is discontinued, and the Contractor shall provide access for the Engineer to do the inspection. A crack may require repair by the Contractor as determined by the Engineer. The Contractor shall be responsible for the repair of all cracks. Protective coat or a concrete sealer shall be applied to a crack less than 0.007 in. (0.18 mm)

in width. A crack that is 0.007 in. (0.18 mm) or greater shall be pressure injected with epoxy according to Section 590." (IDOT, 2016)

- "Any cracks in the structural element greater than 0.012" resulting from the contractor's inability to properly maintain concrete temperature differentials, shall be repaired using epoxy injection at no additional cost to the Department." (NYSDOT, 2019)

APPENDIX D

BRIDGE SEAL ANALYSIS WITH A RECTANGULAR COLUMN

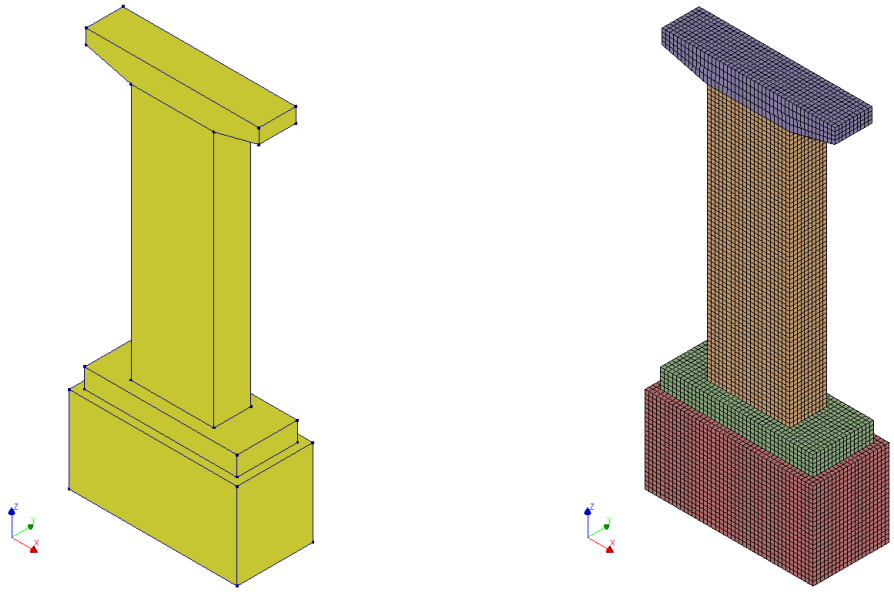

(a) three-dimensional geometry (b) meshing of the model

Figure D.1 – Bridge bent mass concrete structure with rectangular column in DIANA.

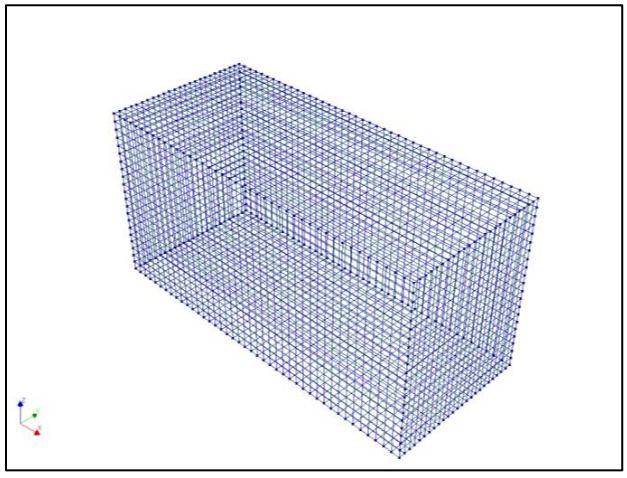

Figure D.2 – Rebar arrangement in the bridge seal.

D.1 Winter Placement Condition:

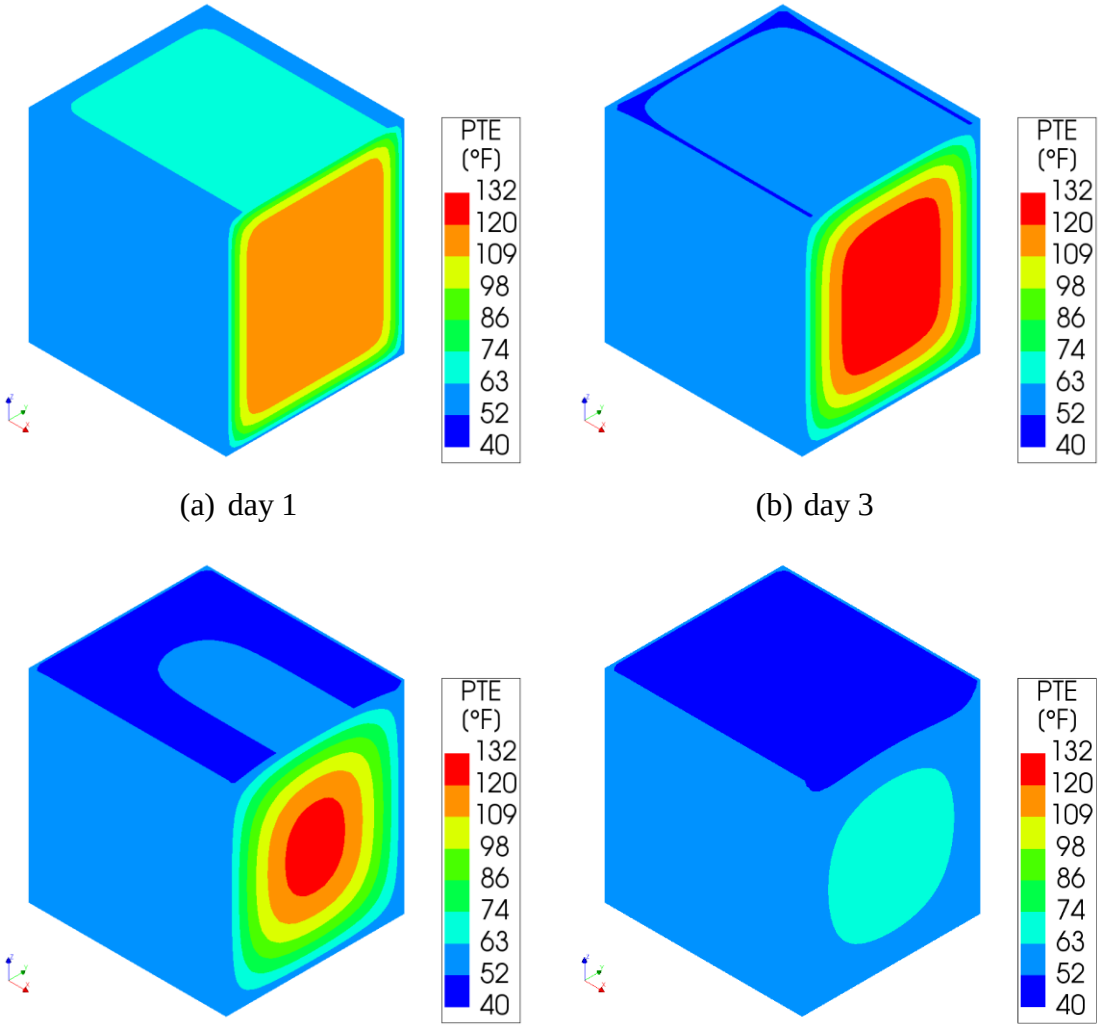

(a) day 1 (b) day 3

(c) day 7 (d) day 28

Figure D.3 – Temperature distribution in the bridge seal up to 28 days after seal placement in winter condition.

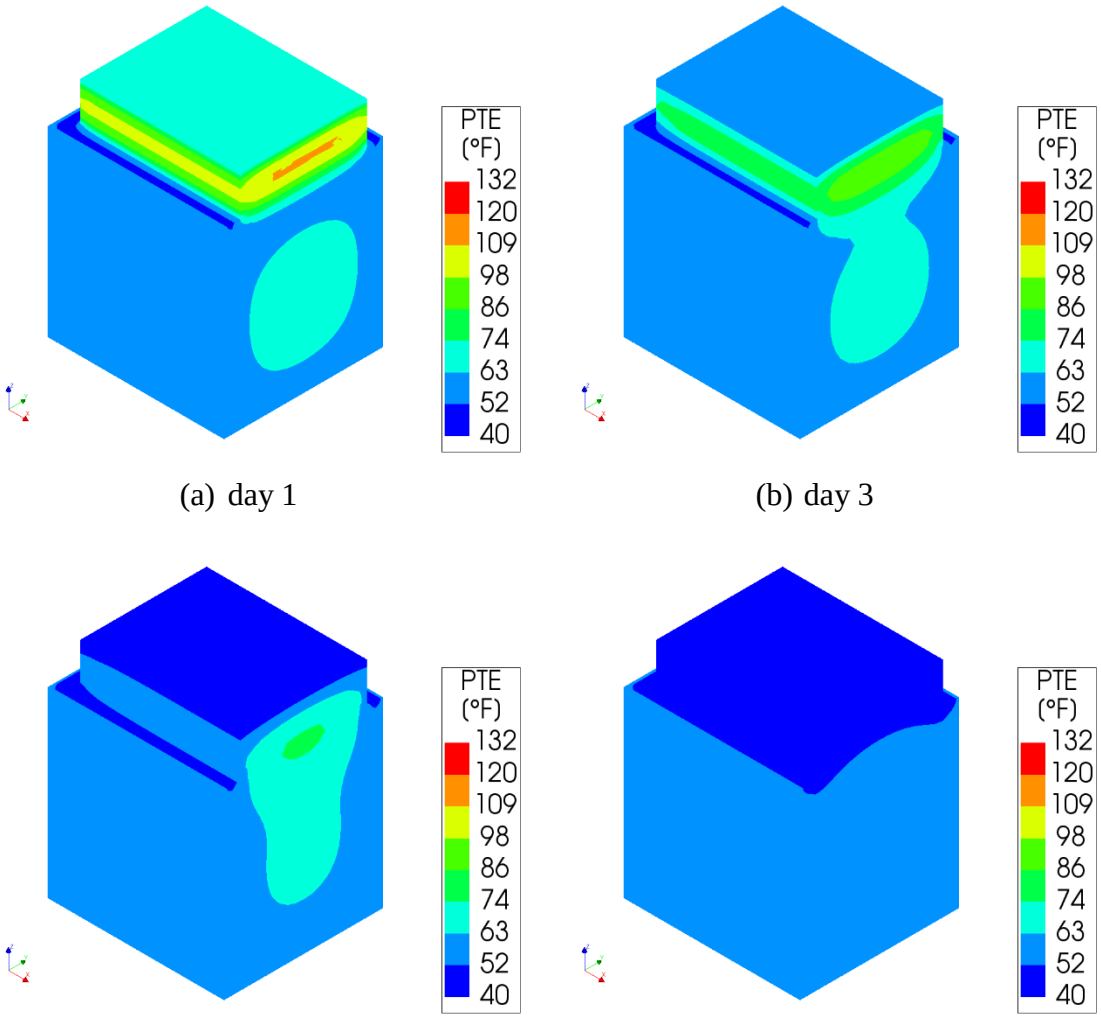

(a) day 1 (b) day 3

(c) day 7 (d) day 28

Figure D.4 – Temperature distribution in the bridge seal and footing up to 28 days after bridge footing placement in winter condition.

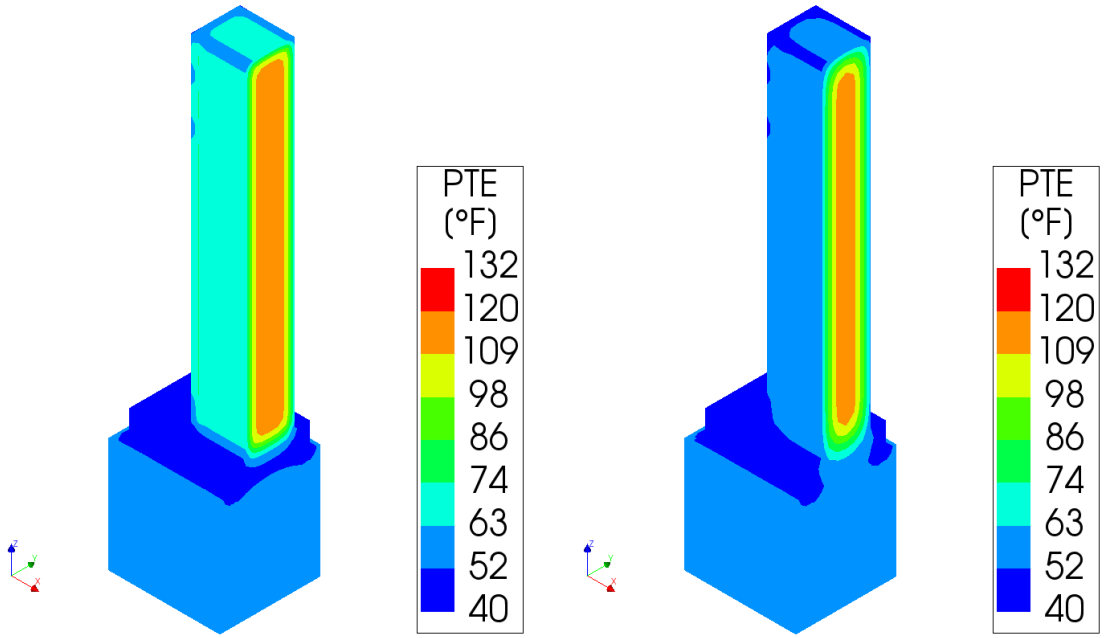

(a) day 1

(b) day 3

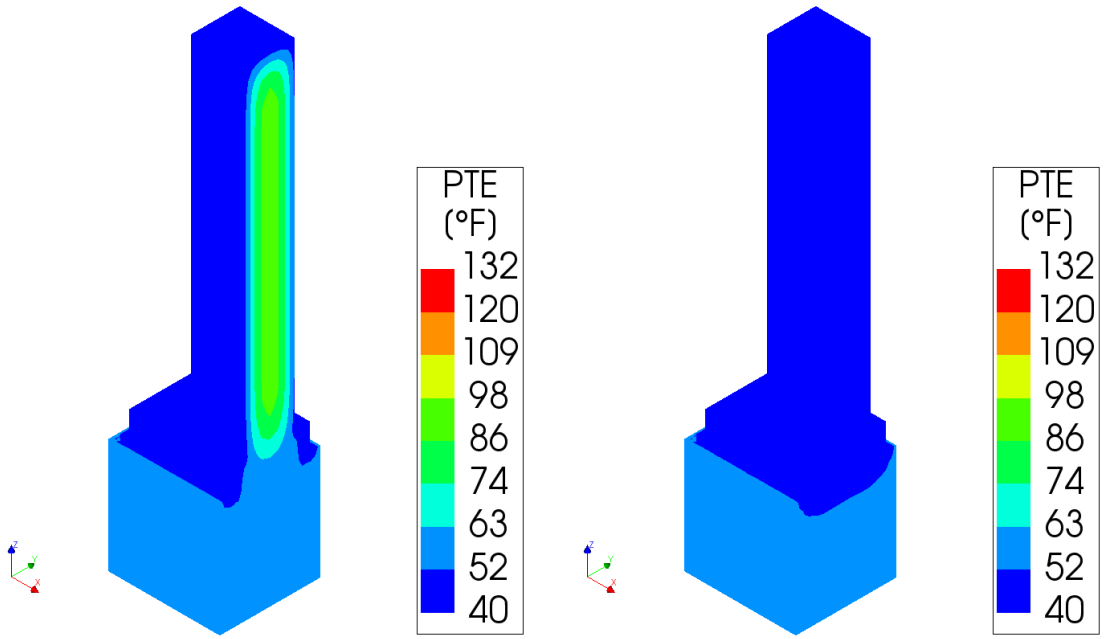

(c) day 7

(d) day 28

Figure D.5 – Temperature distribution in the bridge seal, footing, and column up to 28 days after column placement in winter condition.

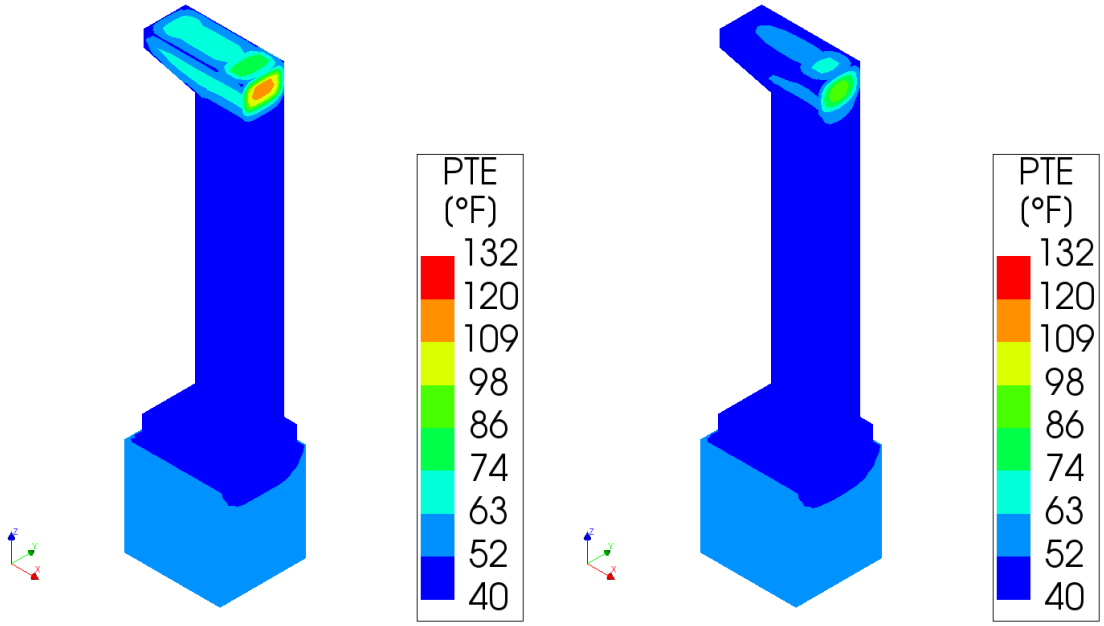

(a) day 1 (b) day 3

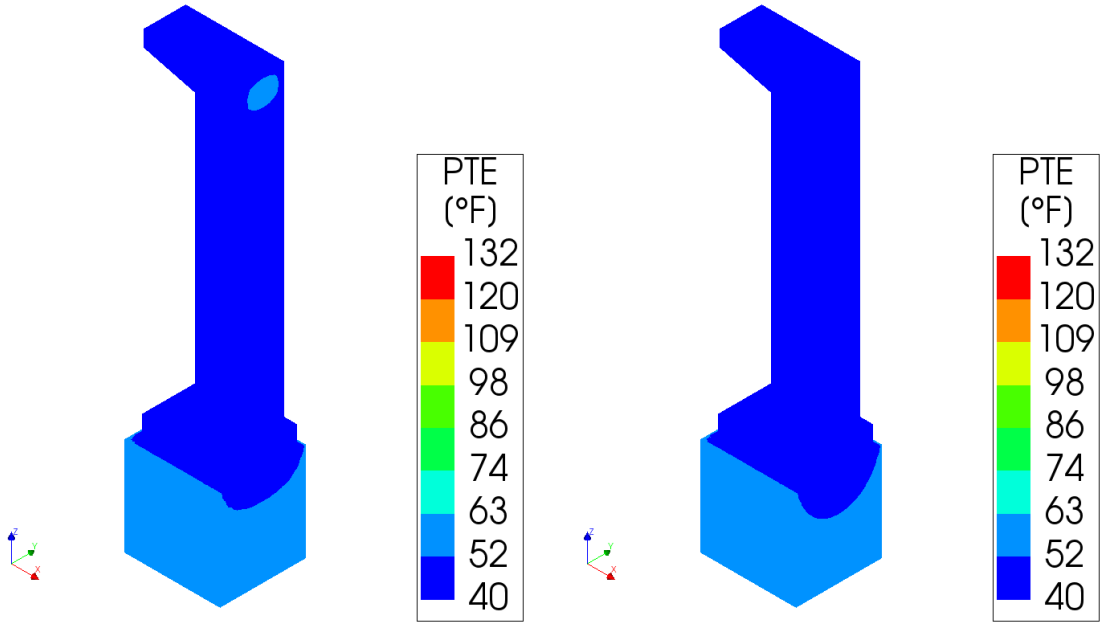

(c) day 7 (d) day 28

Figure D.6 – Temperature distribution in the bridge seal, footing, column, and cap up to 28 days after cap placement in winter condition.

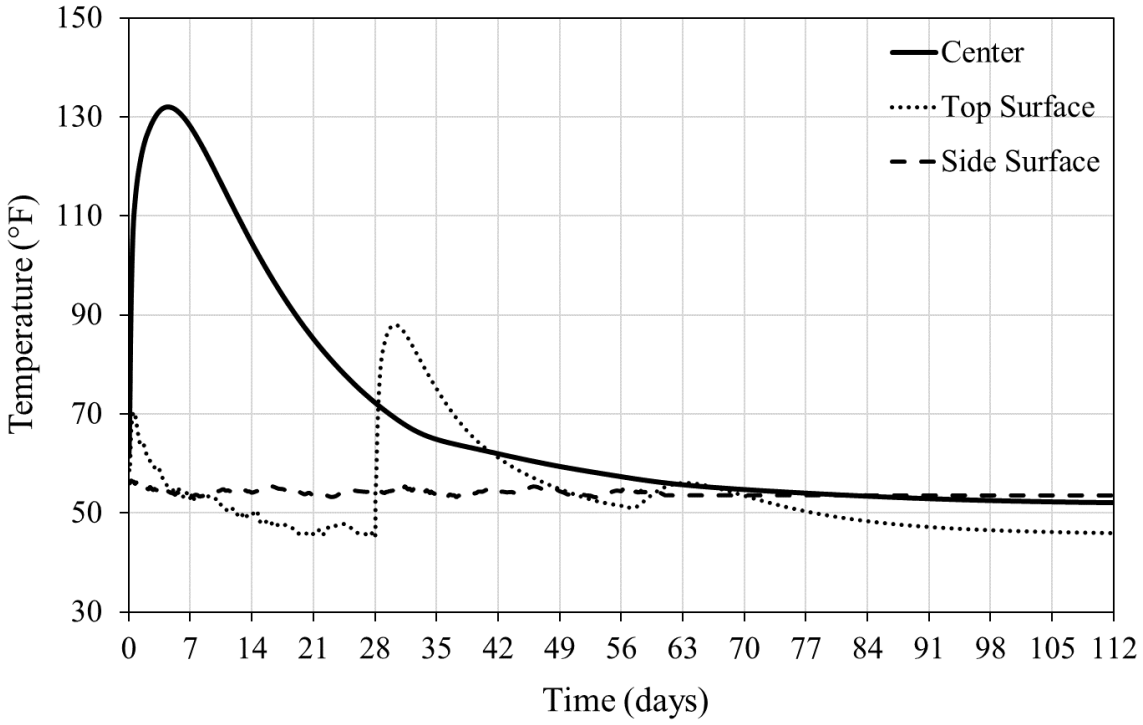

Figure D.7 – Temperature development in the bridge seal in winter placement.

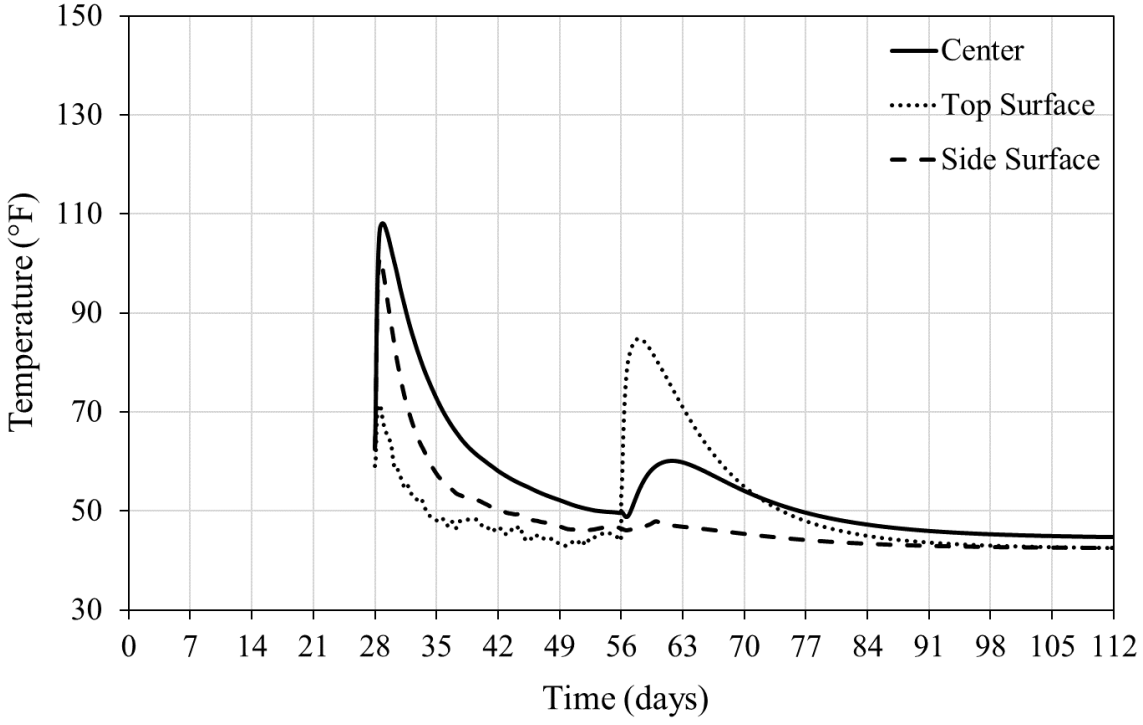

Figure D.8 – Temperature development in the footing in winter placement.

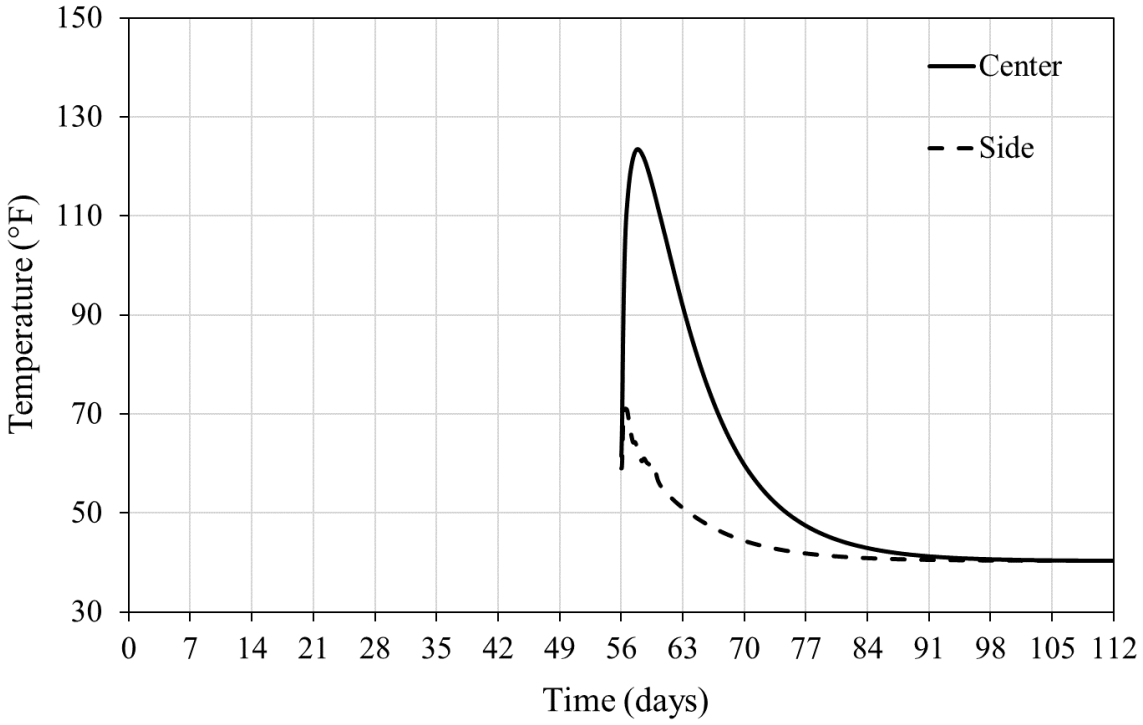

Figure D.9 – Temperature development in the column in winter placement.

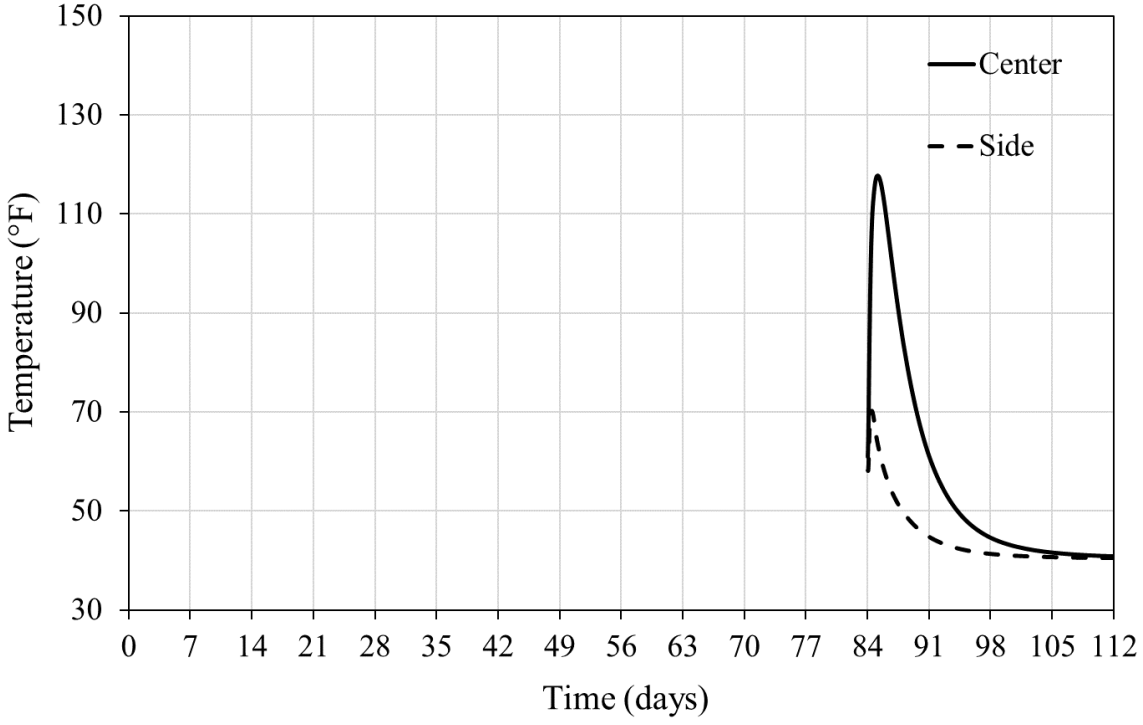

Figure D.10 – Temperature development in the cap in winter placement.

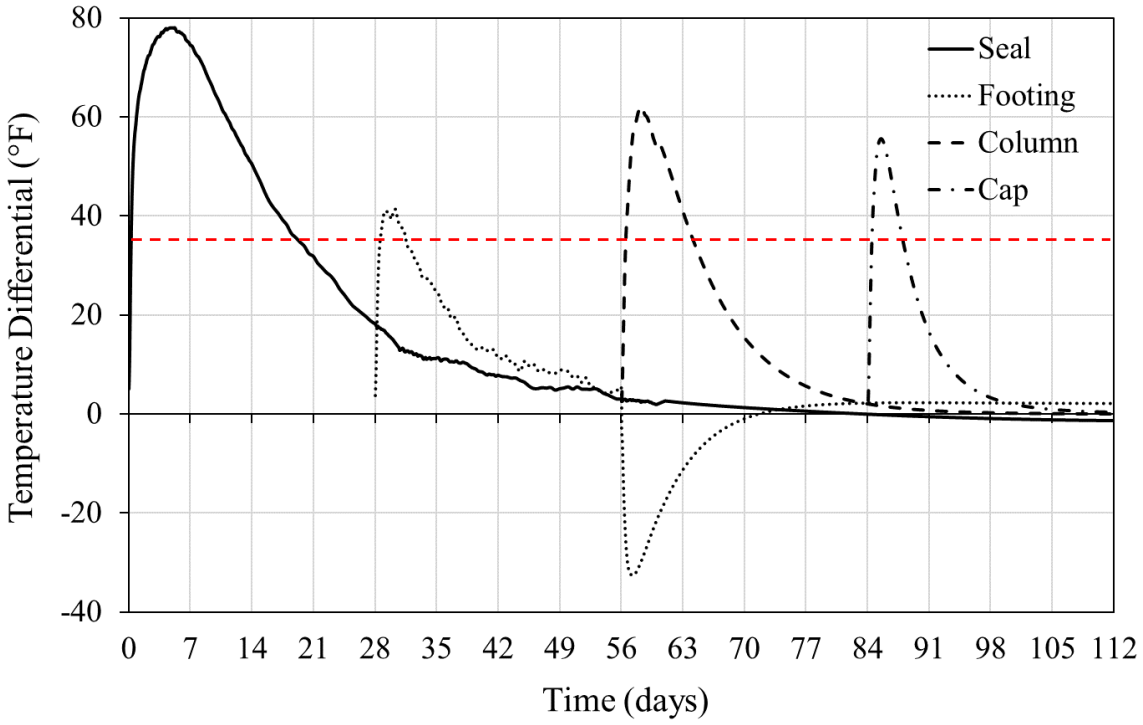

Figure D.11 – Temperature differential development in the bridge seal structure in winter placement

APPENDIX E

VALIDATION OF STRAIN FROM GRADIENT TEMPERATURE

Background

Tensile strain is computed by Eq. E-1, where ε = tensile strain due to temperature change, α=coefficient of thermal expansion, and ΔT=temperature change.

$$\varepsilon = \alpha * \Delta T \quad \text{Eq. E-1}$$

The increased temperature at the core of a mass concrete section results in thermal expansion. However, this expansion is restrained by both the contraction of the cooler surface and by external restraints, if any. To simplify this complexity, it is assumed that the total thermal strain can be estimated by Eq. E-2, where the maximum temperature rise and maximum temperature differential are indicated as $\varepsilon_{temp.rise}$ and $\varepsilon_{temp.diff.}$

$$\varepsilon_{total} = \varepsilon_{temp.rise} + \varepsilon_{temp.diff.} \quad \text{Eq. E-2}$$

By assuming a fully externally restraint condition at the concrete core, the total induced tensile strain is computed by Eq. E-3:

$$\varepsilon_{total} = \alpha * \Delta T_{(temp.rise+temp.diff.)} \quad \text{Eq. E-3}$$

If this tensile strain exceeds the tensile strain capacity of the concrete, the section should crack. To quantify the total strain in concrete, an experimental program is designed. It consists of small concrete cylinder specimens exposed to elevated temperature reflecting the total effect of both temperature rise and temperature differential shown in Table E.1. Three concrete mixtures, FA45, SL30+MK15, and SL40+FA30 are considered. The maximum allowable temperature is commonly limited to 158 °F (70 °C) and the maximum

temperature differential is limited to 35 °F (19.4 °C). In order to evaluate these temperature limits, two cases are considered as shown in Table E.1. This means that the oven temperature for small cylinder specimens must reach 208 °F (97.8 °C), slightly short of the boiling temperature, 212 °F (100 °C).

Table E.1 – Temperature for Measurement Strains.

Cases	Temperature Conditions		
	Maximum Allowable Temperature, °F (°C)	Maximum Temperature Differential, °F (°C)	Oven Temperature (Maximum Temperature + Temperature Differential) °F (°C)
1	158 (70.0)	50 (27.8)	208 (97.8)
2	170 (76.7)	35 (19.4)	205 (96.1)

Testing Procedure

From each mixture, two concrete cylinders are prepared and exposed to the temperature conditions (reaching 208 °F or 97.8 °C), representing the maximum strain state in the core of a mass concrete structure. Temperature and strain measurements recorded for one week (1 day of normal hardening plus six days of exposure to elevated temperature). The procedure in preparing and testing the cylinders for temperature and strain measurements are as follow:

1. Concrete cylinders are prepared for each mixture, and strain and temperature gauges are vertically placed and embedded inside the concrete cylinders during casting.
2. The cylinders are kept in controlled room temperature for 24 hours until they harden. The samples are then demolded at 24 hours after casting.

3. The cylinder specimens are then placed in a bucket full of water and placed in an oven. Marble spheres are placed inside the bucket so that the cylinders are free to expand.
4. The temperature of the oven is then gradually increased to around 205-208 °F (96.1-97.8 °C) and is kept constant for the rest of the test duration. The water level is maintained throughout the test.
5. Strain and temperature measurements are recorded every five minutes.

Figure E-1 shows the embedded vibrating wire strain gauge used for measuring strain and temperature in the specimens. Figure E.2 presents casting of the cylinders and Figure E.3 illustrates the placement of the cylinders in the oven for elevated temperature exposure. Figure E.4 shows the three concrete cylinders from each mixture after being exposed to elevated temperature for six days. Figure E.5 shows the temperature-time history in the oven, which resembles the temperature history obtained at the core of the concrete bridge seal model (see Section 4.9).

Figure E.1 – Embedded vibrating wire strain gauge.

Figure E.2 – Casting concrete specimens with strain and temperature gauge.

(a) cylinder with strain and temperature gauge

(b) marble spheres under the cylinders inside the bucket

Figure E.3 – Placing cylinder specimens inside the oven.

Figure E.4 – Concrete cylinders after being exposed to elevated temperature.

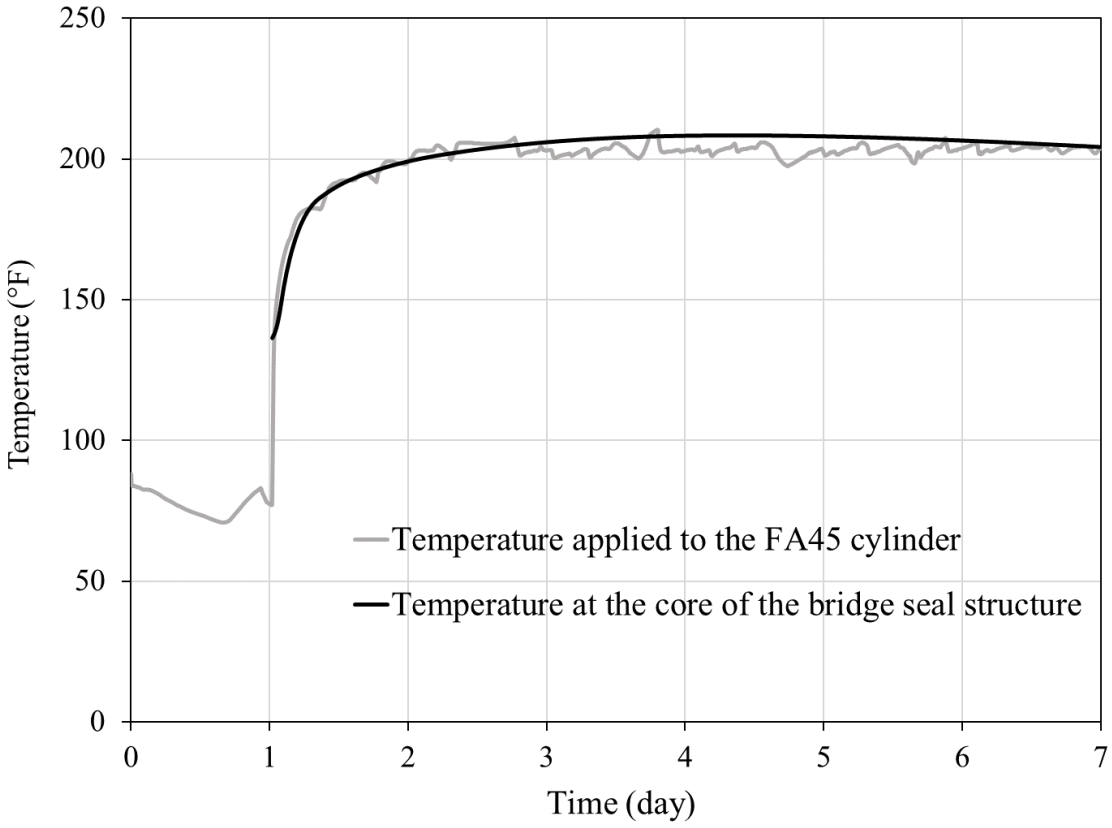

Figure E.5 – Temperature applied to the cylinders resembling the temperature history at the core of the bridge seal model.

Experimental Results

The strain and temperature measurements from the FA45, SL30+MK15, and SL40+FA30 specimens are shown in Figures E.6 through E.8. Table E.2 summarizes the strain and temperature developed in each of the samples within the first three days after casting. In the table, the maximum strain and temperature experienced within the first day of casting in each specimen are labeled as (0-1 day). Figure E.9 compares strains among the three mixtures.

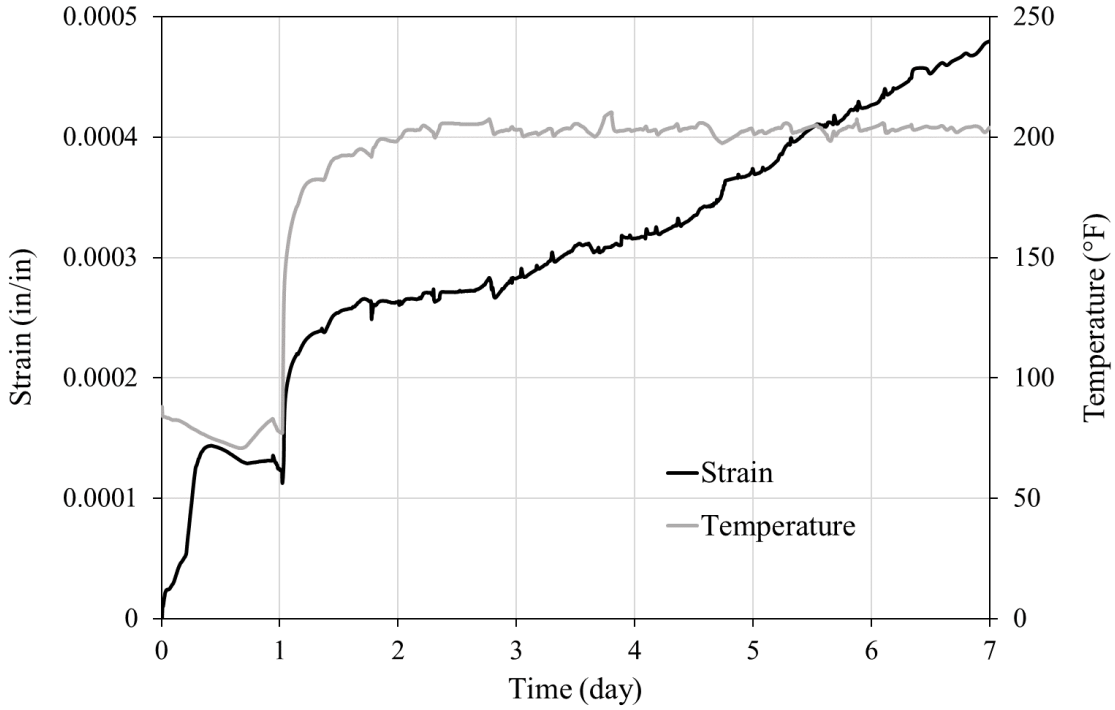

Figure E.6 – Strain and temperature development in the FA45 specimen exposed to elevated temperature.

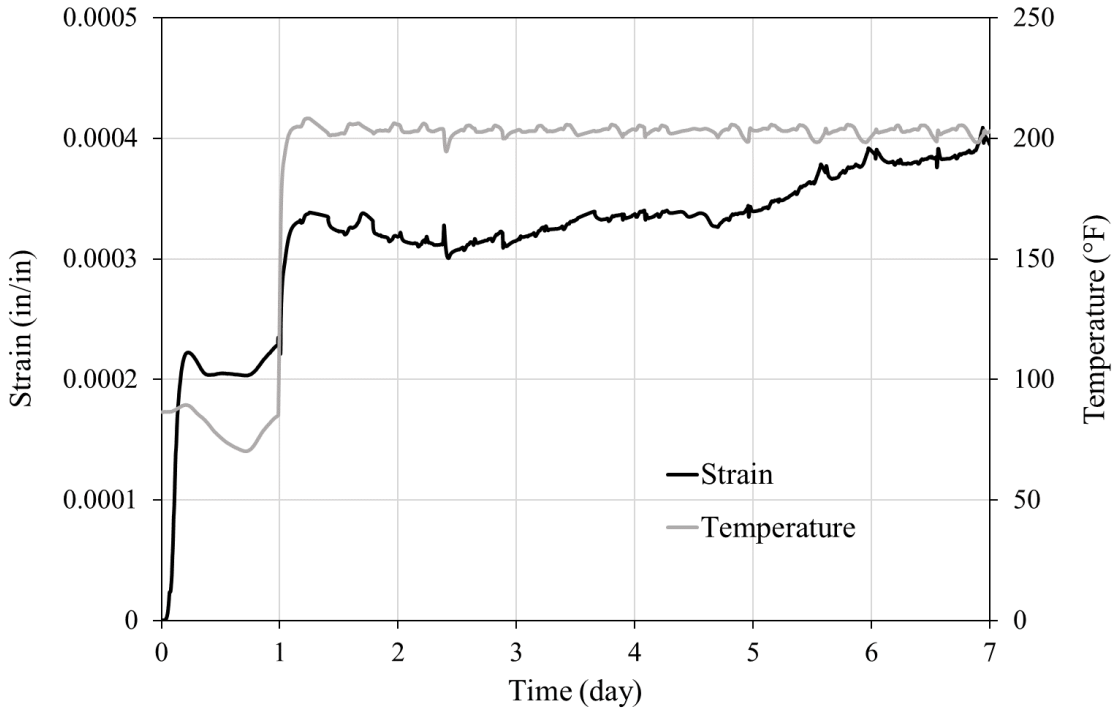

Figure E.7 – Strain and temperature development in the SL30+MK15 specimen exposed to elevated temperature.

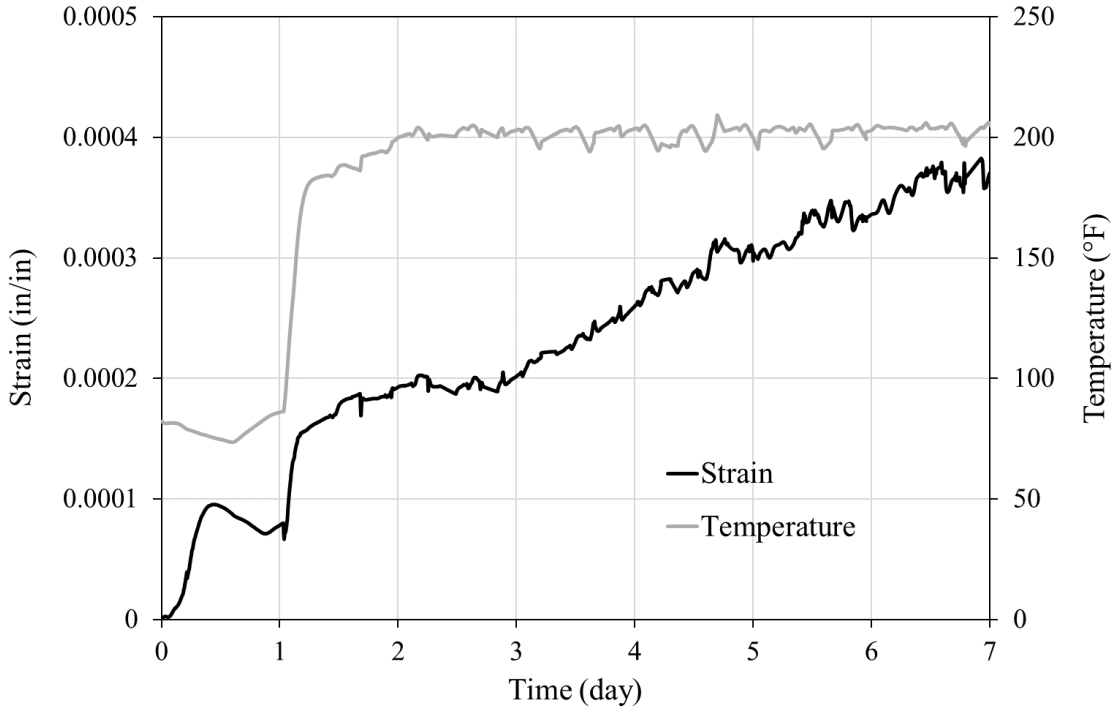

Figure E.8 – Strain and temperature development in the SL40+FA30 specimen exposed to elevated temperature.

Table E.2 – Summary of strains in different concrete mixtures exposed to elevated temperature.

Time (day)	FA45		SL30+MK15		SL40+FA30	
	Temperature (°F)	Strain (με)	Temperature (°F)	Strain (με)	Temperature (°F)	Strain (με)
0-1	74	143	89	222	75	95
2	199	263	206	319	200	193
3	203	283	203	315	203	202

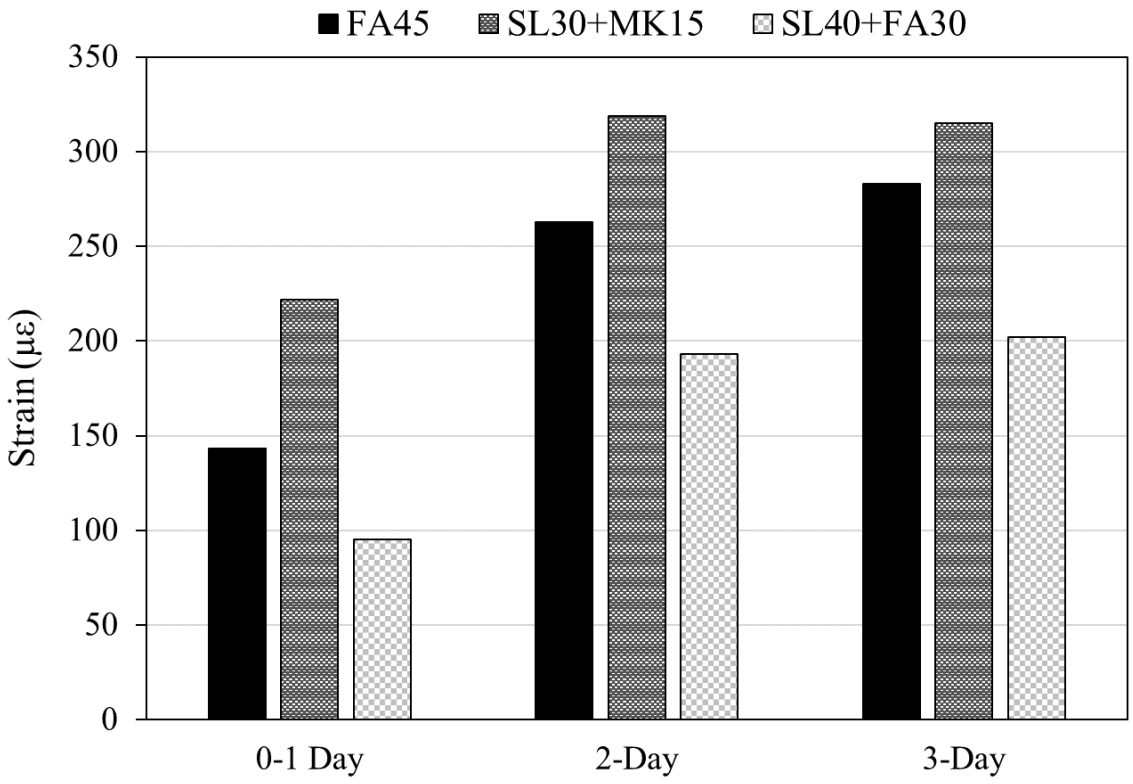

Figure E.9 – Comparison graph of strain development in different concrete mixtures.

Table E.3 and Figure E.10 present the maximum tensile strain developed for critical temperature thresholds.

Table E.3 – Strains vs. Temperature.

Equivalent Gradient Temperature (°F)	Temperature (°F)	Strain (με)		
		FA45	SL30+MK15	SL40+FA30
0	158	202	230	150
35	192	255	296	183
50	205-208	270	329	201

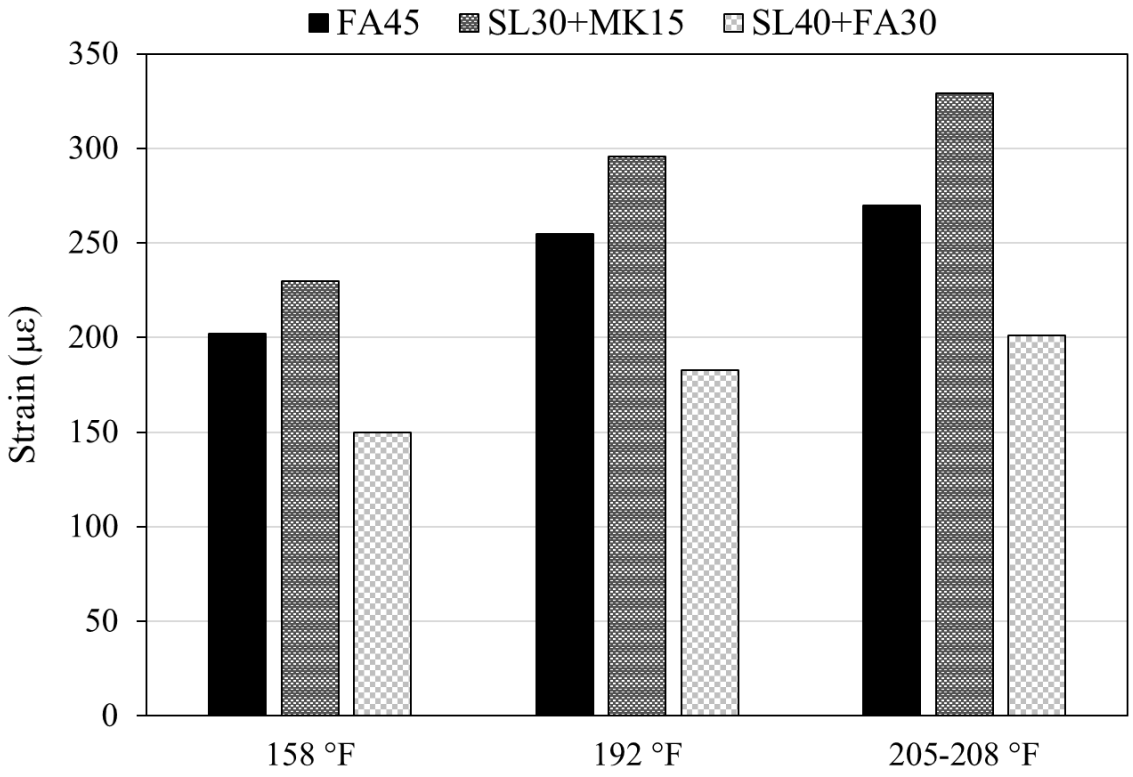

Figure E.10 – Strain vs. Temperature.

The visual inspection of the specimens after the week-long heat exposure indicates that no visual cracks are observed in the FA45 and SL40+FA30 specimens. However, a noticeably visible crack is observed in the SL30+MK15 specimen (see Figure E.11). A replacement level of 55% with slag and 15% metakaolin is recommended to reduce the tensile strain.

Figure E.11 – Crack found in the SL30+MK15 specimen.

Validation of Strain Results with Experimental Results

Table E.4 presents a comparison between the strain measurements from the FEA analysis (Section 4.9) and small-scale cylinder specimen test presented herein.

Table E.4 – Strains from FEA analysis vs. small-scale test specimens.

Mixtures	FEA Analysis		Small-test	
	Gradient 35 °F	Gradient 50 °F	Gradient 35 °F	Gradient 50 °F
FA45	0.0002-0.00075	0.00030-0.0010	0.00037	0.00050
SL30+MK15	0.0004-0.00075	0.00040-0.0010	0.00037	0.00040
SL40+FA30	0.0002-0.00075	0.00025-0.0011	0.00037	0.00038

The experimentally measured strains fall within the range of the analytically determined strains, and the average total strain agrees well. Overall, strains predicted by the FEA analysis are higher due to the fact that the crack strains are determined at integration points and averaged over the length of the element; beyond the crack initiation points, the effect of crack growth at the integration points significantly affects the total strains.

Discussion of the Results

The results illustrate that different concrete mixtures respond differently to elevated temperature. The ternary mixture with 40% slag and 30% Class F fly ash (SL40+FA30) develops the least amount of strain (least expansion), followed by the FA45 and SL30+MK15 mixtures, respectively. These results indicate that it is possible to apply varying maximum temperature and temperature differential limits based on the type of cementitious materials and replacement levels used in a concrete mixture.

APPENDIX F

DETAILED PROCEDURES FOR TESTING METHODOLOGY AND SELECTING SUITABLE MIXTURES FOR MASS CONCRETE PLACEMENTS

In this section, two methods are described on how to select suitable mixture designs for controlling the temperature in mass concrete placements. The methods are based on the methodologies and outcomes of this study. The first method includes performing certain experimental and analytical investigations based on the ability of the agency (these investigations are conducted at the University of Georgia's STRENGTH Laboratory). The second method uses the design charts developed in this study (see Chapter 5) to identify mixtures in order to meet the required temperature allowables in the mass concrete placement.

First Method:

The following steps are recommended in investigating and selecting suitable mixture designs in mass concrete placements:

1. Perform an isothermal calorimetry on the desired mixture following the ASTM C1702 standards and collect the heat of hydration data for one week
    a. Follow standard procedures to prepare paste mixtures, OR
    b. Prepare mortar samples by screening out the coarse aggregate from concrete mixtures using sieve #5.

(Note) Maintain the same consistency in preparing different mixtures. Compare the heat of hydration results between the tested paste OR mortar mixtures to predict a relative decrease or increase in the maximum temperature rise. This is an efficient method in which a large number of mixtures can be evaluated and a good estimate is obtained on the suitability of the mixtures in reducing the temperature in mass concrete placements.

2. After performing the first step (or even if the first step is not applicable), cast a 2 ft x 2 ft x 2 ft concrete specimen (for 1-3 shortlisted mixtures) insulated on all six sides by insulation materials (with a total R-value of 50 °F·ft^2·h/BTU or greater). Follow the methodology presented in Section 3.2 to build the system and quantify temperature measurements from the cube specimens using the desired concrete mixtures. This step allows the user to measure the exact temperature rise at the core of the mass concrete placement and select the most suitable mixture design for the placement.
3. Evaluate the mechanical, durability, and dimensional stability properties of the concrete mixtures selected from steps 1 and 2. The mechanical properties include compressive strength, tensile strength, and modulus of elasticity. The durability properties include permeability, sulfate resistance, and alkali-silica reactivity. The dimensional stability properties include coefficient of thermal expansion and shrinkage. The testing can be performed following the standard procedures presented in Chorzepa et al. (2017).
4. After the experimental steps, it is strongly recommended to perform an analytical investigation to analyze the thermal and structural behavior of the mass concrete structure following the methodology presented in Chapter 4 of this study. DIANA finite

element software is recommended to perform coupled transient thermal analysis and nonlinear structural analysis considering the effect of heat of hydration, mixture design properties, formwork and insulation, expected ambient temperatures surrounding the structure, placement conditions, and boundary conditions. From this step, the temperature distribution, maximum temperature and temperature differential, and cracking are predicted in the mass concrete structure.

Second Method:

This method uses the design charts presented in Chapter 5 of this study to predict the maximum temperature and maximum temperature differential in underwater mass concrete foundations and mass concrete columns with a wide range of volume-to-surface-area ratios (V/A). The effect of different mixture designs, replacement levels, insulation materials, and placement conditions are included in the design charts. From each of the design charts, we select a calculated V/A ratio from the horizontal axis. Then, we draw a vertical line to the curves associated with each mixture design. From the point of intersection with the curve, we then draw a horizontal line to the vertical axis. The point where the horizontal line intersects the vertical axis gives the value of the maximum temperature or maximum temperature differential depending on the type of the graph utilized. The maximum temperature predictions are based on the placement conditions of 85 °F (29.4 °C) and 60 °F (15.6 °C) for summer and winter, respectively. The maximum temperature values may need to be adjusted for more severe placement conditions and mixture designs significantly deviating from the mixtures studied herein. A design example is provided here to guide the user with using those charts.

Example 1:

It is required to select a suitable mixture design for an underwater mass concrete foundation with a volume to surface area ratio (V/A) of 2.5. The maximum temperature in the foundation is limited to 158 °F and the maximum temperature differential is limited to 35 °F. Consider placing in summer with an initial concrete placement temperature of 85 °F. The total cementitious content in the mixture design is considered to be 711 lb/yd^3 (422 kg/m^3).

How to approach the problem and solutions:

From the design charts (Figures 132 through 157), Figure 137 shows three mixture designs during summer placement. Selecting a V/A=2.5 from the horizontal axis, we draw a vertical line until it intersects with the curves. Reading the maximum temperature value on the vertical axis, the FA45 mixture results in a maximum temperature of 158 °F, which meets the maximum temperature requirement.

Following the same steps, Figure 138 shows that the FA45 mixture results in a maximum temperature differential of 73 °F, which is significantly higher than the allowable temperature differential limit of 35 °F. In order to meet the 35 °F requirement, it is required to use insulation material with R-value of 3 °F·ft^2·h/BTU. Providing this insulation will bring down the maximum temperature differential to under 35 °F, as shown in Figure 155 with a Control mixture.

It is important to mention that providing insulation materials may result in a slight increase (about 2-3 °F) in the maximum temperature value. In this case, the FA45 mixture will result in a maximum temperature slightly higher than 158 °F. This temperature can be

lowered to under 158 °F by lowering the placement temperature of the concrete. Additionally, other mixtures, such as SL55+MK15 and SL40+FA30, also meet the maximum temperature requirement of 158 °F, and they result in even lower maximum temperature compared to the FA45 mixture, as shown in Figure 146. The maximum temperature differential limit of 35 °F is also met with these mixtures if insulation materials with a R-value of 3 °F·ft^2·h/BTU or greater are used.

In conclusion, the FA45 mixture is suitable for the mass concrete placement when insulation with R-value of 3 °F·ft^2·h/BTU is provided and the concrete placement temperature is kept under 80 °F. Alternatively, active cooling options should be investigated.

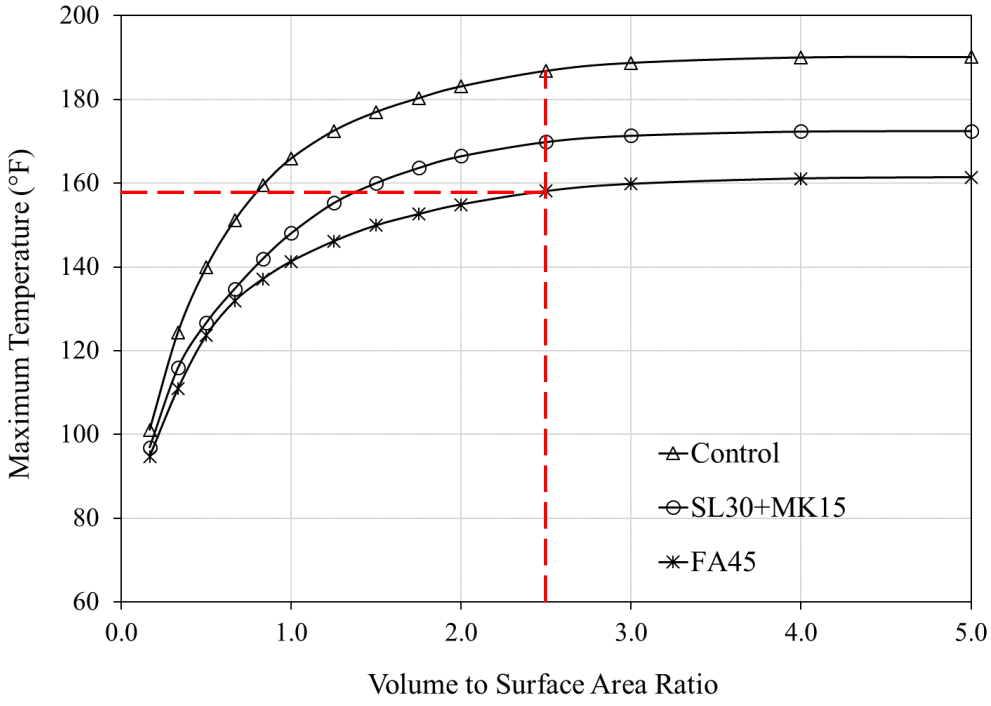

Figure 137 – Effect of 45% replacement mixtures on maximum temperature – foundation (summer).

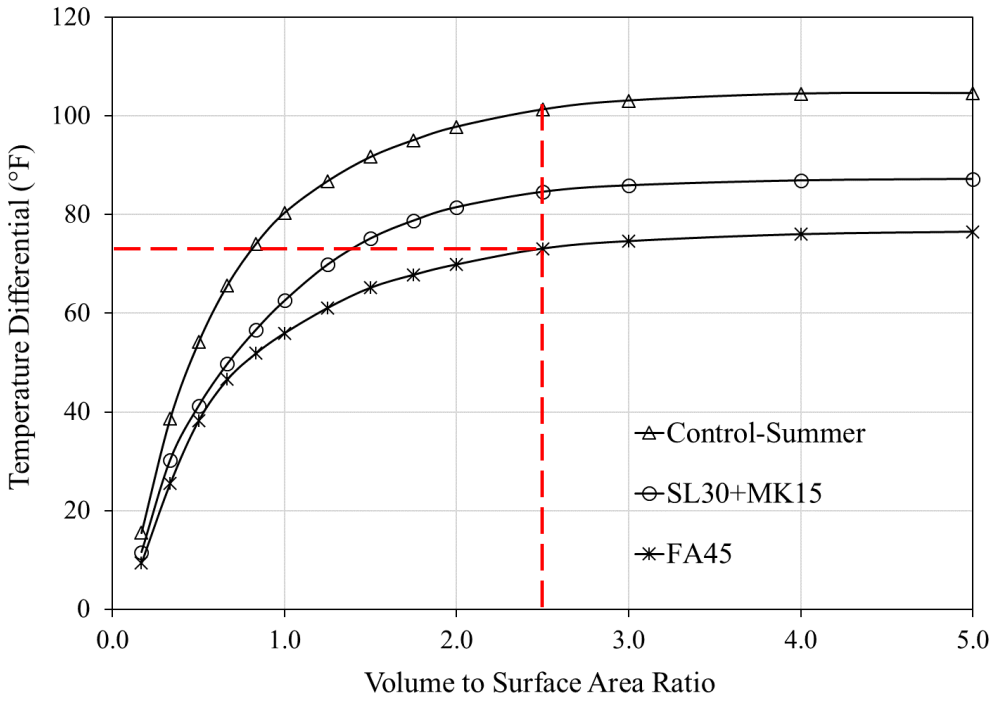

Figure 138 – Effect of 45% replacement mixtures on temperature differential – foundation (summer).

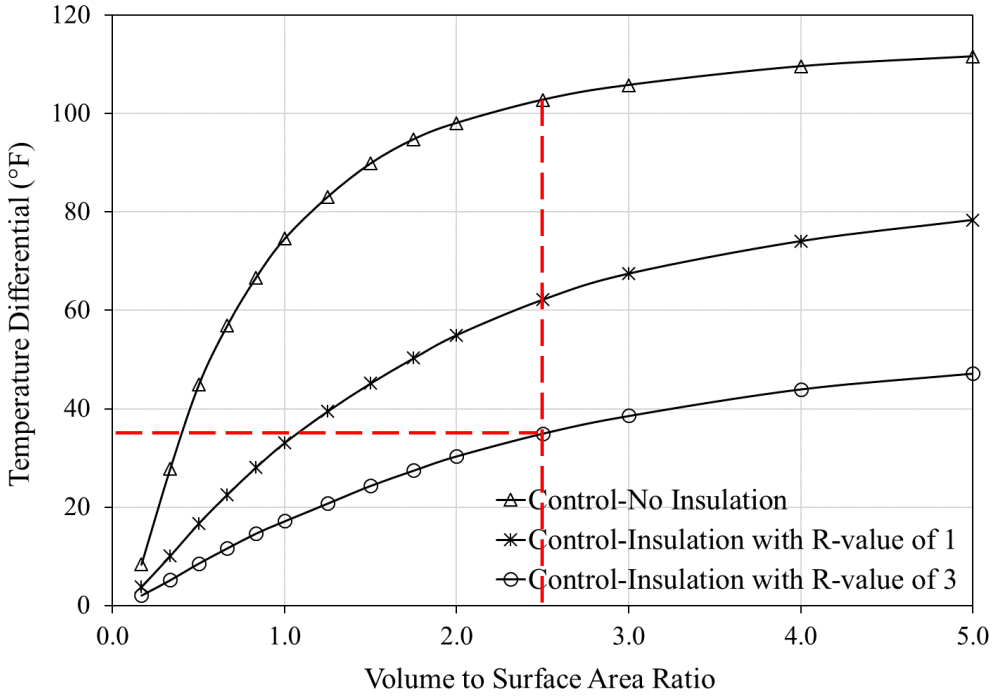

Figure 155 – Effect of insulation on temperature differential – foundation (summer).

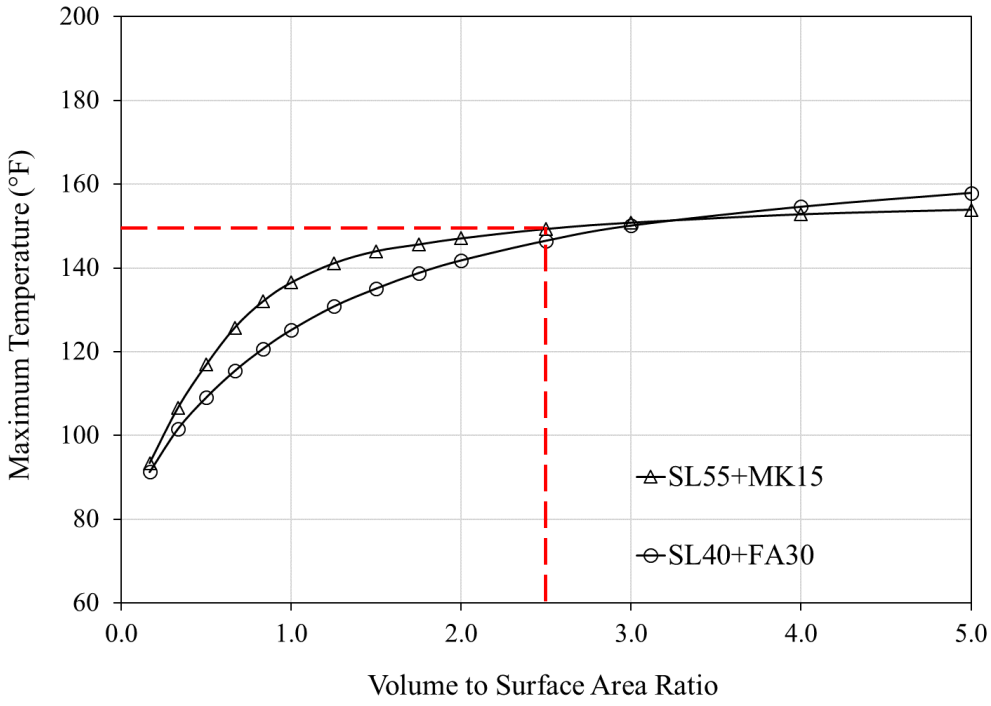

Figure 146 – Effect of ternary mixtures with 70% replacement level on maximum temperature – foundation (summer).

Example 2:

It is required to select a suitable mixture design for a mass concrete column with a volume to surface area ratio (V/A) of 2.5. The maximum temperature in the column is limited to 158 °F and the maximum temperature differential is limited to 35 °F. Consider placing in summer with an initial concrete placement temperature of 85 °F. The total cementitious content in the mixture design is assumed 711 lb/yd^3 (422 kg/m^3) in this example.

How to approach the problem and solutions:

From the design charts (Figures 159 through 187), Figure 164 shows three mixture designs during summer placement. Selecting a V/A=2.5 from the horizontal axis, we draw a vertical line until it intersects with the curves. Reading the maximum temperature value on

the vertical axis, the FA45 mixture results in a maximum temperature of 155.4 °F, which meets the maximum temperature requirement.

Following the same steps, Figure 165 shows that the FA45 mixture results in a maximum temperature differential of 57.4 °F. However, Figure 185 shows that when insulation material with a R-value of 2 is used, the FA45 mixture results in a maximum temperature differential of 27.3 °F, which meets the requirement.

If desired, other mixtures, such as SL55+MK15 and SL40+FA30, also meet the maximum temperature and differential requirements if insulation materials with a R-value of 2 °F·ft^2·h/BTU or greater are used.

In conclusion, the FA45 mixture is suitable for the mass concrete placement when insulation with an R-value of 2 °F·ft^2·h/BTU is used.

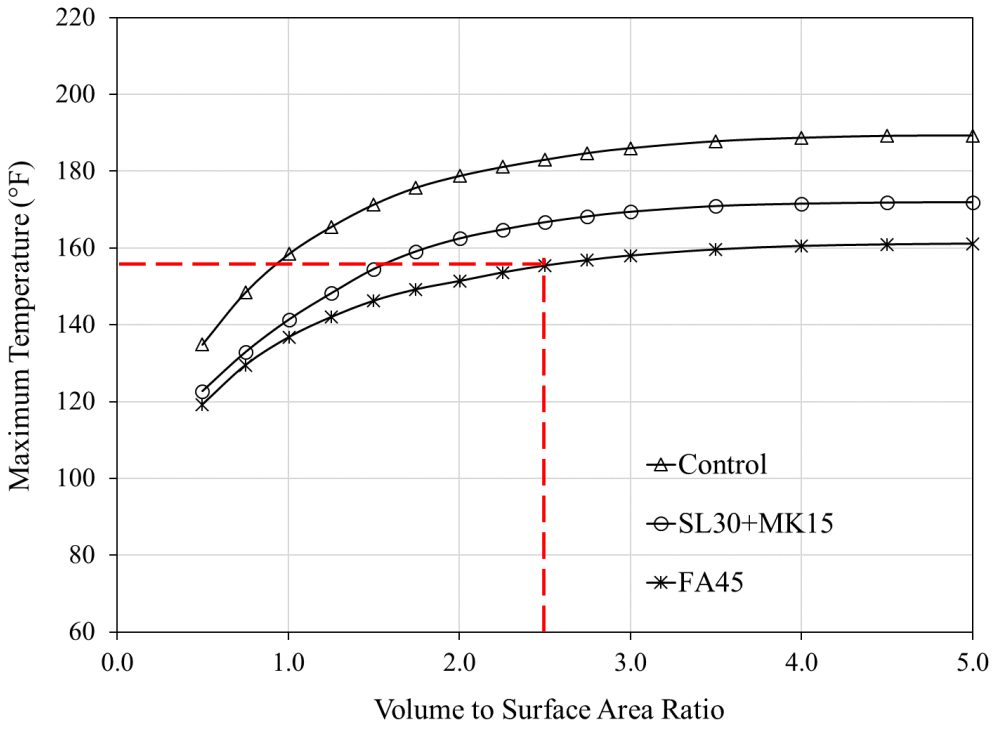

Figure 164 – Effect of 45% replacement mixtures on maximum temperature – column (summer).

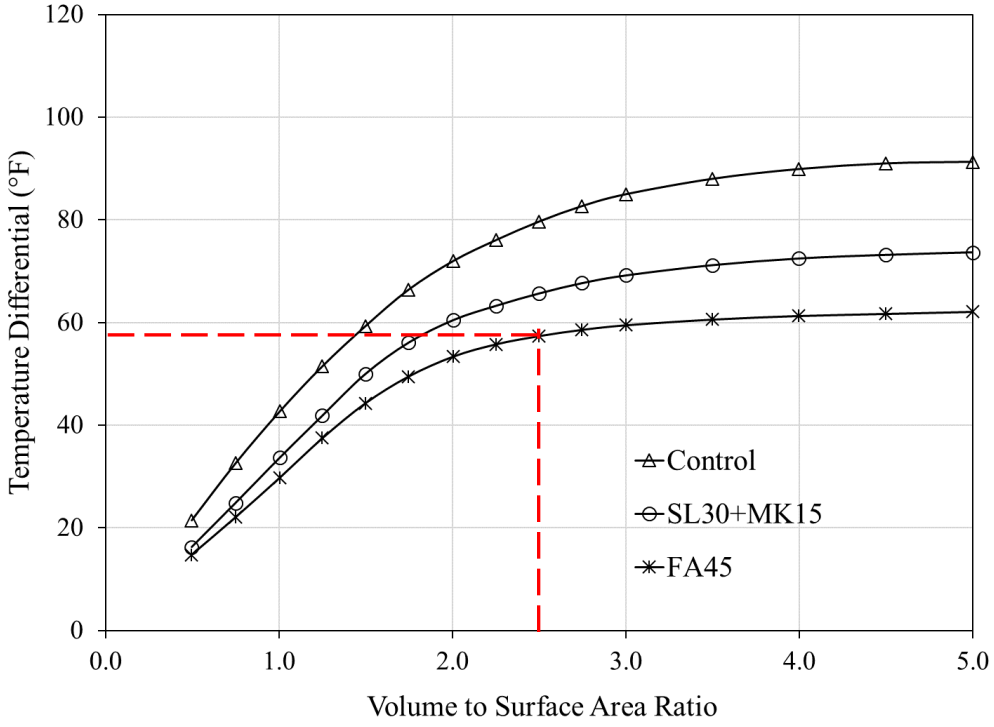

Figure 165 – Effect of 45% replacement mixtures on temperature differential – column (summer).

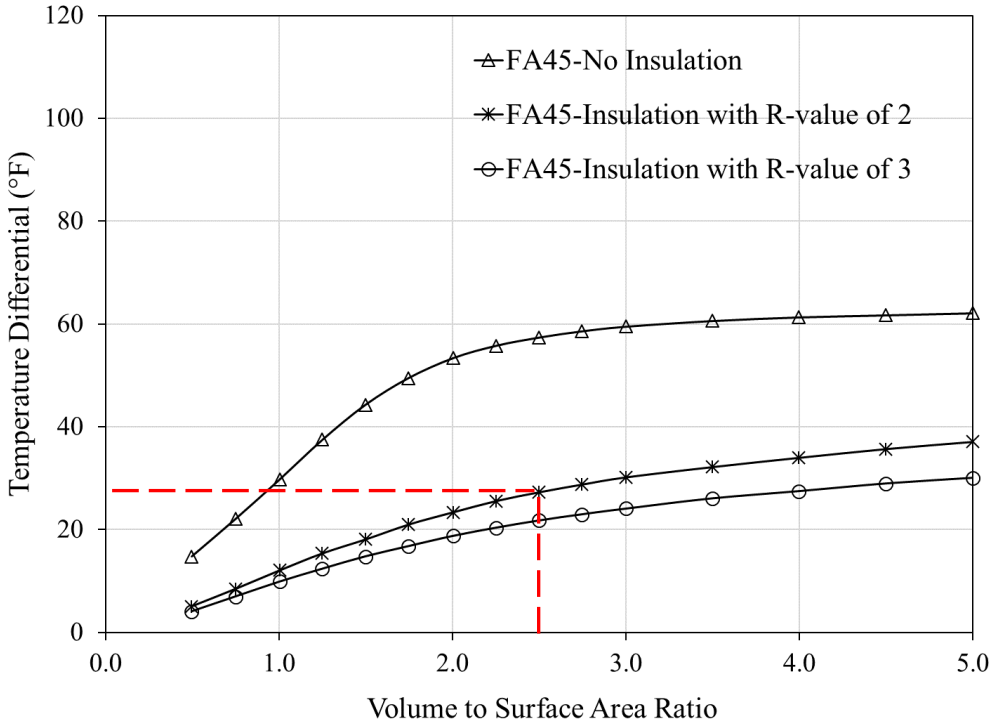

Figure 185 – Effect of insulation on temperature differential with FA45 mixture – column (summer).

Here, the mixture design is based on the cement content of 711 lb/yd^3 (422 kg/m^3). The temperature prediction for a Portland cement mixture with a different cement content may be adjusted by 12.8 °F for every 100 lb/yd^3 (12 °C for every 100 kg/m^3) of cement increased (or decreased) from the base mixture. On contrary, temperature predictions for any binary or ternary mixtures with different cementitious content may be adjusted by 10 °F for every 100 lb/yd^3 (9.4 °C for every 100 kg/m^3) of cementitious material increased (or decreased) from the base mixture.

The methods for cooling down concrete temperatures consist of pre-cooling of the concrete ingredients and post-cooling of the concrete placement. The common pre-cooling practices include: using ice in the mixing water (no frozen pieces of ice after mixing), storing cement and aggregates in cool or shaded locations, sprinkle coarse aggregate with water or wet the stockpile, controlling rate of concrete placement, placing concrete at times of day when the ambient temperature is lowest (in summer) or highest (in winter), and use of liquid nitrogen system to cool the concrete mass before placement. The most common post-cooling practice includes the use of mechanical cooling pipes in the concrete to control the internal temperature of mass concrete during curing and conformance with the Thermal Control Plan.

The methods for controlling temperature differentials, in addition to the practices with lowering internal temperature, include: insulating the concrete forms and the surface of the concrete, providing supplemental external heat at the concrete surface to prevent any heat loss.